

Université de Montréal

Développement d'outils de surveillance biologique pour l'évaluation des risques pour  
la santé des humains exposés à quatre pesticides et au méthylmercure

Par  
Nathalie Gosselin

Département de santé environnementale et santé au travail  
Université de Montréal  
Faculté de médecine

Thèse présentée à la Faculté des études supérieures  
en vue de l'obtention du grade de doctorat  
en santé publique  
option toxicologie de l'environnement

Septembre, 2005

© Nathalie Gosselin, 2005



WA

5

U58

2005

V. 016

C



## AVIS

L'auteur a autorisé l'Université de Montréal à reproduire et diffuser, en totalité ou en partie, par quelque moyen que ce soit et sur quelque support que ce soit, et exclusivement à des fins non lucratives d'enseignement et de recherche, des copies de ce mémoire ou de cette thèse.

L'auteur et les coauteurs le cas échéant conservent la propriété du droit d'auteur et des droits moraux qui protègent ce document. Ni la thèse ou le mémoire, ni des extraits substantiels de ce document, ne doivent être imprimés ou autrement reproduits sans l'autorisation de l'auteur.

Afin de se conformer à la Loi canadienne sur la protection des renseignements personnels, quelques formulaires secondaires, coordonnées ou signatures intégrées au texte ont pu être enlevés de ce document. Bien que cela ait pu affecter la pagination, il n'y a aucun contenu manquant.

## NOTICE

The author of this thesis or dissertation has granted a nonexclusive license allowing Université de Montréal to reproduce and publish the document, in part or in whole, and in any format, solely for noncommercial educational and research purposes.

The author and co-authors if applicable retain copyright ownership and moral rights in this document. Neither the whole thesis or dissertation, nor substantial extracts from it, may be printed or otherwise reproduced without the author's permission.

In compliance with the Canadian Privacy Act some supporting forms, contact information or signatures may have been removed from the document. While this may affect the document page count, it does not represent any loss of content from the document.

Université de Montréal  
Faculté des études supérieures

Cette thèse intitulée :

Développement d'outils de surveillance biologique pour l'évaluation des risques pour  
la santé des humains exposés à quatre pesticides et au méthylmercure

Présentée par :  
Nathalie Gosselin

a été évaluée par un jury composé des personnes suivantes :

Robert Tardif  
président-rapporteur

Gaétan Carrier  
directeur de recherche

Robert Brunet  
codirecteur

Pierre Ayotte  
examineur externe

France Varin  
examineur interne

Robert Tardif  
représentant du doyen de la FES

## RÉSUMÉ

Dans notre environnement, il y a une multitude de substances toxiques potentiellement absorbables par les êtres vivants, incluant les humains. Les organismes gouvernementaux doivent se doter d'outils fiables pour identifier, évaluer et gérer les risques toxicologiques associés à ces substances afin de prévenir les problèmes de santé humaine.

Cette thèse présente des outils de surveillance biologique facilement applicables pour analyser les risques toxicologiques chez les humains exposés à cinq contaminants environnementaux : trois insecticides de la famille des organophosphorés (parathion, malathion et chlorpyrifos), un phytocide largement utilisé comme herbicide (triclopyr), et finalement le méthylmercure. Ces outils visent à évaluer avec suffisamment de précision les quantités de substance qu'un individu a absorbées à partir de la mesure des niveaux de la substance-mère ou de ses métabolites dans une ou plusieurs matrices biologiques. Une analyse de sensibilité des paramètres impliqués a permis de proposer une procédure d'utilisation optimale de chaque outil dans le cadre de programmes d'évaluation et de prévention des risques toxicologiques.

Un modèle cinétique a été développé ou adapté pour chacune des substances étudiées afin d'établir les liens entre les niveaux de biomarqueurs, les charges corporelles de la substance-mère et de ses métabolites et les doses absorbées suite à différents scénarios d'exposition (unique, répété, chronique, intermittent ; cutané, oral et pulmonaire) et différentes stratégies d'échantillonnage des matrices biologiques. Ces outils

mathématiques se basent sur des systèmes d'équations différentielles qui assurent en tout temps la conservation des masses molaires.

Pour chacun des quatre pesticides ciblés, un modèle cinétique spécifique a servi à déterminer des niveaux de biomarqueurs urinaires en-dessous desquels aucun effet toxique n'est susceptible de se développer. Ces valeurs de référence biologiques correspondent aux quantités de la substance-mère, ou de ses métabolites, mesurées dans les urines collectées durant une période donnée chez un individu ayant absorbé, lors de son quart de travail, une dose pour laquelle il n'y a pas eu d'effets observés (DSEO). Une analyse de sensibilité des paramètres des modèles cinétiques a montré que l'hypothèse d'absorption entièrement par la peau donne des valeurs de référence biologiques plus conservatrices que l'hypothèse d'absorption par les autres voies possibles d'entrée. L'application de ces valeurs de référence assure ainsi une bonne protection des personnes exposées quelle que soit la voie d'absorption de ces substances.

Les outils développés dans cette thèse ont été utilisés pour estimer l'exposition et les risques encourus par des travailleurs exposés au malathion ou au triclopyr ainsi que pour des populations autochtones exposées au méthylmercure. Les comparaisons entre les niveaux de biomarqueurs mesurés chez les travailleurs et les valeurs de référence biologiques ont démontré que les risques découlant de cette exposition étaient négligeables ou nuls au moment de cette évaluation. D'autre part, les apports quotidiens en méthylmercure estimés à partir du modèle cinétique et des concentrations

de mercure total mesurées dans les segments consécutifs coupés dans les mèches de cheveux se sont avérés plus bas et plus cohérents avec les données biologiques que ceux estimés à partir de questionnaires alimentaires.

Mots clés : surveillance biologique, analyse des risques, exposition, biomarqueur, toxicocinétique, parathion, malathion, chlorpyrifos, triclopyr, méthylmercure.

## ABSTRACT

In our environment, there is a multitude of toxic chemicals that may be absorbed by living organisms, including humans. Government agencies must thus obtain reliable tools to identify, evaluate and manage the toxicological risks associated with these chemicals in order to prevent damages to human health.

This thesis presents easily applicable biological monitoring tools to analyze the toxicological risks for humans exposed to five environmental contaminants: three insecticides of the organophosphate family (parathion, malathion and chlorpyrifos), a phytocide largely used as herbicide (triclopyr), and finally methylmercury. These tools allow estimation of the absorbed amounts of chemical with sufficient precision starting from the levels of the substance or its metabolites in one or several biological matrices of the exposed individual. A sensitivity analysis of the relevant model parameters led to the proposal of an optimal method for utilizing each tool as part of a program for the evaluation and prevention of toxicological risks.

A kinetic model was developed or adapted for each studied substance in order to establish the links between the levels of biomarkers, the body burdens of the substance and its metabolites and the cumulative intake following various exposure scenarios (single, intermittent, repeated, chronic; dermal, oral and pulmonary) and any collection period of the biological matrices. These mathematical tools are based on systems of differential equations which ensure at any time the conservation of the molar masses.

For each of the four targeted pesticides, a specific kinetic model was used to determine the levels of urinary biomarkers below which toxic effects are not likely to appear. These biological reference values correspond to the amounts of the substance, or their metabolites, measured in urines collected over a chosen period for a worker having absorbed, during the work shift, a dose for which no toxic effect has been observed (NOEL). An analysis on the parameters of the kinetic models showed that the hypothesis of absorption entirely by the skin gives more conservative biological reference values than assuming that absorption occurred through the other possible absorption routes. Use of these reference values thus ensures a good protection for the exposed persons, and this whatever the route-of-entry.

The tools developed in this thesis were applied to estimate the exposure and the risks for workers exposed to malathion or to triclopyr and for indigenous populations exposed to methylmercury. Comparisons between measured levels of biomarkers in workers and the reference values showed that the risk related to this exposition were negligible at the moment of the evaluation. The daily intakes of methylmercury estimated with the kinetic model and starting from the total mercury concentrations measured in hair segments turn out to be lower and more consistent with the biological data than those estimated from dietary questionnaires.

Key words : biological monitoring, risk analysis, exposure, biomarker, toxicokinetics, parathion, malathion, chlorpyrifos, triclopyr, methylmercury.

## TABLES DES MATIÈRES

<b>RÉSUMÉ</b> .....	<b>III</b>
<b>ABSTRACT</b> .....	<b>VI</b>
<b>TABLES DES MATIÈRES</b> .....	<b>VIII</b>
<b>LISTE DES TABLEAUX</b> .....	<b>X</b>
<b>LISTE DES FIGURES</b> .....	<b>XII</b>
<b>LISTE DES ABRÉVIATIONS ET DES SIGLES</b> .....	<b>XVII</b>
<b>CHAPITRE 1 : INTRODUCTION</b> .....	<b>1</b>
<i>PROBLÉMATIQUE</i> .....	2
<i>OBJECTIFS</i> .....	7
<i>STRUCTURE DE LA THÈSE</i> .....	7
<b>CHAPITRE 2 : GÉNÉRALITÉS SUR LA SURVEILLANCE BIOLOGIQUE</b> <b>11</b>	
<i>LES CONDITIONS D'UTILISATION DE LA SURVEILLANCE BIOLOGIQUE</i> ..	12
<i>LES CARACTÉRISTIQUES D'UN BON BIOMARQUEUR D'EXPOSITION</i> .....	13
<i>LES VALEURS DE RÉFÉRENCE</i> .....	13
<i>LA MODÉLISATION CINÉTIQUE</i> .....	18
<b>CHAPITRE 3 : ARTICLE 1, MALATHION</b> .....	<b>23</b>
<i>ABSTRACT</i> .....	25
<i>INTRODUCTION</i> .....	27
<i>METHOD AND MODEL PRESENTATION</i> .....	31
<i>RESULTS</i> .....	40
<i>DISCUSSION</i> .....	47
<i>ACKNOWLEDGMENTS</i> .....	53
<i>APPENDIX</i> .....	54
<i>REFERENCES</i> .....	56
<b>CHAPITRE 4 : ARTICLE 2, PARATHION</b> .....	<b>83</b>
<i>ABSTRACT</i> .....	85
<i>INTRODUCTION</i> .....	87
<i>METHOD</i> .....	92
<i>RESULTS</i> .....	103
<i>DISCUSSION</i> .....	110
<i>ACKNOWLEDGMENT</i> .....	117
<i>APPENDIX</i> .....	118
<i>REFERENCES</i> .....	121
<b>CHAPITRE 5 : ARTICLE 3, CHLORPYRIFOS</b> .....	<b>151</b>
<i>ABSTRACT</i> .....	153
<i>INTRODUCTION</i> .....	155
<i>METHODS</i> .....	158
<i>RESULTS</i> .....	166
<i>DISCUSSION</i> .....	170
<i>ACKNOWLEDGMENT</i> .....	178
<i>APPENDIX</i> .....	179
<i>REFERENCE</i> .....	181
<b>CHAPITRE 6 : ARTICLE 4, TRICLOPYR</b> .....	<b>206</b>

<i>ABSTRACT</i> .....	208
<i>INTRODUCTION</i> .....	209
<i>METHODS</i> .....	211
<i>RESULTS</i> .....	217
<i>DISCUSSION</i> .....	219
<i>ACKNOWLEDGMENTS</i> .....	225
<i>APPENDIX</i> .....	226
<i>REFERENCES</i> .....	228
<b>CHAPITRE 7 : ARTICLE 5, MÉTHYLMERCURE</b> .....	<b>241</b>
<i>ABSTRACT</i> .....	243
<i>INTRODUCTION</i> .....	244
<i>METHODS</i> .....	248
<i>RESULTS</i> .....	254
<i>DISCUSSION</i> .....	262
<i>CONCLUSION</i> .....	267
<i>ACKNOWLEDGMENT</i> .....	269
<i>REFERENCES</i> .....	270
<b>CHAPITRE 8 : CONCLUSION GÉNÉRALE</b> .....	<b>288</b>
<b>BIBLIOGRAPHIE</b> .....	<b>294</b>
<b>APPENDICE : CONTRIBUTION</b> .....	<b>299</b>

## LISTE DES TABLEAUX

### **CHAPITRE 3 : ARTICLE 1, MALATHION**

Table 1. Symbols Used in the Conceptual and Functional Representation of the Model .....	62
Table 2. Numerical Values of Parameters Used in the Model .....	64
Table 3. Comparison of Model Simulations With the Experimental Data of Jellinek et al. (2000) on the Cumulative Urinary Excretion of Malathion Metabolites 0-12, 0-24 and 0-48 h Following a Single Oral Exposure to 0.5, 1.5, 10 and 15 mg/kg of Malathion in Male and Female Human Volunteers .....	66
Table 4. Effect of Variations in the Absorption Rate Constant on the Simulated Cumulative Urinary Excretion of Total Metabolites Over Different Time Periods Following a Single Dermal Exposure to Malathion .....	68
Table 5. Predicted Cumulative Urinary Excretion of Total Metabolites (the Sum of Mono- and Di-Carboxylic Acids and Phosphoric Derivatives) at Different Time Periods Following the Onset of an 8-h Dermal Exposure to Malathion .....	69
Table 6. Excretion of Mono- and Di-Carboxylic Acids in 24-h Urine Samples of Botanical Garden Workers Exposed to Malathion and Comparison With the Biological Reference Values Proposed in This Study .....	71

### **CHAPITRE 4 : ARTICLE 2, PARATHION**

Table 1. Symbols Used in the Conceptual and Functional Representation of the Model .....	130
Table 2. Parameter Values Used for Model Simulations of the Kinetics of Parathion and That of <i>p</i> -Nitrophenol and Alkyl Phosphate Metabolites .....	131
Table 3. Ranges of Values of the Normalized Sensitivity Coefficient R .....	132
Table 4. Biological Reference Values for <i>p</i> -Nitrophenol and Alkyl Phosphates in Urine .....	134
Table 5. Predicted Daily Amounts of <i>p</i> -Nitrophenol and Alkyl Phosphates in Urine During a Repeated 8-h Daily Dermal Exposure to Parathion .....	135
Table 6. Cumulative Urinary Amounts of <i>p</i> -Nitrophenol and Alkyl Phosphates Over Different Collection Periods Following Either an Instantaneous Exposure or the Onset of a 4-h Dermal Exposure to the Chosen NOEL Dose of Parathion .....	136

### **CHAPITRE 5 : ARTICLE 3, CHLORPYRIFOS**

Table 1. Symbols used in the functional representation of the model .....	190
Table 2. Model parameter values .....	191
Table 3. Values of the normalized sensitivity coefficient R .....	193
Table 4. Biological reference values for 3,5,6-trichloro-2-pyridinol and alkyl phosphates in urine: cumulative amounts over different collection periods from the onset of exposure .....	194

Table 5. Comparison of the data of Fenske and Elkner<sup>(6)</sup>, on the cumulative urinary excretion of 3,5,6-trichloro-2-pyridinol (3,5,6-TCP) over 24 and 48 hours in workers exposed to chlorpyrifos following structural control treatments of houses, with the proposed biological reference values<sup>A</sup> ..... 195

**CHAPITRE 6 : ARTICLE 4, TRICLOPYR**

Table 1. Symbols used in the conceptual and functional representation of the modified kinetics model of triclopyr developed by Carmichael *et al.* (1989).....231

Table 2. Amounts of triclopyr measured in the 22-hr cumulative urinary samples (mg) of the workers and their body weights (kg) .....232

Table 3. Effect of variations in the relative contributions of the dermal and pulmonary routes on model predictions of different exposure parameters following a 8-hr exposure to triclopyr resulting in a 22-hr cumulative urinary excretion of triclopyr equal to 56.4 µg/kg .....233

Table 4. The lower-bound, the mean and the upper-bound estimates of daily absorbed dose (mg) for each worker assuming that the absorption occurs only via the skin .....235

Table 5. Comparison of the lower-bound, mean and upper-bound estimates of daily absorbed dose (mg/kg-bw) with the dose corresponding to the no-observed-effect level (NOEL) observed in rats: 5 mg/kg-bw.....237

**CHAPITRE 7 : ARTICLE 5, MÉTHYLMERCURE**

Table 1. Effect on the maximum concentration of total mercury in blood (µg/l) and in hair (µg/g) of variations in the value of the assumed metabolic rate of transformation of organic mercury into inorganic mercury.....276

Table 2. Simulated ratio of total mercury concentration in the 1<sup>st</sup> centimeter of hair closest to the root (µg/g) and in blood (µg/ml) as function of collection times and different durations of methylmercury daily intakes. ....277

Table 3. Descriptive statistics on average daily intakes of methylmercury (µg/kg body weight) for the women from the Inuvik cohort (Walker *et al.*, 2002): *i*) estimated from the model simulations based on the total mercury concentrations measured in the consecutive segments of hair; *ii*) average daily intakes as estimated by the questionnaire. ....278

## LISTE DES FIGURES

### CHAPITRE 2: GÉNÉRALITÉS SUR LA SURVEILLANCE BIOLOGIQUE

- Figure 1. Schéma général des relations entre la dose absorbée dans l'organisme, les biomarqueurs et les effets nocifs sur la santé humaine. .... 17

### CHAPITRE 3 : ARTICLE 1, MALATHION

- Figure 1. Conceptual representation of the kinetics of malathion and its metabolites. Symbols are described in Table 1. .... 73
- Figure 2. Model simulations (lines) compared with experimental data of Feldmann and Maibach (1974) (symbols) on the cumulative urinary excretion time course of total  $^{14}\text{C}$  (% of administered dose) in male human volunteers following an intravenous (A) and dermal (B) exposure to  $1\ \mu\text{Ci}$  of  $^{14}\text{C}$ -malathion. Each point represents mean value of experimental data ( $n = 6$  per exposure group). .... 73
- Figure 3. Model simulations (lines) compared with experimental data of Maibach *et al.* (1971) (symbols) on the cumulative urinary excretion time course of total  $^{14}\text{C}$  (% of administered dose) in male human volunteers following a dermal exposure to  $^{14}\text{C}$ -malathion ( $4\ \mu\text{g}/\text{cm}^2$ ) on the forearm ( $\times$ ), the palm of the hand (+), the hand dorsum ( $\square$ ) and the forehead ( $\diamond$ ). Each point represents mean value of experimental data ( $n = 6$  per exposure group). .... 73
- Figure 4. Model simulations (lines) compared with experimental data of Dennis and Lee (1999) (symbols) on the cumulative urinary excretion time course of phosphoric derivative metabolites (the sum of DMDTP, DMTP and DMP) (nmol) in human volunteers following a dermal exposure (on an intact skin) to an aqueous-based head lice formulation containing on average  $0.126\ \text{g}$  of malathion (O) and an alcohol-based head lice formulation containing on average  $0.089\ \text{g}$  of malathion ( $\square$ ). Each point represents mean value of experimental data ( $n = 5$  to  $10$  volunteers per treatment group). .... 73
- Figure 5. Simulation of the time course of malathion and its metabolites (% of administered dose) in body (A) and excreta (B) compartments of the model following a single oral exposure to malathion. B(t), malathion in blood and tissues in dynamical equilibrium with blood as a function of time; S(t), malathion in storage tissues as a function of time; M(t), total metabolites in the body as a function of time; Q(t), systemic body burden of malathion and its metabolites as a function of time;  $U_{\text{MCA}}(t)$ , MCA metabolite in urine as a function of time,  $U_{\text{DCA}}(t)$ , DCA metabolite in urine as a function of time,  $U_{\text{MP}}(t)$ , phosphoric derivative metabolites in urine as a function of time. For comparison purposes, Figure 5B also shows the average urinary excretion of MCA ( $\times$ ), DCA (O) and phosphoric derivatives ( $\square$ ) during the 0-12, 0-24 and 0-48 h following an oral administration of 0.5, 1.5, 10 and 15 mg/kg of malathion in volunteers, as determined from the data of Jellinek *et al.* (2000). .... 74

- Figure 6. Simulation of the time course of malathion and its metabolites (% of administered dose) in the model compartments following a single dermal exposure to malathion.  $B(t)$ , malathion in blood and tissues in dynamical equilibrium with blood as a function of time;  $S(t)$ , malathion in storage tissues as a function of time;  $M(t)$ , total metabolites in the body as a function of time;  $Q(t)$ , systemic body burden of malathion and its metabolites as a function of time;  $U_{MCA}(t)$ , MCA metabolite in urine as a function of time,  $U_{DCA}(t)$ , DCA metabolite in urine as a function of time,  $U_{MP}(t)$ , phosphoric derivative metabolites in urine as a function of time.....74
- Figure 7. Simulation of the time course of malathion and its metabolites (fraction of absorbed daily dose) in the model compartments following a repeated dermal exposure to malathion, 8 h/day, 5 consecutive days/week for 4 weeks.  $B(t)$ , malathion in blood and tissues in dynamical equilibrium with blood as a function of time;  $S(t)$ , malathion in storage tissues as a function of time;  $M(t)$ , total metabolites in the body as a function of time. ....75

#### **CHAPITRE 4 : ARTICLE 2, PARATHION**

- Figure 1. Biotransformation pathways of parathion. .... 137
- Figure 2. Conceptual representation of the kinetics of parathion and its metabolites. Symbols and abbreviations are described in Table 1. One mole of parathion absorbed in the body is broken down into one mole of alkyl phosphates and one mole of *p*-nitrophenol. .... 137
- Figure 3. Model simulations (lines) compared with experimental data of Feldmann and Maibach (1974) (symbols) on the time course of total ethyl-<sup>14</sup>C urinary excretion rate (% of administered dose/h) in male human volunteers following an intravenous (○) and percutaneous (×) administration of ethyl-<sup>14</sup>C parathion (1 μCi). Each point represents mean value of experimental data (*n* = 6 per exposure group). .... 137
- Figure 4. Model simulations (lines) compared with experimental data of Maibach et al. (1971) (symbols) on the time course of total ethyl-<sup>14</sup>C cumulative urinary excretion (% of administered dose) in male human volunteers following a percutaneous administration of ethyl-<sup>14</sup>C parathion (4 μg/cm<sup>2</sup>) on the forearm (×), the palm of the hand (+), the hand dorsum (□) and the scalp (◇). Each point represents mean value of experimental data (*n* = 6 per exposure group). .... 137
- Figure 5. Model simulation (line) compared with experimental data (symbols) of Hartwell et al. (1964) on the time course of *p*-nitrophenol urinary excretion rate in a human volunteer exposed by inhalation to parathion vapors for 2.5 h, under an exposure temperature of 38°C..... 138
- Figure 6. Model simulation (line) compared with experimental data (symbols) of Hayes et al. (1964) on the time course of *p*-nitrophenol urinary excretion rate in a human volunteer exposed for 2 hours, on 5 consecutive days, to 5 g of 2% parathion dust on a hand and forearm secured in a polyethylene bag, at a constant exposure temperature of 41°C. .... 138

- Figure 7. Model simulation (line) compared with experimental data (symbols) of Michalke (1984) on the time course of *p*-nitrophenol cumulative urinary excretion in a human subject intoxicated orally with parathion. .... 138
- Figure 8. Model simulation (line) compared with experimental data (symbols) of Wolfe et al. (1970) on the time course of *p*-nitrophenol cumulative urinary excretion in a worker following an 8-h application period, in orchards, of a formulation containing parathion..... 138
- Figure 9. Model simulations of the time course of (A) *p*-nitrophenol and (B) alkyl phosphates cumulative excretion in urine (expressed as a fraction of total amounts excreted in urine) following the onset of an 8-h exposure to parathion considering different dermal absorption rate values: —  $k_{\text{abs-dermal}} = 0.04 \text{ h}^{-1}$ ; - - - -  $k_{\text{abs-dermal}} = 0.09 \text{ h}^{-1}$ ; · · · · ·  $k_{\text{abs-dermal}} = 0.3 \text{ h}^{-1}$  ..... 139
- Figure 10. Model simulations of the time course of (A) parathion burden at the site-of-entry  $R(t)$ , and (B) parathion and paraoxon in storage tissues  $S(t)$  (expressed as a fraction of absorbed daily dose) during and following a consecutive 5-day-per-week dermal exposure to parathion, 8 h per day, repeated over two weeks, considering a dermal absorption rate of  $0.04 \text{ h}^{-1}$  (—) or  $0.3 \text{ h}^{-1}$  (- - - -). ..... 139
- Figure 11. Model simulations (lines) of the concentration-time course of *p*-nitrophenol in urine following the onset of an 8-h dermal exposure to parathion where the daily absorbed dose corresponds to the NOEL of  $58 \mu\text{g}/\text{kg}$  of body weight/day with a urinary flow rate of  $1.5 \text{ l}/\text{day}$  and different dermal absorption rate values: —  $k_{\text{abs-dermal}} = 0.04 \text{ h}^{-1}$ ; - - - -  $k_{\text{abs-dermal}} = 0.09 \text{ h}^{-1}$ ; · · · · ·  $k_{\text{abs-dermal}} = 0.3 \text{ h}^{-1}$ . ... 139

### CHAPITRE 5 : ARTICLE 3, CHLORPYRIFOS

- Figure 1. Chlorpyrifos biotransformation pathways. .... 196
- Figure 2. Conceptual representation of the kinetics of chlorpyrifos and its metabolites. Symbols and abbreviations are described in Table 1. One mole of chlorpyrifos absorbed in the body is eventually broken down into one mole of 3,5,6-trichloro-2-pyridinol and one mole of alkyl phosphates (the sum of diethyl phosphate and diethyl thiophosphate), either directly or through the formation of chlorpyrifos-oxon..... 196
- Figure 3. Model simulations (lines) compared with experimental data of Nolan et al.<sup>(12)</sup> (symbols) on (A) the blood concentration-time course of 3,5,6-trichloro-2-pyridinol (×), the urinary excretion rate time course of 3,5,6-trichloro-2-pyridinol (○) and (B) the cumulative urinary-excretion time course of 3,5,6-trichloro-2-pyridinol in male volunteers orally administered  $0.5 \text{ mg}$  chlorpyrifos per kg of body weight deposited onto lactose tablets. Each point represents mean value of experimental data ( $n = 6$ ). ..... 196
- Figure 4. Model simulations (lines) compared with experimental data (symbols) of Drevenkar et al.<sup>(24)</sup> on (A) the blood concentration-time course of chlorpyrifos (□) and alkyl phosphates (×), the urinary excretion rate time course of alkyl phosphates (○) and (B) the cumulative urinary-excretion time course of alkyl phosphates (the sum of diethyl phosphate and diethyl thiophosphate) in a poisoned subject who ingested a commercial insecticide formulation containing chlorpyrifos. .... 196

- Figure 5. Model simulations (lines) compared with experimental data of Nolan *et al.*<sup>(12)</sup> (symbols) on (A) the blood concentration-time course of 3,5,6-trichloro-2-pyridinol and (B) the cumulative urinary excretion time course of 3,5,6-trichloro-2-pyridinol in male volunteers dermally applied 5 mg chlorpyrifos per kg of body weight on the forearm. Each point represents mean value of experimental data (n = 5). ..... 197
- Figure 6. Model simulations (lines) compared with experimental data of Brzak *et al.*<sup>(14)</sup> (symbols) on (A) the blood concentration-time course of 3,5,6-trichloro-2-pyridinol and (B) the cumulative urinary excretion time course of 3,5,6-trichloro-2-pyridinol in 6 male and 6 female volunteers orally administered 0.5 (○), 1 (×) and 2 (□) mg chlorpyrifos per kg of body weight in capsule form. Each point represents mean experimental value and error bars are standard deviations. .... 197
- Figure 7. Model simulations compared with experimental data (symbols) of Griffin *et al.*<sup>(13)</sup> on the cumulative urinary excretion time course of alkyl phosphates (the sum of diethyl phosphate and diethyl thiophosphate) in volunteers orally administered 1 mg of chlorpyrifos placed on a sugar cube. Each point represents mean value of experimental data (n = 5, four men and one women). The solid line represents model simulation using an oral absorption fraction of 0.93 as reported by Griffin *et al.*<sup>(13)</sup>, an oral absorption rate of 0.13 hr<sup>-1</sup>, a CPF storage rate, k<sub>BS</sub>, of 0.12 hr<sup>-1</sup> and the other parameters as reported in Table 2..... 197

**CHAPITRE 6 : ARTICLE 4, TRICLOPYR**

- Figure 1. Modified model of the kinetics of triclopyr developed by Carmichael *et al.* (1989). Symbols are described in Table 1. .... 238
- Figure 2. Model simulations of the time-course of cumulative excretion of triclopyr in urine (expressed as a fraction of the daily absorbed dose) following the onset of an 8-hour day with two 15-minute breaks in the morning and in the after-noon and a 30 minutes break for lunch with absorption only through the skin: (—) k<sub>abs</sub>=0.04 hr<sup>-1</sup>, k<sub>BS</sub>=0.13 hr<sup>-1</sup>, k<sub>SB</sub>=0.46 hr<sup>-1</sup>, k<sub>e</sub>= 0.19 hr<sup>-1</sup>, F<sub>u</sub>=0.74 ; (·-·-·-·) k<sub>abs</sub>=0.06 hr<sup>-1</sup>, k<sub>BS</sub>=0.13 hr<sup>-1</sup>, k<sub>SB</sub>=0.23 hr<sup>-1</sup>, k<sub>e</sub>= 0.35 hr<sup>-1</sup>, F<sub>u</sub>=0.90 ; (-----) k<sub>abs</sub>=0.04 hr<sup>-1</sup>, k<sub>BS</sub>=0.14 hr<sup>-1</sup>, k<sub>SB</sub>=0.28 hr<sup>-1</sup>, k<sub>e</sub>= 0.30 hr<sup>-1</sup>, F<sub>u</sub>=0.81. .... 238

**CHAPITRE 7 : ARTICLE 5, MÉTHYLMERCURE**

- Figure 1. Model simulations of the time-profiles of total mercury concentration in blood (—) and in the 1<sup>st</sup> centimeter of hair closest to the root (----) following ingestion of a once a week intake of 1 µg of methylmercury/kg of body weight: 3-months exposure (A) and 14-months exposure (B). .... 279
- Figure 2. (i) Historical reconstruction of daily intakes of methylmercury (µg/kg of body weight) prior to the hair collection at time 0 (—) from model simulation (----) of the measured data (□) on mercury concentration in successive centimeters of hair (µg/g) in 4 women from the Inuvik cohort (Walker *et al.*, 2002). (ii) Simulated time-profile (·-·-·) of total mercury concentration in blood (µg/l) from the reconstructed intake compared to measured data (×)..... 279

- Figure 3. Comparison between measured and simulated total mercury concentration in blood ( $\mu\text{g/l}$ ) for the 16 women from the Inuvik cohort with mercury levels in the proximal cm of hair above the detection limit (Walker et al., 2002). The simulated value for each woman was obtained using the model of Carrier et al. (2001) in combination with their measured time-profile of total mercury concentration in hair. The line (—) represents the linear equation  $y=x$ . .....279
- Figure 4. (i) Historical reconstruction of daily intake of methylmercury ( $\mu\text{g/kg}$  of body weight) prior to the hair collection at time 0 (—) from model simulation (----) of the measured data ( $\square$ ) on mercury concentration in successive centimeters of hair ( $\mu\text{g/g}$ ) in 2 natives from the Amazon cohort (Lebel et al., 1998; Dolbec et al., 2001). .....280

**LISTE DES ABRÉVIATIONS ET DES SIGLES**

3,5,6-TCP : 3,5,6-trichloro-2-pyridinol

ACGIH<sup>®</sup> : American Conference of Governmental Industrial Hygienists

AChE : acetylcholinesterase

AP : alkyl phosphates

BAT : Biological Tolerance Value

BEI<sup>®</sup> : Biological Exposure Indice

BRVs : Biological Reference Values

bw : body weight

ChE : cholinesterase

CPF : chlorpyrifos

DCA : di-carboxylic acids

DEP : diethylphosphoric acid

DETP : diethylphosphorothioic acid

DMDTP : dimethyl dithiophosphate

DMENO : dose minimale avec un effet nocif observé

DMP : dimethyl phosphate

DMTP : dimethyl thiophosphate

DSEO : dose sans effet observé

DSENO : dose sans effet nocif observé

FAO : Food and Agriculture Organization of the United Nations

GC/MS : capillary gas chromatography/mass spectrometry

GCIHH : German Commission for the Investigation of Health Hazards of Chemical Compounds in the Work Area

INSPQ : Institut National de Santé Publique du Québec

IRSST : Institut de Recherche Robert-Sauvé en Santé et Sécurité du Travail

iv : intravenous

LC-ESI-MS : liquid chromatography-electrospray ionization-mass spectrometry

LOEL : lowest observed effect level

MCA : mono-carboxylic acids

MCK : modèle cinétique classique à multi-compartiment  
MeHg : méthylmercure  
MW : poids moléculaire  
NIOSH<sup>®</sup> : National Institute for Occupational Safety and Health  
NOEL : no observed effect level  
OP : organophosphoré  
PBPK : modèle cinétique à base physiologique  
PCDD : polychloro-dibenzo-p-dioxines  
PCDF : polychloro-dibenzofurannes  
*p*-NP : *p*-nitrophenol  
QSSA : quasi steady state approximations  
RBC : red blood cells  
RBC-AChE : cholinesterase activity in red blood cells  
RfD : reference dose  
TLV<sup>®</sup> : Threshold Limit Values  
TLV-TWA<sup>®</sup> : time-weighted average threshold limit value  
USEPA : United States Environmental Protection Agency  
VLE : valeur limites d'exposition  
WHO : World Health Organization

## LES REMERCIEMENTS

Je remercie mes deux directeurs, Gaétan Carrier et Robert Brunet, qui m'ont soutenue tout au long de la grande aventure qu'a été mon doctorat. Je suis bien heureuse qu'ils m'aient donné, il y a plus de 3 ans, leur confiance afin que je puisse poursuivre à leurs côtés des études dans le domaine de l'analyse des risques toxicologiques. Leur assiduité constante lors de mes travaux de recherche et, surtout, lors de la rédaction de la présente thèse m'a encouragée à mener ce travail à terme.

Je tiens à remercier les autres co-auteurs des articles de ma thèse pour leur excellent travail d'équipe. Je désire particulièrement souligner le support, autant intellectuel qu'amical, de Michèle Bouchard tout au long de mon doctorat.

Je remercie aussi l'Institut de recherche Robert-Sauvé en santé et en sécurité au travail d'avoir cru en mon potentiel de chercheuse et d'avoir financé les deux dernières années de mon doctorat.

Je désire exprimer ma gratitude à mes parents qui m'ont, depuis toujours, encouragée à persévérer à l'atteinte de mes objectifs. Plusieurs remerciements doivent être offerts à mon amoureux, Guillaume Rouleau, pour m'avoir si bien supportée et encouragée à chaque étape du doctorat. Finalement, je gratifie Éliane Rouleau, ma fille d'un an et demi, pour, d'une part, m'avoir donné une belle grossesse et, d'autre part, d'avoir été pendant sa première année de vie un bébé exemplaire pour toutes les mères aux études.

## **CHAPITRE 1 : INTRODUCTION**

## ***PROBLÉMATIQUE***

Notre environnement est contaminé par une multitude de substances toxiques, résultat d'activités humaines: production de biens, transport, chauffage, élimination et récupération de déchets industriels et domestiques ainsi que les activités agricole, horticole et forestière. Cette contamination atteint tous les milieux avec lesquels les êtres vivants sont en contact (air, eau, sol, nourriture) et, conséquemment, l'être humain lui-même est atteint. Les travailleurs qui manipulent des substances toxiques sont généralement les plus susceptibles d'être exposés à ces produits, mais personne n'y échappe. Il existe malheureusement des situations, accidentelles ou non, lors desquelles les êtres humains absorbent des quantités de substances toxiques à des niveaux qui induisent des problèmes de santé. Afin de prévenir ces problèmes, les organismes gouvernementaux doivent établir des moyens d'identification, d'évaluation et de gestion des risques tant à l'égard de l'environnement qu'à l'égard des êtres vivants.

Pour répondre à cette préoccupation, la communauté scientifique consacre de plus en plus d'efforts au développement de différentes approches méthodologiques pour l'analyse des risques toxicologiques pour la santé humaine. Cette analyse se définit comme étant la somme des processus qui permettent de déterminer la probabilité que des effets indésirables sur la santé se produisent à la suite d'une exposition donnée. L'analyse des risques comprend, entre autres, deux volets complémentaires : l'évaluation de l'exposition et l'évaluation de la réponse toxique des êtres humains à cette exposition. Pour être utiles, il importe donc que les méthodes utilisées pour ces

évaluations soient les plus précises, car une mauvaise évaluation peut entraîner des conséquences néfastes pour la société en général. Une bonne analyse des risques reliés à une substance toxique ou à une famille de substances toxiques doit aussi s'appliquer à n'importe quelle condition d'exposition en situation réelle.

En matière d'évaluation de l'exposition, le défi est d'estimer avec suffisamment de précision les quantités de substances absorbées par les personnes exposées en tenant compte de toutes les voies d'entrée dans l'organisme et de tous les types d'exposition. Bien qu'idéalement, la part de la quantité absorbée attribuable à une source spécifique par rapport à l'ensemble des sources d'exposition devrait être déterminée, c'est souvent l'exposition interne totale qui est estimée lors d'une analyse des risques toxicologiques. Il est bon de rappeler que, dans le jargon des toxicologues, la quantité absorbée est souvent appelée dose absorbée ou exposition interne. Dans la présente étude, les outils concernant l'évaluation de l'exposition sont développés pour la détermination de la dose absorbée totale.

Pour évaluer la dose absorbée totale des personnes à des substances toxiques, deux procédures de surveillance sont souvent employées. La première, appelée évaluation environnementale, estime l'exposition interne de façon indirecte en deux temps : 1) par la mesure de la contamination dans les échantillons collectés dans les divers milieux (air, eau, sol, nourriture) et 2) par l'estimation de l'exposition de ces individus à ces milieux et du degré d'absorption des quantités de substances avec lesquelles ils sont en contact lors de leur présence dans ces milieux. La seconde procédure, appelée

surveillance biologique, est plus directe puisqu'elle estime les doses absorbées au moyen de mesures de cette contamination dans des échantillons biologiques (p.ex., sang, urine, cheveux) prélevés directement chez les personnes en contact avec la substance à l'étude.

Pour estimer l'exposition des personnes à l'étude sur la base de mesures environnementales, il faut recueillir une quantité importante d'échantillons individuels afin d'assurer une représentation fidèle de l'exposition réelle. Cette représentation se réalise à l'aide d'analyses statistiques des données recueillies. Par exemple, pour effectuer l'évaluation de l'exposition d'un travailleur exposé par inhalation ou par voie cutanée à une substance quelconque, la fréquence et la durée de l'échantillonnage doivent être adéquates. Les données recueillies doivent en fait tenir compte du temps passé dans un site donné par le travailleur, de sa mobilité dans les lieux fréquentés, des différentes tâches effectuées par ce travailleur, de la fréquence de ces tâches, de la variation des émissions de polluants d'une tâche à l'autre, de la variation des concentrations dans le milieu au cours d'une même journée, d'une journée à l'autre et d'une saison à l'autre. Aux nombreux facteurs de variabilité décrits ci-dessus s'ajoutent la variation des mesures de protection prises par les individus et la variation du degré d'absorption d'un individu à l'autre. Devant tous ces paramètres impliqués dans l'estimation de l'exposition interne, il apparaît donc difficile d'estimer avec précision les doses absorbées par les individus exposés en utilisant uniquement l'échantillonnage environnemental.

En revanche, l'évaluation biologique de l'exposition interne évite les considérants environnementaux et les facteurs d'absorption. Elle vise la reconstruction, à postériori, de la dose absorbée à partir de mesures effectuées dans des matrices biologiques appropriées telles que l'urine, les cheveux, le sang ou l'air exhalé. Les niveaux de biomarqueurs sont en fait les quantités mesurées du contaminant lui-même (substance-mère) ou d'une ou des substances dérivées des processus de biotransformation (métabolites) présents dans les échantillons biologiques.

La caractérisation du risque par l'une ou l'autre de ces deux procédures de surveillance s'établit en comparant les doses absorbées avec des données sur la relation « dose absorbée-réponse toxique chez l'humain ». En général, compte tenu que le but recherché est de prévenir tout risque, on cherche à connaître les niveaux d'exposition en-dessous desquels des effets toxiques n'ont jamais été constatés chez l'humain. Ces niveaux permmissibles se définissent à l'aide des doses DSENO (dose sans effet nocif observé) ou DMENO (dose minimale avec un effet nocif observé). De ces doses résultent des valeurs de référence qui sont, pour la plupart, déterminées en divisant la DSENO ou la DMENO par des facteurs de sécurité. En principe, ces valeurs de référence ainsi calculées assurent la protection de tout le monde, même les plus susceptibles. Conséquemment, en comparant la dose absorbée par un individu avec la valeur de référence spécifique à une substance, on possède un outil de surveillance utile pour prévenir les risques de développer des effets nuisibles sur la santé humaine.

Les valeurs de référence basées sur l'absence d'effets s'appliquent généralement aux doses visant la prévention d'effets non cancérigènes. Quand une substance est considérée posséder un potentiel cancérigène, il y a absence de consensus dans la communauté scientifique sur l'existence d'un seuil sans effet. Les limites admissibles d'exposition sont souvent établies, principalement en Amérique, à un niveau représentant un excès de risque jugé socialement acceptable. Cependant, puisque la détermination de ces limites dépend de nombreux facteurs autres que scientifiques, une discussion sur la caractérisation du risque pour les effets cancérigènes dépasse largement le cadre de ce travail.

Au Québec, les valeurs limites admissibles font généralement référence à des évaluations environnementales. Le Ministère de l'environnement établit les normes pour la contamination de l'air, l'eau et les sols (L.R.Q., c. Q-2), le Ministère de l'agriculture, pêcheries et alimentation détermine celles de la contamination des aliments (L.R.Q., c., P-29), alors que la Commission de la santé et de la sécurité du travail (RQMT, 2001) établit les normes pour le milieu de travail. Pour ce dernier milieu, à quelques exceptions près, les valeurs de référence sont exprimées en concentrations mesurées dans l'air ambiant.

## **OBJECTIFS**

### ***Objectif principal***

Les objectifs principaux de cette recherche sont de développer des outils de surveillance biologique pour cinq contaminants, le méthylmercure (MeHg) et quatre pesticides (parathion, malathion, chlorpyrifos et triclopyr), et de proposer pour chacun une procédure pour déterminer ou utiliser adéquatement des valeurs de référence dans le cadre de programmes d'évaluation et de prévention des risques pour la santé humaine. Ces outils doivent être facilement applicables en situations réelles et être plus précis que ceux déjà existants pour estimer l'exposition humaine à ces substances, autant chez les travailleurs que chez la population générale.

### ***Objectif secondaire***

L'objectif secondaire de cette recherche est d'appliquer ces outils pour étudier l'exposition et les risques en situations réelles. Les applications portent sur l'exposition de travailleurs exposés au malathion et au triclopyr alors que pour le méthylmercure, il porte sur l'exposition de populations autochtones du Canada et du Brésil.

## **STRUCTURE DE LA THÈSE**

Dans ce qui suit, une description sommaire des chapitres de la présente thèse est offerte en fonction des objectifs spécifiques à atteindre pour chaque substance ciblée.

### ***Chapitre 2 : Généralités sur la surveillance biologique***

Dans ce chapitre est présentée une brève discussion sur les caractéristiques d'une étude de surveillance biologique, sur différentes stratégies pour évaluer la dose absorbée et pour déterminer les valeurs repères ainsi que sur les approches de modélisation cinétique. Ce chapitre permet de mieux cerner les enjeux, les mérites et les exigences d'une analyse de risques toxicologiques basée sur des mesures biologiques.

### ***Chapitre 3, 4 et 5 : Pesticides de type organophosphoré (ARTICLES 1, 2 et 3)***

Ces trois chapitres présentent le développement d'outils d'évaluation biologique d'exposition et les propositions de valeurs de référence des marqueurs biologiques utilisés pour trois pesticides organophosphorés : le parathion, le malathion et le chlorpyrifos. Pour ce faire, un modèle cinétique chez l'humain a dû être développé pour chaque organophosphoré à partir de profils temporels, présentés dans la littérature, de la substance-mère et de ses métabolites dans le sang et l'urine collectés chez des humains. Ces modèles permettent d'établir des liens entre la dose absorbée, les charges corporelles et les niveaux de biomarqueurs et ce, pour tous scénarios d'exposition et d'échantillonnage probables. Ensuite, pour chaque substance, le modèle cinétique a été utilisé pour déterminer des valeurs de référence biologiques en milieu de travail sous forme de biomarqueurs urinaires accumulés lors d'une période d'échantillonnage déterminée. Ces valeurs se basent sur les relations entre les quantités absorbées de l'insecticide et l'inhibition des acétylcholinestérases dans le sang; ces

relations « dose absorbée-réponse toxique», établies à partir d'expériences chez des humains, sont aussi tirées de la littérature scientifique.

#### ***Chapitre 6 : Pesticide de type pyridine (ARTICLE 4)***

Pour le triclopyr, herbicide de la famille des pyridines, il existait déjà dans la littérature un modèle cinétique développé à partir d'une étude expérimentale chez l'humain (Carmichael et coll., 1989). Dans le présent ouvrage, ce modèle a été adapté pour travailler avec des charges plutôt que des concentrations dans le but de reconstruire la charge corporelle et les quantités de triclopyr absorbées à partir de la mesure du biomarqueur accumulé dans l'urine. Ce modèle a aussi été modifié afin de permettre cette reconstruction lors de divers scénarios d'exposition. Une fois adapté, ce modèle a été utilisé pour quantifier la dose absorbée afin d'estimer le risque de dépassement d'une dose de référence chez dix travailleurs québécois qui appliquaient du triclopyr sur la végétation sous des lignes de haute tension.

#### ***Chapitre 7 : Méthylmercure (ARTICLE 5)***

Un modèle de la cinétique du MeHg chez l'humain avait déjà été publié (Carrier et coll., 2001). Ce modèle possède déjà les attributs nécessaires pour une reconstruction des profils temporels de charges et de concentrations de mercure organique et inorganique dans le corps, le sang et autres tissus sur la base des concentrations de mercure total mesurées dans les segments consécutifs coupés dans les mèches de cheveux. La contribution originale dans le cadre de cette thèse a principalement consisté à développer des moyens pour reconstruire l'historique des taux d'exposition

par ajustements statistiques des projections du modèle aux concentrations de mercure observées dans les cheveux. Ce travail a été réalisé à partir de données déjà publiées sur les concentrations de mercure total mesurées dans les mèches de cheveux provenant de populations autochtones du Canada et du Brésil (Lebel et coll., 1996, 1998 ; Dolbec et coll., 2000 ; Walker et coll., 2002). L'apport en MeHg ainsi reconstruit a permis d'estimer l'évolution du risque pour la santé en comparaison avec les apports recommandés par Santé Canada. Ce travail a également permis de proposer des stratégies concernant les collectes des matrices biologiques (cheveux et sang) selon le type d'exposition des individus échantillonnés.

### ***Chapitre 8 : Conclusion générale***

Dans ce chapitre sont énoncées les conclusions des résultats de cette thèse ainsi que leurs principales contributions pour le domaine de la surveillance biologique.

**CHAPITRE 2 : GÉNÉRALITÉS SUR LA SURVEILLANCE  
BIOLOGIQUE**

Ce chapitre présente une synthèse de connaissances sur la problématique d'utilisation des biomarqueurs pour l'évaluation des risques associés à l'exposition des êtres humains aux substances toxiques. Une analyse critique de ces connaissances est réalisée dans le but de dégager les principaux concepts à la base des différentes approches mises en œuvre pour atteindre les objectifs de la présente recherche.

### ***LES CONDITIONS D'UTILISATION DE LA SURVEILLANCE BIOLOGIQUE***

Il faut d'emblée préciser que la surveillance biologique n'est pas applicable à tous les contaminants environnementaux ; il est nécessaire d'avoir accès à des mesures biologiques qui permettront une reconstruction fiable de la dose absorbée. C'est le devenir de la substance absorbée dans la circulation sanguine qui dicte quel est le meilleur biomarqueur d'exposition à retenir lors d'une étude d'analyse des risques. En effet, connaître les métabolites potentiels de la substance-mère, les tissus dans lesquels la substance-mère et les métabolites sont plausiblement stockés de même que connaître leurs principales voies d'élimination aident à déterminer, d'une part, la molécule à mesurer et, d'autre part, la matrice biologique où seront faits les prélèvements. De plus, la connaissance de la cinétique du contaminant est essentielle pour établir des liens quantitatifs entre la dose absorbée et son taux d'absorption, d'élimination ou de stockage. Ces liens permettent particulièrement de choisir l'horaire idéal pour effectuer les prélèvements dans la matrice biologique retenue.

## ***LES CARACTÉRISTIQUES D'UN BON BIOMARQUEUR D'EXPOSITION***

Un bon biomarqueur d'exposition doit satisfaire un certain nombre de critères : 1) être le plus spécifique possible au contaminant étudié, 2) permettre sa mesure par une méthode analytique fiable et peu dispendieuse, 3) être facilement accessible et 4) fournir des mesures suffisamment sensibles pour permettre une détection de l'exposition bien inférieure au niveau pour lequel des effets toxiques apparaissent chez les plus sensibles. De plus, il faut que la molécule quantifiée soit assez stable dans la matrice échantillonnée pour permettre des mesures reproductibles.

## ***LES VALEURS DE RÉFÉRENCE***

### ***American Conference of Governmental Industrial Hygienists (ACGIH<sup>®</sup>)***

Au Canada, pour les milieux de travail, les recommandations sur les niveaux d'exposition à ne pas dépasser sont principalement celles proposées par l'American Conference of Governmental Industrial Hygienists (ACGIH<sup>®</sup>). L'ACGIH<sup>®</sup> est un organisme sans but lucratif créé il y a plus de 60 ans qui joue aujourd'hui un rôle primordial à travers le monde dans la prévention des maladies professionnelles. Une de ses missions est l'établissement de valeurs limites d'exposition (VLE) à des agents toxiques pour assurer la protection des travailleurs de l'industrie. Cet organisme produit un guide contenant des valeurs seuils de concentrations de contaminants en milieu ambiant (Threshold Limit Values : TLV<sup>®</sup>) et, lorsque possible, des indices biologiques d'exposition (Biological Exposure Indices : BEIs<sup>®</sup>). S'appuyant sur la

littérature scientifique, des spécialistes voient à la mise à jour des connaissances et à la révision périodique de ces valeurs guides. Cette agence américaine proposait, en 2003, des indices biologiques d'exposition (BEI<sup>®</sup>) pour 39 substances ou groupes de substances (ACGIH, 2003). Ces indices identifient les niveaux de biomarqueurs en deçà desquels les travailleurs ne devraient pas subir d'effets délétères pour leur santé.

Les BEI<sup>®</sup> sont généralement établis en considérant que l'exposition se fait exclusivement par inhalation. Les valeurs ainsi proposées sont déterminées en utilisant rarement des modèles cinétiques qui simulent une exposition pendant une semaine de 5 journées de travail de 8 heures à une concentration de la substance dans l'air ambiant équivalente à la valeur limite d'exposition moyenne pondérée sur huit heures (TLV-TWA<sup>®</sup>) (ACGIH, 2003). Toutefois, de tels liens entre les TLV-TWA<sup>®</sup> et les BEI<sup>®</sup> ne sont pas valables pour les contaminants dont la TLV-TWA<sup>®</sup> protège le travailleur contre des effets locaux (p.ex., irritation des yeux et de la gorge) ou pour ceux dont la principale voie d'absorption est autre que les voies respiratoires (ACGIH, 2003). Dans ces cas, les valeurs des BEI<sup>®</sup> sont déterminées à partir du lien direct entre l'apparition d'effets néfastes sur la santé et les niveaux de biomarqueurs mesurés chez des individus exposés sous des conditions professionnelles. Les BEI<sup>®</sup> du plomb, du cadmium et du parathion ont été établis à partir de tels liens directs. Il faut de plus mentionner que l'ACGIH<sup>®</sup> propose un BEI<sup>®</sup> sur la base d'un biomarqueur d'effets mesurables suite à l'exposition aux pesticides des familles des organophosphorés et des carbamates. Ce BEI<sup>®</sup> correspond à un niveau d'inhibition de 30% de l'activité normale de l'acétylcholinestérase érythrocytaire. Pour se servir de cette approche, il est alors

nécessaire de faire au moins deux prélèvements sanguins, soit avant et après la période d'application de la substance étudiée.

Les BEI<sup>®</sup> urinaires proposés par cet organisme sont basés sur la concentration de la substance-mère ou ses métabolites mesurée dans l'urine d'une seule miction collectée à un moment donné (ACGIH, 2003). Le moment approprié pour recueillir celle-ci est mentionné pour chaque BEI<sup>®</sup>; selon les caractéristiques cinétiques de la substance à l'étude, la miction doit être échantillonnée au commencement, pendant ou à la fin du quart de travail. Lorsque la molécule à mesurer est principalement éliminée par filtration glomérulaire, la concentration du biomarqueur dans l'échantillon est ajustée en fonction de la quantité de créatinine qui y est mesurée. Selon l'ACGIH<sup>®</sup>, cet ajustement permet d'obtenir une concentration indépendante du débit urinaire, jugé très variable en comparaison de l'excrétion de la créatinine, et permet ainsi d'obtenir un meilleur lien entre les mesures de biomarqueurs et les niveaux d'exposition (ACGIH, 2003). Par contre, plusieurs études expérimentales chez les humains rapportent d'importantes variations quant à l'excrétion de la créatinine. En effet, son taux d'excrétion varie beaucoup d'un sujet à l'autre (0,5 – 3 g/jour), sans compter que ce taux chez un même individu est sujet à des variations inter-journalières (63 – 244%) et intra-journalières ( $\geq 200\%$ ) (Curtis et Fogel, 1970; Greenblatt et coll., 1976; Alesio et coll., 1985; Boeniger et coll., 1993). Ces variations, combinées avec l'incertitude et la variabilité inhérentes à la cinétique des substances, contribuent à réduire la fiabilité des estimations de l'exposition interne obtenues à partir d'un seul échantillon urinaire.

### *Proposition d'une nouvelle approche*

Une approche différente de celle préconisée par l'ACGIH<sup>®</sup> a été proposée par Carrier et Brunet (1999) dans le but de déterminer des valeurs de référence biologiques visant la prévention d'effets toxiques chez les humains exposés à l'azinphosméthyle, un pesticide de la famille des organophosphorés. La démarche proposée par ces auteurs s'est faite en deux étapes: 1) le développement d'un modèle mathématique de la cinétique de cette substance et de ses métabolites chez l'humain capable, entre autres, de reconstruire la dose absorbée et l'évolution des charges dans le corps à partir de mesures des biomarqueurs appropriés dans l'urine et 2) la mise à profit des travaux d'autres chercheurs ayant réalisé des études de toxicité chez l'humain. Cette approche a permis de définir pour l'azinphosméthyle les relations entre la dose absorbée, les niveaux de biomarqueurs et le risque de développer des effets nuisibles sur la santé humaine (voir Figure 1) et ce, pour tout scénario d'exposition probable. C'est sur la base de ces relations que Carrier et Brunet (1999) ont déterminé des niveaux de biomarqueurs en deçà desquels on évite l'apparition d'effets toxiques.

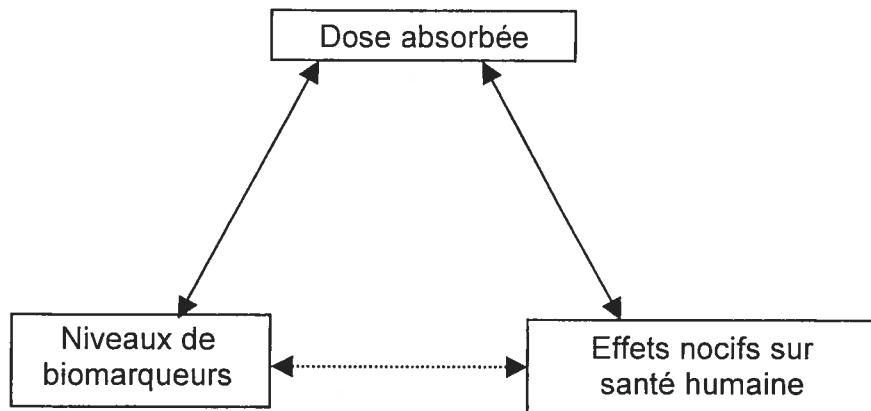


Figure 1. Schéma général des relations entre la dose absorbée dans l'organisme, les biomarqueurs et les effets nocifs sur la santé humaine.

Cette démarche se distingue de l'approche de l'ACGIH<sup>®</sup> par l'utilisation du modèle cinétique ainsi que par le choix de la période de collecte urinaire. D'une part, l'ACGIH<sup>®</sup> utilise les modèles cinétiques principalement pour établir les liens entre l'exposition externe à la TLV-TWA<sup>®</sup> et les niveaux de biomarqueurs (ACGIH, 2003) alors que l'approche de Carrier et Brunet (1999) a été utilisée pour déduire la relation entre niveaux de biomarqueurs et effets nocifs telle que présentée à la Figure 1. En fait, le modèle de Carrier et Brunet (1999) sert à reconstruire les doses absorbées à partir des niveaux de biomarqueurs urinaires accumulés durant une certaine période prédéfinie ainsi qu'à estimer les niveaux de biomarqueurs correspondant à la dose sans effet nocif (DSENO) absorbée sous des conditions d'exposition habituellement vécues en milieu professionnel. Ayant constaté que, sur le plan cinétique, l'estimation de l'exposition à partir d'une seule mesure du biomarqueur était très peu précise, la reconstruction de la dose absorbée avec une précision acceptable est, selon eux, possible seulement sur la base des biomarqueurs urinaires accumulés sur une période

relativement longue. Ainsi, au lieu de collecter une seule miction à un temps spécifié et d'y mesurer la concentration de biomarqueurs, normalisée ou non sur la créatinine, tel que proposé par l'ACGIH<sup>®</sup>, Carrier et Brunet (1999) suggèrent pour l'azinhosphométhyle d'effectuer une collecte urinaire pendant 24 heures consécutives depuis le début d'une journée d'exposition et d'y mesurer la quantité totale des biomarqueurs excrétée sur cette période. Cette stratégie de collecte n'est plus ainsi soumise à l'influence du débit urinaire ou de l'excrétion de la créatinine lors de la reconstruction de l'exposition interne à partir des niveaux de biomarqueurs urinaires.

Avec leur approche, les valeurs de référence de biomarqueurs correspondant aux doses jugées sécuritaires ont été déterminées selon l'hypothèse que l'absorption se fait uniquement par la peau, voie d'absorption la plus importante chez les travailleurs exposés aux pesticides (Temple et Smith, 1996). En effet, une analyse par simulations des paramètres du modèle cinétique a montré que l'absorption par la peau donne des valeurs de référence biologiques plus conservatrices que par les autres voies d'entrée. L'application de ces valeurs en vue de prévenir les risques assure ainsi une bonne protection des personnes exposées, quelque soit la voie d'absorption de ces substances.

### ***LA MODÉLISATION CINÉTIQUE***

La cinétique des substances chimiques dans un organisme vivant est modélisée par une ou l'autre de deux approches compartimentales : soit les modèles classiques à multi-

compartiments (MCK), soit les modèles à base physiologique (PBPK). Pour simuler la cinétique des substances, ces deux approches reposent sur la mise au point de systèmes d'équations différentielles qui assurent la conservation des masses. Ce principe, sur lequel repose théoriquement les modèles MCK et PBPK, respecte une règle d'or en physico-chimie : après l'exposition, la dose absorbée est égale (en moles) à la somme des charges de la substance-mère biodisponibles dans les organes ou tissus d'absorption (poumons, tube digestif, peau) plus les charges absorbées de la substance-mère et de tous ses métabolites contenues dans l'organisme ainsi qu'accumulées dans les excréta (urine, fèces, air expiré, sueur). Dans ces deux types de modèles, ces charges sont représentées par des compartiments représentant des organes ou regroupement d'organes et tissus. À chaque compartiment est associée une équation différentielle qui décrit la différence, par unité de temps, entre les quantités entrantes de la substance-mère ou des métabolites et les quantités sortantes.

Les divergences entre les approches de modélisation MCK et PBPK reposent sur la manière de construire les modèles (représentation des organes ou regroupement d'organes et unités des paramètres) et sur la manière de déterminer les paramètres impliqués dans le modèle (Leung, 1991 ; Gosselin, 2001 ; Dixit et coll., 2003). Dans les modèles PBPK, les paramètres impliqués représentent, entre autres, des caractéristiques physiologiques (p.ex., le débit sanguin et le volume des organes et tissus) de même que des caractéristiques biochimiques (p.ex., le coefficient de partition). Les valeurs de ces derniers paramètres sont souvent déterminées à l'aide d'expériences *in vitro* (sur des cellules ou tissus) ou *in vivo* chez l'animal et, ensuite,

extrapolées à des valeurs correspondantes chez l'humain. Par ailleurs, avec les modèles MCK, les valeurs des paramètres sont déterminées par ajustement optimal entre les profils temporels simulés par le modèle et ceux observés directement chez l'humain. Les profils de la substance-mère et/ou de ses métabolites mesurés dans le sang et dans les excréta (urine, fèces, air exhalé) sont obtenus expérimentalement ou en clinique.

En cinétique, il importe que les modèles utilisés représentent les principaux facteurs gouvernant la cinétique de la substance-mère et de ses métabolites dans l'organisme et surtout, que le modèle permette de répondre à l'objectif visé. Ainsi, si on veut reconstruire la charge corporelle ou la dose absorbée à partir de mesures sur un ou des métabolites d'une substance à laquelle on est exposé, il est primordial que le modèle intègre aussi la cinétique de ces métabolites. C'est même essentiel pour garantir la conservation des masses du système en tout temps. Notre analyse de la littérature nous amène à constater qu'il est très rare qu'un modèle de type PBPK intègre la cinétique de la substance-mère et celle de ses métabolites. En effet, ces modèles considèrent la cinétique de biotransformation de la substance en ses métabolites (généralement au niveau du foie) comme moyen d'élimination sans toutefois décrire la cinétique de ces métabolites. En théorie, l'intégration de cette cinétique dans les modèles PBPK est possible, mais difficile à cause de la nécessité de déterminer les paramètres des métabolites impliqués pour établir leur distribution dans l'ensemble des compartiments classiques des PBPK (i.e., sang artériel et veineux, regroupement de tissus faiblement perfusés et hautement perfusés, foie, tissus adipeux).

L'équipe de la Chaire en analyse des risques toxicologiques pour la santé humaine de l'Université de Montréal a développé des modèles qui permettent l'intégration des principaux facteurs cinétiques avec une approche modifiée des MCK. Les modèles MCK suivants ont été développés principalement pour satisfaire les besoins d'une étude de surveillance biologique: polychloro-dibenzo-p-dioxines et polychloro-dibenzofurannes (PCDD/PCDF) (Carrier et coll., 1995), azinphosméthyle (Carrier et Brunet, 1999), MeHg (Carrier et coll., 2001) et méthanol (Bouchard et coll., 2001). Ce qui distingue ces modèles de la plupart des modèles MCK classiques tient à son insistance d'assurer la conservation des masses molaires; dans ce but, les compartiments de ces modèles représentent une charge et non une concentration. Ceci favorise l'établissement des liens entre les quantités de biomarqueurs accumulées dans les excréta, les charges corporelles et la dose totale absorbée. De plus, ces modèles ont été développés à partir de données expérimentales chez l'humain tirées de différentes expériences ou différents cas cliniques rapportés dans la littérature. Cet éventail de données a donc permis de valider ces modèles pour diverses voies d'entrées, périodes d'exposition et quantités absorbées. Ainsi, une fois les valeurs paramétriques validées chez l'humain, ces modèles ont la capacité d'estimer l'évolution dans le temps des niveaux de biomarqueurs suite à différents scénarios d'exposition (unique, répété, chronique, intermittent; cutanée, orale et pulmonaire). Ces estimations se font simplement en variant les taux d'entrée de la substance lors de la résolution des systèmes d'équations différentielles.

Notre analyse mathématique des modèles cinétiques nous amène à constater que l'approche de modélisation MCK tire avantage des différences entre les échelles de temps des processus cinétiques de la substance et de ses métabolites pour faire des regroupements de tissus. C'est effectivement à cause de ces différences d'échelle de temps qu'il existe souvent un équilibre dynamique entre les quantités de la substance-mère et/ou de ses métabolites mesurées dans le sang et celles mesurées dans certains fluides corporels, tissus et organes. Cet état de quasi-équilibre amène l'apparition rapide d'un rapport constant entre des quantités variables dans le temps; ce qui permet alors le regroupement de ces quantités dans un même compartiment (Segel, 1988; Segel et Slemrod, 1989) et ainsi une simplification du modèle sans fausser la cinétique générale.

Les modèles cinétiques développés dans cette thèse sont basés sur les principes de modélisation proposés dans le cadre des travaux de la Chaire en analyse des risques toxicologiques pour la santé humaine. Cette approche a été retenue principalement à cause de l'accessibilité à de nombreuses données dans la littérature sur les profils temporels des substances-mères et de leurs métabolites mesurés dans le sang et l'urine collectés chez des humains.

**CHAPITRE 3 : ARTICLE 1, MALATHION**

Cet article a été publié en 2003 dans *Toxicological Sciences* 73, pages 182-194.

**A Toxicokinetic Model of Malathion and Its Metabolites as a Tool to  
Assess Human Exposure and Risk through Measurements of Urinary  
Biomarkers**

Michèle Bouchard\*, Nathalie H. Gosselin\*, Robert C. Brunet†, Onil Samuel‡, Marie-  
Josée Dumoulin\* and Gaétan Carrier\*

\* Chaire en analyse des risques toxicologiques pour l'humain and Département de  
santé environnementale et santé au travail, Faculté de Médecine, Université de  
Montréal, C.P. 6128, Succursale Centre-ville, Montréal, Québec, Canada, H3C 3J7

† Département de Mathématiques et de Statistique and Centre de Recherches  
Mathématiques, Faculté des arts et des sciences, Université de Montréal, C.P. 6128,  
Succursale Centre-ville, Montréal, Québec, Canada, H3C 3J7

‡ Institut national de santé publique du Québec. Direction de la toxicologie humaine.  
Centre de toxicologie, 945 avenue Wolfe, Ste-Foy, Québec, Canada, G1V 5B3

Running title: Malathion Kinetics and Risk Assessment

Offprint requests: Gaétan Carrier  
Département de Santé environnementale et santé au travail  
Université de Montréal  
C.P. 6128, Succursale Centre-ville, Montréal, Québec  
H3C 3J7, CANADA  
Telephone number: (514) 343-6111 ext 3108  
Fax number: (514) 343-2200  
E-mail: [gaetan.carrier@umontreal.ca](mailto:gaetan.carrier@umontreal.ca)

## ***ABSTRACT***

A toxicokinetic model is proposed to predict the time evolution of malathion and its metabolites, mono- and di-carboxylic acids (MCA, DCA) and phosphoric derivatives (dimethyl dithiophosphate (DMDTP), dimethyl thiophosphate (DMTP) and dimethyl phosphate (DMP)), in the human body and excreta, under a variety of exposure routes and scenarios. The biological determinants of the kinetics were established from published data on the in vivo time profiles of malathion and its metabolites in the blood and urine of human volunteers exposed by intravenous, oral and dermal routes. In the model, body and excreta compartments were used to represent the time varying amounts of each of the following: malathion, MCA, DCA, DMDTP, DMTP and DMP. The dynamic of inter-compartment exchanges was described mathematically by a differential equation system that ensures conservation of mass at all times. The model parameters were determined by adjusting statistically the explicit solution of the differential equations to the experimental human data. Simulations provide a close approximation to kinetic data available in the published literature. When simulating a dermal exposure to malathion, the main route-of-entry for workers, the model predicts that it takes on average 11.8 h to recover half of the absorbed dose of malathion eventually excreted in urine as metabolites compared to 3.2 h following an intravenous injection and 4.0 h after oral administration. This shows that, following a dermal exposure, the absorption rate governs the urinary excretion rate of malathion metabolites, because the dermal absorption rate is much slower than biotransformation and renal clearance processes. The model served to establish biological reference

values for malathion metabolites in urine since it allows links to be made between the absorbed dose of malathion and the time course of cumulative amounts of metabolites excreted in urine. From the “no observed effect level” (NOEL) of  $0.61 \mu\text{mol/kg/day}$  derived from the data of Moeller and Rider (1962), the model predicts corresponding biological reference values for MCA, DCA and phosphoric derivatives of 44, 13 and 62 nmol/kg, respectively, in 24-h urine samples. The latter were used to assess the health risk of workers exposed to malathion in botanical greenhouses starting from urinary measurements of MCA and DCA metabolites.

**Key Words:** malathion; mono-carboxylic acids; di-carboxylic acids; phosphoric derivatives; toxicokinetics; risk assessment.

## ***INTRODUCTION***

Malathion (O,O-dimethyl S-1,2-di(ethoxycarbonyl)ethyl phosphorodithioate) is an organophosphate (OP) insecticide widely used in agriculture and residential settings as well as in public health programs for mosquito-borne disease control (Environnement Québec, 2002; U.S. EPA, 2000). It is also used in some countries for the treatment of head lice (Roberts, 2002). Like other OP insecticides, malathion exerts its neurotoxic action in humans, as in insects, through cholinesterase (ChE) inhibition. This results in the accumulation of acetylcholine within synapses leading to over-stimulation of postsynaptic receptors (Liu and Pope, 1998). In acutely exposed individuals, clinical signs of OP intoxication usually appear at inhibition of 60-70% of acetylcholinesterase (AChE) activity in red blood cells (RBC). However, light clinical signs and symptoms were reported in subjects with 30 to 60% reduction in RBC-AChE activity (Sidell, 1994).

The American Conference of Governmental Industrial Hygienists proposed a biological exposure index (BEI®) for AChE inhibiting pesticides to prevent cholinergic health effects (ACGIH, 2002). A RBC-AChE activity of 70% of the individual's baseline (i.e. 30% inhibition of the activity) is proposed as a biological reference. However, a BEI® based on the measurement of urinary biomarkers of malathion has not been proposed so far although this is desirable since it would give an earlier warning of possible effects than AChE inhibition. Indeed, it is clearly established that urinary biomarkers of exposure to malathion are more sensitive

exposure indices since they can be measured at exposure doses lower than those necessary to induce a measurable inhibition of AChE activity.

Experimental studies in animals and humans show that malathion is oxidized by cytochrome P-450, in small amounts (4-6% in rats), to malaoxon which is responsible for ChE inhibition (U.S. EPA, 2000). Both malathion and malaoxon are rapidly detoxified by carboxylesterases to mono-acid and di-acid derivatives, which are excreted mainly in urine; these acids can further be metabolically converted to phosphoric derivatives, also primarily excreted in urine (Ecobichon, 1992; Feldmann and Maibach, 1974; Jellinek et al., 2000; U.S. EPA, 2000).

To assess exposure to malathion in field studies, malathion mono- and di-carboxylic acids (MCA and DCA) in urine are thus used as specific biomarkers (Adgate et al., 2001; MacIntosh et al., 1999; Márquez et al., 2001) while the phosphoric derivatives dimethyl dithiophosphate (DMDTP), dimethyl thiophosphate (DMTP) and dimethyl phosphate (DMP) serve as non specific urinary biomarkers (Cocker et al., 2002; Coyes et al., 1986; Fenske, 1988; Fenske and Leffingwell, 1989).

The use of these urinary biomarkers to assess risk is dependent on the establishment of a link between their measurements and critical biological effects. Some authors established a relationship between the exposure dose and urinary biomarkers in controlled human studies (Feldmann and Maibach, 1974; Jellinek et al., 2000) while others studied links between the exposure dose and the inhibition of AChE activity in

volunteers (Moeller and Rider, 1962). In some reports, attempts were also made to link urinary biomarkers to the appearance of early biological effects under experimental conditions but the administered doses were not sufficient to induce an inhibition of AChE activity (Dennis and Lee, 1999; Jellinek et al., 2000). In field studies in exposed workers, these relationships cannot be established directly on the basis of measurements of external doses (ambient air concentrations or skin deposits). In the context of malathion exposure in occupational settings, which occurs mainly through dermal contact (ACGIH, 2002; Tuomainen et al., 2002), knowledge of the kinetics is essential since dermal absorption is subject to large variations among individuals and depending on the exposed skin site (Cohen and Rice, 2001; Feldmann and Maibach, 1974).

If links can be established between (i) the cumulative amounts of urinary biomarkers and the absorbed dose of malathion whatever the exposure route (oral, dermal, pulmonary) or scenario (single, repeated, intermittent or continuous exposure) and (ii) the absorbed dose and the appearance of biological effects, it then becomes possible to use urinary biomarkers to assess risk in workers exposed to malathion. These links can be made through toxicokinetic modeling provided appropriate experimental data on the metabolism and disposition of malathion and its metabolites are available. A physiologically-based pharmacokinetic model has been developed to describe the human dermal absorption, metabolism and excretion of malathion (Rabovsky and Brown, 1993). This model did not however seek to describe the urinary excretion

kinetics of specific metabolites, and thus does not allow reconstruction of the absorbed dose starting from urinary measurements.

The objectives of this study were (i) to develop a toxicokinetic model for humans linking the dose of malathion absorbed under different exposure routes and scenarios to the time courses of malathion metabolites in urine and (ii) to use this model as a framework to relate published human “no observed effect level” (NOEL) to associated amounts of metabolites in urine, which are to be proposed as convenient biological reference values to prevent health effects.

## ***METHOD AND MODEL PRESENTATION***

### ***Model development***

**Conceptual and functional representation.** The disposition kinetics of malathion and its metabolites following intravenous, oral or dermal exposure was modeled using a multi-compartment dynamical system, described mathematically by a mass balance differential equation system (see Appendix). The model conceptual and functional representation was designed to describe the data provided by Feldmann and Maibach (1974) and Jellinek *et al.* (2000) on the kinetics of malathion and its metabolites in human volunteers.

The model conceptual representation is depicted in Figure 1. Symbols and abbreviations used in this study are described in Table 1. The model uses a specific body compartment for the malathion burden in blood and tissues in dynamical equilibrium with blood, *i.e.* tissues that rapidly reach and maintain a fixed ratio with blood (referred to later as the blood compartment  $B(t)$  for simplicity). Another compartment regroups the malathion stored in tissues  $S(t)$ , *i.e.* malathion in lipids or bound to tissue proteins. A compartment  $M(t)$  is also used to describe the whole body burden of total metabolites. In addition, different compartments are introduced for cumulative amounts of each specific malathion metabolites in either urine or feces, that is for malathion mono-carboxylic acids (MCA), di-carboxylic acids (DCA), and for the phosphoric derivatives dimethyl dithiophosphate (DMDTP), dimethyl thiophosphate

(DMTP) and dimethyl phosphate (DMP). The route-of-entry, gastro-intestinal tract or skin, is also represented as a separate input compartment. In the model, all amounts are initially expressed on a mole basis.

The compartment  $M(t)$  regroups unconjugated MCA, DCA, DMDTP, DMTP and DMP metabolites, which are generated in cascade, together with their conjugates, in accordance with the metabolism described by Ecobichon (1992). Since phase I and II biotransformation processes occur on a much more rapid time-scale than renal and fecal clearance of the metabolites, the fractions of total body metabolites excreted from the body as specific metabolites are mainly function of the competition between phase II conjugation and further phase I metabolism. For instance, the amounts of MCA eliminated from the body are dependent on the competition between conjugation and biotransformation to DCA, DMDTP and DMTP. Consequently, if 36% of an absorbed dose is recovered in excreta as MCA and 4% of malathion is metabolized to malaaxon, it indicates that 36% of the absorbed dose has been metabolized to MCA and conjugated while 60% has been biotransformed to other metabolites. Without competition between conjugation and the biotransformation cascade, unconjugated metabolites would all be metabolized to DMP.

In the model, the rates of change in the amounts of a substance in a given compartment are described mathematically as the difference between compartment rates of uptake and loss. Exchange rates between compartments represent either the physical transfer of the same substance or the transfer (on a mole to mole basis) through

biotransformation of malathion to its metabolites or one metabolite to another. Solving the system of differential equations yields the mathematical function of the time courses of malathion and its metabolites in the different compartments.

**Determination of parameters.** The model parameters were determined from the *in vivo* time profiles provided by Feldmann and Maibach (1974) and Jellinek *et al.* (2000). The parameters were determined by: (i) statistical best-fits of the explicit solutions of differential equations to experimental human time course data, or (ii) log-linear regression on the time profile data (using in both cases reported average values). A professional edition of a MathCad software was used for this purpose (MathSoft Inc., Cambridge, MA).

Extensive use was made of the different time scales involved in the biological processes to simplify differential equations, using quasi steady state approximations (QSSA) (Segel, 1988; Segel and Slemrod, 1989). This enabled no more than two model parameters to be estimated per fit. In short, QSSA predicts that compartments with rapid attrition reach a dynamic equilibrium with their slow varying “feeder” compartment. For instance, the output transfer rate,  $k_{BM} + k_{BS}$ , of malathion in blood  $B(t)$  to total body metabolites  $M(t)$  and to storage tissues  $S(t)$  was considered large compared to the rates of change of its feeder compartments:  $R(t)$  for absorption or  $S(t)$  for storage release, because the burden of malathion in blood is quickly depleted under a oral dose (Jellinek *et al.*, 2000).

The transfer rate constant of total metabolites in the body to urine,  $k_{MU}$ , was estimated by least square fit adjustment of the model general solution to the data of Feldmann and Maibach (1974) on the urinary excretion time course of average total  $^{14}C$  in male human volunteers ( $n = 6$ ) exposed intravenously (iv) to  $1 \mu Ci$  of  $^{14}C$ -labeled malathion (dose in mole or g not specified). These authors reported the time course of total  $^{14}C$  urinary excretion rate (% of the administered dose per h). For the fitting of experimental data and to determine the  $k_{MU}$  parameter, the experimental values were converted to cumulative burdens expressed as a fraction of the administered dose. Log-linear regression on the time course of average total  $^{14}C$  urinary excretion rate reported by Feldmann and Maibach (1974) during the 24- to 120-h period following the iv injection also served to determine the low transfer rate constant  $k_{SB}$  of malathion from storage tissues to blood.

The transfer rate constants of malathion in blood to total body metabolites,  $k_{BM}$ , and to storage tissues,  $k_{BS}$ , could not be determined precisely for lack of available detailed time profile data of malathion in blood shortly following malathion exposure in human volunteers. However, the sum of  $k_{BM} + k_{BS}$  could be approximated from the data of Jellinek *et al.* (2000). These authors showed that 1 h following a single oral dose of 15 mg/kg of malathion in human volunteers, blood concentrations of malathion were below the limit of detection (102 ng/ml). This corresponds to an attrition half-life of blood malathion of at most 12 min, which is consistent with a very rapid distribution or biotransformation of malathion. These findings indicate that the rate value of the sum of  $k_{BM} + k_{BS}$  must be greater or equal to  $\frac{\ln 2}{12 \text{ min}}$  or  $3.47 \text{ h}^{-1}$ . The individual values of

$k_{BM}$  and  $k_{BS}$  parameters were determined by adjustment of the numerical solution of the system of differential equations to the data of Feldmann and Maibach (1974) in volunteers exposed iv to  $^{14}\text{C}$ -malathion.

The data of Jellinek *et al.* (2000) were used to determine the fractions of total body metabolites recovered as each of the five metabolites: MCA, DCA, DMDTP, DMTP and DMP ( $f_{\text{MU-MCA}}$ ,  $f_{\text{MU-DCA}}$ ,  $f_{\text{MU-DMDTP}}$ ,  $f_{\text{MU-DMTP}}$  and  $f_{\text{MU-DMP}}$ , respectively). These authors reported mean urinary excretion of these metabolites (as a % of the administered dose) for the 0-12, 12-24 and 24-48 h periods following a single oral malathion dose of 0.5, 1.5, 10 and 15 mg/kg of body weight in male human volunteers as well as 15 mg/kg in female volunteers ( $n = 5$  per group). The fractions of specific body metabolites to total body metabolites were thus obtained from the molar ratio of specific metabolites excreted in urine to total metabolites in urine. This amounts to assuming that the metabolites are produced in different proportions, but are excreted in urine at the same  $k_{\text{MU}}$  rate. This simplification was necessary given the lack of detailed blood and urinary excretion time profiles for each metabolite and the paucity of data on the conjugation reactions of malathion metabolites and their renal clearance. However, the data of Feldmann and Maibach (1974), from which the  $k_{\text{MU}}$  was derived, together with the data of Jellinek *et al.* (2000) show that elimination of the metabolites to urine is almost complete 12 to 24 h following an iv or oral exposure. It is thus reasonable to assume that the renal clearance of the different conjugated malathion metabolites is more or less the same.

The oral absorption fraction used in simulations was that reported by Jellinek *et al.* (2000). The experimental data did not allow for the exact determination of the oral absorption rate constant; a range of values was tested, consistent with data from studies on related compounds (Nolan *et al.*, 1984; Carmichael *et al.*, 1989) together with the duration of intestinal transit up to the main absorption site of malathion (jejunum). For dermal exposures, the absorption fraction and the absorption rate constant were estimated by least square fit adjustment of the model general solution to the data of Feldmann and Maibach (1974) on the urinary excretion time course of average total  $^{14}\text{C}$  in male human volunteers ( $n = 6$ ) exposed dermally to  $1 \mu\text{Ci}$  of  $^{14}\text{C}$ -labeled malathion on the forearms.

**Model simulations.** Once the parameters were estimated as described above, numerical solution of the complete model was performed by the Runge-Kutta method on the differential equation system. Simulations were conducted using a professional edition of a Mathcad Software (MathSoft Inc., Cambridge, MA). The model predicts the amounts of malathion and its metabolites in the body and in excreta at any time point postexposure for any route of exposure and scenario.

Simulations of exposure scenarios, where continuous or repeated intermittent doses are administered through time, were performed by introducing a non-homogenous term,  $g(t)$ , describing these varying inputs (see Appendix).

### ***Model validation***

The model developed using the previously mentioned data was validated using different sets of experimental data: Maibach *et al.* (1971), Wester *et al.* (1983) and Dennis and Lee (1999). Only in the study of Dennis and Lee (1999) were the data presented in graphical form. Those graphs were thus scanned and the data were read using a Sigma Plot Graphing Software (Jandel Corporation, San Rafael, CA).

### ***Determination of biological reference values***

Biological reference values for MCA, DCA and phosphoric derivatives amounts in 24-h urine samples are proposed here based on model predictions and the data of Moeller and Rider (1962). These authors exposed male human volunteers repeatedly, once a day, to gelatin capsules containing malathion. The dosage regimen was 8 mg/day (0.1 mg/kg/day) for 32 days, 16 mg/day (0.2 mg/kg/day) for 47 days or 24 mg/day (0.3 mg/kg/day) for 56 days ( $n = 5$  per exposure group). Plasma and erythrocyte cholinesterase activities were measured twice weekly before, during and after administration. No clinical signs or symptoms of toxicity were observed during the study period at all dose levels. The exposure doses “no observed effect level” (NOEL) and “lowest observed effect level” (LOEL) were estimated by Moeller and Rider (1962) to be 0.2 and 0.3 mg/kg/day, respectively, based on a >10% inhibition of both plasma and erythrocyte cholinesterases as compared to baseline values. We reanalyzed the data of Moeller and Rider (1962) considering as significant an inhibition of  $\geq 19\%$  plasma and  $\geq 12\%$  erythrocyte cholinesterases in two successive measurements, as proposed by several authors (Gage, 1967; Heath and Vale, 1992; Larsen *et al.*, 1982).

Though we used a different criterion, the NOEL and LOEL arrived at are identical to those of Moeller and Rider (1962). From the NOEL value of 0.2 mg/kg/day, the corresponding absorbed dose was estimated and, using the model, associated urinary amounts of MCA, DCA and phosphoric derivatives were obtained.

To determine biological reference values starting from the amounts of MCA, DCA and phosphoric derivatives accumulated in urine 0-24 h following the onset of exposure, the model input conditions were set to generate biological reference values with a safety margin. This was achieved with an 8-h/day absorbed NOEL dose using the slowest absorption rate constant found compatible with the various experimental data available. The fractions of total metabolites recovered in urine as MCA, DCA and phosphoric derivatives were also attributed the smallest individual values determined using data from the study of Krieger and Dinoff (1999) who were the only authors to report individual values of MCA, DCA and phosphoric derivatives in urine. These input conditions ensure a “minimal” urinary excretion of the metabolites for a given dose. This provides a safety margin through a possible overestimation of the dose absorbed when starting from urinary measurements.

### ***Application***

The proposed biological reference values were applied to assess health risk in workers exposed to malathion. Unpublished urinary excretion data from botanical garden workers, collected by the Institut national de santé publique du Québec (INSPQ), Direction de la toxicologie humaine (Québec, Canada), were used. Twenty-four-hour

urine samples were collected in male and female subjects ( $n = 9$  and  $2$ , respectively) following a 2- to 3-h workshift in greenhouses which had been sprayed with malathion 12 to 15 h earlier. The workers studied had not participated in the application of malathion.

Samples were analyzed for  $\alpha$ - and  $\beta$ -MCA and DCA metabolite contents at the INSPQ. Urinary levels were determined by capillary gas chromatography/mass spectrometry (GC/MS) after acidification, extraction on  $C_{18}$  micro-columns and derivatization with diazomethane. Analysis was performed using a model 5890 gas chromatography system (Hewlett Packard), a model 5972 mass spectrometer (Hewlett Packard) and a fused silica capillary column HP-5MS ( $30\text{ m} \times 0.32\text{ mm}$ ,  $0.25\text{ }\mu\text{m}$ ). The limit of detection for MCA and DCA was respectively  $2$  and  $1\text{ }\mu\text{g/l}$ . Average recovery of urine samples spiked with  $10\text{ }\mu\text{g/l}$  of authentic reference standards was  $113\%$  and  $108\%$  for MCA and DCA, respectively ( $n = 10$  samples). Inter-day coefficient of variation for replicate analysis of the same urine sample spiked with  $10\text{ }\mu\text{g/l}$  of reference standard was  $5.6\%$  and  $4.8\%$  for MCA and DCA, respectively ( $n = 10$  days).

## **RESULTS**

### ***Model development***

Table 2 presents parameter values of the model determined using the data of Feldmann and Maibach (1974) and Jellinek *et al.* (2000). Figure 2 shows that with these parameter values, the model reproduces closely the data of Feldmann and Maibach (1974) on the cumulative urinary excretion time course of total  $^{14}\text{C}$  in human volunteers exposed intravenously and dermally to  $^{14}\text{C}$ -labeled malathion. The model, with the same parameters, also simulates well the data of Jellinek *et al.* (2000) on the cumulative urinary excretion of malathion metabolites 0-12, 0-24 and 0-48 h following an oral exposure to malathion in human volunteers (see Table 3). Asymptotically, the model predicts that 90% of the absorbed dose is excreted in urine; the rest is predicted to be excreted in feces, which is compatible with the rat data of Lechner and Abdel-Rahman (1986).

### ***Model validation***

The proposed model was applied to the data collected by Maibach *et al.* (1971) (Fig. 3) and Wester *et al.* (1983) (data not shown) on the urinary excretion time profile of average total  $^{14}\text{C}$  in male human volunteers following a single dermal application of  $^{14}\text{C}$ -labeled malathion at different anatomical regions of the body. The parameter values in Table 2 were used for these model simulations except for the dermal absorption fraction and rate constant, which are known to vary largely according to the exposed region of the skin as well as from one individual to another. To simulate the

experimental data of Maibach *et al.* (1971), the best fit values for the dermal absorption fraction were: 0.075, 0.062, 0.134 and 0.25 for applications to the forearm, the palm of the hand, the hand dorsum and the forehead, respectively. The corresponding values for the absorption rate constant were: 0.103, 0.05, 0.11 and 0.11 h<sup>-1</sup>. To simulate the data of Wester *et al.* (1983) in volunteers exposed dermally to 6.25 μCi of <sup>14</sup>C-malathion on the forearm, the dermal absorption fraction was found to be 0.04 and the absorption rate constant 0.05 h<sup>-1</sup>.

The model was also validated through simulations of the data of Dennis and Lee (1999) on the urinary excretion time course of phosphoric derivative metabolites (the sum of DMDTP, DMTP and DMP) in volunteers exposed to an aqueous or alcohol-based head lice formulation containing malathion (Fig. 4). The model provided a close approximation to the data presented by these authors using the model parameter values in Table 2, except for the dermal absorption fraction and rate constant. For the simulation of exposure to the aqueous-based formulation, the absorption fraction was set equal to 0.075; the value of the absorption rate constant was left as that reported in Table 2. For the simulation of exposure to the alcohol-based solution, the absorption fraction was set equal to 0.068 and the absorption rate constant to 0.123 h<sup>-1</sup>.

### ***Inferences of the model***

**Prediction of the time course of malathion and its metabolites in the body and excreta under different exposure scenarios.** The model was used to predict the time course of malathion and its metabolites in the body and in accessible biological

matrices (blood, urine) under different exposure scenarios likely to occur in practice. Figures 5 and 6 show model predictions of the time profiles of malathion and its metabolites in the body and urine that would result from a single oral or dermal exposure to malathion. Following oral exposure, with an absorption fraction of 0.738 and absorption rate constant of  $1.373 \text{ h}^{-1}$  (half-life of 30 min) as reported in Table 2, the predicted time course of malathion in blood  $B(t)$  shows maximum level 19 min postexposure, which represents 10.6% of the exposure dose (14.4% of the absorbed dose). Because of an early partial storage in tissues and a slow return from these tissues to blood, elimination of malathion from blood follows a bi-exponential pattern with a more rapid phase followed by a slower phase (Fig. 5A). Model simulations predict a low transfer of blood malathion to storage tissues  $S(t)$ , where the maximum storage level represents 2.6% of the exposure dose (3.5% of the absorbed dose) (Fig. 5A). As mentioned above, return to blood from  $S(t)$  is however relatively slow; the predicted half-life for this process is 19.8 h. Malathion is also readily and extensively metabolized in the body and its metabolites are rapidly eliminated once formed; the maximum level of total metabolites  $M(t)$  is reached 1.7 h postexposure and represents 48.9% of the exposure dose (66.3% of the absorbed dose) (Fig. 5A). The cumulative urinary excretion time courses of malathion metabolites show that the different metabolites are rapidly eliminated (Fig. 5B); the model predicts that 79, 90 and 98% of total amounts recovered in urine are excreted during the first 8, 12 and 24 h postexposure, respectively. Asymptotically, urinary MCA, DCA and phosphoric derivatives represent respectively 36.1, 8.7 and 21.6% of the exposure dose (48.9, 11.8 and 29.2% of the absorbed dose).

Following a single dermal exposure, using an absorption fraction of 0.070 and an absorption rate constant of  $0.103 \text{ h}^{-1}$  (half-life of 6.7 h) as reported in Table 2, the predicted time courses of malathion in blood  $B(t)$  and in storage tissues  $S(t)$ , and the total metabolites in the body  $M(t)$  show respective peak levels 0.67, 16.1, 6.5 h postexposure (Fig. 6A). Since the dermal absorption of malathion is small and relatively slow compared to metabolism cum elimination, maximum values for  $B(t)$ ,  $S(t)$  and  $M(t)$  only amount to 0.11, 0.16 and 1.55% of the exposure dose, respectively (1.6, 2.3 and 22.0% of the absorbed dose). Also, because dermal absorption of malathion is slow compared to its biotransformation, a dynamic equilibrium is quickly reached between the skin compartment  $R(t)$  and blood compartment  $B(t)$ . Consequently,  $B(t)$  begins its attrition at the rate of the absorption rate constant of  $0.103 \text{ h}^{-1}$  (half-life of 6.7 h), which is not the case following an oral exposure where absorption is more rapid than elimination processes (see Fig. 5A).

From the cumulative urinary excretion time courses of malathion metabolites (Fig. 6B), the model predicts that 32, 51 and 83% of total amounts recovered in urine are excreted during the first 8, 12 and 24 h, respectively, following a dermal exposure. Asymptotically, urinary MCA, DCA and phosphoric derivatives represent 3.45, 0.83 and 2.06% of exposure dose (48.9, 11.8 and 29.2% of the absorbed dose; these latter excretions are identical to those after oral exposure, as should be). These simulations show that following a dermal exposure to malathion, the absorption rate constant governs the overall urinary excretion rate of the metabolites, because the dermal

absorption rate,  $k_{\text{abs-dermal}}$ , is small compared to the biotransformation rate and renal clearance (represented in the model by  $k_{\text{BM}}$  and  $k_{\text{MU}}$ , respectively). According to model predictions, to recover half of the absorbed dose of malathion eventually excreted in urine as metabolites takes 11.8 h following a single dermal application compared to 3.2 h following an intravenous injection and 4.0 h after oral exposure. Furthermore, as mentioned previously, the dermal absorption rate constant varies among individuals and depends on the skin region exposed to malathion. Table 4 shows that, for dermal exposure to malathion, varying the absorption rate constant affects markedly the cumulative urinary excretion time course of total metabolites (the sum of MCA, DCA and phosphoric derivatives).

The proposed model can also predict the time evolution of malathion and its metabolites in the body and excreta following repeated exposures to malathion. Simulations of an 8 h per day dermal exposure, 5 days a week for 4 consecutive weeks are shown in Fig. 7. With the parameter values given in Table 2, during a week of exposure, there is a slight increase from day to day in peak burdens of malathion in blood  $B(t)$  and in storage tissues  $S(t)$  and total body metabolites  $M(t)$  (measured as a fraction of the absorbed daily dose). However, there is no significant week to week increase in daily maximum levels because, at the end of a 2-day break in exposure, the elimination is nearly complete.

**Reconstruction of the absorbed dose of malathion starting from urinary measurements of the metabolites.** The model can help estimate, through back calculations, the absorbed dose of malathion starting from urinary measurements of the metabolites provided the periods of exposure and urine collection are known. Table 5 shows simulations of the cumulative urinary excretion of total metabolites, expressed as a fraction of the absorbed dose, at different time periods following the onset of an 8-h workshift, assuming zero background levels. Simulations are performed under two dermal exposure scenarios: one with a high value for the absorption rate constant ( $0.12 \text{ h}^{-1}$ ) and another with a low value ( $0.05 \text{ h}^{-1}$ ). Given the importance of the absorption rate constant in determining dermal exposure, the excretion values, reported in Table 5, can be viewed as “best” and “worst” case scenarios. From Table 5, the dose absorbed by workers can be inferred from measurements of the amounts of metabolites in urine, when the urine collection time period following the beginning of a workshift is known as well as the workshift duration.

**Biological reference values.** The model also served to establish biological reference values for malathion metabolites in urine since it links the absorbed dose to the amounts of metabolites excreted in urine over different time periods. From the data of Moeller and Rider (1962), a NOEL oral exposure dose of  $0.61 \mu\text{mol/kg/day}$  ( $0.2 \text{ mg/kg/day}$ ) was derived. With the estimated oral absorption fraction (see Table 2), this corresponds to an absorbed dose NOEL of  $0.45 \mu\text{mol/kg/day}$  ( $0.15 \text{ mg/kg/day}$ ). The corresponding biological reference values for MCA, DCA, phosphoric derivatives are

then 44, 13 and 62 nmol/kg, respectively, in 24-h urine samples. The values for the sum of acids or total metabolites are thus 57 and 119 nmol/kg, respectively.

### *Application*

The model was used to assess the health risk related to malathion exposure in botanical garden workers starting from measurements of the amounts of MCA and DCA metabolites in 24-h urine samples (as described in the Method section). The workers exhibited excretion values of MCA and DCA in their 24-h urine samples corresponding to a range of 0.017 to 0.210 times the biological reference value proposed for MCA and a range of 0.011 to 0.324 times the value proposed for DCA, indicating a negligible health risk for those workers (see Table 6).

## ***DISCUSSION***

A heuristic toxicokinetic model was developed, which integrates a wealth of experimental *in vivo* time profile data, to uncover the critical biological determinants of the kinetics of malathion and its metabolites in humans. The model provides a good understanding of the time evolution of malathion and its metabolites in the body and in urine, under different exposure scenarios (single, repeated, continuous or intermittent exposure). With this model, it is also possible to assess the effect of the route-of-entry on time course data. In the context of biological monitoring, the model facilitates the interpretation of urinary measurements collected over different time periods. It can also be used to propose optimum sampling strategies for routine biological monitoring.

The model showed that, upon absorption, malathion in blood is either readily biotransformed or transferred to storage tissues, though only a small fraction of the absorbed dose of malathion is in fact transferred to storage tissues. Metabolites are also rapidly excreted in urine and feces. Consequently, the exposure route determines the time-dependent urinary excretion rate of malathion metabolites, because different routes-of-entry imply different absorption rates. For example, when simulating a single oral exposure, 80-89% of the absorbed dose is eliminated from the body within 12 h, whereas, after a single dermal application, only between 29-53% of the absorbed dose is excreted during the same time period. (These value ranges are obtained by considering the lowest and highest absorption rate constant used to simulate the various available data.) In workers, who are typically exposed to malathion mainly through the

skin, the absorption rate thus limits the output rates of metabolites in urine, because dermal absorption is much slower than biotransformation rate and renal clearance. This is not the case in individuals exposed by the oral or pulmonary routes, where the absorption rate is not a limiting step in the excretion kinetics.

Considering a continuous 8-h dermal exposure during a workday, the model predicts that 52-80% of the absorbed dose will be eliminated from the body within the 24-h period following the onset of exposure as compared to 84-98% within 48 h. Consequently, for the biological monitoring of worker exposure to malathion through measurements of the amounts of urinary metabolites, collection of 24-h urine samples, starting at the beginning of the workshift, appears as an adequate sampling strategy. In the case of workers subjected to exposure day after day, malathion is predicted by the model to build up in storage tissues during the course of a workweek, thus resulting in a progressive increase in total body burden. Repeating the exposure from week to week does not however cause any significant increase in maximum and minimum body burdens. In this situation, it is best to collect the 24-h urine samples on the last day of a workweek. Measurements should be repeated periodically when exposure levels are suspected to vary significantly with time.

It is interesting to note that based on the data of Jellinek *et al.* (2000), cumulative amounts of metabolites in urine (expressed as a percentage of the malathion exposure dose) appear in the following order: MCA > phosphoric derivatives > DCA. These findings combined with the fact that the MCA metabolite is specific to malathion

exposure (Márquez *et al.*, 2001; Tuomainen *et al.*, 2002), suggest that MCA in urine is the most useful individual biological indicator of exposure to malathion. Of course, measurements of phosphoric derivatives can also be of interest as non specific bioindicators of exposure to organophosphate compounds (Cocker *et al.*, 2002; Coye *et al.*, 1986).

The model enables links to be established at all times between the dose, the body burden of malathion and that of its metabolites and the amounts of specific metabolites excreted in urine. The model can thus be used to reconstruct, through back calculations, the absorbed dose of malathion following oral or dermal exposure, starting from measurements of cumulative amounts of a specific metabolite excreted in urine over a given period of time. Reconstructing the absorbed dose from metabolites in urine avoids unnecessary assumptions or approximations about the absorption fraction, which is known to be subject to large inter-individual variations and, in the case of dermal exposure, to vary according to anatomical skin regions (ACGIH, 2002; Cohen and Rice, 2001; Feldmann and Maibach, 1974).

It was also possible, with the model, to propose biological reference values with a margin of safety by simulating a dermal exposure scenario typical of a daily worker exposure and using a combination of kinetic parameters that overestimates the reconstructed absorbed dose starting from urinary measurements. The establishment of biological reference values based on a dermal exposure scenario rather than an oral or pulmonary exposure contributes to safe estimates whatever the exposure route. Indeed,

in an individual exposed to malathion mainly by inhalation or ingestion, the urinary excretion of metabolites is more rapid than following a dermal exposure and hence urinary excretion values in 24-h urine samples collected at the beginning of an exposure period are more important. It should also be reminded that the biological reference values were determined with the model using the slowest absorption rate found compatible with the available literature data on excretions, together with the lowest individual values found for the fractions of total metabolites recovered in urine as MCA, DCA or phosphoric derivatives. This was to consider the variations in the absorption rate among individuals and depending on the exposed skin regions (Feldmann and Maibach, 1974) as well as the reported variations from one study to another in the fractions of total metabolites recovered in urine as MCA, DCA and phosphoric derivatives (Bradway and Shafik, 1977; Jellinek *et al.*, 2000; Krieger and Dinoff, 2000). However, the study of Jellinek *et al.* (2000) showed that over the 0.5 to 15 mg/kg oral dose range, the fraction of total metabolites recovered in urine as MCA, DCA and phosphoric derivatives was independent of the dose.

To assess the risk of exposure to malathion, the amounts of MCA, DCA and phosphoric derivatives in the 24-h urine samples of exposed subjects can be compared to the proposed reference values. Ideally, it is best to establish the risk from measurements of the sum of acids rather than MCA or DCA individually, for a specific but more precise estimate. Otherwise, the risk can be estimated from measurements of the sum of all metabolites in urine which, despite not being entirely specific to malathion exposure, allows to bypass uncertainties about the relative weights of each

metabolite in total excretion. Also, when 24-h urine samples cannot be collected for practical reasons, collection periods can be shortened; the Table 5 can be used to estimate the 24-h urinary excretion in exposed subjects starting from measurements over other urine collection periods. For a “safe side” estimation, excretion values in Table 5 obtained from the slowest absorption rate should be used. However, to minimize the effects of inter-individual and inter-site variations of absorption rates on urinary outputs, it is best to collect urine samples over the longest possible time period.

The model and proposed biological reference values were used in this study to assess the risk for workers exposed to malathion in a botanical garden. The risk was predicted to be negligible given that the measurements of MCA and DCA in 24-h urine samples were lower than the proposed biological reference values. In general, these workers appear to be less exposed than the greenhouse workers of a recent Spanish report (Márquez *et al.*, 2001) where MCA was measured in the urine of three individuals following applications of malathion. The total amounts of MCA excreted during the 24-h period following applications were calculated to be 134, 182 and 671  $\mu\text{g}$ , corresponding to 31.7, 8.6, and 6.3 nmol/kg, assuming a body weight of 70 kg. These values represent respectively 0.72, 0.20 and 0.14 of the proposed biological reference value.

In summary, the toxicokinetic model was developed that accounts for the constraints related to significant variations in some of the parameters: (i) variations in the dermal absorption fraction and the rate of absorption among individuals and according to the

exposed skin regions and (ii) variations from one report to another in the fractions of total metabolites recovered in urine as MCA, DCA and phosphoric derivatives. In this study, the model was used to reconstruct the absorbed dose starting from measurements of urinary biomarkers; the effect of varying absorption fractions was thus bypassed. Variations in the absorption rate constant and relative proportions of the different metabolites in urine can impair accurate estimation of the absorbed dose starting from the amounts of biomarker in urine. Under these conditions, to calculate biological reference values with a margin of safety, the smallest rate values for the latter parameters afforded by the literature were used. This leads to a possible overestimation of the corresponding values for the reconstructed dose. The model also assumes the absence of saturation in the metabolism and clearance processes. Over the exposure dose range modeled in this study, the available data in volunteers and workers were accurately predicted without having to introduce saturation. The model cannot, however, be used to predict the kinetics in the saturating exposure dose ranges, as expected in the case of intoxicated subjects. The available literature data remained sufficient to build a robust model to better understand the kinetics of malathion and its metabolites and to propose convenient biological reference values together with sampling strategies. These can be of use immediately for the biological monitoring of malathion exposure through measurements of metabolites in urine.

## ***ACKNOWLEDGMENTS***

This study was funded by the "Institut de recherche en santé et sécurité du travail du Québec". Authors wish to thank Pierre Dumas of the "Institut national de santé publique du Québec" for the analysis of malathion metabolites in urine.

## APPENDIX

### *First order linear differential equations for each compartment*

From Figure 1, the following differential equations are obtained (see Table 1 for definitions of symbols and abbreviations):

$$\frac{dR(t)}{dt} = g(t) - k_{abs} \times R(t)$$

where  $g(t)$  is the absorbed oral or dermal dose  $D_{abs}$  per unit of time.  $D_{abs} = D_{exp} \times f_{abs}$

where  $f_{abs}$  is the absorption fraction and  $D_{exp}$  is the exposure dose.

For intravenous injection,  $g(t) = 0$  for  $t > 0$  and at time  $t = 0$ :  $B(0) = D_{abs}$ .

$$\frac{dB(t)}{dt} = k_{abs} \times R(t) + k_{SB} \times S(t) - (k_{BS} + k_{BM}) \times B(t)$$

$$\frac{dS(t)}{dt} = k_{BS} \times B(t) - k_{SB} \times S(t)$$

$$\frac{dM(t)}{dt} = k_{BM} \times B(t) - (k_{MU} + k_{MF}) \times M(t)$$

$$\frac{dF(t)}{dt} = k_{MF} \times M(t)$$

$$\frac{dM_i(t)}{dt} = f_i \times k_{BM} \times B(t) - (k_{MU} + k_{MF}) \times M_i(t)$$

$$\frac{dU_i(t)}{dt} = k_{MU} \times M_i(t)$$

where:  $i \in \{MCA - C, DCA - C, DMDTP - C, DMTP - C, DMP - C\}$ ,  $\sum_i f_i = 1$  and

$$\sum_i M_i(t) = M(t)$$

## **REFERENCES**

ACGIH (2002). *Documentation of the Threshold Limit Values and Biological Exposure Indices*, 7th Ed. American Conference of Governmental Industrial Hygienists, Cincinnati, OH.

Adgate, J.L., Barr, D.B., Clayton, C.A., Eberly, L.E., Freeman, N.C.G., Lioy, P.J., Needham, L.L., Pellizzari, E.D., Quackenboss, J.J., Roy, A., and Sexton, K. (2001). Measurement of children's exposure to pesticides: analysis of urinary metabolite levels in a probability-based sample. *Environ. Health Perspect.* **109**(6), 583-590.

Bradway, D.E., and Shafik, T.M. (1977). Malathion exposure studies. Determination of mono- and dicarboxylic acids and alkyl phosphates in urine. *J. Agric. Food Chem.* **25**(6), 1342-1344.

Carmichael, N.G., Nolan, R.J., Perkins, J.M., Davies, R., and Warrington, S.J. (1989). Oral and dermal pharmacokinetics of triclopyr in human volunteers. *Human Toxicol.* **8**, 431-439.

Cocker, J., Mason, H.J., Garfitt, S.J., and Jones, K. (2002). Biological monitoring of exposure to organophosphate pesticides. *Toxicol. Lett.* **134**, 97-103.

Cohen, D.E., and Rice, R.H. (2001). Toxic responses of the skin. In *Casarett & Doull's Toxicology: The Basic Science of Poisons*, Sixth Edition (C.D. Klaassen, Ed.), pp. 653-671. McGraw-Hill, New York.

Coye, M.J., Lowe, J.A., and Maddy, K.J. (1986). Biological monitoring of agricultural workers exposed to pesticides: II. Monitoring of intact pesticides and their metabolites. *J. Occup. Med.* **28(8)**, 628-636.

Dennis, G.A., and Lee, P.N. (1999). A phase 1 volunteer study to establish the degree of absorption and effect on cholinesterase activity of four head lice preparations containing malathion. *Clin. Drug Invest.* **18**, 105-115.

Ecobichon, D.J. (1992). *The Basis of Toxicity Testing*, Second edition. CRC Press, Boca Raton, New York.

Environnement Québec (2002). *Bilan des Ventes de Pesticides au Québec en 1997*. Gouvernement du Québec, Québec, Canada.

Feldmann, R.J., and Maibach, H.I. (1974). Percutaneous penetration of some pesticides and herbicides in man. *Toxicol. Appl. Pharmacol.* **28**, 126-132.

Fenske, R.A. (1988). Correlation of fluorescent tracer measurements of dermal exposure and urinary metabolite excretion during occupational exposure to malathion. *Am. Ind. Hyg. Assoc. J.* **49(9)**, 438-444.

Fenske, R.A., and Leffingwell, J.T. (1989). Method for the determination of dialkyl phosphate metabolites in urine for studies of human exposure to malathion. *J. Agric. Food Chem.* **37**, 995-998.

Gage, J.C. (1967). The significance of blood cholinesterase activity measurements. *Residue Rev.* **18**, 159-73.

Heath, A.J.W., and Vale, J.A. (1992). Clinical presentation and diagnosis of acute organophosphorus insecticide and carbamate poisoning. In *Clinical and Experimental Toxicology of Organophosphates and Carbamates* (B. Ballantyne and T.C. Marrs, Eds.), pp.513-519. Butterworth-Heinemann Ltd., Oxford.

Jellinek, Schwartz and Connolly, Inc (2000). *The Effects and Pharmacological Disposition of a Single Oral Dose of Malathion Administered to Human Volunteers*. Cheminova, Lemvig, Denmark. Unpublished report, CHA Doc. No.: 299 FYF Amdt-4. Submitted to EPA on 5/17/00, MRID 45125601.

Krieger, R.I., and Dinoff, T.M. (2000). Malathion deposition, metabolite clearance, and cholinesterase status of date dusters and harvester in California. *Arch. Environ. Contam. Toxicol.* **38**, 546-553.

Larsen, K.-O., and Hanel, H.K. (1982). Effect of exposure to organophosphorus compounds on cholinesterase in workers removing poisonous depots. *Scand. J. Environ. Health* **8**, 222-8.

Lechner, D.W., and Abdel-Rahman, M.S. (1986). Kinetics of carbaryl and malathion in combination in the rat. *J. Toxicol. Environ. Health* **18**, 241-256.

Liu, J, and Pope, C.N. (1998). Comparative presynaptic neurochemical changes in rat striatum following exposure to chlorpyrifos or parathion. *J. Toxicol. Environ. Health, Part A* **53**, 531-544

MacIntosh, D.L., Needham, L.L, Hammerstrom, K.A., and Ryan, P.B. (1999). A longitudinal investigation of selected pesticide metabolites in urine. *J. Exp. Anal. Environ. Epidemiol.* **9**, 494-501.

Maibach, H.I., Feldmann, R.J., Milby, T.H., and Serat, W.F. (1971). Regional variation in percutaneous penetration in man: pesticides. *Arch. Environ. Health* **23**, 208-211.

Márquez, M.C., Arrebola, F.J., Egea González, F.J., Castro Cano, M.L., and Martínez Vidal, J.L. (2001). Gas chromatographic-tandem mass spectrometric analytical method for the study of inhalation, potential dermal and actual exposure of agricultural workers to the pesticide malathion. *J. Chromatogr. A* **939**, 79-89.

Moeller, H.C., and Rider, J.A. (1962). Plasma and red blood cholinesterase activity as indications of the threshold of incipient toxicity of ethyl-*p*-nitrophenyl thionobenzene-phosphonate (EPN) and malathion in human beings. *Toxicol. Appl. Pharmacol.* **4**, 123-130.

Nolan, R.J., Rick, D.L., Freshour, N.L., and Saunders J.H. (1984). Chlorpyrifos pharmacokinetics in human volunteers. *Toxicol. Appl. Pharmacol.* **73**, 8-15.

Rabovsky, J. and Brown, J.P. (1993). Malathion metabolism and disposition in mammals. *J. Occup. Med. Toxicol.* **2**, 131-168.

Roberts, R.J. (2002). Head lice. *New Eng. J. Med.* **346(21)**, 1645-1650.

Segel, L.A. (1988). On the validity of the Steady State Approximation of enzyme kinetics. *Bull. Math. Biol.* **50**, 579-593.

Segel, L.A., and Slemrod, M. (1989). The Quasi-Steady State Approximation: A case study in perturbation. *SIAM Rev.* **31**, 446-476.

Sidell F.R. (1994). Clinical effects of organophosphorus cholinesterases inhibitors. *J. Appl. Toxicol.* **14**, 111-113.

Tuomainen, A., Kangas, J.A., Meuling W.J.A., and Glass, R.C. (2002). Monitoring of pesticide applicators for potential dermal exposure to malathion and biomarkers in urine. *Toxicol. Lett.* **134**, 125-132.

U.S. EPA (2000). *Malathion*. Office of Prevention, Pesticides and Toxic Substances, Environmental Protection Agency, Washington, DC.

Wester, R.C, Maibach, H.I, Bucks, D.A.W., and Guy, R.H. (1983). Malathion percutaneous absorption after repeated administration to man. *Toxicol. Appl. Pharmacol.* **68**, 116-119.

**Table 1. Symbols Used in the Conceptual and Functional Representation of the Model**

Variables and parameters Symbols or abbreviations	Description
Variables	
$g(t)$	Dose per unit of time which can describe time varying inputs
$R(t)$	Burden of malathion at the site-of-entry (gastro-intestinal (GI) tract or skin) as a function of time
$Q(t)$	Systemic body burden of malathion and its metabolites as a function of time
$B(t)$	Burden of malathion in blood and tissues in dynamical equilibrium with blood as a function of time
$S(t)$	Burden of malathion in storage tissues as a function of time
$M(t)$	Burden of total malathion metabolites in the body as a function of time
$M_{MCA}(t)$	Burden of unconjugated MCA metabolite in the body as a function of time
$M_{DCA}(t)$	Burden of unconjugated DCA metabolite in the body as a function of time
$M_{DMDTP}(t)$	Burden of unconjugated DMMDTP metabolite in the body as a function of time
$M_{DMTP}(t)$	Burden of unconjugated DMTP metabolite in the body as a function of time
$M_{DMP}(t)$	Burden of unconjugated DMP metabolite in the body as a function of time
$M_{MCA-C}(t)$	Burden of conjugated MCA metabolite in the body as a function of time
$M_{DCA-C}(t)$	Burden of conjugated DCA metabolite in the body as a function of time
$M_{DMMDTP-C}(t)$	Burden of conjugated DMMDTP metabolite in the body as a function of time
$M_{DMTP-C}(t)$	Burden of conjugated DMTP metabolite in the body as a function of time
$M_{DMP-C}(t)$	Burden of conjugated DMP metabolite in the body as a function of time
$U(t)$	Cumulative burden of total malathion metabolites in urine as a function of time
$U_{MCA}(t)$	Cumulative burden of MCA metabolite in urine as a function of time
$U_{DCA}(t)$	Cumulative burden of DCA metabolite in urine as a function of time
$U_{DMDTP}(t)$	Cumulative burden of DMMDTP metabolite in urine as a function of time
$U_{DMTP}(t)$	Cumulative burden of DMTP metabolite in urine as a function of time
$U_{DMP}(t)$	Cumulative burden of DMP metabolite in urine as a function of time
$F(t)$	Cumulative burden of total malathion metabolites in feces as a function of time

$F_{MCA}(t)$	Cumulative burden of MCA metabolite in feces as a function of time
$F_{DCA}(t)$	Cumulative burden of DCA metabolite in feces as a function of time
$F_{DMDTP}(t)$	Cumulative burden of DMDTP metabolite in feces as a function of time
$F_{DMTP}(t)$	Cumulative burden of DMTP metabolite in feces as a function of time
$F_{DMP}(t)$	Cumulative burden of DMP metabolite in feces as a function of time
Constants	
$f_{abs-oral}$	Oral absorption fraction of malathion
$f_{abs-dermal}$	Dermal absorption fraction of malathion
$k_{abs-oral}$	Oral absorption rate constant of malathion ( <i>i.e.</i> transfer rate from the mouth through the GI and into blood)
$k_{abs-dermal}$	Dermal absorption rate constant of malathion ( <i>i.e.</i> transfer rate from skin surface to blood)
$k_{BS}$	Blood to storage tissues transfer coefficient of malathion
$k_{SB}$	Storage tissues to blood transfer coefficient of malathion
$k_{BM}$	Metabolism rate constant of malathion to total metabolites in the body
$k_{MU}$	Whole body to urine transfer coefficient of total malathion metabolites
$k_{MF}$	Whole body to feces transfer coefficient of total malathion metabolites
Metabolite fractions	
$f_{MU-MCA}$	Fraction of total body metabolites recovered as MCA
$f_{MU-DCA}$	Fraction of total body metabolites recovered as DCA
$f_{MU-DMDTP}$	Fraction of total body metabolites recovered as DMDTP
$f_{MU-DMTP}$	Fraction of total body metabolites recovered as DMTP
$f_{MU-DMP}$	Fraction of total body metabolites recovered as DMP

*Note.* MCA = malathion mono-carboxylic acids; DCA = malathion di-carboxylic acids; phosphoric derivatives = the sum of dimethyl dithiophosphate (DMDTP), dimethyl thiophosphate (DMTP) and dimethyl phosphate (DMP).

**Table 2. Numerical Values of Parameters Used in the Model**

Constant parameters		Values
Absorption fractions	$f_{\text{abs-oral}}$	0.738
	$f_{\text{abs-dermal}}^a$	0.0705
Transfer rates ( $\text{h}^{-1}$ )	$k_{\text{abs-oral}}^b$	0.345 - 1.373
	$k_{\text{abs-dermal}}^a$	0.103
	$k_{\text{BM}}^c$	6.000
	$k_{\text{BS}}^c$	0.240
	$k_{\text{SB}}$	0.035
	$k_{\text{MU}}$	0.215
	$k_{\text{MF}}$	0.0239
	$k_{\text{DMP}}$	0.0239
Metabolite fractions	$f_{\text{MCA}}$	0.544
	$f_{\text{DCA}}$	0.131
	$f_{\text{DMDTP}}$	0.019
	$f_{\text{DMTP}}$	0.182
	$f_{\text{DMP}}$	0.124

*Note.* The description of constant parameters is given in Table 1. Absorption fractions and transfer rates were determined in this study by statistical best-fits; metabolite fractions were obtained from the literature.

<sup>a</sup>These values were determined from the data of Feldmann and Maibach (1974). However, the dermal absorption fraction and absorption rate constants are known to be subject to variations among individuals and depending on the exposed skin region. To

simulate the various data presented in this article, the value range for  $f_{\text{abs-dermal}}$  was found to be 0.04 - 0.25 and for  $k_{\text{abs-dermal}}$  0.05 - 0.123  $\text{h}^{-1}$ .

<sup>b</sup>Different values for  $k_{\text{abs-oral}}$  were used, corresponding to absorption half-lives between 30 min and 2 h.

<sup>c</sup>Using the  $k_{\text{MU}}$  value of 0.215  $\text{h}^{-1}$  determined from the data of Feldmann and Maibach (1974), the best fit was obtained for a  $\frac{k_{\text{BM}}}{k_{\text{BS}}}$  ratio equal to 25 and a rate value for the sum of  $k_{\text{BM}} + k_{\text{BS}}$  equal to 6.24  $\text{h}^{-1}$ , indicating that  $(k_{\text{BM}} + k_{\text{BS}}) \gg k_{\text{MU}}$  and malathion biotransformation is a very rapid process ( $k_{\text{BM}} = 6 \text{ h}^{-1}$ ).

**Table 3. Comparison of Model Simulations With the Experimental Data of Jellinek et al. (2000) on the Cumulative Urinary Excretion of Malathion Metabolites 0-12, 0-24 and 0-48 h Following a Single Oral Exposure to 0.5, 1.5, 10 and 15 mg/kg of Malathion in Male and Female Human Volunteers**

Malathion metabolite	Urine collection period (h)	Observed cumulative urinary excretion						Predicted cumulative urinary excretion (% of the administered dose recovered in urine as specific metabolites)
		(% of the administered dose recovered in urine as specific metabolites)						
		Oral exposure dose						
		0.5 mg/kg (male)	1.5 mg/kg (male)	10 mg/kg (male)	15 mg/kg (male)	15 mg/kg (female)	Mean	
MCA	0-12	39.5	33.6	30.7	41.3	29.6	35.0	32.5
	0-24	39.7	34.0	31.5	42.6	30.1	35.6	35.2
	0-48	39.9	34.0	31.6	42.7	30.3	35.7	35.8
DCA	0-12	11.4	3.7	3.4	10.0	3.9	6.5	7.8
	0-24	13.1	7.1	4.8	11.9	4.4	8.3	8.5
	0-48	15.9	7.3	5.0	12.1	4.6	9.0	8.6
Phosphoric derivatives	0-12	15.0	21.7	18.0	24.8	15.9	20.1	19.4
	0-24	15.9	24.4	19.5	26.6	16.9	20.6	21.0

0-48	17.2	24.7	20.0	26.9	17.5	21.3	21.4
------	------	------	------	------	------	------	------

*Note.* MCA = malathion mono-carboxylic acids; DCA = malathion di-carboxylic acids; phosphoric derivatives = the sum of dimethyl dithiophosphate (DMDTP), dimethyl thiophosphate (DMTP) and dimethyl phosphate (DMP). The predicted values reported in this

Table were obtained using an oral absorption rate of  $1.373 \text{ h}^{-1}$ .

**Table 4. Effect of Variations in the Absorption Rate Constant on the Simulated Cumulative Urinary Excretion of Total Metabolites Over Different Time Periods Following a Single Dermal Exposure to Malathion**

Urine collection period postexposure (h)	Cumulative urinary excretion of total metabolites (fraction of the absorbed dose)			
	$k_{\text{abs}} = 0.12 \text{ h}^{-1}$	$k_{\text{abs}} = 0.10 \text{ h}^{-1}$	$k_{\text{abs}} = 0.07 \text{ h}^{-1}$	$k_{\text{abs}} = 0.05 \text{ h}^{-1}$
	0-4	0.09	0.08	0.06
0-8	0.30	0.26	0.20	0.15
0-12	0.48	0.43	0.34	0.26
0-16	0.62	0.56	0.46	0.37
0-24	0.77	0.73	0.64	0.53
0-36	0.86	0.84	0.78	0.69
0-48	0.88	0.87	0.84	0.78
0-200	0.90	0.90	0.90	0.90

*Note.*  $k_{\text{abs}}$  = dermal absorption rate constant values, which are in the range of those used for simulations of the various dermal data presented in this article.

**Table 5. Predicted Cumulative Urinary Excretion of Total Metabolites (the Sum of Mono- and Di-Carboxylic Acids and Phosphoric Derivatives) at Different Time Periods Following the Onset of an 8-h Dermal Exposure to Malathion**

Urine collection period following the onset of exposure (h)	Cumulative urinary excretion of total metabolites (fraction of the absorbed dose)	
	$k_{\text{abs}} = 0.12 \text{ h}^{-1}$	$k_{\text{abs}} = 0.05 \text{ h}^{-1}$
	0-4	0.02
0-6	0.06	0.03
0-8	0.13	0.06
0-12	0.32	0.16
0-16	0.49	0.27
0-20	0.62	0.38
0-24	0.72	0.46
0-36	0.84	0.65
0-48	0.88	0.76
0-60	0.89	0.82
0-72	0.89	0.85

*Note.* The predicted cumulative urinary excretion of total metabolites over different time periods is given considering two dermal exposure scenarios, with a relatively high and low absorption rate constants ( $0.12$  and  $0.05 \text{ h}^{-1}$ , respectively). Background urinary

excretion is considered negligible. Also note that, eventually, no more than 90% of absorbed dose will be excreted in urine.  $k_{abs}$  = Dermal absorption rate constant.

**Table 6. Excretion of Mono- and Di-Carboxylic Acids in 24-h Urine Samples of Botanical Garden Workers Exposed to Malathion and Comparison With the Biological Reference Values Proposed in This Study**

Subjects	Sex <sup>a</sup>	Cumulative 24-h urinary excretion (nmol)		Fraction of the proposed biological reference values <sup>b</sup>	
		MCA	DCA	MCA	DCA
1	F	47.3	7.9	0.020	0.011
2	F	159.4	69.4	0.066	0.097
3	F	205.0	75.5	0.085	0.106
4	F	80.8	12.9	0.033	0.018
5	F	42.2	10.3	0.017	0.014
6	F	113.4	23.8	0.047	0.033
7	M	51.4	31.5	0.017	0.035
8	F	98.5	45.5	0.041	0.064
9	M	228.7	105.9	0.074	0.116
10	F	62.4	15.5	0.026	0.022
11	F	509.0	231.7	0.210	0.324

*Note.* MCA = malathion mono-carboxylic acids; DCA = malathion di-carboxylic acids.

<sup>a</sup>F = female and M = male, which are considered to weigh, as default values, 55 and 70 kg of body weight, respectively.

<sup>b</sup>Biological reference values proposed in this study for MCA and DCA are respectively 44 and 13 nmol/kg in 24-h urine samples.

## CAPTIONS TO FIGURES

**Figure 1.** Conceptual representation of the kinetics of malathion and its metabolites. Symbols are described in Table 1.

**Figure 2.** Model simulations (lines) compared with experimental data of Feldmann and Maibach (1974) (symbols) on the cumulative urinary excretion time course of total  $^{14}\text{C}$  (% of administered dose) in male human volunteers following an intravenous (A) and dermal (B) exposure to 1  $\mu\text{Ci}$  of  $^{14}\text{C}$ -malathion. Each point represents mean value of experimental data ( $n = 6$  per exposure group).

**Figure 3.** Model simulations (lines) compared with experimental data of Maibach *et al.* (1971) (symbols) on the cumulative urinary excretion time course of total  $^{14}\text{C}$  (% of administered dose) in male human volunteers following a dermal exposure to  $^{14}\text{C}$ -malathion ( $4 \mu\text{g}/\text{cm}^2$ ) on the forearm ( $\times$ ), the palm of the hand (+), the hand dorsum ( $\square$ ) and the forehead ( $\diamond$ ). Each point represents mean value of experimental data ( $n = 6$  per exposure group).

**Figure 4.** Model simulations (lines) compared with experimental data of Dennis and Lee (1999) (symbols) on the cumulative urinary excretion time course of phosphoric derivative metabolites (the sum of DMDTP, DMTP and DMP) (nmol) in human volunteers following a dermal exposure (on an intact skin) to an aqueous-based head

lice formulation containing on average 0.126 g of malathion (O) and an alcohol-based head lice formulation containing on average 0.089 g of malathion (□). Each point represents mean value of experimental data ( $n = 5$  to 10 volunteers per treatment group).

**Figure 5.** Simulation of the time course of malathion and its metabolites (% of administered dose) in body (A) and excreta (B) compartments of the model following a single oral exposure to malathion.  $B(t)$ , malathion in blood and tissues in dynamical equilibrium with blood as a function of time;  $S(t)$ , malathion in storage tissues as a function of time;  $M(t)$ , total metabolites in the body as a function of time;  $Q(t)$ , systemic body burden of malathion and its metabolites as a function of time;  $U_{MCA}(t)$ , MCA metabolite in urine as a function of time,  $U_{DCA}(t)$ , DCA metabolite in urine as a function of time,  $U_{MP}(t)$ , phosphoric derivative metabolites in urine as a function of time. For comparison purposes, Figure 5B also shows the average urinary excretion of MCA (×), DCA (O) and phosphoric derivatives (□) during the 0-12, 0-24 and 0-48 h following an oral administration of 0.5, 1.5, 10 and 15 mg/kg of malathion in volunteers, as determined from the data of Jellinek *et al.* (2000).

**Figure 6.** Simulation of the time course of malathion and its metabolites (% of administered dose) in the model compartments following a single dermal exposure to malathion.  $B(t)$ , malathion in blood and tissues in dynamical equilibrium with blood as a function of time;  $S(t)$ , malathion in storage tissues as a function of time;  $M(t)$ , total metabolites in the body as a function of time;  $Q(t)$ , systemic body burden of malathion

and its metabolites as a function of time;  $U_{MCA}(t)$ , MCA metabolite in urine as a function of time,  $U_{DCA}(t)$ , DCA metabolite in urine as a function of time,  $U_{MP}(t)$ , phosphoric derivative metabolites in urine as a function of time.

**Figure 7.** Simulation of the time course of malathion and its metabolites (fraction of absorbed daily dose) in the model compartments following a repeated dermal exposure to malathion, 8 h/day, 5 consecutive days/week for 4 weeks.  $B(t)$ , malathion in blood and tissues in dynamical equilibrium with blood as a function of time;  $S(t)$ , malathion in storage tissues as a function of time;  $M(t)$ , total metabolites in the body as a function of time.

Fig. 1

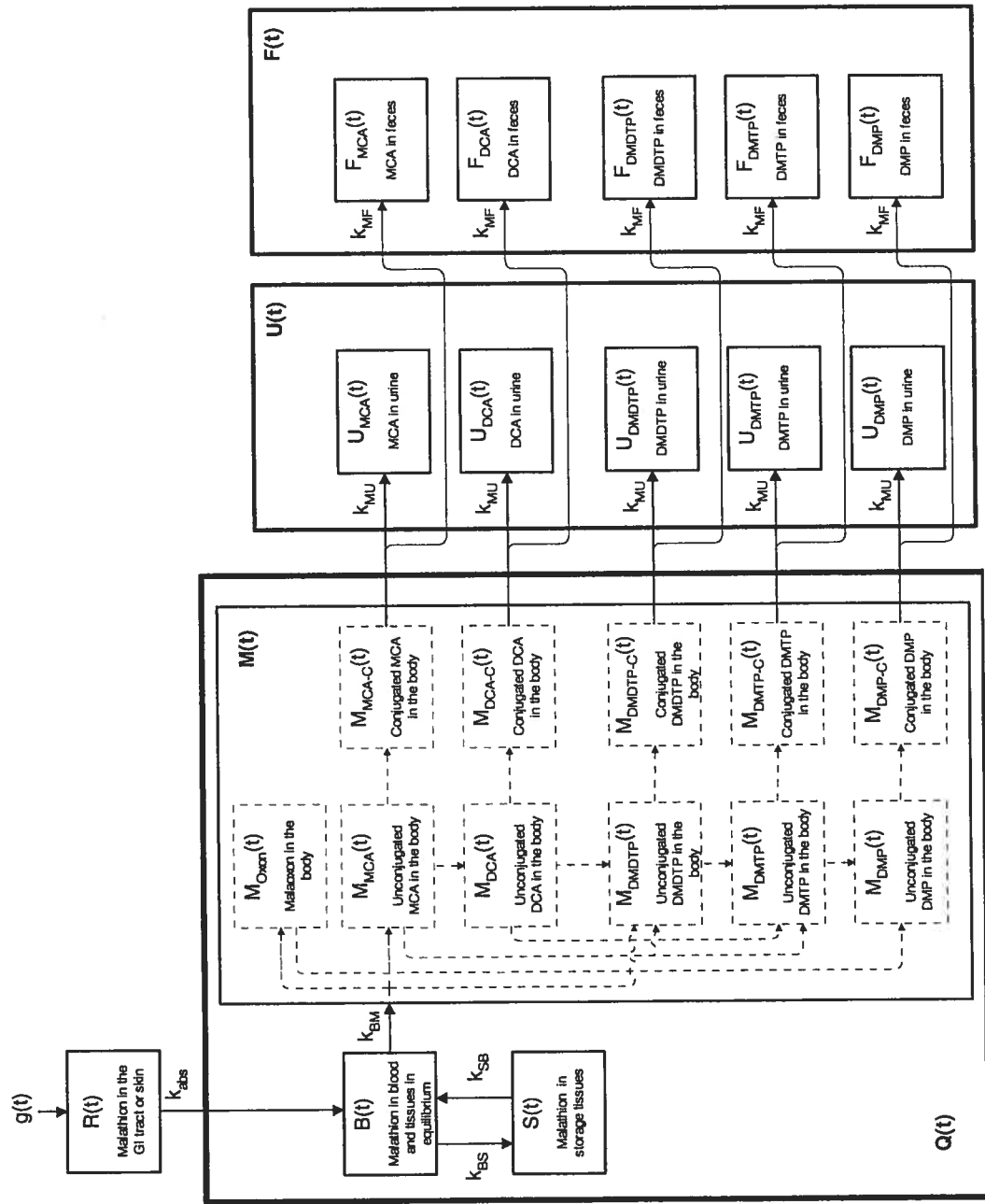


Fig. 2.

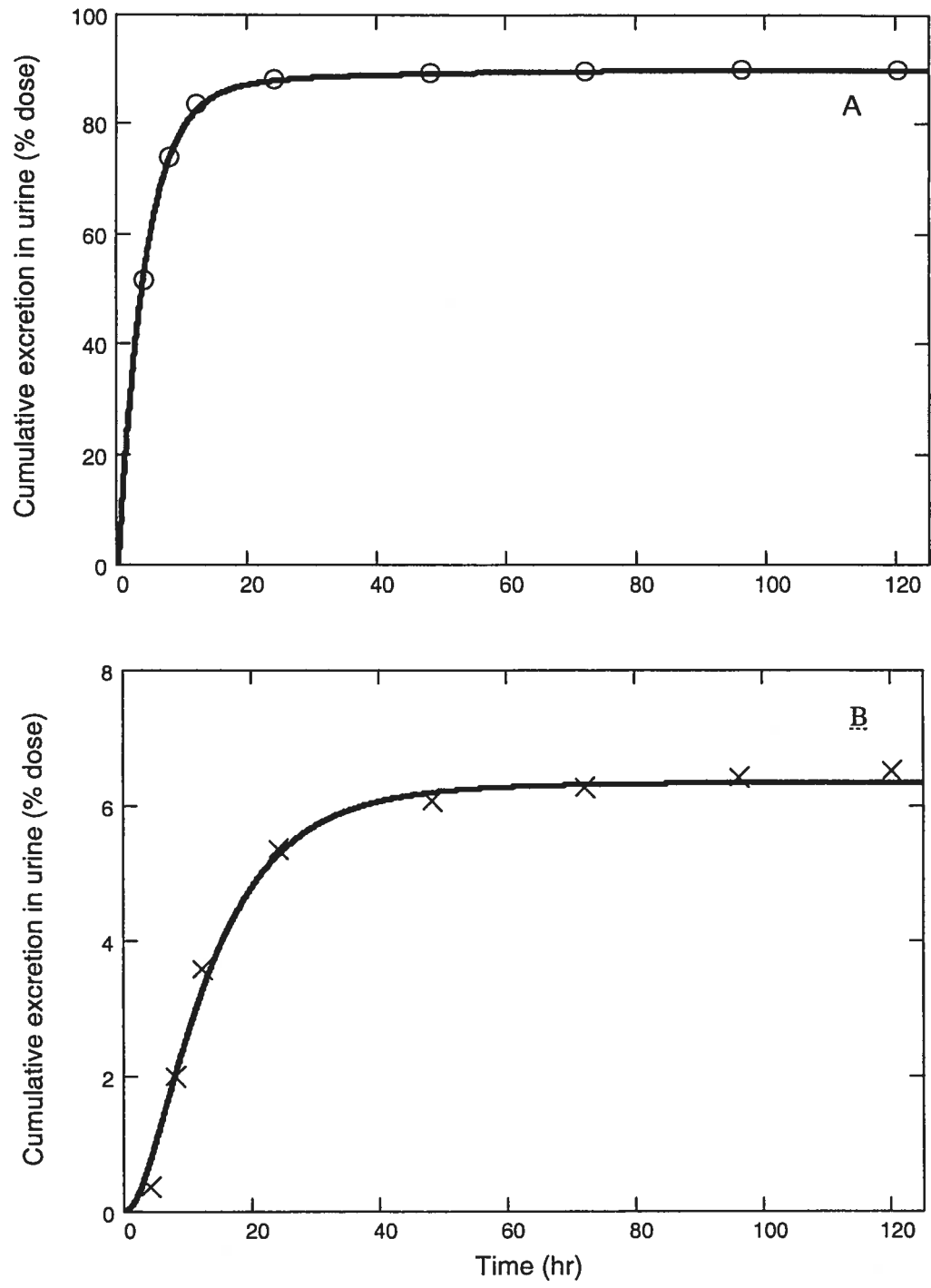


Fig. 3.

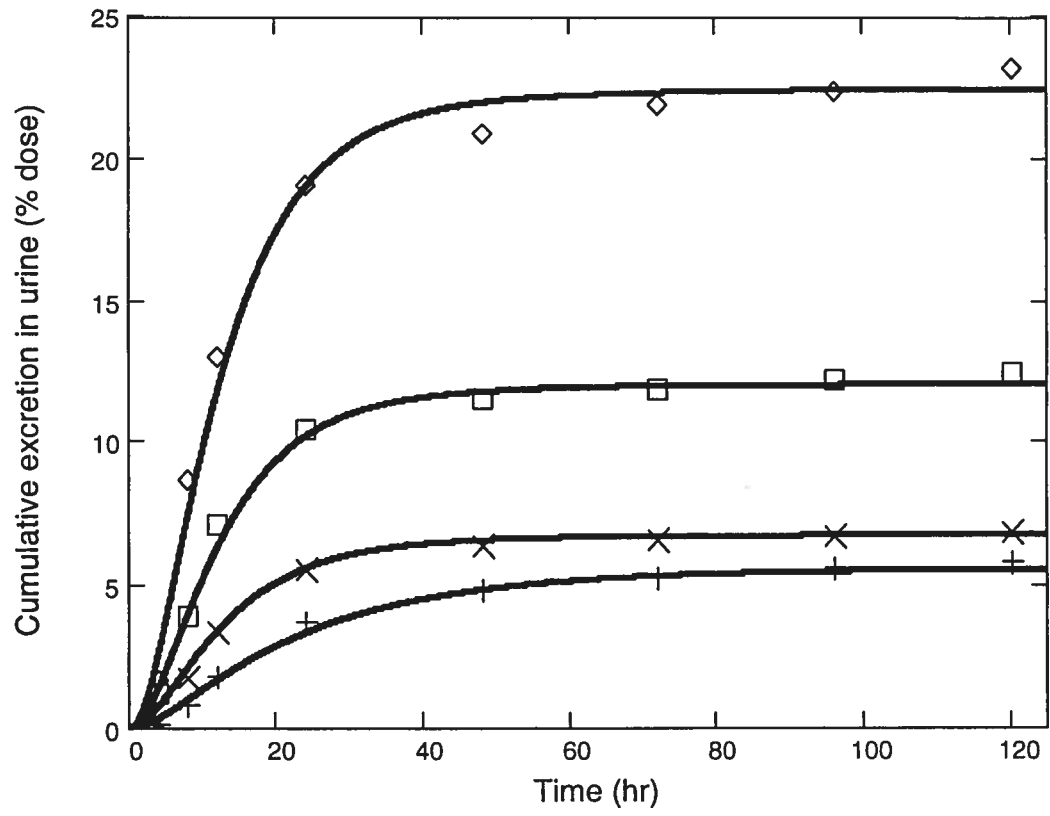


Fig. 4.

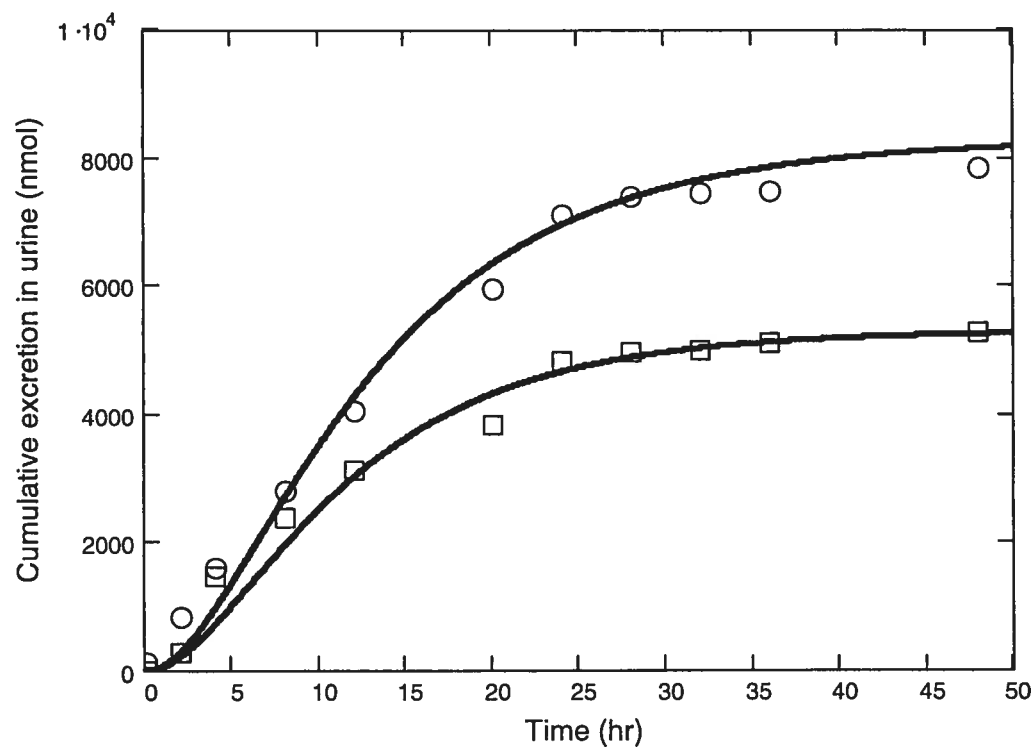


Fig. 5.

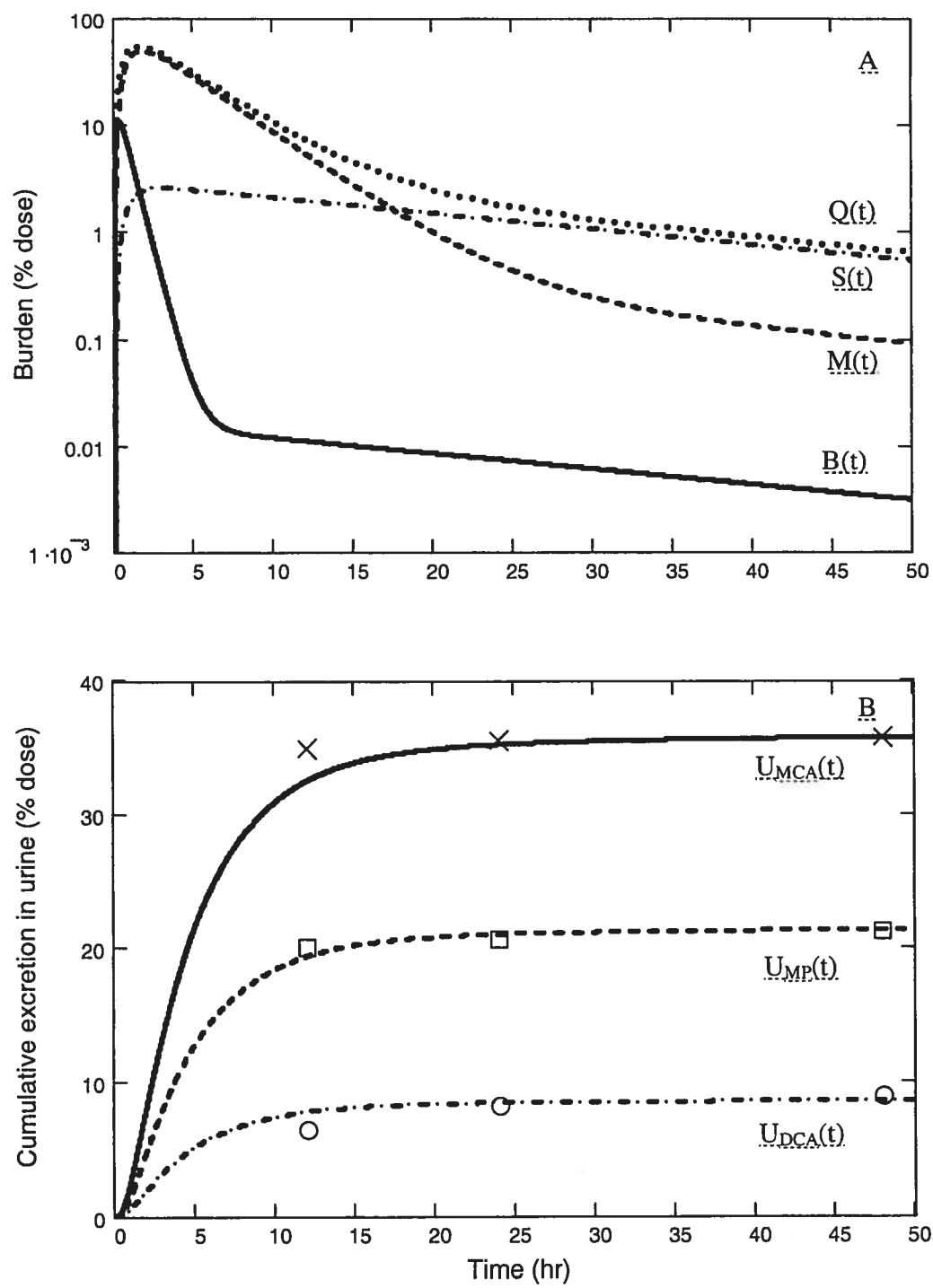


Fig. 6.

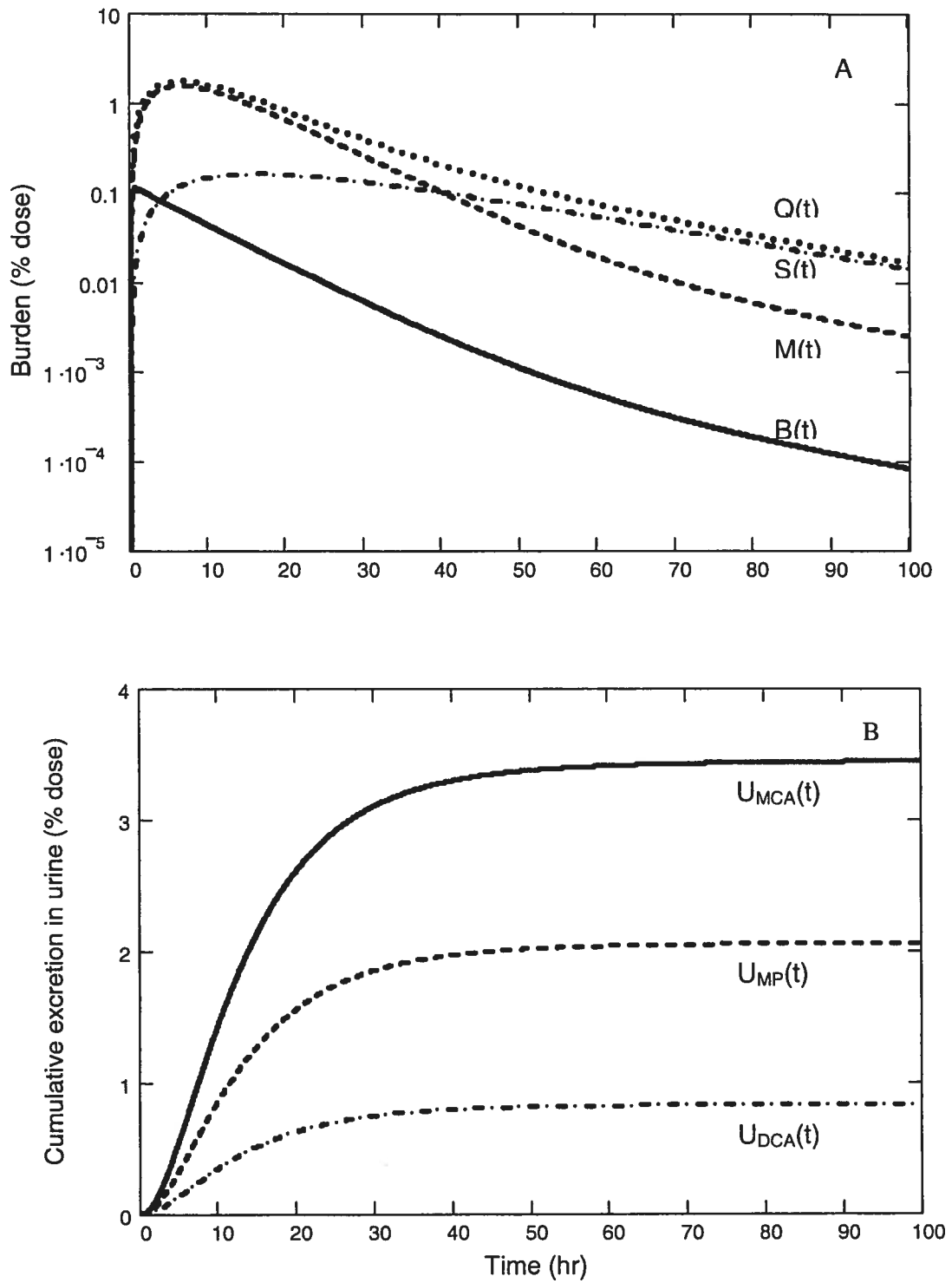
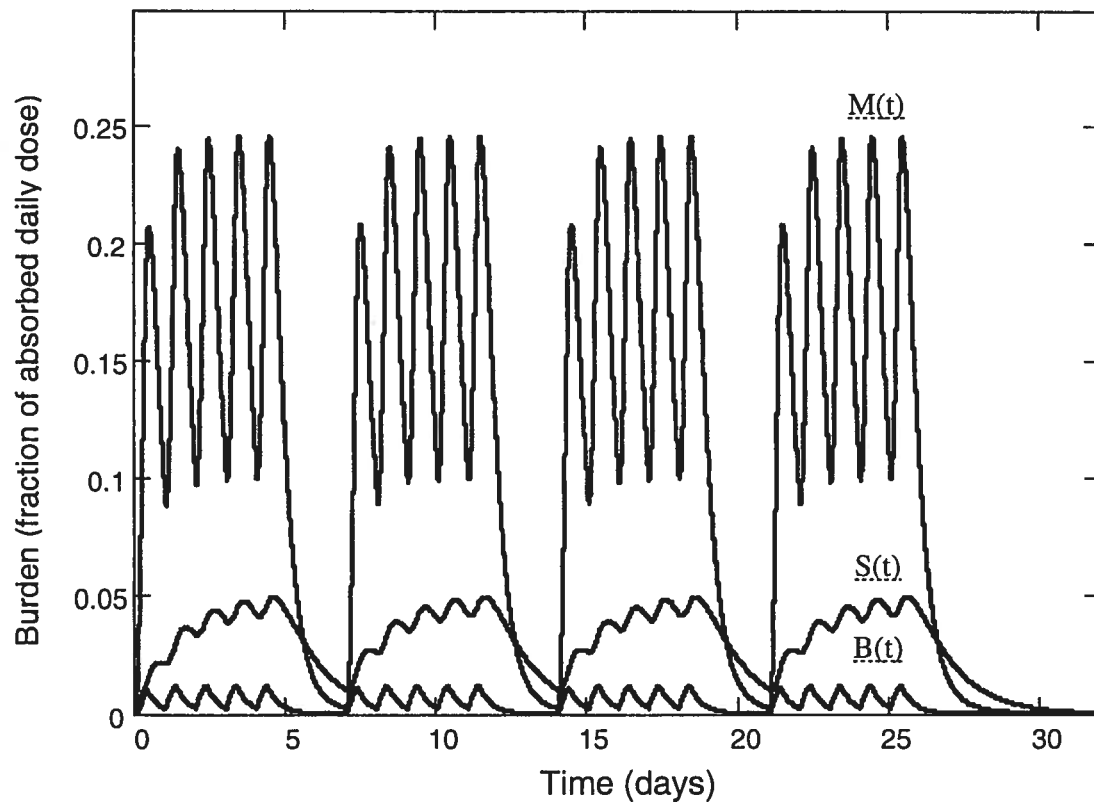


Fig. 7.



**CHAPITRE 4 : ARTICLE 2, PARATHION**

Cet article a été publié en janvier 2005 dans *Toxicology Mechanism and Methods* 15, pages 33-52.

**Toxicokinetic Modeling of Parathion and Its Metabolites in Humans  
for the Determination of Biological Reference Values**

Nathalie H. Gosselin<sup>\*</sup>, Michèle Bouchard<sup>\*</sup>, Robert C. Brunet<sup>†</sup>, Marie-Josée Dumoulin<sup>\*</sup>  
and Gaétan Carrier<sup>\*</sup>

<sup>\*</sup> Chaire en analyse des risques toxicologiques pour l'humain and Département de santé environnementale et santé au travail, Faculté de Médecine, Université de Montréal, P.O. Box 6128, Main Station, Montreal (Quebec), Canada, H3C 3J7

<sup>†</sup> Département de Mathématiques et de Statistique and Centre de Recherches Mathématiques, Faculté des arts et des sciences, Université de Montréal, P.O. Box 6128, Main Station, Montreal (Quebec), Canada, H3C 3J7

Running title: Modeling of parathion kinetics

Offprint requests: Gaétan Carrier  
Département de Santé environnementale et santé au travail  
Université de Montréal  
P.O. Box 6128, Station centre-ville, Montréal (Québec) H3C 3J7  
CANADA  
Telephone number: (514) 343-6111 ext 3108  
Fax number: (514) 343-2200  
E-mail: gaetan.carrier@umontreal.ca

## ***ABSTRACT***

A multi-compartment kinetic model was developed to describe the kinetics of parathion and its metabolites, *p*-nitrophenol (*p*-NP) and alkyl phosphates (AP), in order to assess worker exposure and health risks. Model compartments represent body burdens and excreta of parathion and its metabolites; to minimize the number of compartments and free parameters, regrouping was carried out on the basis of the time scales of the kinetic processes involved. Burden variations in time were described mathematically by differential equations that ensure conservation of mass on a mole basis. Model parameter values were determined from statistical fits to published *in vivo* kinetic data in humans. Except for the dermal absorption fraction and absorption rate, which are known to be subject to wide intra- and inter-individual variability, a single set of parameter values for the internal body kinetics enabled the model to simulate accurately the available kinetic data. For dermal exposure to parathion, with a typical absorption rate of  $0.085 \text{ h}^{-1}$ , model simulations show that it takes 20 h to recover half of the total amounts of *p*-NP eventually excreted in urine and 30 h for the AP. The model can be used to estimate the dose of parathion absorbed under different exposure routes and temporal scenarios, based on measurements of amounts of metabolites accumulated in urine over given time periods. Using the above dose-excreta links and the human no-observed-effect level for parathion reported in the literature for the inhibition of cholinesterase activities, biological reference values are proposed in the form of specific amounts of urinary metabolites excreted over chosen time periods.

**Key Words:** parathion; *p*-nitrophenol; alkyl phosphates; toxicokinetics; urinary biomarkers; risk assessment.

## ***INTRODUCTION***

Parathion (O,O-diethyl O-*p*-nitrophenyl phosphorothioate) is an organophosphorus insecticide widely used in agriculture. In humans, as in insects, this pesticide exerts its neurotoxic action by inhibiting nervous system acetylcholinesterases (AChE), enzymes responsible for the degradation of acetylcholine. Clinical signs of intoxication usually occur at an inhibition of 60-70% of the cholinesterase activity in red blood cells (RBC-AChE), an enzyme closely related to nervous system cholinesterases (Sidell, 1994). Some clinical signs and symptoms were however reported in subjects with a RBC-AChE inhibition of 30-60% (Sidell, 1994).

In 1991, due to the high toxicity of parathion, the U.S. EPA and most of the registrants of products containing parathion reached an agreement to restrict the application of parathion to agricultural crops of alfalfa, barley, corn, cotton, canola, sorghum, soybean, sunflower and wheat (U.S. EPA, 1999). Additional label restrictions which include aerial-only application and mechanical-only harvesting were further agreed upon to reduce health risks in workers (U.S. EPA, 1999). Yet, following these restrictions, some exposure incidents related to parathion spray drift or equipment maintenance have still been documented. The 1999 U.S. EPA Human Health Risk Assessment Report also states that postapplication exposure of agricultural workers remains a concern in the United States (U.S. EPA, 1999). The use of parathion is still a concern in many other countries (Denga et al., 1995; Akgür et al., 1999).

Most plausibly, occupational exposure to parathion occurs mainly through the skin due to the low volatility and high lipophilic properties of this substance. Given the large variations and uncertainties in dermal absorption, to estimate the dose of parathion that actually penetrates in the body, and consequently to assess the health risks, the measurement of biomarkers is more accurate than environmental monitoring (ACGIH, 2002).

The ACGIH<sup>®</sup>, NIOSH<sup>®</sup> and the German Commission for the Investigation of Health Hazards of Chemical Compounds in the Work Area (GCIHH) all proposed biological reference values based on the prevention of RBC-AChE inhibition. A 30% inhibition of the RBC-AChE activity compared to the individual's baseline was proposed by these three organizations as a biological limit value. However, the inhibition of RBC-AChE activity is not specific to parathion exposure but rather to the whole class of acetylcholinesterase inhibiting pesticides, namely organophosphorus and carbamate pesticides. The ACGIH<sup>®</sup> and GCIHH proposed more specific biological reference values based on the urinary concentration of *p*-nitrophenol (*p*-NP), a metabolite of parathion but also of other pesticides such as methyl parathion (O,O-dimethyl O-*p*-nitrophenyl phosphorothioate) and EPN (phenylphosphonothioic acid O-ethyl O-*p*-nitrophenyl ester). The ACGIH<sup>®</sup> proposed a biological exposure index (BEI<sup>®</sup>) of 0.5 mg of *p*-NP/g of creatinine (0.34 mmol *p*-NP/mol creatinine) and the GCIHH suggested a biological tolerance value (BAT) of 0.5 mg of *p*-NP/L of urine. Both organizations recommended collecting a spot urine sample as soon as possible after work. The *p*-NP urinary biomarker gives an earlier warning of possible adverse

cholinergic effects than the inhibition of RBC-AChE activity since *p*-NP in urine is detectable far before any inhibition of enzymatic activity occurs (Arterberry et al., 1961; Richter et al., 1992).

The proposed BEI<sup>®</sup> and BAT are expressed in concentrations, either adjusted or not for creatinine contents. For the interpretation of measurements of *p*-NP in a spot urine sample, the timing of sample collection is critical since urinary concentration values vary significantly with time. For chemicals eliminated through the kidneys by glomerular filtration or active secretion and not passively reabsorbed, as is the case for parathion metabolites (Michalke, 1984; Jokanović, 2001), the urinary concentrations decrease with increasing urinary flow rate (Boeniger et al., 1993). Although creatinine is often taken to be excreted in urine at a constant rate, several authors reported that its excretion rate is subjected to significant inter-individual variations (0.5 – 3 g/day) as well as inter-day (63 – 244%) and intra-day ( $\geq 200\%$ ) variations in the same individual (Curtis & Fogel, 1970; Greenblatt et al., 1976; Alesio et al., 1985; Boeniger et al., 1993). The main factors influencing the urinary excretion rate of creatinine are diurnal variations, body mass index, gender, age, pregnancy, diet, exercise and diuresis. These important variations with time, in either metabolite concentrations or creatinine excretion rate, suggest that the measurement of amounts of metabolites accumulated in urine over a given period of time is a more reliable means of assessing occupational health risks.

In order to make good use of amounts of urinary biomarkers as a means of determining exposure and health risks, it appears important to develop a toxicokinetic model that would permit reconstruction of the absorbed dose from biomarker measurements, and the choice of any convenient urine collection periods. This modeling should also allow simulation of different temporal scenarios (single, repeated intermittent or continuous exposures) and exposure routes (oral, dermal, respiratory). Models have been developed to describe the toxicokinetics of parathion in rodents (Sultatos, 1990; Gearhart et al., 1994) but these models did not describe the kinetics of parathion metabolites excreted in urine and were not adapted nor validated for humans.

After systemic absorption, parathion is either stored in lipids or biotransformed mainly in the liver; the biotransformation is a rapid hydrolysis to *p*-NP and diethylphosphorothioic acid (DETP), which are excreted in urine and feces, or an oxidation to paraoxon, the metabolite responsible for the inhibition of cholinesterases (Menzie, 1969; Poore & Neal, 1972; Hayes, 1982; Jokanović, 2001). According to an *in vitro* study with human liver microsomes (Mutch et al., 1999), the rate of detoxification of parathion into *p*-NP is 4 to 7 times greater than the rate of activation of parathion into paraoxon, indicating that roughly 80% of the biotransformed parathion is directly hydrolyzed to *p*-NP while 20% of parathion is converted to paraoxon. Once formed, paraoxon is either broken down by a A-esterase into *p*-NP and diethylphosphoric acid (DEP), which are excreted in urine and feces, or it binds to proteins such as AChE (Menzie, 1969; Hayes, 1982; Jokanović, 2001). Hence, less than 20% of the parathion absorbed dose forms AChE bound oxon. In rats, about 65-

74% of the amount of AChE bound oxon undergoes spontaneous hydrolysis (reversible binding) while the rest undergoes aging (irreversible binding) (Carr & Chambers, 1996). Upon binding with AChE, paraoxon releases a *p*-NP molecule (Gallo & Lawryk, 1991; Lotti, 1991; Zhang & Sultatos, 1991). In turn, the oxon reversibly bound to AChE, during hydrolysis, gives rise to DEP (Gallo & Lawryk, 1991; Lotti, 1991). The irreversibly bound oxon, upon turnover of the AChE enzyme, releases an alkyl residue, a monoethyl phosphate (Gallo & Lawryk, 1991; Lotti, 1991). The main metabolites of parathion found in urine are therefore *p*-NP and alkyl phosphates (AP): essentially DETP and DEP (see Figure 1).

The objectives of this study were thus: *i*) to develop a toxicokinetic model predicting the time course of *p*-NP and AP metabolites in human urine associated with a given absorbed amount of parathion under various exposure routes and temporal scenarios and *ii*) to propose, using model predictions, biological reference values for parathion metabolites, *p*-NP and AP, based on the measurement of cumulative amounts of metabolites in successive urine collections following the onset of occupational exposure.

## METHOD

### *Model Development*

**Conceptual and Functional Representation** The urinary excretion kinetics of parathion and its metabolites was modeled using a multi-compartment dynamical system. The conceptual model is depicted in Figure 2 and symbols and abbreviations are described in Table 1. Compartments represent the burdens or cumulative excreta of parathion or its metabolites as a function of time and arrows stand for the rates of transfer or biotransformation of parathion and its metabolites. The evolution of burdens is described mathematically by differential equations where the rate of change of the amounts in each compartment is the difference between the incoming and outgoing transfer rates (see Appendix for differential equations). Once the parameters of the internal dynamics of parathion have been determined using time course data under controlled exposure conditions, the differential equation system can then be solved for other time modulated inputs and absorption rates. The model can thus be used to predict the time courses of parathion and its metabolites under different exposure scenarios (intravenous (iv), oral, dermal and/or inhalation, single or repeated intermittent or continuous exposures).

The model uses specific input compartments,  $D(t)$ ,  $GI(t)$ ,  $RT(t)$ , to describe the amounts of parathion bioavailable at the skin surface, the gastrointestinal tract and the respiratory tract, respectively. Tissue burdens of parathion and paraoxon that rapidly reach and maintain a fixed ratio with the blood burden were regrouped with the blood

burden in a single compartment,  $B(t)$ , since all these quantities evolve in unison. Another compartment,  $S(t)$ , regroups storage tissue burdens of parathion and paraoxon that are slowly returned to blood. This  $S(t)$  compartment was introduced in the model to account for the biphasic elimination kinetics of parathion metabolites in the urine of volunteers intravenously exposed to parathion (Feldmann & Maibach, 1974). The terminal elimination phase of this urinary time course curve is most plausibly due to the slow release to blood of parathion and paraoxon accumulated in lipids or covalently bound to tissue proteins.

To simulate the time courses of the urinary biomarkers, there are two key elements to consider in the biotransformation process. The first one: each mole of parathion in the body is eventually broken down into one mole of  $p$ -NP and one mole of AP (DETP, DEP or other alkyl phosphates), either directly or through the formation of paraoxon (Menzie, 1969; Gallo & Lawryk, 1991; Lotti, 1991; Zhang & Sultatos, 1991; Jokanović, 2001). This requires two distinct mass balance differential equation systems (on a mole basis), one for the production and elimination of  $p$ -NP and another for AP (see the Appendix for differential equations). The second one: phase I and phase II biotransformation of parathion and paraoxon into  $p$ -NP or AP occurs on a much more rapid time-scale than renal and fecal clearance of the metabolites (Michalke, 1984). Consequently, the rate of formation of  $p$ -NP or AP, directly from parathion or through the formation of paraoxon, is very rapid compared to the relatively slow metabolite elimination.

It was also considered that as soon as the AP or *p*-NP metabolites are formed, they rapidly undergo phase II conjugations (Michalke, 1984) and become highly hydrosoluble. Single metabolite specific compartments,  $M_{AP}(t)$  or  $M_{NP}(t)$ , were thus used to represent either AP (the sum of DETP and DEP) or *p*-NP burdens in blood and in tissues in dynamic equilibrium with blood (for short, compartments  $M_{AP}(t)$ ,  $M_{NP}(t)$  and  $B(t)$  will usually be referred to as blood burden compartments). The compartments  $M_{AP}(t)$  and  $M_{NP}(t)$  comprise the sum of free and conjugated forms of the metabolites since, in the studies used to develop the model, total *p*-NP and AP were measured analytically, after acidic or enzymatic hydrolysis of samples (Elliott et al., 1960; Shafik et al., 1973a,b; Michalke, 1984).

Analysis of the experimental data of Feldmann and Maibach (1974) and Michalke (1984) further served to detail the part of the model representing the kinetics of *p*-NP and AP metabolites. Michalke (1984) reported the concentration-time course of *p*-NP in the blood and urine of a subject intoxicated with parathion. The first two biological specimens were collected 30 min and 10 hr after parathion ingestion. Maximum concentration of *p*-NP in blood was observed in the first collection sample, whereas, maximum concentration in urine was seen in the second sample. This shows that: *i*) *p*-NP is formed rapidly from parathion and paraoxon and *ii*) its subsequent rapid disappearance from blood but long delay before recovery in urine stems most plausibly from a retention of *p*-NP in the kidney. This delay was also observed in animal studies on the detailed time courses of [ $^{14}\text{C}$ ]-*p*-NP in blood and urine (Qiao et al., 1994, 2000; Abu-Qare et al., 2000). This delayed excretion is modeled by the introduction of a

holding compartment  $K_{NP}(t)$  that retains *p*-NP prior to excretion in urine. In a similar matter, the available urinary excretion kinetic data on AP, reported by Feldmann and Maibach (1974), show that peak excretion rate of AP in urine was not reached until 10 hr following an iv injection of labeled parathion in volunteers, indicating a long delay between the rapid biotransformation of parathion and the excretion of its AP metabolites. Indeed, these authors described the time course of total ethyl- $^{14}\text{C}$  excretion rate in the urine of 6 volunteers exposed iv to 1  $\mu\text{Ci}$  of ethyl- $^{14}\text{C}$ -labeled parathion (dose in mole or in gram was not specified). Given that parathion was marked on the alkyl group, the kinetics of AP was followed in that study. In the model, a holding compartment  $K_{AP}(t)$  that retains AP prior to excretion in urine was therefore introduced to account for the observed time of maximum urinary excretion rate of AP.

The compartment  $U_{AP}(t)$  represents the cumulative excretion of total AP observed in urine and  $F_{AP}(t)$  the cumulative excretion of total AP excreted otherwise and not measured, similarly for total *p*-NP with  $U_{NP}(t)$  and  $F_{NP}(t)$ . The metabolite burdens not excreted through urine are likely excreted via feces, as evidenced from mass-balance data in animals (Nye & Dorough, 1976; Prakashchandra & Guthrie, 1983; Carver & Riviere, 1989).

**Determination of the Parameters** The studies of Feldmann and Maibach (1974), Hayes et al. (1964), Hartwell et al. (1964), Maibach et al. (1971) and Morgan et al. (1977) were used to determine model parameter values. Figures reported in those

studies were scanned and the experimental values were read using a Sigma Plot Graphing Software (Jandel Corporation, San Rafael, CA).

Most of the model parameter values were first estimated by least square fits of the approximate analytical solutions of the differential equations to the appropriate human time course data available in the literature. The different time scales involved in the biological processes provided these approximate solutions following the quasi steady state theory (Segel, 1988; Segel & Slemrod, 1989). Starting with these first estimations, the model parameter values were further adjusted by least square fits of exact numerical solutions of the differential equation system to the experimental time course data. A professional edition of a MathCad software was used for this purpose (MathSoft Inc., Cambridge, MA). In the following, the published data used for the determination of each model parameter value are presented.

*Parathion and Paraoxon Kinetics:* The parameter  $k_{BM}$  represents the rate of appearance of *p*-NP or AP in the blood compartment, *i.e.*, the rate at which blood parathion and paraoxon are broken down into *p*-NP and AP. It was determined from the data of Michalke (1984) on the time course of blood *p*-NP in a subject exposed to parathion. According to these data, the maximum concentration of *p*-NP in blood was observed during the initial sampling, that is 30 min postexposure, suggesting that most of the parathion is metabolized by that time. The half-life for the appearance of *p*-NP in blood is thus of the order of 6 min and hence the  $k_{BM}$  biotransformation rate was taken to be  $6.93 \text{ h}^{-1}$ . This rapid biotransformation is supported by the animal data of Sultatos

(1990) on the concentration-time course of parathion in blood, liver, lungs and brain of mice exposed iv to parathion.

The slow transfer rate  $k_{SB}$  of stored parathion and paraoxon back to the blood compartment  $B(t)$  was determined from the data of Feldmann and Maibach (1974) by log-linear regression of the time course of average total ethyl- $^{14}C$  urinary excretion rate during the terminal phase (36 to 120 h) following an iv injection of ethyl- $^{14}C$  parathion in volunteers. The parathion and paraoxon storage rate  $k_{BS}$  was also estimated from the iv data of Feldmann and Maibach (1974) by least square fits of the numerical solution of the differential equation system to the time course of average total ethyl- $^{14}C$  urinary excretion rate 0-120 h postexposure.

*AP Kinetics:* The proportion of blood AP that is eventually excreted in urine as

compared to feces,  $f_{U-AP} = \frac{k_{MK-AP}}{k_{MK-AP} + k_{MF-AP}}$ , was determined also from the iv data of

Feldmann and Maibach (1974) on the average amounts of total ethyl- $^{14}C$  recovered overall in the urine of volunteers during the 120-h collection period, assuming that the urinary excretion of AP is complete at that time. The transfer rates  $k_{MK-AP}$  and  $k_{KU-AP}$  describing the kinetics of urinary AP were estimated by least square fits of the differential equation solution to the iv time course data reported by Feldmann and Maibach (1974) on the urinary excretion rate 0-120 h postexposure.

*p*-NP Kinetics: The proportion of blood *p*-NP that is eventually excreted in urine as compared to feces,  $f_{U-NP} = \frac{k_{MK-NP}}{k_{MK-NP} + k_{MF-NP}}$ , was obtained from the study of Morgan et al. (1977), which reports the percent of *p*-NP excreted in the urine of volunteers ( $n = 4$ ) following an oral administration of 1 or 2 mg of parathion.

The transfer rates  $k_{MK-NP}$  and  $k_{KU-NP}$  describing the kinetics of urinary *p*-NP were estimated by least square fits of the differential equation solution to the data of Hartwell et al. (1964) on the time course of average *p*-NP urinary excretion rate in a volunteer following a 2.5-h inhalation exposure to parathion vapors at 38°C. Respiratory exposure was considered, for input to the model, as equivalent to a drop by drop exposure with instantaneous absorption of inhaled vapors.

*Dermal Absorption Parameters for Parathion:* The parameter  $f_{abs-dermal}$  describes the fraction of the exposure dose that will be absorbed into the systemic circulation. The parameter  $k_{abs-dermal}$  describes the dermal absorption rate of parathion from skin layers, epidermis or dermis, to the systemic circulation. There are known intra- and inter-individual variations in the skin absorption of chemicals depending on the anatomical region of the skin exposed, the skin condition and the environmental temperature and humidity (Maibach et al., 1971; Bronaugh & Maibach, 1999; ACGIH, 2002). These variations appear important for parathion absorption according to the data of Maibach et al. (1971). To account for this variability, the absorption parameter values,  $k_{abs-dermal}$  and  $f_{abs-dermal}$ , were adjusted to the different dermal data sets. However, to ensure the unity of the model, a single set of parameter values was used to describe the kinetics of

parathion and its metabolites once parathion is absorbed in the blood stream. A sensitivity analysis was achieved to study the impact of variations in the dermal absorption rate on metabolites urinary excretion.

The model was used to simulate the data of Feldmann and Maibach (1974) along with the data of Maibach et al. (1971) both on the urinary time course of average ethyl-<sup>14</sup>C equivalents in volunteers exposed to dermal doses of ethyl-<sup>14</sup>C parathion. Feldmann and Maibach (1974) applied 1  $\mu$ Ci of ethyl-<sup>14</sup>C parathion on the forearms of 6 male volunteers (dose in mole or in gram not specified). Maibach et al. (1971) applied 1  $\mu$ Ci of ethyl-<sup>14</sup>C parathion on 13 skin regions of male volunteers ( $n = 6$  per exposure group; dose in mole or g not specified). The most common dermal exposure scenarios reported by these authors were simulated with the model, *i.e.* exposures either on the forearm, the palm, the hand dorsum or the scalp.

The data of Hayes et al. (1964) on the urinary excretion kinetics of *p*-NP was also simulated. These authors established the time course of *p*-NP excretion rate in the urine of a male volunteer exposed 2 h per day, on 5 successive days, to 5 g of 2% parathion dust on the right hand and forearm secured in a polyethylene bag. During the 2-h daily exposure, the temperature was kept constant at 41°C.

**Model Simulations** Once the parameters of the model were determined as described above, simulations of the time courses of parathion and its metabolites in the body and in excreta were carried out by solving numerically the differential equation systems

using the Runge-Kutta method incorporated in MathCad. The same set of parameter values was used to describe the kinetics of parathion once absorbed and that of its metabolites. Only the absorption rates were adjusted according to the site-of-entry. Simulations of different temporal exposure scenarios, where continuous or repeated intermittent doses are administered through time, were performed by introducing time varying inputs (see Appendix).

### ***Sensitivity Analysis***

The capacity of each model parameter value to influence the predicted 12- and 24-h urinary excretion was tested. The model parameter values, obtained above from fits to published mean excretion data, were separately varied as far as  $\pm 50\%$ . The sensitivity tests were based on the following normalized sensitivity coefficient:  $R = \frac{(O_2 - O_1)/O_1}{(I_2 - I_1)/I_1}$

where  $I_1$  is the default value of the parameter analyzed for sensitivity,  $I_2$  its modified value and where  $O_1$  is the predicted 12- or 24-h cumulative urinary using default parameter values,  $O_2$  its predicted value with the modified parameter values.

### ***Establishment of Biological Reference Values***

The biological reference values proposed in the current study are expressed as cumulative amounts of *p*-NP or AP in urine collected over different periods of time following the onset of an exposure to parathion. These values are generated by simulating an 8-h dermal exposure, where the daily absorbed dose corresponds to a human no-observed-effect level (NOEL) reported in the available literature on blood

cholinesterase inhibition following controlled exposures. To provide a safety margin and to protect the more susceptible workers, the slowest absorption rate compatible with the various dermal experimental data presented above was used for these simulations. Further, background values were considered negligible.

**Human NOEL for the Establishment of the Biological Reference Values** Human NOELs for parathion have been reported by Edson et al. (1964) and Rider et al. (1969), based on the inhibition of plasma pseudocholinesterase (plasma-ChE) or RBC-AChE activities in volunteers exposed orally to parathion. In all these studies, volunteers were repeatedly exposed to parathion over more than a month resulting in a response representative of a worker exposure. The clinical signs or symptoms of toxicity were monitored throughout the course of the experiment, but none were observed.

Data provided in the aforementioned studies was reanalyzed since the cholinesterase activity reduction considered then as significant for the determination of the reported NOELs was different from that suggested by several other authors. Given the large inter- and intra-individual variability in baseline plasma-ChE and RBC-AChE activities of unexposed individuals, the inhibition was considered as significant when the degree of inhibition of exposed subjects compared to their baseline activity was  $\geq 19\%$  for plasma-ChE and  $\geq 12\%$  for RBC-AChE (Gage, 1967; Larsen & Hanel, 1982; Heath & Vale, 1992).

Edson et al. (1964) exposed volunteers orally to parathion, once a day, 5 days per week, during 5 to 14 consecutive weeks. The dosage regimens were 0, 0.6, 1.2, 2.4, 4.8 and 7.2 mg/day ( $n = 4$  per exposure group). Plasma-ChE and RBC-AChE activities were measured before, during and after the exposure period. In the group exposed to 7.2 mg/day, an inhibition of 33% of the plasma-ChE activity (*i.e.*, 67% of control activity) and 16% of the RBC-AChE activity (*i.e.*, 84% of control activity) was observed after 6 weeks of exposure. For the other dose regimens, no significant inhibition was reported. From these observations and the cholinesterase inhibition criteria mentioned above, the human NOEL dose value retained for the establishment of our suggested biological reference values was 4.8 mg/day (*i.e.*, 58  $\mu\text{g}/\text{day}/\text{kg}$  of body weight (bw)) as determined by Edson et al. (1964). In the absence of adequate human experimental data, the oral absorption fraction was assumed to be 100%, a value observed in dogs (Braeckman et al., 1983).

The human NOEL dose value of 58  $\mu\text{g}/\text{kg}\text{-bw}/\text{day}$  is corroborated by the experimental study of Rider et al. (1969). The latter authors administered parathion orally to male prisoners during approximately 30 consecutive days. Four groups of 5 volunteers ingested 3, 4.5, 6 or 7.5 mg of parathion per day (or 40, 60, 80 and 100  $\mu\text{g}/\text{kg}\text{-bw}$ , assuming a body weight of 75 kg). The analysis of plasma-ChE and RBC-AChE activities measured in volunteers shows that the NOEL dose of this study is 4.5 mg/day (or 60  $\mu\text{g}/\text{kg}\text{-bw}/\text{day}$ ).

## **RESULTS**

### ***Model Simulations***

Table 2 presents parameter values of the model obtained from fits to available experimental data. With these values, the model reproduced closely the data of Feldmann and Maibach (1974) on the time course of total ethyl-<sup>14</sup>C excretion in the urine of human volunteers exposed to either a single iv or a dermal dose of ethyl-<sup>14</sup>C parathion (Figure 3). The excretion rate data of Feldmann and Maibach (1974) following iv injection, when converted to cumulative values, show that, at the end of the observation period (120 h), 46% of the dose is excreted in urine as AP. Therefore, in the model, the urinary fraction  $f_{U-AP}$  was set to 0.46; the rest is eliminated by other means, most plausibly via the feces. In the data of Feldmann and Maibach (1974) for a dermal dose, only 10% is finally recovered in urine. Combining this with the results of the iv experiment, indicating that only 46% of an absorbed dose is finally excreted as AP in urine, leads to a dermal absorption fraction,  $f_{abs-dermal}$ , equal to 0.21, *i.e.*  $0.21 \times 0.46 = 0.10$ . The absorption rate compatible with the dermal data reported by these authors was found to be  $k_{abs-dermal} = 0.085 \text{ h}^{-1}$ .

The proposed model, with the parameter values of Table 2 describing the kinetics of absorbed parathion and that of AP metabolites, was also applied to the data of Maibach et al. (1971) on the urinary excretion time profiles of total ethyl-<sup>14</sup>C in human volunteers to whom was applied ethyl-<sup>14</sup>C parathion on different skin regions of the body (Figure 4). The data of Maibach et al. (1971) indicated large variations in the

dermal absorption fraction and rate depending on the exposed skin site. For proper model simulations of these data, the average dermal absorption fractions compatible with the data were 0.19, 0.26, 0.46 and 0.72 for applications to the forearm, the palm of the hand, the hand dorsum and the scalp, respectively, while the corresponding absorption rates were 0.06, 0.04, 0.15 and 0.07 h<sup>-1</sup>.

The model, with the parameter values of Table 2 describing the kinetics of absorbed parathion and that of *p*-NP, gave a good fit to the data of Hartwell et al. (1964) on the time course of urinary *p*-NP in a volunteer exposed to parathion vapors by inhalation (Figure 5). The model was also found to predict correctly the data of Hayes et al. (1964) on the time course of *p*-NP excretion in the urine of a volunteer repeatedly exposed to parathion dust through dermal contact at an exposure temperature of 41°C (Figure 6). At this relatively high exposure temperature, the dermal absorption rate (0.5 h<sup>-1</sup>) was found to be much greater than was the case in the studies of Feldmann and Maibach (1974) and Maibach et al. (1971) mentioned above.

The model was also tentatively applied to the data of Michalke (1984) on the cumulative urinary excretion time course of *p*-NP metabolite in a subject intoxicated with parathion, to estimate the unknown absorbed dose. The model provided a close fit to the data presented by this author using the model parameters reported in Table 2 for the kinetics of absorbed parathion and that of *p*-NP along with an oral absorption rate of 0.8 h<sup>-1</sup> (Figure 7). This oral absorption rate value is also compatible with the data on chlorpyrifos, a related compound (Nolan et al., 1984). No saturation function was

necessary to obtain a good fit. Using the value for the urinary *p*-NP fraction reported by Morgan et al. (1977)  $f_{U-NP} = 0.37$ , the model estimates that the absorbed dose of this intoxicated subject was 860  $\mu\text{mol}$  (250 mg).

The model was also used to reproduce the kinetics of parathion and its metabolites under the exposure conditions of agricultural and horticultural workers. Without regard for the specific absorption fraction, the model can be used to reconstruct the actual dose of parathion absorbed in the body of a worker from the amounts of metabolites excreted in urine. Figure 8 compares model simulation to the data of Wolfe et al. (1970) on the time course of *p*-NP cumulative excretion in the urine of an orchard worker applying a formulation containing parathion during a single 8-h period. A good fit to the time course data of this worker was achieved by considering that bioavailable parathion penetrated in the body at a constant rate of  $0.3 \text{ h}^{-1}$  and that, although absorption occurred mostly on the day of application, it continued to some extent on the days following the spraying episode. The absorption rate used here is typical of a dermal exposure under high ambient temperatures as reported by Wolfe et al. (1970). It is compatible with the study of Hayes et al. (1964), which suggests that high exposure temperature accelerates the passage of parathion through the skin. This absorption rate value could also reflect a combined dermal and respiratory exposure. From the cumulative urinary excretion time course data depicted in Figure 8, the overall dose of parathion absorbed in the body of the worker was estimated to be 23  $\mu\text{mol}$  (6.7 mg).

### *Sensitivity Analysis*

Sensitivity analysis were conducted on model parameters using default values reported in Table 2. Under typical worker exposure conditions, a daily dermal exposure over 8 consecutive hours, sensitivity tests through model simulations (see Table 3) have shown that the dermal absorption rate  $k_{\text{abs-dermal}}$  and the excretion rate parameter  $k_{\text{KU}}$  were the main parameters governing the 12- and 24-h cumulative urinary excretion. The effect of variations in these latter rates was more important than the impact of variations in parathion biotransformation rate  $k_{\text{BM}}$ . In sensitivity tests, it was shown that the exact value for the biotransformation rate  $k_{\text{BM}}$  had little bearing on metabolites excretion kinetics provided parathion partitioning between storage and metabolism ( $k_{\text{BS}}/k_{\text{BM}}$ ) remained fixed.

### *Determination of Biological Reference Values*

Biological reference values for *p*-NP and AP amounts in urine samples collected over different time periods are presented in Table 4. To ensure that these biological references values were derived with a safety margin, model inferences under different input conditions are considered in the following.

Figure 9 shows that use of the slowest possible dermal absorption rate ( $k_{\text{abs-dermal}}$ ) is essential in establishing protective biological reference values. For example, when simulating a dermal exposure to parathion where the absorbed dose over 8 h corresponds to the NOEL dose, using a  $k_{\text{abs-dermal}}$  value of  $0.3 \text{ h}^{-1}$ , yields a 24-h cumulative urinary amounts of 55 nmol/kg-bw for *p*-NP and 41 nmol/kg-bw for AP,

whereas using a  $k_{\text{abs-dermal}}$  value of  $0.04 \text{ h}^{-1}$ , the corresponding values are 24 nmol/kg-bw for *p*-NP and 15 nmol/kg-bw for AP. This illustrates that, for dermal exposure, the absorption rates can strongly limit metabolite excretion rates. The effect of the absorption rate on the cumulative urinary amounts reflects the importance of establishing biological reference values based on the simulation of a dermal exposure scenario rather than a pulmonary or oral exposure. In the latter exposures, absorption is so rapid that excreted amounts over a period of time are much larger for a given absorbed dose.

Table 5 illustrates that the determination of biological reference values without consideration of a background also contributes to provide values with a safety margin. As shown in Table 5, when simulating a repeated 8 h/day dermal exposure to parathion, 5 days per week, Monday to Friday, typical of a worker exposure, with an absorption rate of  $0.04 \text{ h}^{-1}$ , daily urinary amounts of *p*-NP and AP are shown to increase over the course of a work-week. Predicted daily urinary excretion of *p*-NP and AP on Friday is, respectively, about 3 and 6 times the values predicted on Monday. This increase occurs because there is not enough time available between the end of a work-shift and the beginning of the next work-shift for the total excretion of metabolites stemming from the daily absorbed dose.

Figure 10A also shows that, when considering this typical worker exposure scenario with a slow absorption rate,  $k_{\text{abs-dermal}} = 0.04 \text{ h}^{-1}$ , a significant fraction of the absorbed daily dose from the previous day remains in the skin layers, epidermis or dermis, and

has not yet reached the systemic circulation. Under this repeated exposure scenario, accumulation of parathion or paraoxon in storage tissues  $S(t)$  further contributes to the increase in the daily urinary excretion of parathion metabolites as the week progresses (see Figure 10B).

If a much faster dermal absorption rate is considered,  $k_{\text{abs-dermal}} = 0.3 \text{ h}^{-1}$ , for these repeated exposures, Figure 10A shows that there is no accumulation from one exposure day to another in the skin burden of parathion. However, even with this rapid dermal absorption, the daily urinary excretion tends to be higher at the end of the work-week, due to the effect of the tissue storage build up and slow release to blood (see Figure 10B). For instance, on the first exposure week, Monday daily urinary excretion of AP is 20.7% of the absorbed daily dose as compared to 45.4% on Friday. It is also noteworthy that, for any  $k_{\text{abs-dermal}}$  values between 0.04 and  $0.3 \text{ h}^{-1}$ , after two weeks of repeated exposures, 8 h/day, 5 days/week, there are no further week to week increase in the daily urinary excretion values of either *p*-NP or AP.

Table 6 presents the cumulative urinary excretion of *p*-NP and AP generated from simulations of either an instantaneous or a 4-h dermal exposure, where the total absorbed dose corresponds to  $58 \mu\text{g}/\text{kg-bw}$ . Since workers are rarely exposed to pesticides for more than 8 consecutive hours, comparison of Table 4 and Table 6 shows that consideration of an 8-h temporal exposure scenario rather than a shorter exposure duration leads to smaller *p*-NP and AP urinary excretion values and thus safer biological reference values based on urinary excretion.

Figure 11 shows simulations of the concentration-time course of *p*-NP in urine following a dermal absorption typical of a daily worker exposure, where the total absorbed dose corresponds to the NOEL. The concentration was obtained by dividing the time-dependent *p*-NP urinary excretion rate ( $\frac{dU_{NP}(t)}{dt}$ ) by the average urinary flow rate in man (equivalent to 1.5 l/day reported by Boeniger et al., 1993). This Figure indicates that urinary concentrations vary significantly with time in addition to being influenced by the dermal absorption rate, the creatinine contents and the urinary flow rate. Thus, to avoid being misled by these important variations in spot value concentrations, it is best to propose a biological reference value expressed in terms of cumulative amounts of the metabolite recovered in urine over a specified time period.

## ***DISCUSSION***

### ***Model Development***

A toxicokinetic model was developed in this study to better assess health risks related to parathion exposure in workers using urinary measurements of metabolites, AP or *p*-NP. The model describes the time courses of urinary biomarkers of parathion under different exposure routes and temporal scenarios. The model was built for biological monitoring purposes and not, for instance, to uncover the links between the formation of paraoxon and the appearance of health effects. It predicts the essential features of the kinetics of parathion and its metabolites in humans without the need for detailed knowledge of internal physiological processes. To develop the model, extensive use was made of the different time scales underlying the critical biological processes governing the urinary excretion dynamics.

A single set of values were used for the model parameters describing the kinetics of parathion, once absorbed, to its excretion as AP and *p*-NP in urine. Only the dermal absorption rate,  $k_{\text{abs-dermal}}$ , and the absorption fraction,  $f_{\text{abs-dermal}}$ , needed to be adjusted to provide good fits to all the considered dermal data sets. These adjustments for the absorption parameters reflect the known wide variations in absorption due to the particularities of each exposed skin region and exposure temperature, as reported by Funckes et al. (1963) and observed from the data of Hayes et al. (1964) and Maibach et al. (1971). The model showed that, depending on the absorption rate, the dynamics of the urinary biomarkers can be markedly altered. For example, following an iv injection,

to recover half of the total amounts of *p*-NP excreted in urine takes 7 h, for AP it takes 20 h, whereas, following a dermal exposure, the corresponding times are 20 h for *p*-NP and 30 h for AP, considering a dermal absorption rate of  $0.085 \text{ h}^{-1}$ .

The model was not validated with an entirely separate data set because such data was not forthcoming. However, a single set of parameter values was capable of describing the internal dynamics of parathion and its metabolites over a variety of data sets with different routes-of-entry and temporal scenarios. The model simulated closely published data on the mean urinary time course of parathion metabolites in volunteers and workers following acute and repeated iv, pulmonary or dermal exposures (Hartwell et al., 1964; Hayes et al., 1964; Wolfe et al., 1970; Maibach et al., 1971; Durham et al., 1972; Feldmann & Maibach, 1974). This gives confidence that the model is a suitable tool to assess exposure and hence health risks in workers using urinary biomarker measurements.

The model can, through back calculations, serve to estimate the dose of parathion absorbed by a worker. There are however constraints related to the wide variations in the absorption rate according to the route of exposure and, in the case of dermal exposure, upon the site of application, skin condition and exposure temperature. Considering that these variations in the absorption rate largely influence the urinary excretion rate (see sensitivity analysis), simulations of an exposure scenario with the slowest and highest absorption rates compatible with the available literature data on excretions can provide a lower- and upper-bound value for the absorbed dose

reconstructed from amounts of biomarkers in urine. In cases where some basic information is available on the approximate time of exposure, the route of absorption and the detailed urinary excretion time course, the model can provide a more accurate estimation of the absorbed dose. This was carried out starting from the *p*-NP urinary time course reported by Michalke (1984) in an intoxicated subject. Even for the relatively high dose estimated for this subject, a good time profile prediction of the urinary excretion data was afforded by the model without the need for any saturation mechanism in the metabolism of parathion (Figure 7). The estimated absorbed dose of parathion for this intoxicated subject was from one to two orders of magnitude higher than the absorbed dose estimated by the model for the orchard workers in Durham et al. (1972) and Wolfe et al. (1970) (data shown only in one case). Attempts were also made to simulate other data in intoxicated subjects (Kuo et al., 1979). However, for the two cases reported in that study, marked saturation processes appeared to govern the kinetics. The cumulative urinary excretion of these subjects were however assessed to be 3.2 and 8.5 mmol, which would correspond, according to the model, to absorbed doses of at least 8.5 and 22.1 mmol, respectively. These are 10 and 26 times greater than that calculated for the intoxicated subject of the study of Michalke (1984) discussed above.

A temporary retention effect of parathion metabolites, prior to excretion in urine, was however apparent from data in exposed volunteers (Feldmann & Maibach, 1974) and an intoxicated subject (Michalke, 1984); it was accounted for in the model by introducing a holding compartment that retains parathion metabolites prior to their

excretion in urine. This process may be due to a retention of actively secreted parathion metabolites in renal tubular cells prior to their transport in the tubular lumen. The mechanisms by which this occurs, possibly an inhibition of renal active transport as reported for the herbicide 2,4,5-trichlorophenoxyacetic acid and for dinitrophenol (Berndt & Grote, 1968; Berndt, 1982), remain to be documented in *in vitro* studies using human cells.

An important feature of the model lies with the determination of its parameters solely from human data in order to avoid uncertainties arising from animal to human extrapolations. Indeed, comparison of the human data of Morgan et al. (1977) and the animal data of Carver and Riviere (1989), Nye and Dorough (1976), and Prakashchandra and Guthrie (1983) shows large differences between animals and humans in the relative proportion of *p*-NP recovered in urine as compared to feces. Morgan et al. (1977) reported that, on average, 37% of the *p*-NP appears to be eliminated by the renal route in humans as compared to 87-90% in rats (Nye & Dorough, 1976; Prakashchandra & Guthrie, 1983) and 96% in pigs (Carver & Riviere, 1989).

The model was built on the basis of a compilation of published mean urinary excretion data for different exposure scenarios. It could be refined if, within a same experimental framework, individual blood and urinary excretion data had been available from volunteers exposed by different routes to a wide dose range of parathion. These data would have helped establishing the inter-individual variability. In the absence of such

data, a sensitivity analysis was implemented for the model to simulate the variation in outcomes under reasonable parameter variations. However, knowing the variations in parameter values describing the internal kinetics is not essential for the purpose of this study, which is the determination of reference values for *p*-NP and AP in urine. Indeed, in the case of a dermal exposure, the main route-of-entry for workers, sensitivity analyses conducted on the model parameter values showed that the absorption rate contributes to a major part of the variability in the urinary excretion rate of parathion metabolites. Within reasonable ranges, the parameters describing the internal kinetics have generally little influence on the 12- or 24-h urinary excretion for dermal absorption.

#### ***Establishment of Biological Reference Values***

Biological reference values for urinary parathion metabolites, *p*-NP and AP, are established in this study to prevent adverse health effects in exposed workers. The proposed biological reference values are expressed as cumulative amounts of *p*-NP or AP in urine over given periods of time rather than in the form of end-of-shift urine samples as the ACGIH<sup>®</sup> suggests. End-of-shift urine concentrations are subject to the influence of the rapid changes in metabolites transfer to urine (see Figure 11) and can vary greatly for identical exposures given that the time elapsed since the previous micturition is usually unknown. With the approach proposed in the current paper, the integration of urinary excretion amounts over given periods of time reduces significantly these variations and avoids the impact of the known variations in urinary flow rate. Furthermore, the ACGIH<sup>®</sup> approach relies on the concentration of

metabolites in urine with respect to that of creatinine; with the proposed approach, it is unnecessary to rely on creatinine, which excretion rate has been documented to vary (Boeniger et al., 1993). The expression of biological reference values in terms of cumulative urinary amounts rather than spot urine sample measurements also facilitates the detection of metabolites at lower exposure levels.

Inferences using the toxicokinetic model show that the worker exposure scenario used to derive the biological reference values provide safe estimates that protect the more susceptible workers. The biological reference values can also be considered protective on the basis of the data of Hayes et al. (1964) in a volunteer dermally exposed to parathion. For this volunteer, where the reported 24-h *p*-NP urinary excretion was 15.9  $\mu\text{mol}$ , there was no significant inhibition of RBC-AChE (0%) and plasma-ChE (6%) activities. Assuming a body weight of 70 kg for this volunteer, this excretion value is approximately 10 times higher than the *p*-NP biological reference value proposed in this study (24 nmol/kg-bw).

These biological reference values can serve to estimate health risks in exposed workers. For instance, Wolfe et al. (1970) determined the urinary excretion of *p*-NP in 7 spraymen exposed to parathion in orchards. It can be calculated from the reported data that, assuming a constant daily exposure over the observation period and a body weight of 70 kg, the *p*-NP daily excretion of the different workers is 50, 230, 40, 60, 30, 20 and 47 nmol/kg-bw. On this basis, only the excretion in one worker is below the biological reference value for *p*-NP (24 nmol/kg) proposed in the current study. These

findings suggest significant occupational exposures for those workers. That study was however conducted long before the U.S. EPA reached, in 1991, an agreement to limit the usage of parathion in the USA and to increase parathion handling and postapplication restrictions (U.S. EPA, 1999). To our knowledge, the extent to which these measures contributed to reduce the adverse health risks cannot be assessed for lack of relevant data published after 1991.

***ACKNOWLEDGMENT***

The authors thank the Institut de Recherche Robert-Sauvé en Santé et Sécurité du Travail (IRSST) for providing financial support.

## APPENDIX

### *First order linear differential equations for each compartment*

**Kinetics of parathion.** From Figure 2, the following differential equations are obtained (see Table 1 for definitions of symbols and abbreviations):

$$\frac{dD(t)}{dt} = g_{\text{dermal}}(t) - k_{\text{abs-dermal}} \times D(t)$$

$$\frac{dGI(t)}{dt} = g_{\text{oral}}(t) - k_{\text{abs-oral}} \times GI(t)$$

$$\frac{dRT(t)}{dt} = g_{\text{inh}}(t) - k_{\text{abs-inh}} \times RT(t)$$

where  $g_{\text{dermal}}(t)$ ,  $g_{\text{oral}}(t)$  and  $g_{\text{inh}}(t)$  are the bioavailable dose  $D_{\text{abs}}$  per unit of time for dermal, oral, or respiratory tract absorption, respectively.

For intravenous injection,  $g(t) = 0$  for  $t \geq 0$  and at time  $t = 0$ :  $B(0) = D_{\text{abs}}$ .

$$\frac{dB(t)}{dt} = k_{\text{abs-oral}} \times GI(t) + k_{\text{abs-inh}} \times RT(t) + k_{\text{abs-dermal}} \times D(t) + k_{\text{SB}} \times S(t) - (k_{\text{BS}} + k_{\text{BM}}) \times B(t)$$

$$\frac{dS(t)}{dt} = k_{\text{BS}} \times B(t) - k_{\text{SB}} \times S(t)$$

### Kinetics of the p-nitrophenol metabolite

$$\frac{dM_{NP}(t)}{dt} = k_{BM} \times B(t) - (k_{MK-NP} + k_{MF-NP}) \times M_{NP}(t)$$

$$\frac{dK_{NP}(t)}{dt} = k_{MK-NP} \times M_{NP}(t) - k_{KU-NP} \times K_{NP}(t)$$

$$\frac{dU_{NP}(t)}{dt} = k_{KU-NP} \times K_{NP}(t)$$

$$\frac{dF_{NP}(t)}{dt} = k_{MF-NP} \times M_{NP}(t)$$

### Kinetics of the alkyl phosphate metabolites

$$\frac{dM_{AP}(t)}{dt} = k_{BM} \times B(t) - (k_{MK-AP} + k_{MF-AP}) \times M_{AP}(t)$$

$$\frac{dK_{AP}(t)}{dt} = k_{MK-AP} \times M_{AP}(t) - k_{KU-AP} \times K_{AP}(t)$$

$$\frac{dU_{AP}(t)}{dt} = k_{KU-AP} \times K_{AP}(t)$$

$$\frac{dF_{AP}(t)}{dt} = k_{MF-AP} \times M_{AP}(t)$$

### *Mass balance verification*

### Kinetics of the p-nitrophenol metabolite

$$D(t) + GI(t) + RT(t) + B(t) + S(t) + M_{NP}(t) + K_{NP}(t) + U_{NP}(t) + F_{NP}(t) - [D(0) + GI(0) + RT(0) + B(0) + S(0) + M_{NP}(0) + K_{NP}(0) + U_{NP}(0) + F_{NP}(0)]$$

$$= \int_0^t [g_{\text{dermal}}(s) + g_{\text{oral}}(s) + g_{\text{inh}}(s)] \times ds =$$

total absorbed dose til time "t"

**Kinetics of the alkyl phosphate metabolites**

$$D(t) + GI(t) + RT(t) + B(t) + S(t) + M_{AP}(t) + K_{AP}(t) + U_{AP}(t) + F_{AP}(t) - \\ [D(0) + GI(0) + RT(0) + B(0) + S(0) + M_{AP}(0) + K_{AP}(0) + U_{AP}(0) + F_{AP}(0)]$$

$$= \int_0^t [g_{\text{dermal}}(s) + g_{\text{oral}}(s) + g_{\text{inh}}(s)] \times ds =$$

total absorbed dose til time "t"

## REFERENCES

Abu-Qare, A.W., Brownie, C.F., and Abou-Donia, M. 2000. Placental transfer and pharmacokinetics of a single oral dose of [<sup>14</sup>C]p-nitrophenol in rats. *Arch. Toxicol.* 74:388-396.

Alessio, L., Berlin, A., Dell'Orto, A., Toffoletto, F., and Ghezzi, I. 1985. Reliability of urinary creatinine as a parameter used to adjust values of urinary biological indicators. *Int. Arch. Occup. Environ. Health* 55:99-106.

Algür, S.A., Öztürk, P., Sözmen, E.Y., Delen, Y., Tanyalçin, T., and Ege, B. 1999. Paraoxonase and acetylcholinesterase activities in humans exposed to organophosphorous compounds. *J. Toxicol. Environ. Health A* 58:469-474.

American Conference of Governmental Industrial Hygienists 2002. *Documentation of the biological exposure indices*, 7th ed.. Cincinnati, OH: ACGIH® Worldwide.

Arterberry, J.D., Durham, W.F., Elliot, J.W., and Wolfe, H.R. 1961. Exposure to parathion. *Arch. Environ. Health* 3:476-485.

Berndt, W.O. 1982. Renal methods in toxicology. In *Principles and Methods of Toxicology*. ed. A. Wallace Hayes, 447-474. New York: Raven Press.

Berndt, W.O., and Grote, D. 1968. The accumulation of C14-dinitrophenol by slices of rabbit kidney cortex. *J. Pharmacol. Exp. Ther.* 164:223-231.

Boeniger, M.F., Lowry, L.K., and Rosenberg, J. 1993. Interpretation of urine results used to assess chemical exposure with emphasis on creatinine adjustments: a review. *Am. Ind. Hyg. Assoc. J.* 54:615-627.

Braeckman, R.A., Audenaert, F., Willems, J.L., Belpaire, F.M., and Bogaert, M.G. 1983. Toxicokinetics of methyl parathion and parathion in the dog after intravenous and oral administration. *Arch. Toxicol.* 54:71-82.

Bronaugh, R.L., and Maibach, H.I. 1999. Percutaneous Absorption. *Drugs – Cosmetics – Mechanisms – Methodology*, 3rd ed.. New York: Marcel Dekker.

Carr, R.L., and Chambers, J.E. 1996. Kinetic analysis of the in vitro inhibition, aging, and reactivation of brain acetylcholinesterase from rat and channel catfish by paraoxon and chlorpyrifos-oxon. *Toxicol. Appl. Pharmacol.* 139:365-373.

Carver, M.P., and Riviere, J.E. 1989. Percutaneous absorption and excretion of xenobiotics after topical and intravenous administration to pigs. *Fundam. Appl. Toxicol.* 13:714-722.

Curtis, G., and Fogel, M. 1970. Creatinine excretion : diurnal variation and variability of whole and part-day measures. *Psychosom. Med.* 32:337-350.

Denga, N., Moldeus, P., Kasilo, O.M.J., and Nhachi, C.F.B. 1995. Use of urinary p-nitrophenol as an index of exposure to parathion. *Bull. Environ. Contam. Toxicol.* 55:296-302.

Durham, W.F., Wolfe, H.R., and Elliott, J.W. 1972. Absorption and excretion of parathion by spraymen. *Arch. Environ. Health* 24:381-387.

Edson, E.F., and colleagues 1964. Summaries of toxicology data : no-effects levels of three organophosphates in the rat, pig and man. *Food Cosmet. Toxicol.* 2:311-316.

Elliott, J.W., Walker, K.C., Penick, A.E., and Durham, W.F. 1960. Insecticide exposure: a sensitive procedure for urinary p-nitrophenol determination as a measure of exposure to parathion. *J. Agric. Food Chem.* 88:111-113.

Feldmann, R.J., and Maibach, H.I. 1974. Percutaneous penetration of some pesticides and herbicides in man. *Toxicol. Appl. Pharmacol.* 28:126-132.

Funckes, A.J., Hayes, G.R., and Hartwell, W.V. 1963. Urinary excretion of paranitrophenol by volunteers following dermal exposure to parathion at different ambient temperatures. *J. Agric. Food Chem.* 11:455-457.

Gage, J.C. 1967. The significance of blood cholinesterase activity measurements. *Residue Rev.* 18:159-173.

Gallo, M.A., and Lawryk, N.J. 1991. Organic phosphorus pesticides. In *Handbook of Pesticide Toxicology*. ed. W.J. Hayes and E.R. Laws, 917-1023. New York: Academic Press.

Gearhart, J.M., Jepson, G.W., Clewell, H.J., Andersen, M.E., and Conolly, R.B. 1994. Physiologically based pharmacokinetic model for the inhibition of acetylcholinesterase by organophosphate esters. *Environ. Health Perspect.* 102 (suppl 11):51-60.

Greenblatt, D.J., Ransil, B.J., Harmatz, J.S., Smith, T.W., Duhme, D.W., and Koch-Weser, J. 1976. Variability of 24-hour urinary creatinine excretion by normal subjects. *J. Clin. Pharmacol.* 16:321-328.

Hartwell, W.V., Hayes, G.R., and Funckes, A.J. 1964. Respiratory exposure of volunteers to parathion. *Arch. Environ. Health* 8:820-825.

Hayes, W.J. 1982. *Pesticides Studied in Man*. Baltimore, MD: Williams & Wilkins.

Hayes, G.R., Funckes, A.J., and Hartwell, W.V. 1964. Dermal exposure of human volunteers to parathion. *Arch. Environ. Health* 8:829-833.

Heath, A.J.W., and Vale, J.A. 1992. Clinical presentation and diagnosis of acute organophosphorus insecticide and carbamate poisoning. In *Clinical and Experimental Toxicology of Organophosphates and Carbamates*, ed. B. Ballantyne and T.C. Marrs, 513-519. Oxford: Butterworth-Heinemann Ltd.

Jokanović, M. 2001. Biotransformation of organophosphorus compounds. *Toxicology* 166:139-160.

Kuo, T.-L., Chen, W.-Y., and Yen, T.-S. 1979. Studies on parathion poisoning. III. A kinetic study of the excretion of urinary p-nitrophenol in acute parathion intoxication. *J. Formosan Med. Assoc.* 78:344-354.

Larsen, K.-O., and Hanel, H.K. 1982. Effect of exposure to organophosphorus compounds on cholinesterase in workers removing poisonous depots. *Scand. J. Environ. Health* 8:222-228.

Lotti, M. 1991. Treatment of acute organophosphate poisoning. *Med. J. Aust.* 154: 51-55.

Maibach, H.I., Feldmann R.J., Milby, T.H., and Serat, W.F. 1971. Regional variation in percutaneous penetration in man: Pesticides. *Arch. Environ. Health* 23:208-211.

Menzie, C.M. 1969. Metabolism of Pesticides. Washington, DC: United States Department of the Interior, Bureau of Sport Fisheries and Wildlife.

Michalke, P. 1984. Determination of p-nitrophenol in serum and urine by enzymatic and non-enzymatic conjugate hydrolysis and HPLC. Application after parathion intoxication. *Z. Rechtsmedizin* 92:95-100.

Morgan, D.P., Hetzler, H.L., Slach, E.F., and Lin, L.I. 1977. Urinary excretion of paranitrophenol and alkyl phosphates following ingestion of methyl and ethyl parathion by human subjects. *Arch. Environ. Contam. Toxicol.* 6:159-173.

Mutch, E., Blain, P.G., and Williams, F.M. 1999. The role of metabolism in determining susceptibility to parathion toxicity in man. *Toxicol. Lett.* 107:177-187.

Nolan, R.J., Rick, D.L., Freshour, N.L., and Saunders J.H. 1984. Chlorpyrifos pharmacokinetics in human volunteers. *Toxicol. Appl. Pharmacol.* 73:8-15.

Nye, D.E., and Dorough, H.W. 1976. Fate of insecticides administered endotracheally to rats. *Bull. Environ. Contam. Toxicol.* 15:291-296.

Poore, R.E., and Neal, R.A. 1972. Evidence of extrahepatic metabolism of parathion. *Toxicol. Appl. Pharmacol.* 23:759-768.

Prakashchandra, V.S., and Guthrie, F.E. 1983. Percutaneous penetration of three insecticides in rats: a comparison of two methods for in vivo determination. *J. Invest. Dermatol.* 80:291-293.

Qiao, G.L., Williams, P.L., and Riviere, J.E. 1994. Percutaneous absorption, biotransformation, and systemic disposition of parathion in vivo in swine. I. Comprehensive pharmacokinetic model. *Drug Metab. Dispos.* 23:459-471.

Qiao, G.L., Chang, S.K., Brooks, J.D., and Riviere, J.E. 2000. Dermatotoxicokinetic modeling of p-nitrophenol and its conjugation metabolite in swine following topical and intravenous administration. *Toxicol. Sci.* 54:284-294.

Richter, E.D., Chuwers, P., and Levy Y. 1992. Health effects from exposure to organophosphate pesticides in workers and residents in Israel. *Isr. J. Med. Sci.* 28:584-598.

Rider, J.A., Moeller, H.C., Puletti, E.J., and Swader, J.I. 1969. Toxicity of parathion, systox, octamethyl pyrophosphoramidate, and methyl parathion in man. *Toxicol. Appl. Pharmacol.* 14:603-611.

Segel, L.A. 1988. On the validity of the steady state approximation of enzyme kinetics. *Bull. Math. Biol.* 50:579-593.

Segel, L.A., and Slemrod, M. 1989. The quasi-steady state approximation: A case study in perturbation. *Society for Industrial and Applied Mathematics Review* 31:446-476.

Shafik, T., Sullivan, H.C., and Enos, H.R. 1973a. Multiresidue procedure for halo- and nitrophenols. Measurement of exposure to biodegradable pesticides yielding these compounds as metabolites. *J. Agric. Food Chem.* 21:295-298.

Shafik, T., Bradway, D.E., Enos, H.R., and Yobs, A.R. 1973b. Human exposure to organophosphorus pesticides. A modified procedure for the gas-liquid chromatographic analysis of alkyl phosphate metabolites in urine. *J. Agric. Food Chem.* 21:625-629.

Sidell, F.R. 1994. Clinical effects of organophosphorus cholinesterases inhibitors. *J. Appl. Toxicol.* 14:111-113.

Sultatos, L.G. 1990. A physiologically based pharmacokinetic model of parathion based on chemical-specific parameters determined in vitro. *J. Amer. Coll. Toxicol.* 9:611-619.

US Environmental Protection Agency 1999. Ethyl parathion: revised human health risk assessment. Washington, DC: Office of Prevention, Pesticides and Toxic Substances.

Wolfe, H.R., Durham, W.F., and Armstrong, J.F. 1970. Urinary excretion of insecticide metabolites. *Arch. Environ. Health* 21:711-716.

Zhang, H.X., and Sultatos, L.G. 1991. Biotransformation of the organophosphorus insecticides parathion and methyl parathion in male and female rat livers perfused in situ. *Drug Metab. Dispos.* 19:473-477.

**Table 1. Symbols Used in the Conceptual and Functional Representation of the Model**

Variables and parameters Symbols or abbreviations		Description
Variables	$g_{\text{dermal}}(t)$	Dermal dose bioavailable (mol) per unit of time (h) which can describe time varying inputs
	$g_{\text{oral}}(t)$	Oral dose bioavailable (mol) per unit of time (h) which can describe time varying inputs
	$g_{\text{inh}}(t)$	Inhaled dose bioavailable (mol) per unit of time (h) which can describe time varying inputs
	$D(t)$	Burden of parathion bioavailable (mol) at the skin surface as a function of time
	$GI(t)$	Burden of parathion bioavailable (mol) in the gastrointestinal tract as a function of time
	$RT(t)$	Burden of parathion bioavailable (mol) in the respiratory tract as a function of time
	$Q(t)$	Systemic body burden of parathion and its metabolites (mol) as a function of time
	$B(t)$	Burden of parathion and paraoxon (mol) in blood and tissues in dynamical equilibrium with blood as a function of time
	$S(t)$	Burden of parathion and paraoxon (mol) in storage tissues as a function of time
	$M_{\text{AP}}(t)$	Burden of alkyl phosphates (mol) in blood and tissues in dynamical equilibrium with blood as a function of time
	$M_{\text{NP}}(t)$	Burden of <i>p</i> -nitrophenol (mol) in blood and tissues in dynamical equilibrium with blood as a function of time
	$K_{\text{AP}}(t)$	Burden of alkyl phosphates (mol) in body reservoir as a function of time
	$K_{\text{NP}}(t)$	Burden of <i>p</i> -nitrophenol (mol) in body reservoir as a function of time
	$U_{\text{AP}}(t)$	Cumulative burden of alkyl phosphates (mol) in urine as a function of time
	$U_{\text{NP}}(t)$	Cumulative burden of <i>p</i> -nitrophenol (mol) in urine as a function of time
	$F_{\text{AP}}(t)$	Cumulative burden of alkyl phosphates (mol) in feces as a function of time
	$F_{\text{NP}}(t)$	Cumulative burden of <i>p</i> -nitrophenol (mol) in feces as a function of time
	Parameters	$k_{\text{abs-oral}}$
$k_{\text{abs-inh}}$		Pulmonary absorption rate of parathion ( $\text{h}^{-1}$ )
$k_{\text{abs-dermal}}$		Dermal absorption rate of parathion ( <i>i.e.</i> , transfer rate from skin surface to blood) ( $\text{h}^{-1}$ )
$k_{\text{BS}}$		Blood to storage tissues transfer coefficient of parathion and paraoxon ( $\text{h}^{-1}$ )
$k_{\text{SB}}$		Storage tissues to blood transfer coefficient of parathion and paraoxon ( $\text{h}^{-1}$ )
$k_{\text{BM}}$		Rate of body parathion and paraoxon biotransformation into <i>p</i> -nitrophenol and alkyl phosphates ( $\text{h}^{-1}$ )
$k_{\text{MK-AP}}$		Blood to body reservoir transfer coefficient of alkyl phosphates ( $\text{h}^{-1}$ )
$k_{\text{MK-NP}}$		Blood to body reservoir transfer coefficient of <i>p</i> -nitrophenol ( $\text{h}^{-1}$ )
$k_{\text{KU-AP}}$		Body reservoir to urine transfer coefficient of alkyl phosphates ( $\text{h}^{-1}$ )
$k_{\text{KU-NP}}$		Body reservoir to urine transfer coefficient of <i>p</i> -nitrophenol ( $\text{h}^{-1}$ )
$k_{\text{MF-AP}}$		Blood to feces transfer coefficient of alkyl phosphates ( $\text{h}^{-1}$ )
$k_{\text{MF-NP}}$		Blood to feces transfer coefficient of <i>p</i> -nitrophenol ( $\text{h}^{-1}$ )

**Table 2. Parameter Values Used for Model Simulations of the Kinetics of Parathion and That of *p*-Nitrophenol and Alkyl Phosphate Metabolites**

Transfer coefficients	Values (h <sup>-1</sup> )
<i>Absorption parameters for parathion</i>	
$k_{\text{abs-oral}}$	0.8
$k_{\text{abs-dermal}}$	0.04 - 0.5
<i>Parathion and paraoxon kinetic parameters</i>	
$k_{\text{BM}}$	6.93
$k_{\text{BS}}$	2.40
$k_{\text{SB}}$	0.0457
<i>Alkyl phosphate kinetic parameters</i>	
$k_{\text{MK-AP}}$	0.0997
$k_{\text{KU-AP}}$	0.0749
$k_{\text{MF-AP}}$	0.117
<i><i>p</i>-Nitrophenol kinetic parameters</i>	
$k_{\text{MK-NP}}$	0.463
$k_{\text{KU-NP}}$	0.166
$k_{\text{MF-NP}}$	0.788

**Table 3. Ranges of Values of the Normalized Sensitivity Coefficient R**

Model parameters	Normalized sensitivity coefficient R range <sup>a</sup>			
	<i>p</i> -Nitrophenol		Alkyl phosphates	
	12-h cumulative urinary excretion	24-h cumulative urinary excretion	12-h cumulative urinary excretion	24-h cumulative urinary excretion
$k_{SB}$	(0.03, 0.03)	(0.06, 0.07)	(0.03, 0.03)	(0.05, 0.06)
$k_{BS}$	(-0.26, -0.20)	(-0.21, -0.18)	(-0.26, -0.20)	(-0.23, -0.18)
$k_{BM}$	(0.18, 0.40)	(0.14, 0.33)	(0.19, 0.41)	(0.15, 0.35)
$k_{BM}^b$	(0.01, 0.04)	(0.00, 0.01)	(0.02, 0.06)	(0.01, 0.02)
$k_{MK}^c$	(0.10, 0.27)	(0.03, 0.08)	(0.50, 0.76)	(0.23, 0.52)
$k_{KU}$	(0.51, 0.78)	(0.21, 0.52)	(0.75, 0.90)	(0.51, 0.78)
$k_{abs-dermal}^d$	(0.59, 0.93)	(0.28, 0.83)	(0.64, 0.94)	(0.36, 0.86)

<sup>a</sup>  $R = \frac{(O_2 - O_1)/O_1}{(I_2 - I_1)/I_1}$ , where  $I_1$  is the default value of the parameter given in Table 2,  $I_2$  its modified value ( $\pm$  up to 50%  $I_1$ ).  $O_1$  is the predicted 12- or 24-h cumulative urinary using default parameter values and  $O_2$  its predicted value with the modified parameter value. The cumulative urinary  $O_1$  and  $O_2$  were obtained by model simulations of an 8-h dermal exposure to parathion, where the daily absorbed dose corresponds to a unit dose.

<sup>b</sup>  $k_{BS}$  and  $k_{BM}$  are varied simultaneously but such as to maintain a constant partitioning ratio between storage and metabolism ( $k_{BS}/k_{BM}$ ).

<sup>c</sup> The proportion of blood metabolite that is eventually excreted in urine as compared to feces is kept constant ( $k_{MK}/k_{MK}+k_{MF}$ ).

<sup>d</sup> The default parameter value is  $0.085 \text{ h}^{-1}$ , value determined from the data of Feldmann and Maibach (1974) on the time course of total ethyl-<sup>14</sup>C urinary excretion rate in volunteers following a percutaneous administration of ethyl-<sup>14</sup>C parathion.

**Table 4. Biological Reference Values for *p*-Nitrophenol and Alkyl Phosphates in Urine**

Period of urine collection (h) following the onset of exposure	Proposed biological reference values <sup>a</sup> (nmol/kg of body weight)	
	<i>p</i> -Nitrophenol	Alkyl phosphates
12	6	2
24	24	15

<sup>a</sup> Expressed as cumulative amounts over different periods of urine collection. These amounts were obtained using model simulations of an 8-h dermal exposure to parathion, where the daily absorbed dose corresponds to the human NOEL of 58  $\mu\text{g}/\text{kg}$  of body weight and the dermal absorption rate is equal to  $0.04 \text{ h}^{-1}$ .

**Table 5 Predicted Daily Amounts of *p*-Nitrophenol and Alkyl Phosphates in Urine During a Repeated 8-h Daily Dermal Exposure to Parathion**

Day of the onset of the 24-h urine collection	24-h cumulative urinary excretion <sup>a</sup> (% of absorbed daily molar dose)			
	<i>p</i> -Nitrophenol		Alkyl phosphates	
	First week of exposure	Second week of exposure	First week of exposure	Second week of exposure
Monday	11.8	17.5	7.5	18.4
Tuesday	24.7	27.4	24.0	29.2
Wednesday	31.2	32.4	34.9	37.4
Thursday	34.3	34.9	40.7	41.8
Friday	35.7	36.0	43.5	44.0
Saturday	24.6	24.7	37.3	37.6
Sunday	12.0	12.1	21.5	21.6

<sup>a</sup> Obtained using model simulations of an 8-h dermal exposure to parathion, Monday to Friday, repeated over two weeks, where the dermal absorption rate is equal to 0.04 h<sup>-1</sup>.

**Table 6. Cumulative Urinary Amounts of *p*-Nitrophenol and Alkyl Phosphates Over Different Collection Periods Following Either an Instantaneous Exposure or the Onset of a 4-h Dermal Exposure to the Chosen NOEL Dose of Parathion**

Period of urine collection (h) following the onset of exposure	Cumulative urinary excretion <sup>a</sup> (nmol/kg of body weight)			
	<i>p</i> -Nitrophenol		Alkyl phosphates	
	Instantaneous exposure	4-h exposure	Instantaneous exposure	4-h exposure
	12	12	9	5
24	29	26	21	18

<sup>a</sup> Obtained using model simulations of a dermal exposure, where the daily absorbed dose corresponds to the human NOEL of 58  $\mu\text{g}/\text{kg}$  of body weight and the dermal absorption rate is equal to  $0.04 \text{ h}^{-1}$ .

## CAPTIONS TO FIGURES

**Figure 1.** Biotransformation pathways of parathion.

**Figure 2.** Conceptual representation of the kinetics of parathion and its metabolites. Symbols and abbreviations are described in Table 1. One mole of parathion absorbed in the body is broken down into one mole of alkyl phosphates and one mole of *p*-nitrophenol.

**Figure 3.** Model simulations (lines) compared with experimental data of Feldmann and Maibach (1974) (symbols) on the time course of total ethyl-<sup>14</sup>C urinary excretion rate (% of administered dose/h) in male human volunteers following an intravenous (○) and percutaneous (×) administration of ethyl-<sup>14</sup>C parathion (1 μCi). Each point represents mean value of experimental data (*n* = 6 per exposure group).

**Figure 4.** Model simulations (lines) compared with experimental data of Maibach et al. (1971) (symbols) on the time course of total ethyl-<sup>14</sup>C cumulative urinary excretion (% of administered dose) in male human volunteers following a percutaneous administration of ethyl-<sup>14</sup>C parathion (4 μg/cm<sup>2</sup>) on the forearm (×), the palm of the hand (+), the hand dorsum (□) and the scalp (◇). Each point represents mean value of experimental data (*n* = 6 per exposure group).

**Figure 5.** Model simulation (line) compared with experimental data (symbols) of Hartwell et al. (1964) on the time course of *p*-nitrophenol urinary excretion rate in a human volunteer exposed by inhalation to parathion vapors for 2.5 h, under an exposure temperature of 38°C.

**Figure 6.** Model simulation (line) compared with experimental data (symbols) of Hayes et al. (1964) on the time course of *p*-nitrophenol urinary excretion rate in a human volunteer exposed for 2 hours, on 5 consecutive days, to 5 g of 2% parathion dust on a hand and forearm secured in a polyethylene bag, at a constant exposure temperature of 41°C.

**Figure 7.** Model simulation (line) compared with experimental data (symbols) of Michalke (1984) on the time course of *p*-nitrophenol cumulative urinary excretion in a human subject intoxicated orally with parathion.

**Figure 8.** Model simulation (line) compared with experimental data (symbols) of Wolfe et al. (1970) on the time course of *p*-nitrophenol cumulative urinary excretion in a worker following an 8-h application period, in orchards, of a formulation containing parathion.

**Figure 9.** Model simulations of the time course of (A) *p*-nitrophenol and (B) alkyl phosphates cumulative excretion in urine (expressed as a fraction of total amounts excreted in urine) following the onset of an 8-h exposure to parathion considering different dermal absorption rate values: —  $k_{\text{abs-dermal}} = 0.04 \text{ h}^{-1}$ ; - - - - -  $k_{\text{abs-dermal}} = 0.09 \text{ h}^{-1}$ ; ······  $k_{\text{abs-dermal}} = 0.3 \text{ h}^{-1}$ .

**Figure 10.** Model simulations of the time course of (A) parathion burden at the site-of-entry  $R(t)$ , and (B) parathion and paraoxon in storage tissues  $S(t)$  (expressed as a fraction of absorbed daily dose) during and following a consecutive 5-day-per-week dermal exposure to parathion, 8 h per day, repeated over two weeks, considering a dermal absorption rate of  $0.04 \text{ h}^{-1}$  (—) or  $0.3 \text{ h}^{-1}$  (- - - - -).

**Figure 11.** Model simulations (lines) of the concentration-time course of *p*-nitrophenol in urine following the onset of an 8-h dermal exposure to parathion where the daily absorbed dose corresponds to the NOEL of  $58 \mu\text{g}/\text{kg}$  of body weight/day with a urinary flow rate of 1.5 l/day and different dermal absorption rate values: —  $k_{\text{abs-dermal}} = 0.04 \text{ h}^{-1}$ ; - - - - -  $k_{\text{abs-dermal}} = 0.09 \text{ h}^{-1}$ ; ······  $k_{\text{abs-dermal}} = 0.3 \text{ h}^{-1}$ .

FIGURE 1

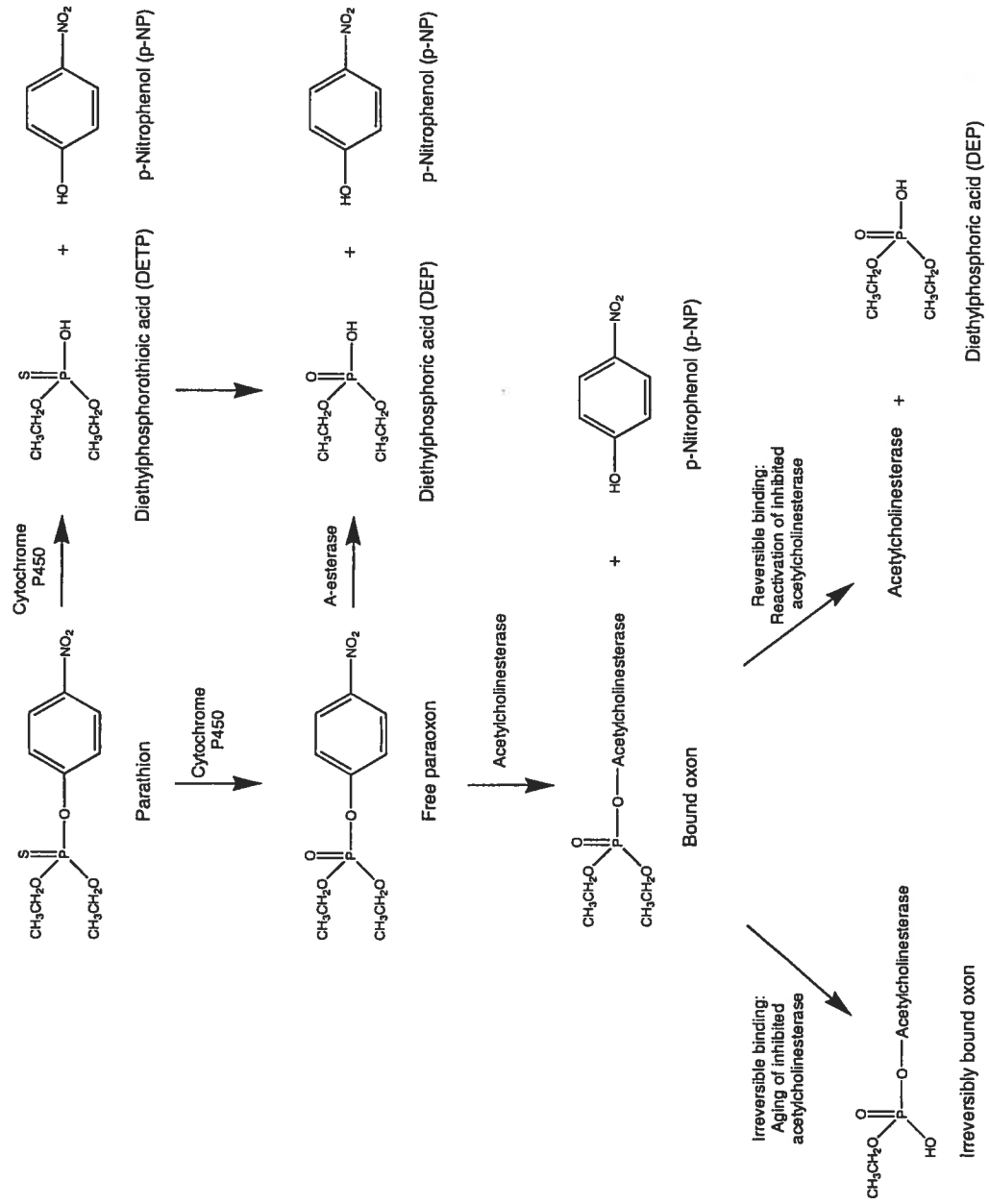


FIGURE 2

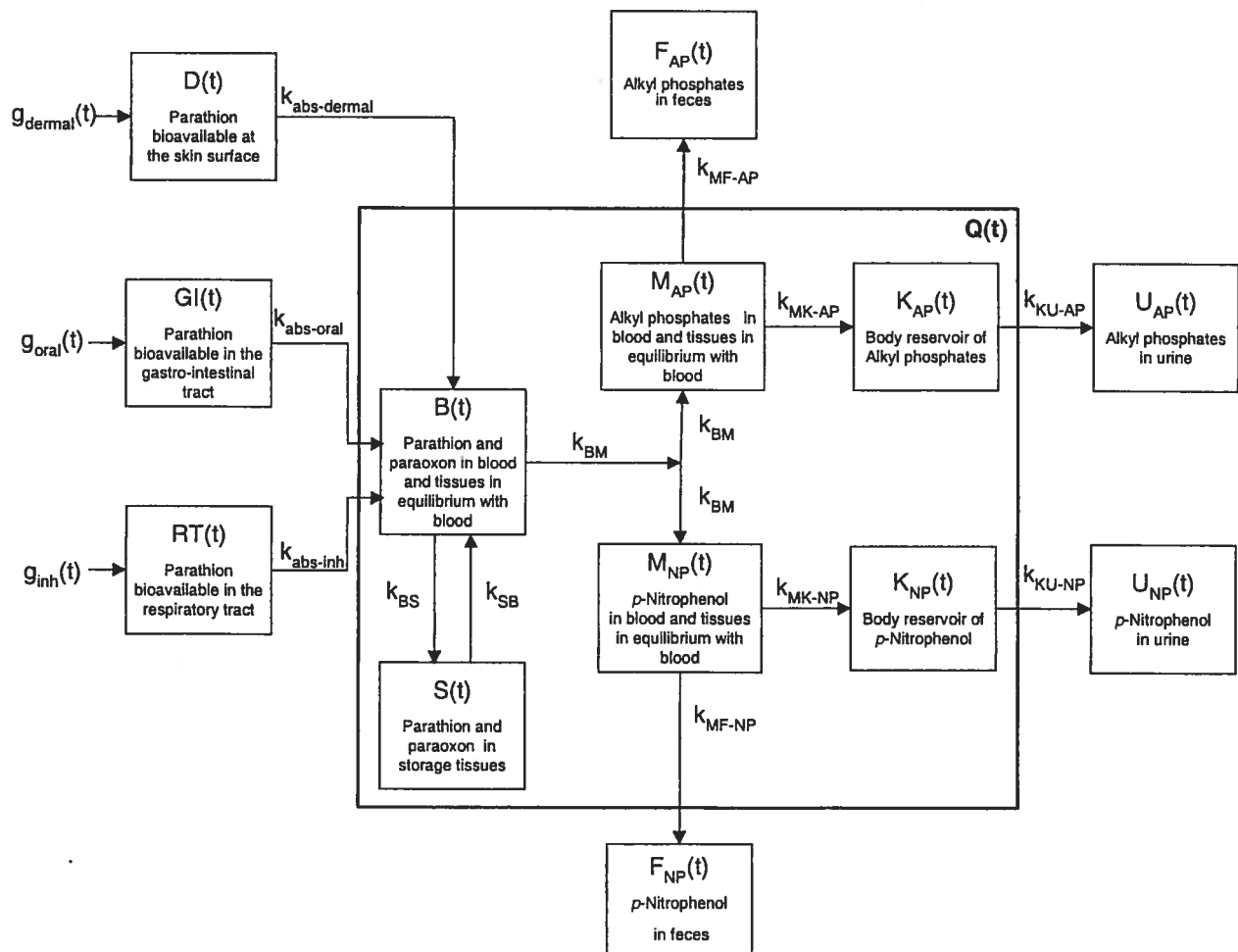


FIGURE 3

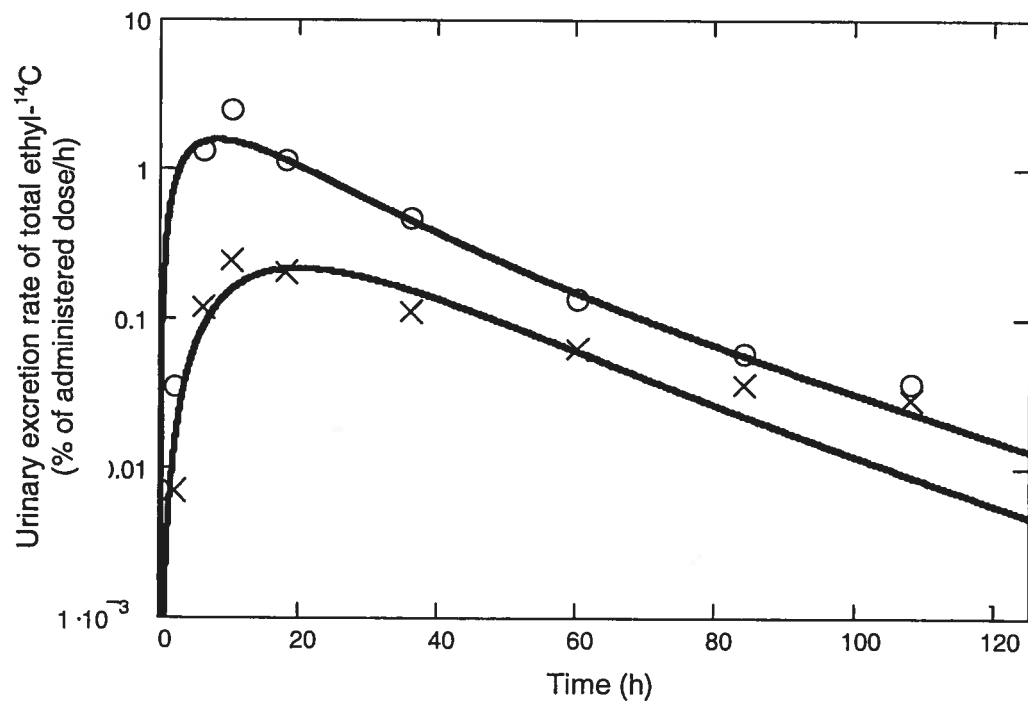


FIGURE 4

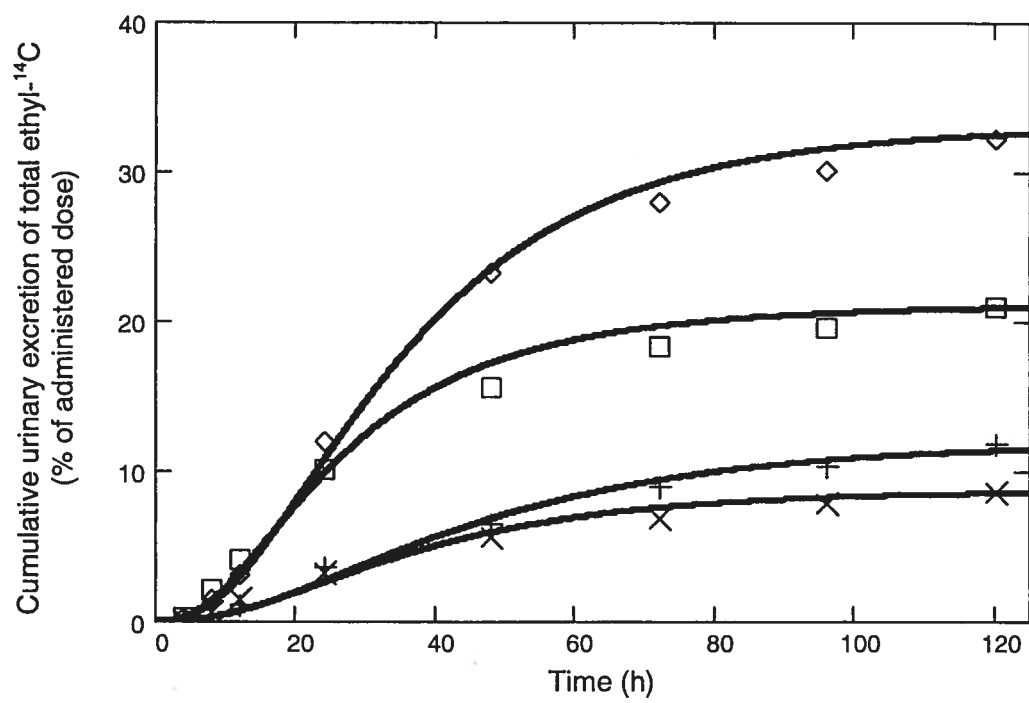


FIGURE 5

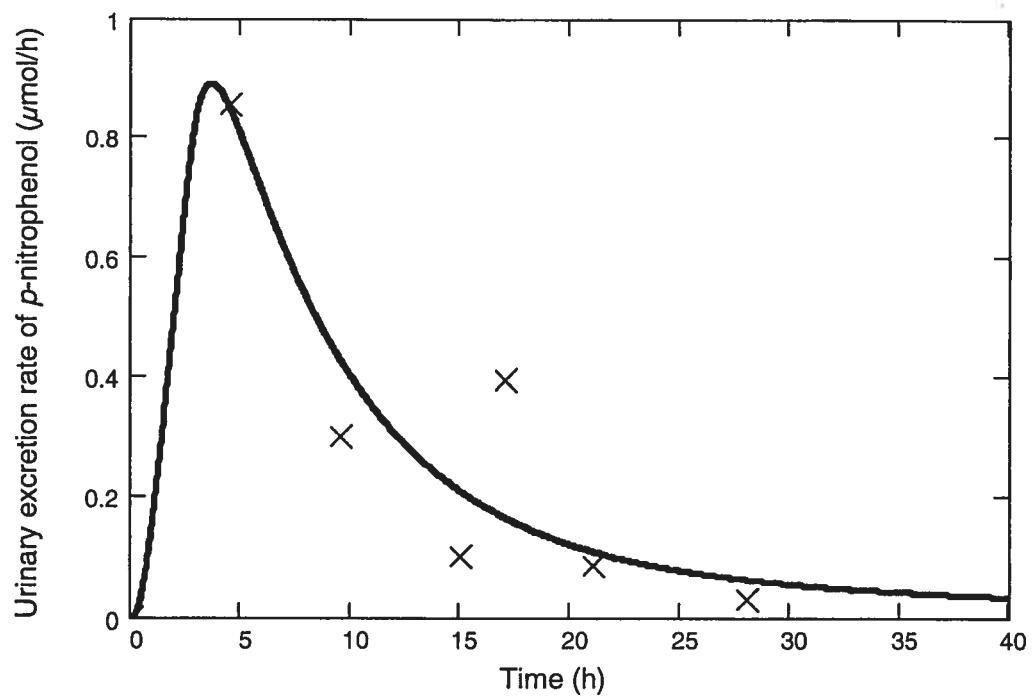


FIGURE 6

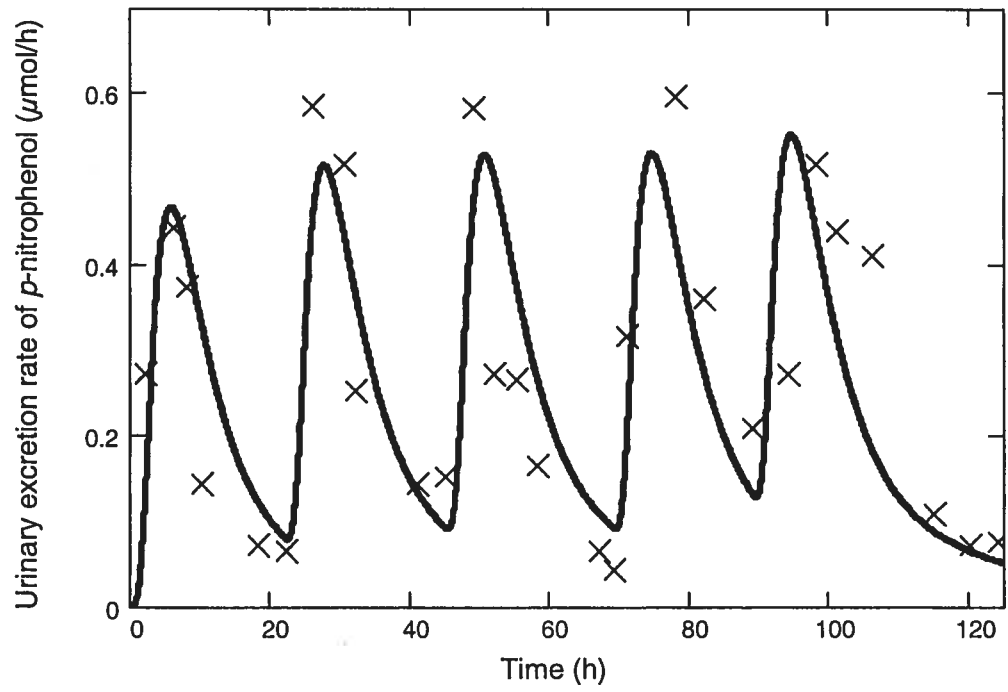


FIGURE 7

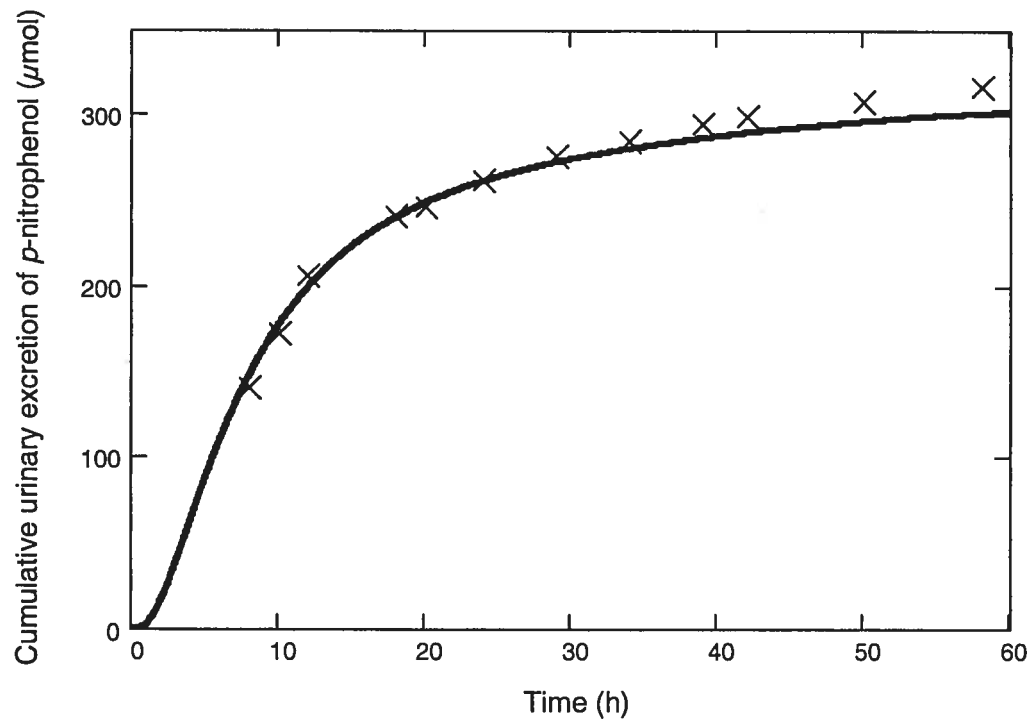


FIGURE 8

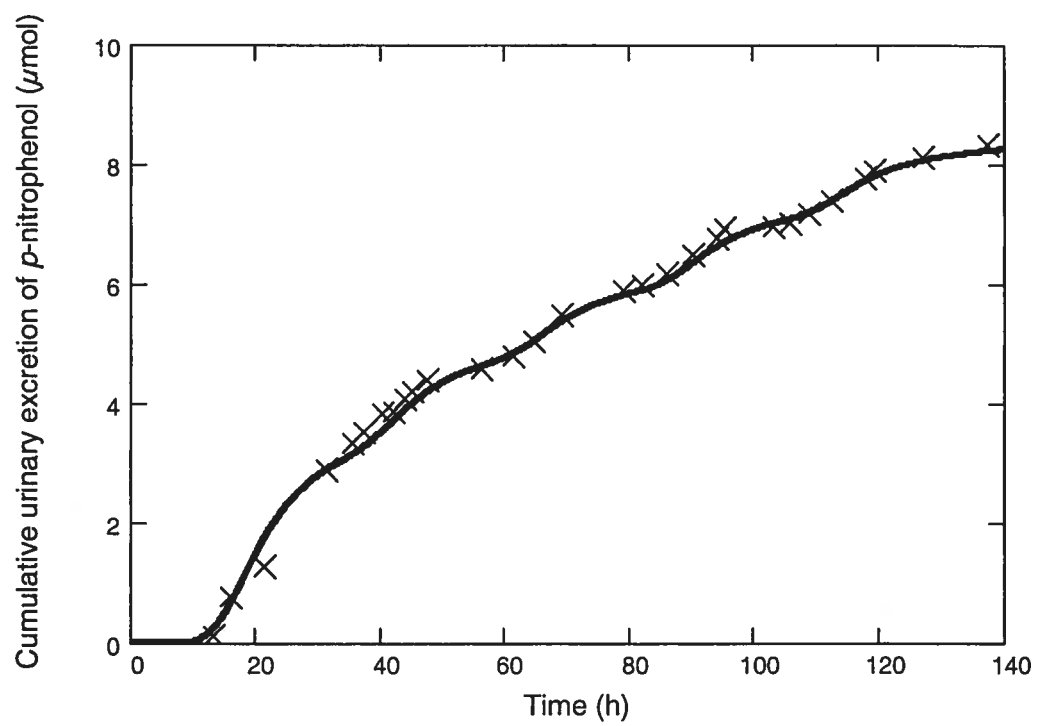


FIGURE 9

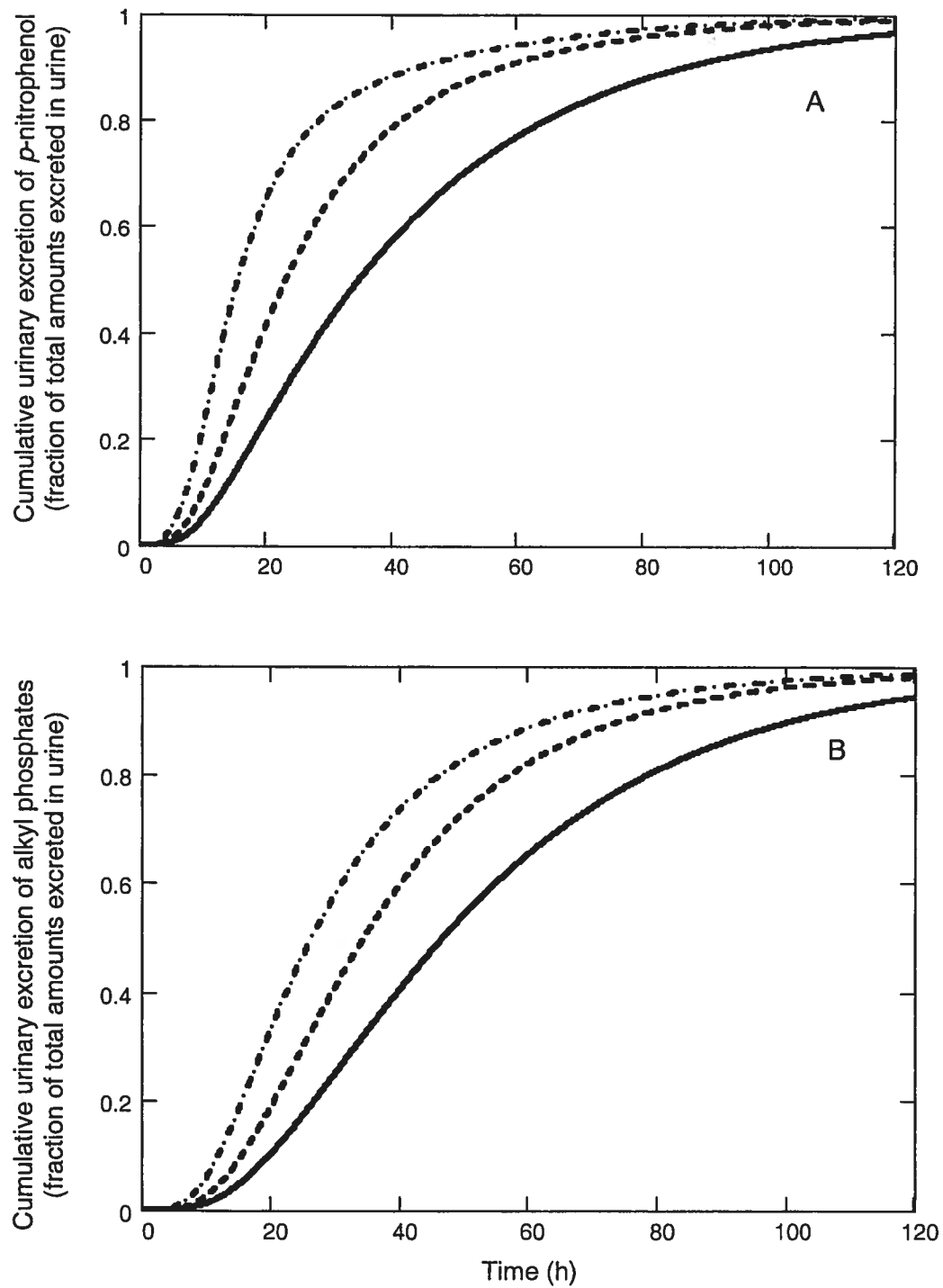


FIGURE 10

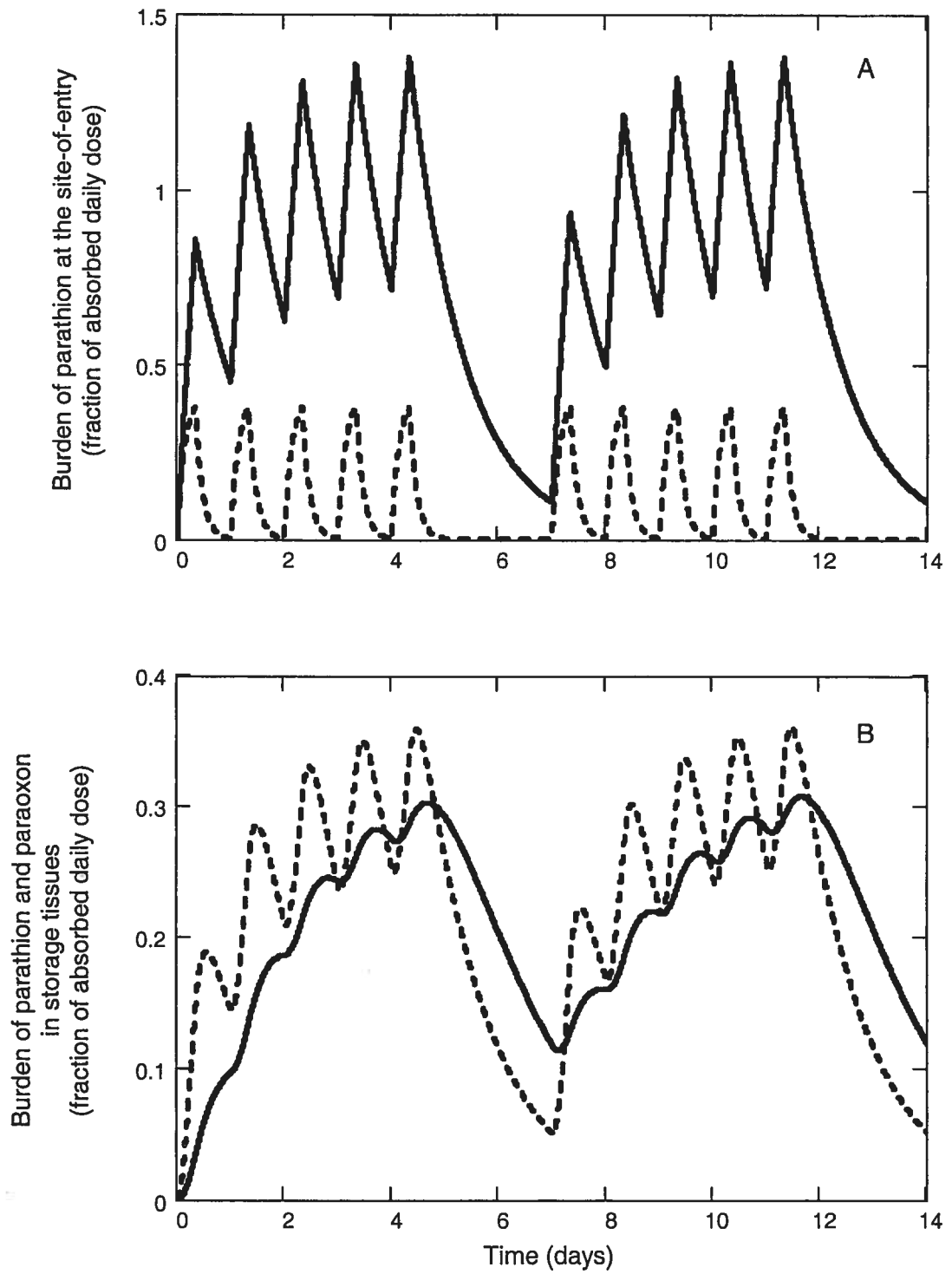
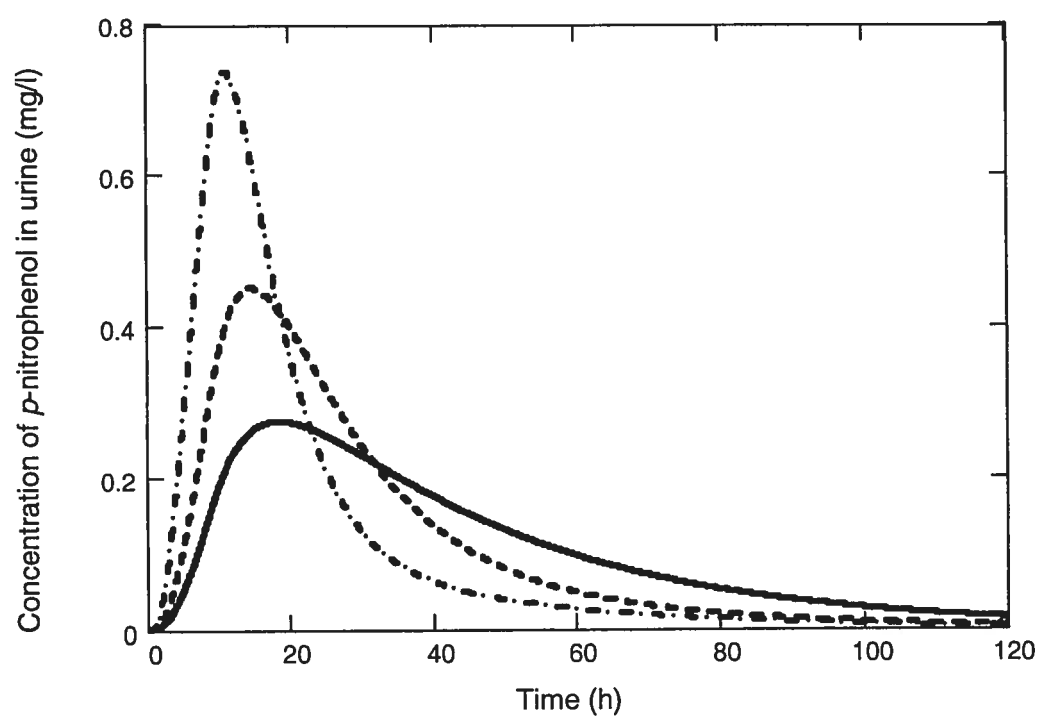


FIGURE 11



**CHAPITRE 5 : ARTICLE 3, CHLORPYRIFOS**

Cette version finale de l'article a été acceptée en novembre 2004 pour publication dans *Journal of Occupational and Environmental Hygiene*.

## **Determination of Biological Reference Values for Chlorpyrifos Metabolites in Human Urine Using a Toxicokinetic Approach**

Michèle Bouchard<sup>1</sup>, Gaétan Carrier<sup>1</sup>, Robert C. Brunet<sup>2</sup>, Yvette Bonvalot<sup>1</sup>, Nathalie H.  
Gosselin<sup>1</sup>

<sup>1</sup> Chaire en analyse des risques toxicologiques pour la santé humaine and Département de santé environnementale et santé au travail, Faculté de Médecine, Université de Montréal, P.O. Box 6128, Main Station, Montreal (Quebec), Canada, H3C 3J7

<sup>2</sup> Département de Mathématiques et de Statistique and Centre de Recherches Mathématiques, Faculté des arts et des sciences, Université de Montréal, P.O. Box 6128, Main Station, Montreal (Quebec), Canada, H3C 3J7

Offprint requests: Gaétan Carrier  
Département de Santé environnementale et santé au travail  
Université de Montréal  
P.O. Box 6128, Station centre-ville, Montreal (Quebec) H3C 3J7  
CANADA  
Telephone number: (514) 343-6111 ext 3108  
Fax number: (514) 343-2200  
E-mail: gaetan.carrier@umontreal.ca

## ***ABSTRACT***

Urinary biomarkers of chlorpyrifos (CPF) exposure are often measured in field studies although biological guidelines are not yet available to assess health risks in workers. The aim of this study was to propose biological reference values (BRVs) for CPF metabolites in urine based on a toxicokinetic approach. As a first step, a toxicokinetic model for CPF and its metabolites was developed and validated using the human kinetic time course data available in the literature. The model was built to link the absorbed dose of CPF under a variety of exposure routes and temporal scenarios to the urinary excretion of its major metabolites, 3,5,6-trichloro-2-pyridinol (3,5,6-TCP) and alkyl phosphates (AP). The model was then used to propose BRVs of urinary biomarkers of CPF exposure below which workers should not experience adverse health effects, whatever their exposure conditions. This was achieved by linking *i*) a literature reported repeated CPF no-observed-effect level (NOEL) daily exposure dose for the inhibition of red-blood-cell acetylcholinesterase (RBC-AChE) activity to a corresponding absorbed daily dose, on the one hand and *ii*) this absorbed daily dose to the urinary excretion of CPF metabolites, on the other hand. Model simulations under a variety of exposure scenarios showed that the safest BRVs are obtained from a dermal exposure scenario with the slowest absorption rate compatible with the available literature data rather than from respiratory or oral exposure scenarios. Also, model simulations showed that, for a given total absorbed dose, absorption over 8 hours results in smaller 3,5,6-TCP and AP urinary excretion rates than those obtained from the same absorbed dose over shorter exposure durations, although eventually the

cumulative amounts found in urine would be the same. From these considerations, BRVs were derived by simulating an 8-hour dermal CPF exposure such that the total absorbed daily dose corresponds to the absorbed NOEL. The reference values are proposed in the form of total amounts of 3,5,6-TCP and AP metabolites excreted in urine over chosen time periods (24 and 48 hours).

**Keywords** Chlorpyrifos, 3,5,6-Trichloro-2-Pyridinol, Alkyl Phosphates, Biological Reference Values, Biomarkers, Toxicokinetics, Occupational Exposure

## ***INTRODUCTION***

Chlorpyrifos (*O,O*-diethyl-*O*-[3,5,6-trichloro-2-pyridyl]phosphorothioate, CAS Registry No. 2921-88-2) is an organophosphorus (OP) pesticide used in LORSBAN<sup>®</sup> and DURSBAN<sup>®</sup> formulations to control agricultural and horticultural insect pests. Chlorpyrifos-induced toxicity results primarily from the inhibition of neuronal acetylcholinesterase (AChE) activity by the chlorpyrifos (CPF) bioactivation product, CPF-oxon.<sup>(1-3)</sup>

To prevent health risks from airborne exposures in occupational settings, a time-weighted average threshold limit value (TLV-TWA<sup>®</sup>) of 0.2 mg CPF/m<sup>3</sup> of air has been proposed.<sup>(4)</sup> However, in the majority of occupational cases, respiratory exposure to pesticides accounts for only a small fraction of the overall exposure.<sup>(5)</sup> Like many other OP insecticides, CPF's lipophilic property favors its absorption through the skin.<sup>(4)</sup> Fenske and Elkner<sup>(6)</sup> have estimated that, during structural control treatments of houses with DURSBAN<sup>®</sup>, 73 percent of urinary CPF metabolite excretion was attributable to dermal exposure.

Since occupational exposure to CPF potentially occurs through multiple routes, particularly by skin contact, the assessment of health risks based on the compliance to biological guidelines rather than environmental guidelines (TLV<sup>®</sup>) appears more suitable.<sup>(7,8)</sup> A Biological Exposure Index (BEI<sup>®</sup>) has been proposed based on the measurement of the inhibition of red-blood-cell (RBC)-AChE activity by OP and

carbamate insecticides.<sup>(4)</sup> However, a BEI<sup>®</sup> based on the measurement of urinary metabolites of CPF has not been proposed so far; this is desirable since urinary biomarkers give an earlier warning of exposure and biological effects than the inhibition of AChE activity and are more specific.<sup>(9)</sup>

According to both animal and human studies, whatever the exposure route, CPF is eventually nearly completely converted to equimolar amounts of 3,5,6-trichloro-2-pyridinol (3,5,6-TCP) and alkyl phosphate (AP) metabolites (diethyl phosphate (DEP) and diethyl thiophosphate (DETP)) (see Figure 1), which are essentially excreted through the renal route.<sup>(10-14)</sup> To assess exposure to CPF, urinary metabolites are thus often being measured: 3,5,6-TCP as a more specific biomarker and AP as less specific biomarkers.<sup>(6,15,16)</sup> Nonetheless, given the absence of biological guidelines for 3,5,6-TCP and AP metabolites, these urinary biomarkers cannot currently be used to assess health risks.

Most BEIs<sup>®</sup> are based on urinary biomarker concentrations at TLV-TWA<sup>®</sup> airborne exposure.<sup>(4)</sup> In the case of CPF, for which exposure occurs through multiple routes, the establishment of a BEI<sup>®</sup> on the basis of airborne concentrations of CPF does not ensure a safe estimate for all working conditions because of very different absorption fractions and absorption rates arising from the different routes of exposure. BEIs<sup>®</sup> have also been proposed based on links between urinary biomarkers and effects under worker exposure situations<sup>(4)</sup>, but these links have not yet been established for CPF. Recently, biological reference values (BRVs) have been proposed for the specific urinary

metabolites of the following OP insecticides: azinphosmethyl<sup>(17)</sup>, malathion<sup>(18)</sup> and parathion<sup>(19)</sup>. These BRVs are given as urinary excretions corresponding to safe levels of absorption for workers, whatever the exposure scenario. This was accomplished through the development, for each of these OP insecticides, of a toxicokinetic model relating the dose of the parent compound absorbed in the body to *i*) the time course of urinary biomarkers under different exposure scenarios, on the one hand, and *ii*) to OP insecticides exposure doses causing inhibition of RBC-AChE activity, on the other hand.

The objective of this study was to use a similar approach to propose BRVs for CPF metabolites in urine, with a margin of safety. The model developed in the current work links the absorbed dose of CPF to the urinary excretion of its major metabolites, 3,5,6-TCP and alkyl phosphates (the sum of DEP and DETP). The modeling approach used here, similar to that used in previous works on malathion<sup>(18)</sup> and parathion<sup>(19)</sup>, is a refinement of classical compartment models in that a biological significance is attributed to each compartment and mass balance tracking is emphasized.

## ***METHODS***

### ***Model Development and Validation***

A multi-compartment dynamical model was developed to describe the biodisposition kinetics of CPF and its metabolites in humans. It seeks to predict the essential biological features of the kinetics of CPF with a minimum number of compartments and parameters. To limit the number of compartments, regrouping of tissues and functions was carried out on the basis of the different time scales relevant to the essential biological processes. Parameters were determined from direct fits to available human data on the time courses of the parent compound and its metabolites in biological matrices (blood and urine).

### ***Model Functional Representation***

The model functional representation was based on the available literature on the time-course data of CPF and its metabolites, 3,5,6-TCP and AP, in blood and urine of individuals exposed orally and dermally to CPF. The model is depicted in Figure 2 and symbols and abbreviations are described in Table I. Compartments represent burdens, on a mole basis, of CPF or its metabolites in the body or cumulative excretion of CPF metabolites as a function of time. Arrows stand for the transfer rate of CPF or its metabolites from one compartment to another or the biotransformation rate of CPF to one of its metabolites. The variations with time in compartment burdens were described mathematically by systems of differential equations where the rate of change

in a compartment burden is the difference between its input and output rates (see Appendix for differential equations).

The amounts of CPF bioavailable at the skin surface, in the gastro-intestinal tract and in the respiratory tract were each represented by a specific input compartment,  $D(t)$ ,  $GI(t)$ ,  $RT(t)$ , respectively. A specific compartment  $B(t)$  was used to describe the CPF blood burden (i.e. arterial and venous blood including tissue blood). A storage compartment  $S(t)$  was used to represent CPF in lipids or reversibly bound to tissue proteins.

In the model, which aims at relating the absorbed dose of CPF to the excretion of 3,5,6-TCP and AP metabolites, each mole of CPF in the body was taken to be eventually broken down into one mole of 3,5,6-TCP and one mole of AP<sup>(10)</sup>; this occurs directly or through the formation of CPF-oxon (in vitro half life of the oxon in human blood of 55 seconds).<sup>(20-23)</sup> Thus, a mass-balance system of differential equations was developed for CPF absorption, storage and metabolism into 3,5,6-TCP and AP. After CPF breakdown, the kinetics of 3,5,6-TCP and AP were described by two different mass-balance (on a mole basis) differential equation systems. Accordingly, metabolite specific compartments  $M_{TCP}(t)$  and  $M_{AP}(t)$  were used to represent the body burden of 3,5,6-TCP and AP metabolites. Similarly, the cumulative urinary excretions of 3,5,6-TCP and AP metabolites were represented by compartments  $U_{TCP}(t)$  and  $U_{AP}(t)$ . The model considers that excretion of CPF metabolites occurs through the renal route, as indicated in the literature.<sup>(10-14)</sup>

### *Determination of Parameter Values*

The model parameters were determined using the experimental data of Nolan et al.<sup>(12)</sup> and Drevenkar et al.<sup>(24)</sup> in individuals orally exposed to CPF. Nolan et al.<sup>(12)</sup> exposed 6 volunteers orally to 0.5 mg CPF per kg of body weight and established the detailed blood concentration-time profile of 3,5,6-TCP along with the time course of 3,5,6-TCP urinary excretion rate. These time profiles were shown to evolve in parallel on a semi-log plot, indicating that the 3,5,6-TCP urinary excretion rate is proportional to the 3,5,6-TCP body burden, a fact incorporated in the model kinetics.

Drevenkar et al.<sup>(24)</sup> determined the blood concentration-time profiles of CPF and AP as well as the urinary excretion time course of AP metabolites in a subject orally intoxicated with CPF. After an initial disposition phase, blood concentration-time profiles of CPF and AP are parallel on a semi-log plot. Peak blood concentration levels were observed during the first sample collection (i.e. 2 to 5 hours after ingestion) and concentration values dropped rapidly at subsequent time periods without the observation of an initial zero-order elimination process. Although this subject ingested a dose of CPF sufficiently large to induce signs of acute toxicity, the blood concentration-time courses of CPF and AP metabolites measured after admission to hospital suggest the absence of saturation processes. Also, it can be seen again from the data that the AP urinary excretion rate follows, on a semi-log plot, a time course parallel to the blood concentration of AP metabolites. However, although parallel, these time courses are not straight lines, they rather show an initial rapid decrease

followed by a slower decrease. The rapid decrease is due to two concomitant processes both occurring in the same order of time-scale: the biotransformation of CPF into its metabolites and the transfer of CPF from the blood compartment to a storage compartment. The slower decrease reflects the release of CPF from the storage compartment to blood, released CPF being biotransformed as soon as it reaches the blood compartment.

For the determination of the model parameters, since CPF is eventually broken down into one mole of 3,5,6-TCP and one mole of AP, the experimental data used from the literature (exposure dose and blood and urinary time course data) were expressed in moles. In addition, given that the model is based on the conservation of mass, experimental data used from the literature on the urinary excretion profiles of CPF metabolites which were presented as excretion rates were integrated over time to provide the cumulative burdens necessary for mass conservation. Observed blood concentration values of CPF and its metabolites reported in the literature were also converted to burdens. Amounts of CPF in blood were obtained simply by multiplying reported CPF concentrations in blood by the blood volume (0.08 times the body weight<sup>(25)</sup>). Amounts of metabolites in the body were obtained by multiplying the observed metabolites concentrations in blood by their apparent volume of distribution. The latter was found to correspond to the blood volume in order to ensure conservation of mass at all times in the system i.e. that, at all times, the total bioavailable CPF dose equals the sum of CPF amounts remaining at the site-of-entry, amounts of CPF and its metabolites in the body and amounts of metabolites excreted, in moles. Considering the

blood volume as the volume of distribution of CPF metabolites is consistent with the fact that CPF metabolites are unlikely to diffuse through vascular cells because they rapidly undergo phase II conjugation once formed<sup>(11,12)</sup>. More precisely, this conjugation increases both the water-solubility and the molecular weight (MW of 375, 346 and 330 for the glucurono-conjugates of 3,5,6-TCP, DETP and DEP, respectively, and of 277, 249 and 233 for the sulfo-conjugates of 3,5,6-TCP, DETP and DEP, respectively), which limits the capacity to diffuse through lipid membranes of vascular cells or the passage through aqueous channels of the cellular membranes (this latter process becomes negligible for substances with a MW>150-200).<sup>(26)</sup>

Parameters were determined essentially by least square fits of the explicit solution of differential equations to the observed average blood time courses of CPF, 3,5,6-TCP and AP metabolites (see Table II). The accuracy of parameter values was verified by minimum least square fits to the observed urinary-excretion time courses of CPF metabolites. No more than two parameters were determined per fit. A professional edition of a MathCad software was used for this purpose (MathSoft<sup>®</sup> Inc., Cambridge, MA).

### ***Model Simulations***

Once the parameters of the model were determined as described above, simulations of the time courses of CPF and its metabolites in the body and in excreta were carried out by solving numerically the whole differential equation systems using a fourth-order Runge-Kutta algorithm incorporated in MathCad. The model was used to predict the

time courses of CPF and its metabolites under different exposure routes (oral, dermal and/or inhalation) and temporal scenarios (single or repeated intermittent or continuous exposures). In all these simulations, the same set of parameter values was used to describe the kinetics of CPF, once absorbed, and that of its metabolites. Only the absorption rate constant and the absorption fraction were adjusted according to the route, site and mode of exposure.

To compare model simulations of blood concentrations of CPF and its metabolites with reported experimental results, compartment burdens were simply divided by the blood volume. To compare model simulations of urinary excretions to reported observed data, both the observed excretion rates and the cumulative amounts were examined.

### ***Model Validation***

The model developed using the previously mentioned data was validated using different sets of experimental data. The data of Nolan et al.<sup>(12)</sup> for dermally exposed individuals (on the forearm), the oral data of Brzak et al.<sup>(14)</sup> and that of Griffin et al.<sup>(13)</sup> were used for model validation.

### ***Determination of Biological Reference Values***

BRVs are proposed in this study for 3,5,6-TCP and AP in urine. Since most regulatory agencies and international organizations now rely on the measurement of RBC-AChE inhibition as an early biomarker of cholinergic effects<sup>(27,28)</sup>, the proposed reference values were derived using the available literature data on human exposure to no-

observed-effect level (NOEL) doses for the inhibition of RBC-AChE activity. Plasma cholinesterase activity was not considered because it is now generally accepted that it should not be used for risk assessment since its inhibition is not indicative of an adverse effect; this is well documented by Carlock et al.<sup>(28)</sup> in a review on regulating and assessing risk of cholinesterase-inhibiting pesticides.

In the selection of the NOEL for the establishment of the proposed BRVs, repeated-dose controlled exposures were used since they most resemble worker exposure conditions. The study of Coulston et al.<sup>(29)</sup> is, to our knowledge, the only available controlled study on the assessment of RBC-AChE activity in volunteers repeatedly exposed to CPF. These authors determined RBC-AChE activity in volunteers orally administered tablets containing 0, 0.014, 0.03 and 0.1 mg of CPF per kg of body weight per day for 27, 20 and 9 days, respectively (n = 4 adult male volunteers per exposure group). For all dose regimens, no significant inhibition of RBC-AChE activity was observed. The NOEL for inhibition of RBC-AChE activity was thus taken to be 0.1 mg/kg/day, the highest dose tested. An analysis of the available repeated-dose NOEL data carried out by Mattsson et al.<sup>(30)</sup> also led them to conclude that the repeated-dose human NOEL is  $\approx$  0.1 mg/kg/day. These authors used for their analysis the human data of Coulston et al.<sup>(29)</sup> and corroborated their results with the data of McCollister et al.<sup>(31)</sup> on dogs, which showed that dietary administration of 0.1 mg CPF/kg/day for 1 year did not produce any statistically or clinically significant effect on RBC-AChE activity.

From this repeated exposure-dose NOEL value of 0.1 mg/kg/day (20  $\mu$ mol/day for a 70 kilogram individual), the corresponding absorbed NOEL dose was estimated. BRVs in the form of urinary excretion of metabolites were then derived by simulating with the model an 8-hour dermal CPF exposure such that the total absorbed daily dose corresponds to the absorbed NOEL dose. The proposed reference values are the total amounts of 3,5,6-TCP and AP metabolites excreted in urine over chosen time periods following the onset of exposure. To derive BRVs with a margin of safety, these simulations were carried out: *i*) using the slowest absorption rate compatible with the analyzed experimental time-course data and *ii*) without considering any baseline excretion.

### ***Sensitivity Analysis***

The capacity of each model parameter value to influence the cumulative urinary excretion over conveniently chosen time periods, 12, 24 and 48 hour, was tested. The model parameter values, obtained above from fits to published mean excretion data, were separately varied. The sensitivity tests were based on the following normalized sensitivity coefficient:  $R = \frac{(O_2 - O_1)/O_1}{(I_2 - I_1)/I_1}$  where  $I_1$  is the estimated value of the parameter analyzed for sensitivity and  $I_2$  its locally modified value and where  $O_1$  is the predicted 12-, 24- or 48-hour cumulative urinary amount of metabolite using estimated parameter values and  $O_2$  its predicted value with the modified parameter value.

## **RESULTS**

### ***Model Simulations***

Table II presents parameter values of the model determined using the data of Nolan et al.<sup>(12)</sup> and Drevenkar et al.<sup>(24)</sup> in orally exposed individuals. Figure 3 shows that the model, with these parameter values, provided a close approximation to the data collected by Nolan et al.<sup>(12)</sup> on the blood concentration-time profiles of 3,5,6-TCP as well as the urinary excretion time course of 3,5,6-TCP in volunteers orally administered 0.5 mg CPF per kg of body weight in the form of tablets. Figure 4 shows that the model also reproduced closely the data of Drevenkar et al.<sup>(24)</sup> on the blood concentration-time profiles of CPF and AP together with the time dependent cumulative urinary excretion time course of AP in a subject poisoned with CPF. According to model simulation, the total absorbed dose of this intoxicated subject was estimated to be 731  $\mu\text{mol}$  (the exposure dose was estimated to be  $\approx 4.6$  mg CPF/kg of body weight).

The proposed model was applied to another set of data from Nolan et al.<sup>(12)</sup> on the blood and urinary time profiles of 3,5,6-TCP in dermally exposed volunteers, on the forearm. The parameter values reported in Table II, which describe the kinetics of absorbed CPF and that of 3,5,6-TCP, were used for these simulations. To fit the data, the dermal absorption fraction ( $f_{\text{abs-dermal}}$ ) was found to be 0.010 and the dermal absorption rate ( $k_{\text{abs-dermal}}$ ),  $0.04 \text{ hr}^{-1}$ . These values are near those reported by Nolan et al.<sup>(12)</sup> using a simpler compartment model:  $f_{\text{abs-dermal}} = 0.013$  and  $k_{\text{abs-dermal}} = 0.03 \text{ hr}^{-1}$ .

With the values determined in the present study, Figure 5 shows that simulations of time profiles were in close agreement with the observed data.

The model was further validated with the data of Brzak et al.<sup>(14)</sup> on the blood concentration-time profiles of 3,5,6-TCP as well as on the cumulative urinary excretion time course of 3,5,6-TCP in volunteers orally exposed to capsules containing 0.5, 1 and 2 mg CPF per kg of body weight (see Figure 6). All the parameters of the internal kinetics were kept as determined with the data Nolan et al.<sup>(12)</sup> in orally exposed individuals (Table II). For good predictions of the experimental data, the average absorption fraction was found to be 0.23, 0.23 and 0.19 for the 0.5, 1 and 2 mg/kg dose, respectively, and the absorption rate was found to be  $0.1 \text{ hr}^{-1}$  for all doses. This is congruent with the oral absorption fraction estimate of 0.22 which can be inferred from the average, on all treatment groups, 3,5,6-TCP cumulative excretion in urine reported by Brzak et al.<sup>(14)</sup>. This small absorption rate fraction stems from the fact that CPF was given in the form of capsules rather than in the form of tablets as in the study of Nolan et al.<sup>(12)</sup> and, it appears, the contents of some of the capsules was not completely bioavailable.

The model describing the kinetics of absorbed CPF and that of AP was also applied to the data of Griffin et al.<sup>(13)</sup> in volunteers orally exposed to a low dose of 1 mg of CPF placed on a sugar cube. With the parameter values of Table II, the model predicts too small a rate of elimination for AP in urine. However, a good fit was obtained (see Figure 7) by lowering the storage rate of CPF,  $k_{BS}$ , to  $0.12 \text{ hr}^{-1}$  and by using the oral

absorption fraction of 0.93 reported by Griffin et al.<sup>(13)</sup> and an oral absorption rate of  $0.13 \text{ hr}^{-1}$  while keeping the other parameter values of Table II unchanged.

### ***Sensitivity Analysis***

A sensitivity analysis was performed on model parameters using the values reported in Table II (see Table III). It showed that, under typical worker exposure conditions – an 8 hour per day dermal exposure –, the dermal absorption rate  $k_{\text{abs-dermal}}$  and the urinary excretion rate parameters,  $k_{\text{MU-TCP}}$  and  $k_{\text{MU-AP}}$ , were the main model parameters governing the 12-, 24- and 48-hour cumulative urinary excretion. However, changes in the dermal absorption rate had a greater influence on the cumulative urinary excretion of CPF metabolites over the first 12-hour period than over the 0-24 and 0-48 hour periods.

Changes in the dermal absorption rate  $k_{\text{abs-dermal}}$  and the urinary excretion rate parameters  $k_{\text{MU-TCP}}$  and  $k_{\text{MU-AP}}$  had a larger effect on the excretion than changes in the CPF biotransformation rate  $k_{\text{BM}}$ . Varying the biotransformation rate  $k_{\text{BM}}$  had little impact on metabolites excretion kinetics provided CPF partitioning between storage and metabolism ( $k_{\text{BS}}/k_{\text{BM}}$ ) remained fixed, which is the case in our model. In other words, the value of the  $k_{\text{BS}}/k_{\text{BM}}$  ratio is more important in governing the kinetics than the values of the two parameters separately ( $k_{\text{BS}}$  and  $k_{\text{BM}}$ ).

### ***Determination of Biological Reference Values***

Using the model, which allows links to be made between the absorbed dose and the urinary excretion of metabolites whatever the exposure scenario, BRVs for 3,5,6-TCP

and AP in urine are proposed (see Table IV). These are expressed as cumulative amounts of metabolites (nmol per kg of body weight) in 24- and 48-hour urine collection periods. Although considered, in the interest of robustness, the possibility of a BRV based on a 0-12 hour collection period was excluded because it would be too sensitive to the highly variable absorption rate, as shown by the sensitivity analysis.

## ***DISCUSSION***

This report presents a toxicokinetic approach for the determination of BRVs for CPF metabolites in urine. As a first step, a toxicokinetic model was developed that captures the broad features of CPF kinetics and allows links to be made between the dose of CPF absorbed in the body and the urinary excretion of its metabolites, for different exposure routes and temporal scenarios. As a second step, this model was used to propose reference values of urinary biomarkers of CPF exposure below which workers should not experience adverse health effects.

### ***Model Description of the Kinetics of Chlorpyrifos and Its Metabolites***

To describe the kinetics of CPF once absorbed and that of its metabolites, a single set of parameter values was used (Table II); only the parameters pertaining to the absorption process needed to be adjusted to meet the very different exposure situations encountered (dermal, oral or inhalation routes). The model showed that the blood and urinary excretion kinetics of CPF and its metabolites were most dependent on the absorption rate constant ( $k_{\text{abs}}$ ) and absorption fraction ( $f_{\text{abs}}$ ) of CPF. These parameters are known to differ substantially among individuals (a 10-fold difference in the oral absorption rate, according to Nolan et al.<sup>(12)</sup>, i.e. from 0.3 to 3 hr<sup>-1</sup> (n = 6 individuals)) and from one exposure route to another. Also, for oral exposures, these parameters vary depending on the mode of administration, e.g., tablets versus capsules<sup>(12,14)</sup>, and for dermal exposures, depending on the exposed skin site, the skin condition and the ambient temperature and humidity.<sup>(4,32)</sup>

With these considerations, the model was shown capable of accurately simulating the kinetics of CPF and its metabolites over a wide range of doses (12 to 95  $\mu\text{mol}$  of absorbed CPF) by different exposure routes.<sup>(12,14)</sup> At the lower absorbed dose of 2.7  $\mu\text{mol}$ , as administered by Griffin et al.<sup>(13)</sup>, the CPF storage rate  $k_{BS}$  needed to be reduced substantially for the model to provide a good fit to the urinary excretion time course of AP metabolites reported by these authors. At low doses, one can surmise that the reason for this low storage rate lies with the hepatic first-pass metabolic effect, which is more important than at higher doses. If this is so, a significantly larger part of the CPF dose would be metabolized prior to reaching the systemic circulation from which storage occurs.

However, the model parameter values could not all be validated with an entirely separate data set, under the same exposure conditions, because such data were not forthcoming. Since the model was built to derive BRVs by allowing links to be made between an absorbed daily dose (therefore independent of the absorption fraction), the cumulative urinary amounts of biomarkers and the appearance of critical biological effects, it was not necessary to have the complete range of parameter values. In this context, it is sufficient to use the most conservative parameter values compatible with the available data.

### *Comparison of the Current Model with Others Previously Published*

The current model can be compared to other previously published models. Authors have fitted their experimental time course data to one or two compartment models.<sup>(12,24)</sup> In particular, Nolan et al.<sup>(12)</sup> described mathematically the blood concentration-time profile of 3,5,6-TCP using a one compartment model with first-order elimination leading to a prediction of mono-exponential decrease. In our model, 3,5,6-TCP in the body was also represented by a single compartment; however, the introduction of a storage compartment for the parent compound,  $S(t)$ , results in a bi-exponential pattern for the blood time course of CPF metabolites. This feature corresponds more closely to the combined data of Nolan et al.<sup>(12)</sup> and Drevenkar et al.<sup>(24)</sup> (see Figures 3-5).

Timchalk et al.<sup>(33)</sup> recently proposed a pharmacokinetic model for CPF, CPF-oxon and its 3,5,6-TCP metabolite. These authors described the kinetics of the parent compound using a model with 8 compartments: skin, gastro-intestinal tract, liver, brain, fat, diaphragm, richly and slowly perfused tissues. Their model for the 3,5,6-TCP kinetics was described by a single global compartment from which elimination occurs through excretion in urine. The parameters of their model were determined from a combination of animal data<sup>(22,34,35)</sup>, human data<sup>(12,25)</sup> and mathematical algorithms<sup>(36)</sup>. The model of Timchalk et al.<sup>(33)</sup> considers only the detoxification of CPF into 3,5,6-TCP, whereas our model considers also the AP metabolites, which are as important in quantity since one mole of CPF yields a mole of 3,5,6-TCP and a mole of AP. These authors do not propose a BRV based on their model. Although structurally different, both our model

and that of Timchalk et al.<sup>(33)</sup> provided a close approximation to the data of Nolan et al.<sup>(12)</sup> and Brzak et al.<sup>(14)</sup>.

### ***Proposed Biological Reference Values***

BRVs are proposed in this study for CPF urinary metabolites based on the links between the dose of CPF absorbed and time varying metabolite excretion as provided by the toxicokinetic model, on the one hand, and on experimental data relating CPF exposure dose to the inhibition of RBC-AChE activity, on the other hand. They are expressed as total amounts of 3,5,6-TCP and AP in urine over time periods chosen to provide an accurate assessment of worker exposure, i.e., 24 and 48 hours following the onset of a workshift.

Although it is more practical in field studies to determine concentrations of CPF metabolites in spot urine samples and adjust for creatinine contents, this may lead to serious biases because of important variations with time, in both CPF metabolite concentrations and creatinine excretion rate ( $\geq 200\%$  intra-day and 63 – 244% inter-day variations in creatinine excretion rate in the same individual).<sup>(37-40)</sup> For a more accurate assessment of health risks, it is better to determine total amounts of metabolites in urine collected over the longest feasible period of time. Model simulations showed that it is best to collect urine samples over at least 24 hours, as was done in several studies.<sup>(6, 18, 41-43)</sup> This stems from the fact that *i*) the dermal absorption rate, which is known to be subject to wide intra- and inter-individual variations<sup>(32)</sup>, has a larger influence on the rate of appearance of CPF metabolites in urine at earlier time points than at later times

(see Table III), and *ii*) when considering a  $k_{\text{abs-dermal}}$  of  $0.04 \text{ hr}^{-1}$ , a greater fraction of the absorbed CPF dose is estimated to be excreted in urine as 3,5,6-TCP and AP during the first 24 hours following the onset of an 8-hour dermal exposure to CPF (11.3% and 19.8%, respectively) than during the first 12 hours (2.5% and 5.7%, respectively).

The proposed BRVs aim at protecting the most susceptible workers. According to several authors,<sup>(27,44,45)</sup> the establishment of guidelines on the basis of measurements of RBC-AChE activity as a surrogate for AChE in the nervous system contributes to provide a margin of safety for protecting human health. Indeed, in a study conducted by Nordstrand et al.<sup>(46)</sup> in rats administered a single oral dose of CPF, RBC-AChE was inhibited at least 12-fold more than brain or peripheral tissue AChE. Chen et al.<sup>(27)</sup> reported moreover that the inhibition of RBC-AChE activity consistently occurs at CPF doses below those exerting any clinical signs of cholinergic toxicity.

Using the toxicokinetic model developed, it was possible to explore the conditions (exposure routes and time scenarios) under which an identical total CPF absorbed dose would produce the lowest cumulative urinary excretion of CPF metabolites over chosen time periods. Since the proposed BRVs are based on these cumulative urinary outputs, they can be determined with a margin of safety by basing them on the slowest output situations. It can thus be shown that reference values based on a workday dermal exposure scenario, with slow absorption and thus slow urinary output, are safer than those based on the faster urinary outputs of rapidly absorbed CPF from respiratory or oral exposures. For example, simulation of an 8-hour dermal exposure to CPF leads

to cumulative urinary amounts of 3,5,6-TCP over 24 hours equal to 11.3 percent of the absorbed dose, whereas the corresponding value inferred from an 8-hour inhalation exposure with instantaneous absorption equals 33.2 percent of the absorbed dose. Similarly, simulation of an 8-hour dermal exposure to CPF leads to cumulative urinary amounts of AP over 24 hours equal to 19.8 percent of the absorbed dose, whereas the corresponding value inferred from an 8-hour inhalation exposure equals 48.7 percent of the absorbed dose. In addition, bearing in mind that workers are rarely exposed to pesticides for more than 8 consecutive hours, model simulations were conducted where a given total dose is absorbed over different exposure durations up to 8 hours. These showed that, for a given total absorbed dose, absorption over 8 hours results in smaller 3,5,6-TCP and AP urinary excretion rates than those obtained from shorter exposure durations. This is reasonable since the same total input, when absorbed over a longer period, leads to a lower input rate and consequently a lower output rate, although eventually the cumulative amounts found in urine would be the same. Thus, urinary BRVs based on the 8-hour exposure duration are the more conservative.

Model inferences further indicated that the smaller the absorption rate value, the slower will metabolites be excreted in urine. For inhalation exposure, absorption is very rapid and is similar to a drop by drop infusion; following oral exposure, the average absorption rate compatible with the available data varies between 0.1 and 0.5 hr<sup>-1</sup> (12,14); upon dermal application, the absorption rate was shown to be much slower, in the vicinity of 0.04 hr<sup>-1</sup>.<sup>(12)</sup> In the case of a dermal exposure, the main route-of-entry for workers, sensitivity analyses conducted on model parameter values (see Table III)

showed that the absorption rate contributes to a major part of the variability in the urinary excretion rate of CPF metabolites. The proposed BRVs, based on a dermal exposure with the slowest absorption rate found,  $0.04 \text{ hr}^{-1}$ , are thus protective.

It was also found from model simulations that the derivation of BRVs without adding the background contribution of prior exposure days also contributes to provide safer estimates. Indeed, the daily urinary excretion of CPF metabolites, expressed as a fraction of the absorbed daily dose, was predicted to increase upon repeated daily 8-hour dermal exposures. These findings indicate that for workers exposed to CPF on an almost daily basis, it is best to collect urine at the end of a workweek to account for the yet non-eliminated built up of previous days.

As a measure of their applicability to practical situations, the proposed BRVs were used to assess the health risks of botanical garden workers applying CPF ( $n = 1$ ) to plants or manipulating treated plants ( $n = 3$ ).<sup>(43)</sup> The total amounts of 3,5,6-TCP measured in a 0-24 hour urine sample following an application of CPF were  $1.4 \mu\text{g}$  in the person applying CPF and 6.5, 5.1,  $4.5 \mu\text{g}$  in 3 individuals manipulating plants. These values represent respectively 0.004, 0.018, 0.014 and 0.012 of the proposed BRV, assuming a body weight of 70 kilograms. The proposed BRVs were also used to assess the health risks of workers in the Fenske and Elkner<sup>(6)</sup> study, who were exposed to CPF following structural control treatments of houses. These workers appear to be more exposed than those of the study of Samuel et al.<sup>(43)</sup>. However, from the values shown in Table V, it appears that these workers were at low risk upon comparison of

their 3,5,6-TCP cumulative urinary excretion values over 24 and 48 hours following the onset of a workday to the proposed BRVs for each of these urine collection periods.

The proposed BRVs are convenient and robust. However, they could benefit from further validation in the field for different occupational exposure conditions. This could be achieved by comparing observed amounts of CPF biomarkers with levels of cholinesterase activity in workers in contact with CPF. The accuracy of the proposed BRVs could then be refined, always ensuring that any individual with a urinary excretion value below the BRV has an inhibition of RBC-AChE activity below the BEI<sup>®</sup> of 30%, as proposed by the ACGIH<sup>®(4)</sup>, and this whatever the exposure duration (single or repeated).

***ACKNOWLEDGMENT***

The authors wish to thank the Institut de Recherche Robert-Sauvé en Santé et Sécurité du Travail (IRSST) for providing financial support for this study.

## APPENDIX

### *First Order Linear Differential Equations for Each Model Compartment*

#### **Kinetics of Chlorpyrifos**

From Figure 2, the following differential equations are obtained (see Table I for definitions of symbols and abbreviations):

$$\frac{dD(t)}{dt} = g_{\text{dermal}}(t) - k_{\text{abs-dermal}} \times D(t) \quad [1]$$

$$\frac{dGI(t)}{dt} = g_{\text{oral}}(t) - k_{\text{abs-oral}} \times GI(t) \quad [2]$$

$$\frac{dRT(t)}{dt} = g_{\text{inh}}(t) - k_{\text{abs-inh}} \times RT(t) \quad [3]$$

where  $g_{\text{dermal}}(t)$ ,  $g_{\text{oral}}(t)$  and  $g_{\text{inh}}(t)$  are the bioavailable dose per unit of time for dermal, oral, or respiratory tract absorption, respectively.

For intravenous injection,  $g(t) = 0$  for  $t \geq 0$  and at time  $t = 0$ :  $B(0) = D_{\text{abs}}$ .

$$\frac{dB(t)}{dt} = k_{\text{abs-oral}} \times GI(t) + k_{\text{abs-inh}} \times RT(t) + k_{\text{abs-dermal}} \times D(t) + k_{\text{SB}} \times S(t) - (k_{\text{BS}} + k_{\text{BM}}) \times B(t) \quad [4]$$

$$\frac{dS(t)}{dt} = k_{\text{BS}} \times B(t) - k_{\text{SB}} \times S(t) \quad [5]$$

**Kinetics of 3,5,6-Trichloro-2-Pyridinol**

$$\frac{dM_{\text{TCP}}(t)}{dt} = k_{\text{BM}} \times B(t) - k_{\text{MU-TCP}} \times M_{\text{TCP}}(t) \quad [6]$$

$$\frac{dU_{\text{TCP}}(t)}{dt} = k_{\text{MU-TCP}} \times M_{\text{TCP}}(t) \quad [7]$$

**Kinetics of the Alkyl Phosphates**

$$\frac{dM_{\text{AP}}(t)}{dt} = k_{\text{BM}} \times B(t) - k_{\text{MU-AP}} \times M_{\text{AP}}(t) \quad [8]$$

$$\frac{dU_{\text{AP}}(t)}{dt} = k_{\text{MU-AP}} \times M_{\text{AP}}(t) \quad [9]$$

**REFERENCE**

1. **Namba, T., C.T. Nolte, J.J. Jackrel, and D. Grob:** Poisoning due to organophosphate insecticides. *Am. J. Med.* 50:475-492 (1971).
2. **Huff, R.A., J.J. Corcoran, J.K. Anderson, and M.B. Abou-Donia:** Chlorpyrifos oxon binds directly to muscarinic receptors and inhibits cAMP accumulation in rat striatum. *J. Pharmacol. Exp. Ther.* 269:329-335 (1994).
3. **Sultatos, L.G.:** Mammalian toxicology of organophosphorus pesticides. Invited review. *J. Toxicol. Environ. Health* 43:271-289 (1994).
4. **American Conference of Governmental Industrial Hygienists:** *Documentation of the Threshold Limit Values and Biological Exposure Indices*, 7th Ed. Cincinnati, OH: ACGIH, 2002.
5. **Dowling, K.C., and J.N. Seiber:** Importance of respiratory exposure to pesticides among agricultural populations. *Int. J. Toxicol.* 21:371-381(2002).
6. **Fenske, R.A., and K.P Elkner:** Multi-route exposure assessment and biological monitoring of urban pesticide applicators during structural control treatments with chlorpyrifos. *Toxicol. Ind. Health* 6(3/4):349-371 (1990).

7. **Gil, F., and A. Pla:** Biomarkers as biological indicators of xenobiotic exposure. *J. Appl. Toxicol.* 21:245-255 (2001).
8. **Lauwerys, R., and P. Hoet:** *Industrial Chemical Exposure: Guidelines for Biological Monitoring.* Boca Raton, FL: Lewis Publishers, 2001.
9. **Richter, E.D., P. Chuwers, and Y. Levy:** Health effects from exposure to organophosphate pesticides in workers and residents in Israel. *Isr. J. Med. Sci.* 28:584-598 (1992).
10. **Smith, G.N., B.S. Watson, and F.S. Fischer:** Investigations on Dursban insecticide. Metabolism of [<sup>36</sup>Cl] o,o-diethyl o-3,5,6-trichloro-2-pyridyl phosphorothioate in rats. *J. Agric. Food Chem.* 15:132-138 (1967).
11. **Bakke, J.E., V.J. Feil, and C.E. Price:** Rat urinary metabolites from o,o-diethyl-o-(3,5,6-trichloro-2-pyridyl) phosphorothioate. *J. Environ. Sci. Health B* 11(3):225-230 (1976).
12. **Nolan, R.J., D.L. Rick, N.L. Freshour, and J.H. Saunders:** Chlorpyrifos: pharmacokinetics in human volunteers. *Toxicol. Appl. Pharmacol.* 73:8-15 (1984).
13. **Griffin, P., H. Mason, K. Heywood, and J. Cocker:** Oral and dermal absorption of chlorpyrifos: a human volunteer study. *Occup. Environ. Med.* 56:10-13 (1999).

14. **Brzak, K.A.:** *A Rising Dose Toxicology Study to Determine the No-Observable-Effect-Levels (NOEL) for Erythrocyte Acetylcholinesterase (AChE) Inhibition and Cholinergic Signs and Symptoms of Chlorpyrifos at Three Dose Levels – Part B.* Report No. 981176. Midland, Michigan: Toxicology & Environmental Research and Consulting, Dow Chemical Company, 2000.
  
15. **Jitsunari, F., F. Asakawa, T. Nakajima, and J. Shimada:** Determination of 3,5,6-trichloro-2-pyridinol levels in the urine of termite control workers using chlorpyrifos. *Acta Med. Okayama* 43(5):299-306 (1989).
  
16. **Cocker, J., H.J. Mason, S.J. Garfitt, and K. Jones:** Biological monitoring of exposure to organophosphate pesticides. *Toxicol. Lett.* 134:97-103 (2002).
  
17. **Carrier, G., and R.C. Brunet:** A toxicokinetic model to assess the risk of azinphosmethyl exposure in humans through measures of urinary elimination of alkylphosphates. *Toxicol. Sci.* 47:23-32 (1999).
  
18. **Bouchard, M., N.H. Gosselin, R.C. Brunet, O. Samuel, M.J. Dumoulin, and G. Carrier:** A toxicokinetic model of malathion and its metabolites as a tool to assess human exposure and risk through measurements of urinary biomarkers. *Toxicol. Sci.* 73:182-194 (2003).

19. **Gosselin, N.H., M. Bouchard, R.C. Brunet, M.J. Dumoulin, and G. Carrier:** Toxicokinetic modeling of parathion and its metabolites in humans for the determination of biological reference values. *J. Toxicol. Environ. Health* (in press).
20. **Sultatos, L.G., and S.D. Murphy:** Kinetic analyses of the microsomal biotransformation of the phosphorothioate insecticides chlorpyrifos and parathion. *Fundam. Appl. Toxicol.* 3:16-21 (1983).
21. **Sultatos, L.G., L.D. Minor, and S.D. Murphy:** Metabolic activation of phosphorothioate pesticides: role of the liver. *J. Pharmacol. Exp. Ther.* 232(3):624-628 (1985).
22. **Ma, T., and J.E. Chambers:** Kinetic parameters of desulfuration and dearylation of parathion and chlorpyrifos by rat liver microsomes. *Food Chem. Toxicol.* 32(8):763-767 (1994).
23. **Brzak, K.A., D.W. Harms, M.J. Bartels, and R.J. Nolan:** Determination of chlorpyrifos, chlorpyrifos oxon, and 3,5,6-trichloro-2-pyridinol in rat and human blood. *J. Anal. Toxicol.* 22:203-210 (1998).
24. **Drevenkar, V., Z. Vasilic, B. Stengl, Z. Fröbe, and V. Rumenzak:** Chlorpyrifos metabolites in serum and urine of poisoned persons. *Chem. Biol. Interact.* 87:315-22 (1993).

25. **Brown, R.P., M.D. Delp, S.L. Lindstedt, L.R. Rhomberg, and R.P. Beliles:** Physiological parameter values for physiologically based pharmacokinetic models. *Toxicol. Ind. Health* 13:407-484 (1997).
26. **Seeman, P., and Kalant, H.:** Drug Solubility, Absorption, and Movement Across Body Membranes. In *Principles of Medical Pharmacology*, Sixth Edition, H. Kalant and W.H. E. Roschlau (eds.), pp. 9-25. B.C. Burlington, Ontario: Decker, 1997.
27. **Chen, W.L., J.J. Sheets, R.J. Nolan, and J.L. Mattsson:** Human red blood cell acetylcholinesterase inhibition as the appropriate and conservative surrogate endpoint for establishing chlorpyrifos reference dose. *Regul. Toxicol. Pharmacol.* 29(1):15-22 (1999).
28. **Carlock, L.L., W.L. Chen, E.B. Gordon, J.C. Killeen, A. Manley, L.S. Meyer, et al.:** Regulating and assessing risks of cholinesterase-inhibiting pesticides: divergent approaches and interpretations. *J. Toxicol. Environ. Health B Crit. Rev.* 2(2):105-160 (1999).
29. **Coulston, F., L. Golberg, and T. Griffin:** *Safety Evaluation of Dowco 179 in Human Volunteers*. Accession No. 112118. Albany, New York: Institute of Experimental Pathology and Toxicology, Albany Medical College, 1972.

30. **Mattsson, J.J., L. Holden, D.L. Eisenbrandt, and J.E. Gibson:** Reanalysis with optimized power of red blood cell acetylcholinesterase activity from a 1-year dietary treatment of dogs to chlorpyrifos. *Toxicology* 160:155-164 (2001).
31. **McCollister, S.B., R.J. Kociba, C.G. Humiston, D.D. McCollister, and P.J. Gehring:** Studies of the acute and long-term oral toxicity of chlorpyrifos (o,o-diethyl o-3,5,6-trichloro-2-pyridyl phosphorothioate). *Food Cosmet. Toxicol.* 12:45-61 (1974).
32. **Bronaugh, R.L., and H.I. Maibach:** *Percutaneous Absorption. Drugs – Cosmetics – Mechanisms – Methodology*, 3rd Edition. New York: Marcel Dekker, 1999.
33. **Timchalk, C., R.J. Nolan, A.L. Mendrala, D.A., Dittenber, K.A. Brzak, and J.L. Mattsson:** A physiologically based pharmacokinetic and pharmacodynamic (PBPK/PD) model for the organophosphate insecticide chlorpyrifos in rats and humans. *Toxicol. Sci.* 66:34-53 (2002).
34. **Mortensen, S.R., S.M. Chanda, M.J. Hooper, and S. Padilla:** Maturational differences in chlorpyrifos-oxonase activity may contribute to age-related sensitivity to chlorpyrifos. *J. Biochem. Toxicol.* 11:279-287 (1996).

35. **Sultatos, L.G, M. Shao, and S.D. Murphy:** The role of hepatic biotransformation in mediating the acute toxicity of the phosphorothionate insecticide chlorpyrifos. *Toxicol. Appl. Pharmacol.* 73:60-68 (1984).
36. **Poulin, P., and K. Krishnan:** An algorithm for predicting tissue: blood partition coefficients of organic chemicals from n-octanol: water partition coefficient data. *J. Toxicol. Environ. Health* 46:117-129 (1995).
37. **Curtis, G., and M. Fogel:** Creatinine excretion: diurnal variation and variability of whole and part-day measures. *Psychosom. Med.* 32:337-350 (1970).
38. **Greenblatt, D.J., B.J. Ransil, J.S. Harmatz, T.W. Smith, D.W. Duhme, and J. Kosh-Weser:** Variability of 24-hour urinary creatinine excretion by normal subjects. *J. Clin. Pharmacol.* 16:321-328 (1976).
39. **Alessio, L, A. Berlin, A. Dell'Orto, F. Toffoletto, and I. Ghezzi:** Reliability of urinary creatinine as a parameter used to adjust values of urinary biological indicators. *Int. Arch. Occup. Environ. Health* 55:99-106 (1985).
40. **Boeniger, M.F., L.K. Lowry, and J. Rosenberg:** Interpretation of urine results used to assess chemical exposure with emphasis on creatinine adjustments: a review. *Am. Ind. Hyg. Assoc. J.* 54:615-627 (1993).

41. **Middendorf, P., C. Timchalk, B. Kropscott, B., and D. Rick:** Forest worker exposure to Garlon™ 4 herbicide. *Appl. Occup. Environ. Hyg.* 9:589-594 (1994).
  
42. **Saieva, C., C. Aprea, R Tumino, G. Masala, S. Salvini., G. Frasca, et al.:** Twenty-four-hour urinary excretion of ten pesticide metabolites in healthy adults in two different areas of Italy (Florence and Ragusa). *Sci. Total Environ.* 332:71-80 (2004).
  
43. **Samuel, O., L. St-Laurent, P. Dumas, E. Langlois, and G. Gingras:** *Pesticides en Milieu Serricole – Caractérisation de l'Exposition des Travailleurs et Évaluation des Délais de Réentrée.* Report No. R315. Quebec, Canada : Institut de Recherche en Santé et Sécurité au Travail (IRSST), 2002.
  
44. **Gibson, J.E., W.L. Chen, and R.K.D. Peterson:** How to determine if an additional 10× safety factor is needed for chemicals: a case study with chlorpyrifos. *Toxicol. Sci.* 48:117-122 (1999).
  
45. **Van Gemert, M., M. Dourson, and A. Moretta:** Use of human data for the derivation of a reference dose for chlorpyrifos. *Regul. Toxicol. Pharmacol.* 33:110-116 (2001).

46. Nordstrandt, A.C., S. Padilla, and V.C. Moser: The relationship of oral chlorpyrifos effects on behavior, cholinesterase inhibition and muscarinic receptor density in rats. *Pharmacol. Biochem. Behav.* 58:15-23 (1997).

**Table 1. Symbols used in the functional representation of the model**

Variables and parameters		Description	
Symbols or abbreviations			
Variables	$g_{\text{dermal}}(t)$	Dermal dose bioavailable (mol) per unit of time (hr) which can describe time varying inputs	
	$g_{\text{oral}}(t)$	Oral dose bioavailable (mol) per unit of time (hr) which can describe time varying inputs	
	$g_{\text{inh}}(t)$	Inhaled dose bioavailable (mol) per unit of time (hr) which can describe time varying inputs	
	$D(t)$	Burden of chlorpyrifos bioavailable (mol) at the skin surface as a function of time	
	$GI(t)$	Burden of chlorpyrifos bioavailable (mol) in the gastro-intestinal tract as a function of time	
	$RT(t)$	Burden of chlorpyrifos bioavailable (mol) in the respiratory tract as a function of time	
	$Q(t)$	Systemic body burden of chlorpyrifos and its metabolites (mol) as a function of time	
	$B(t)$	Blood burden of chlorpyrifos (mol) as a function of time	
	$S(t)$	Burden of chlorpyrifos in storage tissues (mol) as a function of time	
	$M_{\text{TCP}}(t)$	Body burden of 3,5,6-trichloro-2-pyridinol (mol) as a function of time	
	$M_{\text{AP}}(t)$	Body burden of alkyl phosphates (mol) as a function of time	
	$U_{\text{TCP}}(t)$	Cumulative amount of 3,5,6-trichloro-2-pyridinol in urine (mol) as a function of time	
	$U_{\text{AP}}(t)$	Cumulative amount of alkyl phosphates in urine (mol) as a function of time	
	Parameters	$f_{\text{abs-oral}}$	Oral absorption fraction of chlorpyrifos
		$f_{\text{abs-inh}}$	Pulmonary absorption fraction of chlorpyrifos
$f_{\text{abs-dermal}}$		Dermal absorption fraction of chlorpyrifos	
$k_{\text{abs-oral}}$		Oral absorption rate of chlorpyrifos ( $\text{hr}^{-1}$ )	
$k_{\text{abs-inh}}$		Pulmonary absorption rate of chlorpyrifos ( $\text{hr}^{-1}$ )	
$k_{\text{abs-dermal}}$		Dermal absorption rate of chlorpyrifos (i.e., transfer rate from skin surface to blood) ( $\text{hr}^{-1}$ )	
$k_{\text{BS}}$		Blood to storage tissues transfer rate of chlorpyrifos ( $\text{hr}^{-1}$ )	
$k_{\text{SB}}$		Storage tissues to blood transfer rate of chlorpyrifos ( $\text{hr}^{-1}$ )	
$k_{\text{BM}}$		Biotransformation rate of chlorpyrifos ( $\text{hr}^{-1}$ )	
$k_{\text{MU-TCP}}$		Transfer rate of 3,5,6-trichloro-2-pyridinol from the body to urine ( $\text{hr}^{-1}$ )	
$k_{\text{MU-AP}}$	Transfer rate of alkyl phosphates from the body to urine ( $\text{hr}^{-1}$ )		

**Table 2. Model parameter values**

Parameters <sup>A</sup>		Values
Absorption fractions	$f_{\text{abs-oral}}$	0.798 <sup>B</sup>
	$f_{\text{abs-dermal}}$	0.00995 <sup>C</sup>
Transfer rates (hr <sup>-1</sup> )	$k_{\text{abs-oral}}$	0.460 <sup>B</sup>
	$k_{\text{abs-dermal}}$	0.0400 <sup>C</sup>
	$k_{\text{BM}}$	1.908 <sup>D</sup>
	$k_{\text{BS}}$	3.061 <sup>D</sup>
	$k_{\text{SB}}$	0.0361 <sup>D</sup>
	$k_{\text{MU-TCP}}$	0.0611 <sup>E,F</sup>
	$k_{\text{MU-AP}}$	0.199 <sup>E,G</sup>

<sup>A</sup> The description of parameters is given in Table I.

<sup>B</sup> The oral absorption fraction and rate are known to vary according to the mode of administration.<sup>(12,14)</sup> These oral absorption fraction and rate values were determined from the oral data of Nolan et al.<sup>(12)</sup> on the average blood time profile of 3,5,6-trichloro-2-pyridinol (3,5,6-TCP) along with the average time course of 3,5,6-TCP cumulative urinary excretion calculated from the urinary excretion rate data presented by these authors.

<sup>C</sup> The dermal absorption fraction and rate are known to vary according to the site of application.<sup>(31)</sup> These dermal absorption rate and fraction values were determined from

the dermal data of Nolan et al.<sup>(12)</sup> on the average blood and urinary time courses of 3,5,6-TCP in volunteers exposed to CPF on the forearm.

<sup>D</sup> Determined from the data of Drevenkar et al.<sup>(24)</sup> on both the blood time courses of chlorpyrifos and alkyl phosphates (AP).

<sup>E</sup> Based on the available human data<sup>(12-14)</sup>, excretion of metabolites from the body was taken to occur through the renal route.

<sup>F</sup> Determined from the average blood time course of 3,5,6-TCP reported by Nolan et al.<sup>(12)</sup> and accuracy was verified from the average urinary excretion time profile of 3,5,6-TCP reported by these authors.

<sup>G</sup> Determined from the blood time course of AP reported by Drevenkar et al.<sup>(24)</sup> and accuracy was verified from the urinary excretion time profile of AP reported by these authors.

**Table 3. Values of the normalized sensitivity coefficient R**

Model parameters	Normalized sensitivity coefficient R <sup>A</sup>					
	3,5,6-Trichloro-2-pyridinol			Alkyl phosphates		
	0-12 hr urinary excretion	0-24 hr urinary excretion	0-48 hr urinary excretion	0-12 hr urinary excretion	0-24 hr urinary excretion	0-48 h urinary excretion
k <sub>SB</sub>	0.06	0.13	0.23	0.06	0.14	0.25
k <sub>BS</sub>	-0.56	-0.55	-0.48	-0.56	-0.54	-0.46
k <sub>BM</sub>	0.59	0.53	0.55	0.58	0.56	0.47
k <sub>BM</sub> <sup>B</sup>	0.05	0.02	0.01	0.04	0.02	0.01
k <sub>MU</sub>	0.83	0.66	0.40	0.57	0.29	0.10
k <sub>abs-dermal</sub>	0.88	0.75	0.52	0.88	0.72	0.47

<sup>A</sup>  $R = \frac{(O_2 - O_1)/O_1}{(I_2 - I_1)/I_1}$ , where  $I_1$  is the estimated value of the parameter as given in Table II,

$I_2$  its locally modified value.  $O_1$  is the predicted 12-, 24- or 48-hour cumulative urinary excretion using the estimated parameter value and  $O_2$  the predicted value with the modified parameter value. The cumulative urinary  $O_1$  and  $O_2$  were obtained by model simulations of an 8-hour dermal exposure to chlorpyrifos, where the daily absorbed dose corresponds to a unit dose.

<sup>B</sup>  $k_{BS}$  and  $k_{BM}$  are varied simultaneously but such as to maintain a constant partitioning ratio between storage and biotransformation ( $k_{BS}/k_{BM}$ ).

**Table 4. Biological reference values for 3,5,6-trichloro-2-pyridinol and alkyl phosphates in urine: cumulative amounts over different collection periods from the onset of exposure**

Urine collection period (hr)	Proposed biological reference values <sup>A,B</sup> (nmol/kg of body weight)	
	3,5,6-Trichloro-2-pyridinol	Alkyl phosphates
0 - 24	26	45
0 - 48	76	99

<sup>A</sup> For comparison of urinary metabolite measurements to the proposed biological reference values, workers should collect all urines from the beginning of a workshift for either of the proposed periods: 24 or 48 hours, preferably at the end of a workweek to capture, for safety, non-eliminated doses from previous days.

<sup>B</sup> Obtained using model simulations of an 8-hour dermal exposure, where the daily absorbed dose corresponds to the estimated human absorbed no-observed-effect level (NOEL) dose of 0.08 mg/kg of body weight and where the dermal absorption rate is equal to 0.04 hr<sup>-1</sup>. The absorbed NOEL dose was obtained by multiplying the oral exposure dose NOEL of 0.1 mg/kg determined by Coulston et al.<sup>(29)</sup> by the oral absorption fraction of 0.798. This latter value was determined from the data of Nolan et al.<sup>(12)</sup> where volunteers were administered chlorpyrifos in the form of tablets as in the study of Coulston et al.<sup>(29)</sup>.

**Table 5. Comparison of the data of Fenske and Elkner<sup>(6)</sup>, on the cumulative urinary excretion of 3,5,6-trichloro-2-pyridinol (3,5,6-TCP) over 24 and 48 hours in workers exposed to chlorpyrifos following structural control treatments of houses, with the proposed biological reference values<sup>A</sup>**

Urine collection period (hr)	Observed 3,5,6 - TCP cumulative urinary excretion over different urine collection periods						
	Biological reference value for same urine collection period						
	Worker 1	Worker 2	Worker 3	Worker 4	Worker 5	Worker 6	Worker 8
0 - 24	0.05	0.12	0.10	0.10	0.09	0.02	0.06
0 - 48	0.04	0.06	0.08	0.08	0.09	0.02	0.04

<sup>A</sup> See Table III for the proposed biological reference values for 3,5,6-TCP in the 24- or 48-hour urine collection periods.

## CAPTIONS TO FIGURES

**Figure 1.** Chlorpyrifos biotransformation pathways.

**Figure 2.** Conceptual representation of the kinetics of chlorpyrifos and its metabolites. Symbols and abbreviations are described in Table 1. One mole of chlorpyrifos absorbed in the body is eventually broken down into one mole of 3,5,6-trichloro-2-pyridinol and one mole of alkyl phosphates (the sum of diethyl phosphate and diethyl thiophosphate), either directly or through the formation of chlorpyrifos-oxon.

**Figure 3.** Model simulations (lines) compared with experimental data of Nolan et al.<sup>(12)</sup> (symbols) on (A) the blood concentration-time course of 3,5,6-trichloro-2-pyridinol ( $\times$ ), the urinary excretion rate time course of 3,5,6-trichloro-2-pyridinol ( $\circ$ ) and (B) the cumulative urinary-excretion time course of 3,5,6-trichloro-2-pyridinol in male volunteers orally administered 0.5 mg chlorpyrifos per kg of body weight deposited onto lactose tablets. Each point represents mean value of experimental data ( $n = 6$ ).

**Figure 4.** Model simulations (lines) compared with experimental data (symbols) of Drevenkar et al.<sup>(24)</sup> on (A) the blood concentration-time course of chlorpyrifos ( $\square$ ) and alkyl phosphates ( $\times$ ), the urinary excretion rate time course of alkyl phosphates ( $\circ$ ) and (B) the cumulative urinary-excretion time course of alkyl phosphates (the sum of

diethyl phosphate and diethyl thiophosphate) in a poisoned subject who ingested a commercial insecticide formulation containing chlorpyrifos.

**Figure 5.** Model simulations (lines) compared with experimental data of Nolan et al.<sup>(12)</sup> (symbols) on (A) the blood concentration-time course of 3,5,6-trichloro-2-pyridinol and (B) the cumulative urinary excretion time course of 3,5,6-trichloro-2-pyridinol in male volunteers dermally applied 5 mg chlorpyrifos per kg of body weight on the forearm. Each point represents mean value of experimental data (n = 5).

**Figure 6.** Model simulations (lines) compared with experimental data of Brzak et al.<sup>(14)</sup> (symbols) on (A) the blood concentration-time course of 3,5,6-trichloro-2-pyridinol and (B) the cumulative urinary excretion time course of 3,5,6-trichloro-2-pyridinol in 6 male and 6 female volunteers orally administered 0.5 (○), 1 (×) and 2 (□) mg chlorpyrifos per kg of body weight in capsule form. Each point represents mean experimental value and error bars are standard deviations.

**Figure 7.** Model simulations compared with experimental data (symbols) of Griffin et al.<sup>(13)</sup> on the cumulative urinary excretion time course of alkyl phosphates (the sum of diethyl phosphate and diethyl thiophosphate) in volunteers orally administered 1 mg of chlorpyrifos placed on a sugar cube. Each point represents mean value of experimental data (n = 5, four men and one women). The solid line represents model simulation using an oral absorption fraction of 0.93 as reported by Griffin et al.<sup>(13)</sup>, an oral

absorption rate of  $0.13 \text{ hr}^{-1}$ , a CPF storage rate,  $k_{BS}$ , of  $0.12 \text{ hr}^{-1}$  and the other parameters as reported in Table 2.

Fig. 1

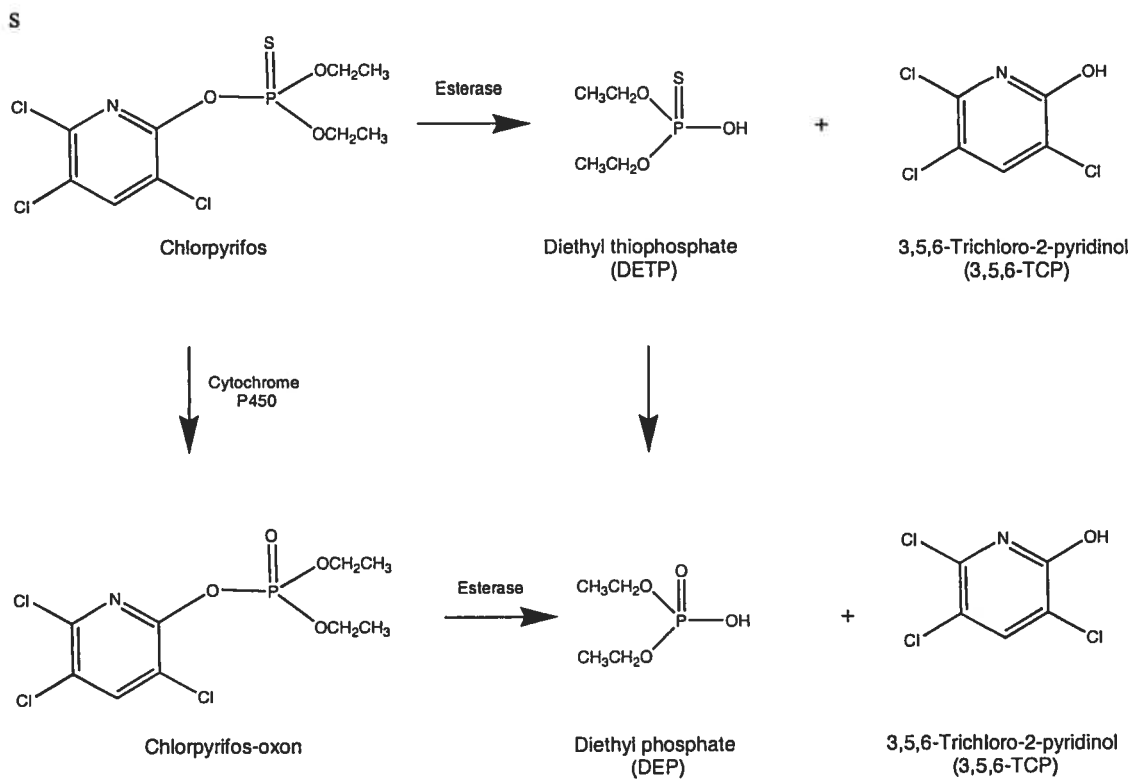


Fig. 2

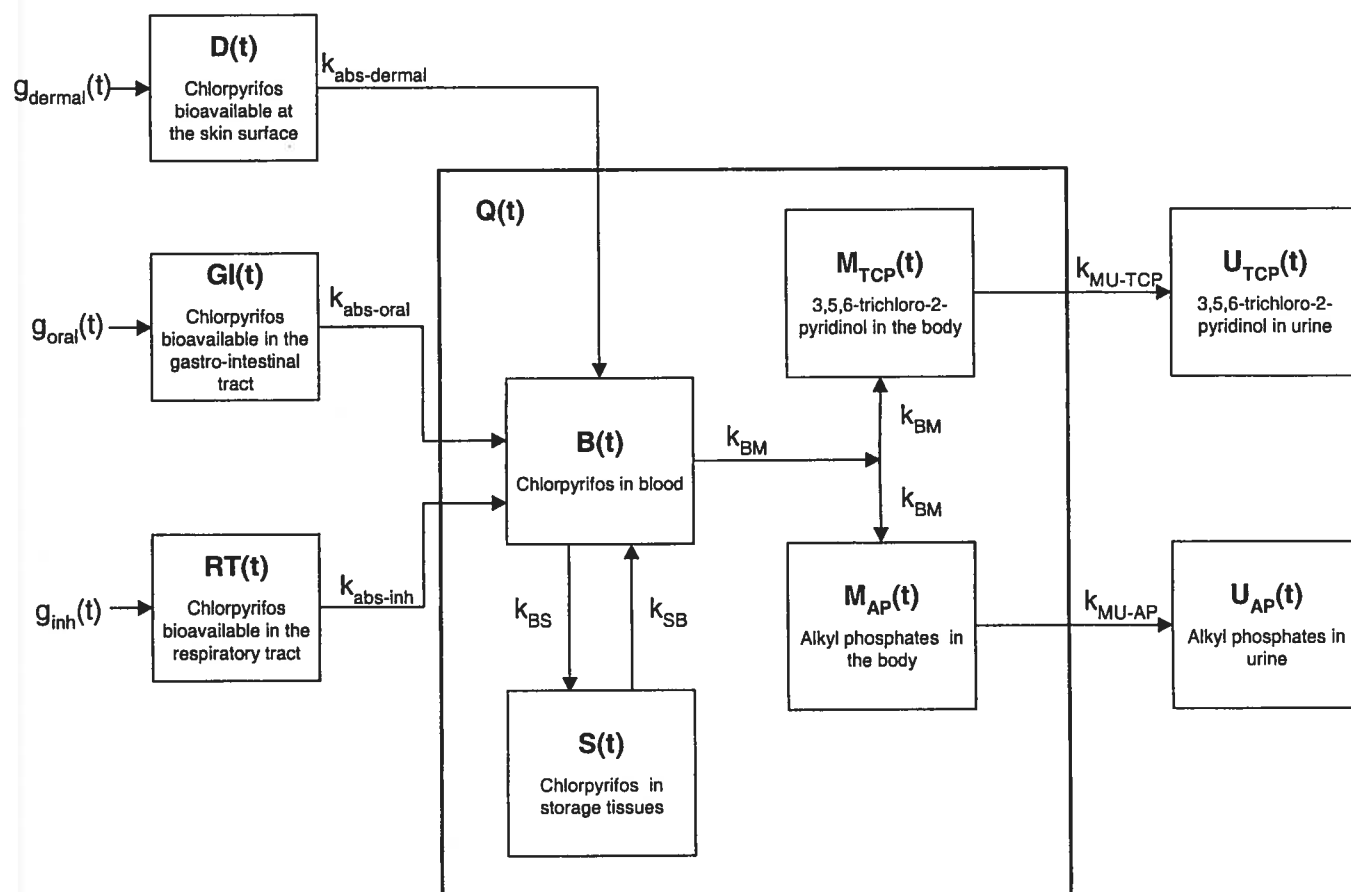


Fig. 3

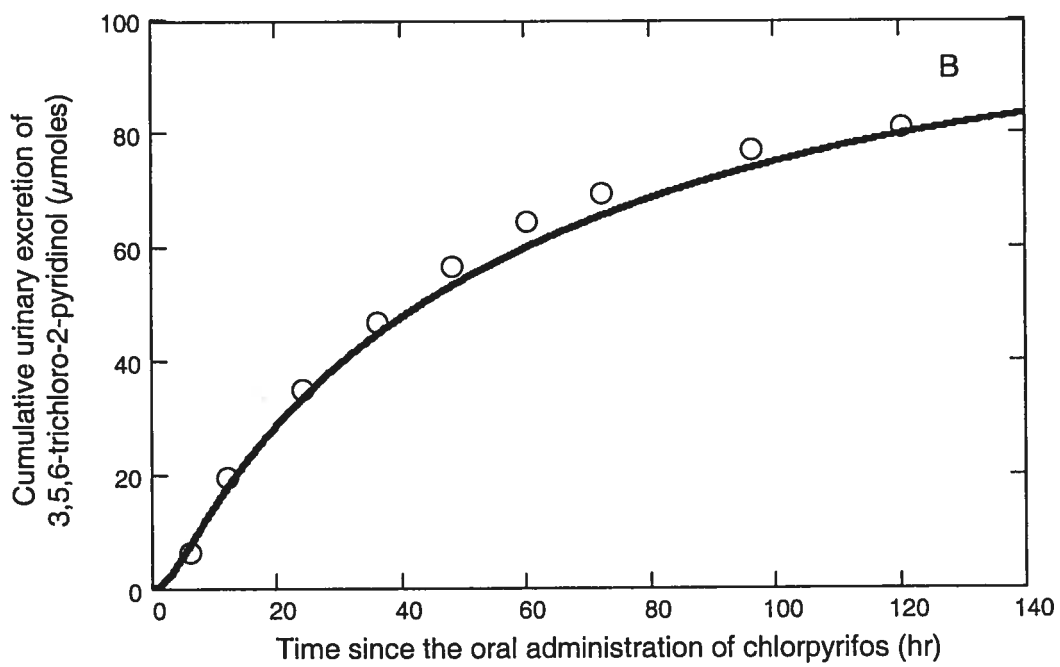
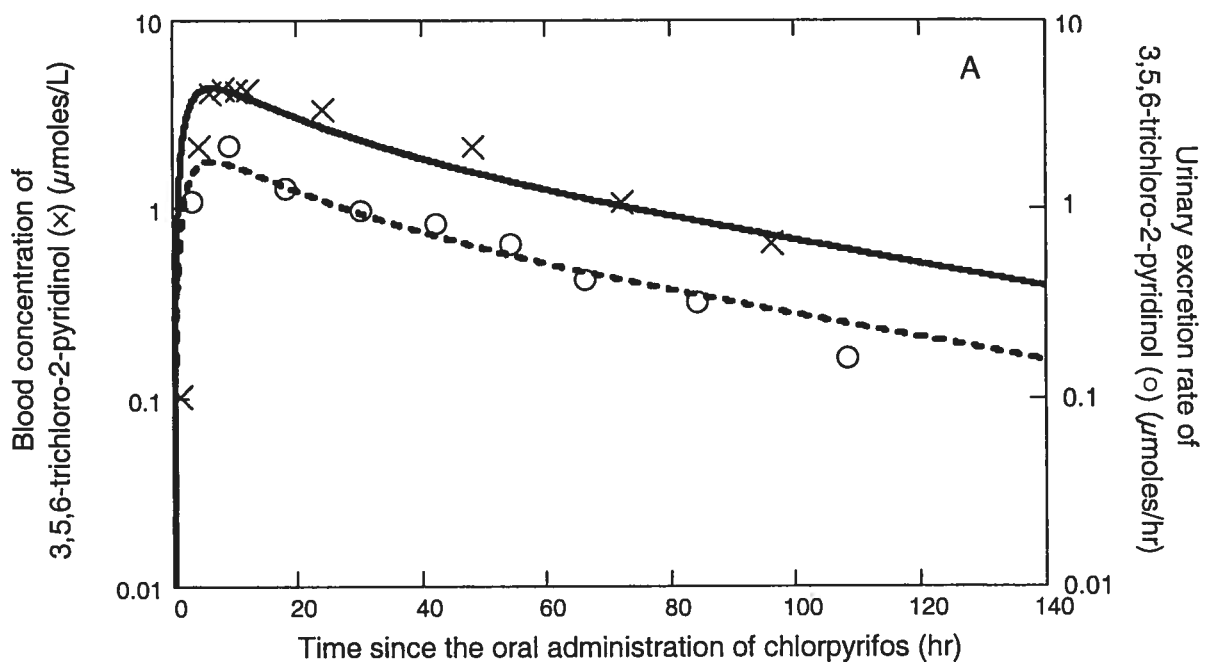


Fig. 4

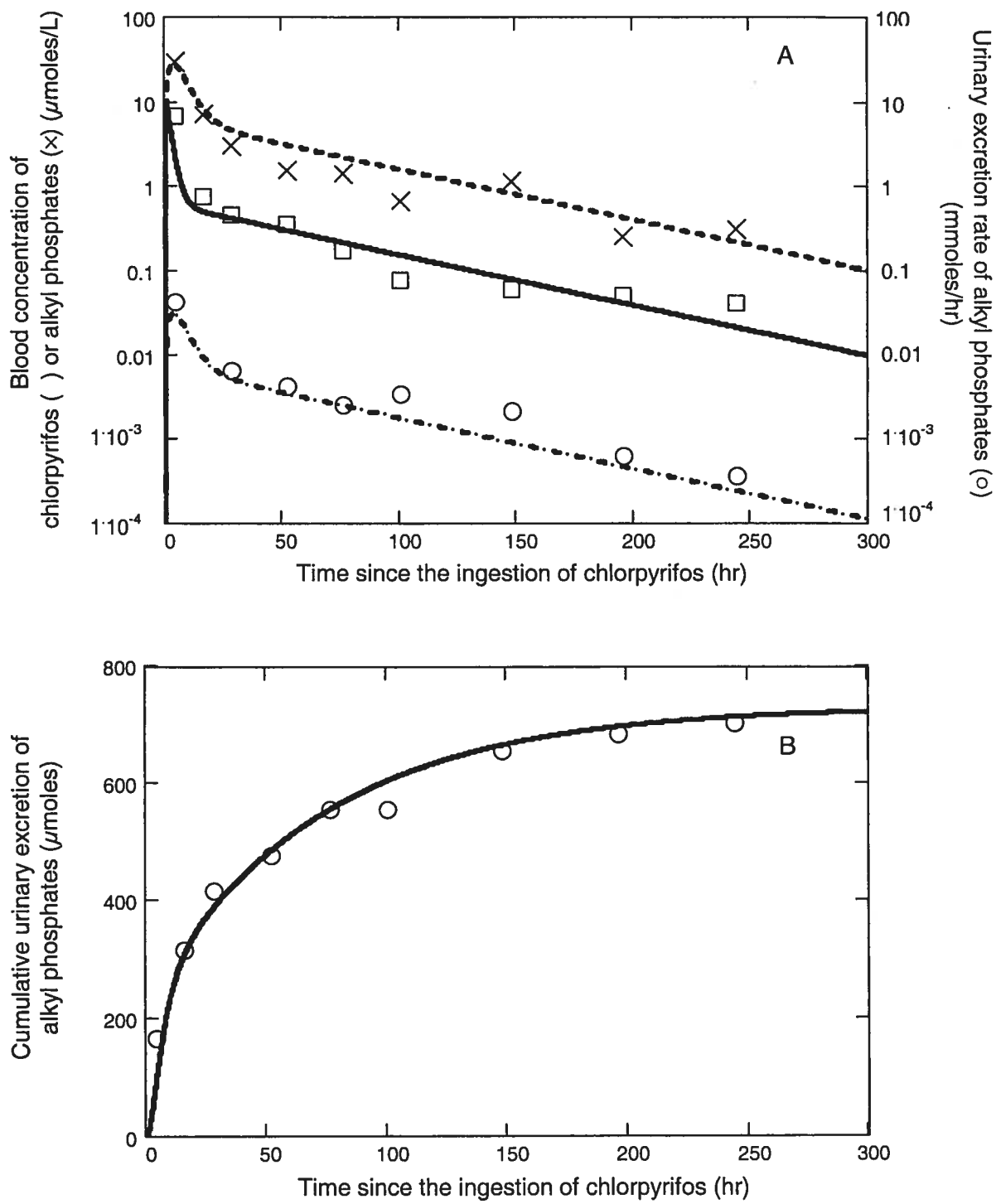


Fig. 5

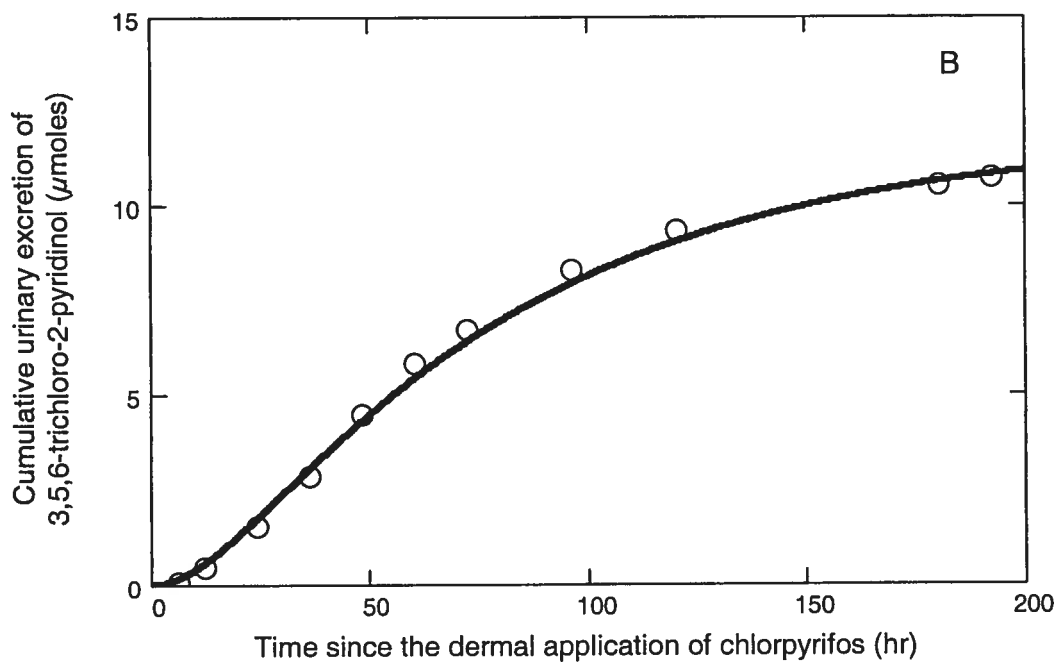
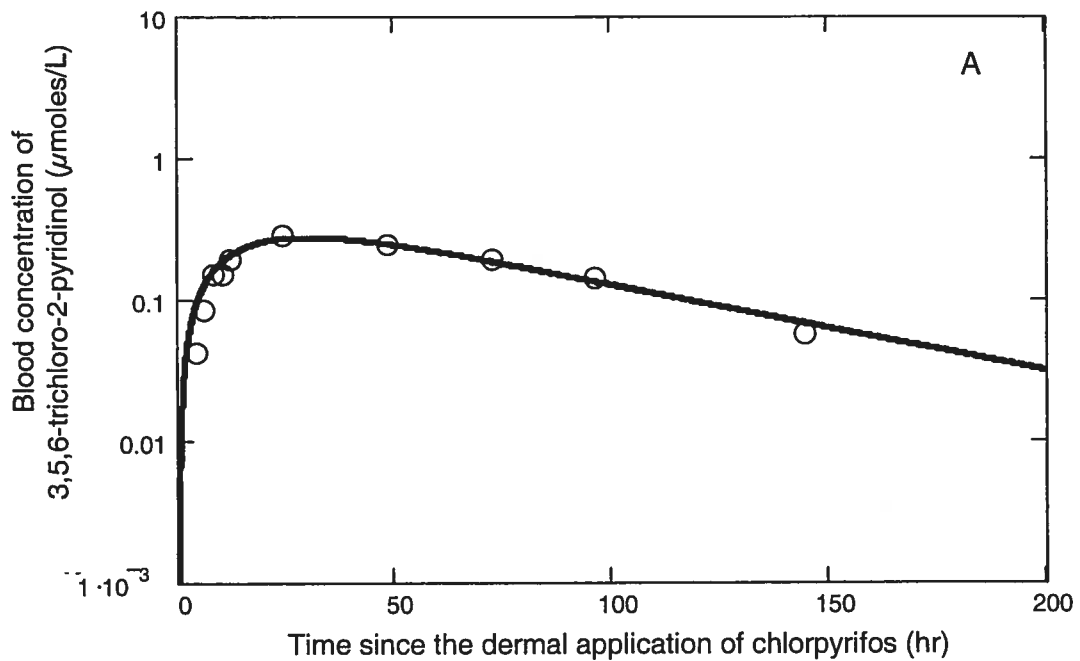


Fig. 6

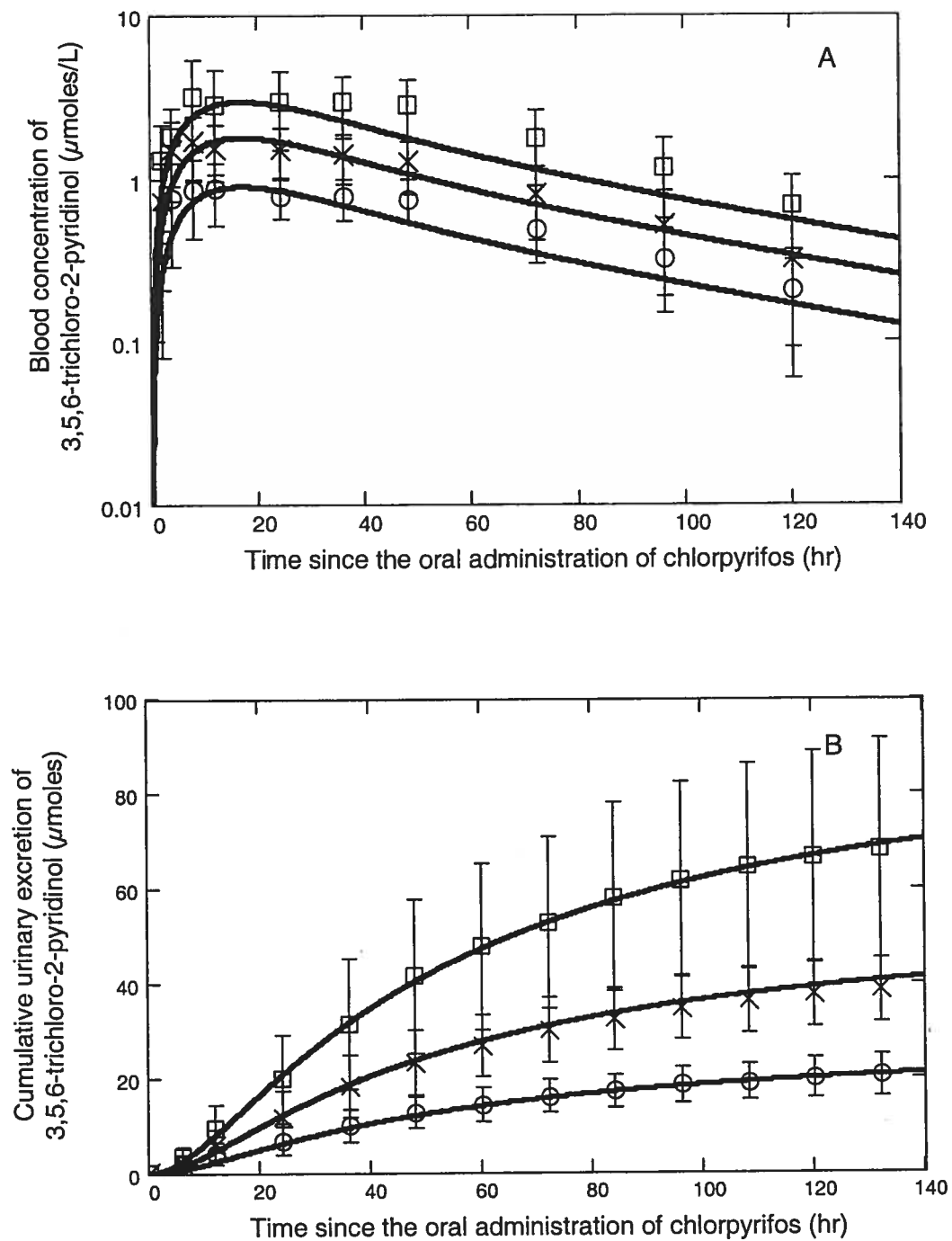
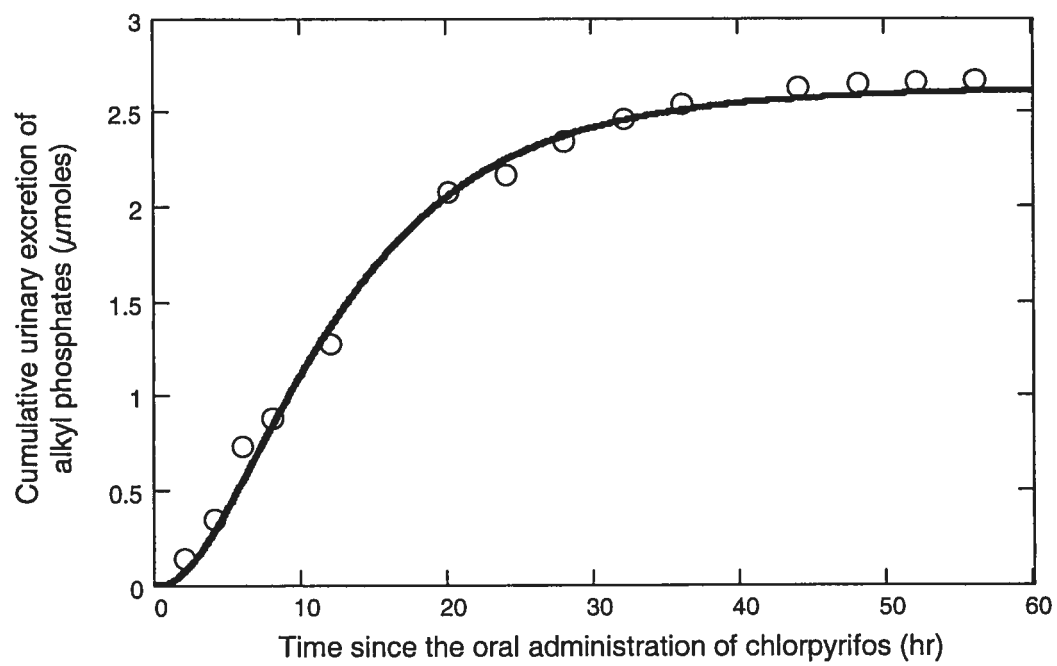


Fig. 7



**CHAPITRE 6 : ARTICLE 4, TRICLOPYR**

Cette version finale de l'article a été acceptée le 5 décembre 2004 dans *Annals of Occupational Hygiene*.

## **WORKER EXPOSURES TO TRICLOPYR: RISK ASSESSMENT THROUGH MEASUREMENTS IN URINE SAMPLES**

Nathalie H. Gosselin<sup>\*</sup>, Robert C. Brunet<sup>†</sup>, Gaétan Carrier<sup>\*</sup> and Amssétou Dosso<sup>\*</sup>

<sup>\*</sup> Chaire en analyse des risques toxicologiques pour l'humain and Département de santé environnementale et santé au travail, Faculté de Médecine, Université de Montréal, P.O. Box 6128, Main Station, Montreal (Quebec), Canada, H3C 3J7

<sup>†</sup> Département de Mathématiques et de Statistique and Centre de Recherches Mathématiques, Faculté des arts et des sciences, Université de Montréal, P.O. Box 6128, Main Station, Montreal (Quebec), Canada, H3C 3J7

Key words: triclopyr, Garlon 4<sup>®</sup>, occupational exposure, health risk assessment, biomonitoring.

***ABSTRACT***

In the province of Quebec (Canada), the phytocide Garlon 4<sup>®</sup>, whose active ingredient is triclopyr, is often used to prevent trees reaching electrical conductors. The object of this paper is to assess the potential health risks in workers coming into contact with Garlon 4<sup>®</sup>. Ten workers collected their micturations during the 22 hours following the beginning of a work-shift. Measured urinary amounts of triclopyr varied between 1 and 13 mg. The absorbed daily doses were estimated from the amounts of triclopyr in urine through the use of a kinetic model that links the rates of triclopyr elimination to absorbed doses. These estimated doses were compared to the no-observed-effect level (NOEL) observed in rats: 5 mg/kg-bw. The upper-bound estimations of the worker daily absorbed doses were found to be 13.3% or less of the rat NOEL.

## ***INTRODUCTION***

Garlon 4<sup>®</sup> is a phytocide employed to control the undesirable growth of woody plants and broadleaf weeds. The active ingredient of Garlon 4<sup>®</sup> is triclopyr (3,5,6-trichloro-2-pyridinyloxyacetic acid), present as a butoxyethyl ester form with a concentration of 61.6%. Its mode of action occurs through imitation of auxin, a natural growth-regulating hormone found in plants, which results in acceleration of the plant's maturation. Since the plant's energy supply is not sufficient to support this rapid growth, the plant dies prematurely. Garlon 4<sup>®</sup> is used on a variety of sites, in particular on power line rights-of-ways to reduce the risk of power outages and to allow safe access to transmission facilities. In the province of Quebec (Canada), this phytocide is, together with Tordon 101<sup>®</sup>, the principal product applied in summer for controlling the growth of trees capable of reaching electrical conductors. Concern for the workers applying the pesticides led the electric utility company to undertake a field study in 2001 to assess the potential occupational health risks from the seasonal application of Garlon 4<sup>®</sup>.

To evaluate occupational exposure to pesticides, biological monitoring through collection and analysis of urine to establish levels of the parent substance or its metabolites is a direct and accurate means. It integrates all routes of exposure and, compared to environmental monitoring, is independent of the absorption fractions of exposed surfaces, the protective equipments used and the climatic conditions. The use of biomarkers to assess health risks is however possible only if the link between their

levels in urinary samples and the critical biological effects is established. This can be achieved by a two step procedure: first, relate absorbed dose to biomarkers levels with a validated toxicokinetic model; second, compare this absorbed dose with a toxicity dose established from observed biological effects. This procedure, retained for the health risk assessment of triclopyr, was already used for other pesticides (Carrier and Brunet, 1999; Bouchard et al., 2003; Gosselin et al., 2005). Since triclopyr, once absorbed by humans, is principally excreted without biotransformation (Carmichael et al., 1989), the suitable biomarker for the biological monitoring of Garlon 4<sup>®</sup> is triclopyr itself in urine. The object of this paper is to assess the health risks incurred by workers through measurements of the amounts of triclopyr in their urine.

## ***METHODS***

### ***Field study***

**Studied Workers:** At the end of June 2001, ten male workers were recruited to participate in a survey of biological monitoring. From June to August 2001, these workers sprayed Garlon 4<sup>®</sup> under high voltage transmission lines in the province of Quebec. Eight of them applied diluted Garlon 4<sup>®</sup> with a backpack unit directly on the stumps of recently cut trees. The diluted solution in the backpack unit was 20% Garlon 4<sup>®</sup> and 80% mineral oil. Dilution manipulations were carried out by the managers of the project; each worker loaded its backpack unit with this solution. The personal protective equipments of these 8 workers were long pants, rubber boots and a helmet. Their work-schedule was an 8-hour day with two 15-minute breaks in the morning and in the afternoon and a 30-minute lunch break. The two other workers pulverized diluted Garlon 4<sup>®</sup> over the leaves under transmission lines from a tractor-mounted boom spray. The tractor reservoir was filled by these two workers with 12.6 liters of Garlon 4<sup>®</sup> and 1800 liters of water. These two workers wore rubber boots, gloves, an overall and a helmet. Their work-schedule was an 11.5-hour day with two 15-minute breaks in the morning and a 30-minute break in the afternoon.

**Urinary sample collection :** On the ultimate day of a 5 day work-week, the workers were instructed to collect all their micturations into a plastic container from the onset of their workday (8 o'clock) until the first micturation of the next day (6 o'clock). Thus the amounts of triclopyr measured in these samples represented the cumulative urinary

excretion of triclopyr during the 22-hr period from the beginning of that day's exposure. The body weight of each worker was recorded at the same time.

Urine samples were analyzed at the Laboratoire du Centre de toxicologie humaine of the Institut national de santé publique du Québec which is accredited by the Canadian Association for Environmental Analytical Laboratories. Samples were kept frozen at  $-20^{\circ}\text{C}$  until analysis. The sum of free and conjugated triclopyr was measured after acidic hydrolysis and extraction with a hexane/ether mixture. The extracts were evaporated to dryness and redissolved in a 25% acetonitrile : 75% ammonium acetate solution. The samples were then analyzed using a Micromass Quattro liquid chromatography-electrospray ionization-mass spectrometry (LC-ESI-MS) system operated in negative MRM mode. The LC system was equipped with a Waters Symmetry C18 column ( $5\mu\text{m}$ ,  $50\text{ mm} \times 2.1\text{ mm}$ ). The limit of detection of triclopyr was  $0.3\ \mu\text{g/L}$  and the limit of quantification was  $0.9\ \mu\text{g/L}$ . Average recovery of triclopyr from urine samples spiked with a  $10\ \mu\text{g/L}$  of reference standard was 97%. Intra-day coefficient of variation for replicate analysis of the same urine sample spiked with  $2\ \mu\text{g/l}$  of reference standard was 4% ( $n = 10$  samples).

### ***Health Risk Analysis***

**Determination of the daily absorbed dose :** The daily absorbed dose of triclopyr for each worker was reconstructed from the following equation:

$$\text{Daily absorbed dose} = \frac{\text{Cumulative amount of triclopyr in the urine collected over T hours}}{F_{\text{exc}}(T)}$$

(1)

Where  $F_{exc}(T)$  is the fraction of the daily absorbed dose of triclopyr recovered in the cumulative urinary sample during  $T$  hours following the onset of exposure.

The results of the pharmacokinetic study of Carmichael *et al.* (1989) were adapted to estimate  $F_{exc}(22 \text{ hrs})$ . These authors exposed five healthy male volunteers to triclopyr via the oral and dermal routes. The dietary doses were 0.1 mg/kg-bw followed three weeks later by 0.5 mg/kg-bw of triclopyr. The five volunteers were later exposed to a dermal dose equivalent to 3.7 mg/kg-bw of triclopyr. After each administration, blood and urinary samples were collected over a period of 72 hours. To fit these time-course data, Carmichael *et al.* (1989) used an open two-compartment pharmacokinetic model. A different set of model parameters was estimated for each administration and for each volunteer.

The original kinetic model of Carmichael *et al.* (1989) was modified in order to assess, for the gradual exposure occurring in typical work shifts, the absorbed dose starting from cumulative amounts of triclopyr excreted in urinary samples collected during the given period of time (see Fig. 1). Since the skin and the lungs are the significant route-of-entries for workers exposed to triclopyr (Middendorf *et al.*, 1994), two functions were included in the model to describe the input dose per unit of time bioavailable at each site of absorption ( $g_{skin}(t)$  and  $g_{lungs}(t)$ ). These two time dependent input functions allow one to simulate the different time tables of exposure encountered in occupational conditions. For skin absorption, an input compartment was necessary to account for the accumulation in skin followed by the slow release of triclopyr to the blood stream. On

the other hand, simulations show that it is not necessary to add an input compartment for lungs, since the absorption is too rapid to observe a sizable time-delay to the blood stream; the pulmonary absorption is in fact similar to a drop by drop intravenous exposure. The differential equation system for this kinetic model is described in the Appendix. The model simulations were performed by solving numerically this system using the Runge-Kutta method incorporated in MathCad 2000 Professional.

In the current study, absorption of triclopyr occurs gradually during the work day and for five consecutive days; the input functions used to simulate this occupational exposure were based on the specified work-schedules for each of the two groups of workers, those with a backpack unit and those using a tractor-mounted boom spray. Estimations of  $F_{exc}(22 \text{ hrs})$ , specific to each work-schedule, were obtained by solving the differential equation system with the appropriate input conditions (see the Appendix). For a unit of absorbed dose, under a given time-table of exposure, the numerical solution of the model predicts a cumulative amount of triclopyr to be observed in the urine collected during the 22 hours following the beginning of exposure. From formula #1, the relevant  $F_{exc}(22 \text{ hrs})$  is then easily obtained.

Since the relative contributions of the dermal route and the pulmonary route cannot be determined by a simple measurement of triclopyr in urine, model simulations with input functions  $g_{skin}(t)$  and  $g_{lungs}(t)$  giving different fractions of the daily absorbed dose arising from the skin and from the lungs ( $f_{skin}$  and  $f_{lungs}$ ) were carried out in order to determine their impact on outcome in urine. For each choice of  $f_{skin}$  and  $f_{lungs}$ , the daily

absorbed dose, the peak of blood concentration and the area under the blood concentration time-curve were estimated by simulating an 8-hr exposure to triclopyr without break time resulting in a 22-hr cumulative urinary excretion of triclopyr equal to the average of triclopyr measured in the urinary samples of workers.

In model simulations, the sets of parameters describing the internal kinetics of triclopyr ( $k_{SB}$ ,  $k_{BS}$ ,  $k_e$ ,  $F_u$ ,  $V_d$ , see the descriptions in Table 1) were the ones estimated from the time-courses of triclopyr in each of the five volunteers orally exposed to 0.1 and 0.5 mg/kg-bw of triclopyr in Carmichael *et al.* (1989). The rates of dermal absorption ( $k_{abs}$ ) used were the ones estimated from the time-courses of dermally absorbed triclopyr in the corresponding volunteers. An average set of parameters was also obtained from the average of these ten individual data sets. Consequently, for each assumed values of skin versus lungs fractions contributing to daily dose ( $f_{skin}$  and  $f_{lungs}$ ), the parameter sets derived from the individual sets presented in Carmichael *et al.* (1989) enabled eleven estimations of  $F_{exc}(22 \text{ hrs})$  for the workers with backpack units as well as for the workers with a tractor-mounted boom spray.

**Determination of the toxicity dose :** To assess the health risks associated with occupational exposure to triclopyr, the estimated daily absorbed dose was compared with the no-observed-effect level (NOEL) proposed by U.S.EPA for chronic exposure (U.S. EPA, 1998). The critical effect used to define it is an increased incidence of proximal tubular degeneration of the kidneys in  $P_1$  and  $P_2$  parental rats observed in a two-generation dietary reproduction study in Sprague-Dawley rats (U.S. EPA, 1998).

In that experimental study, 30 rat-couples per dosage were exposed respectively to 0, 5, 25 and 250 mg/kg-bw/day of triclopyr. The first and second generations P<sub>1</sub> and P<sub>2</sub> ingested triclopyr during respectively 10 and 12 weeks before mating. The NOEL was found to be 5 mg/kg-bw/day and the lowest-observed-effect level (LOEL) was 25 mg/kg-bw/day. The reference dose (RfD) recommended by U.S. EPA is determined by dividing this NOEL by a safety factor of 100-fold to take into account the animal-to-human extrapolation and the inter-individual variability (U.S. EPA, 1998).

## ***RESULTS***

### ***Field study***

The amounts of triclopyr were measured, for each of the 10 workers, in the cumulative urine collected during 22 hours following the onset of a work-day exposure. These data and their body weight are presented in Table 2. The average of the measured urinary amounts is 56.4  $\mu\text{g}/\text{kg-bw}$ .

### ***Health Risk Analysis***

Table 3 presents the exposure parameters estimated from model simulations where the contributions of the dermal absorbed route and the pulmonary route vary. Due to the small rate of dermal absorption, the estimation on the peak of blood concentration is lowest when the absorption occurs only via the skin whereas the estimations of the daily absorbed dose and the area under the blood concentration time-curve are highest.

The two exposure scenarios, the one for the eight workers with a backpack unit and the other for the two workers with tractor-mounted boom spray, were simulated with the kinetics model presented in Fig. 1 and the appropriate input conditions presented in the Appendix. For each exposure scenario, eleven time-courses of triclopyr urinary excretion were calculated using each of the ten individual sets of model parametric values and one set obtained from the average of these ten individual sets. These simulations were carried out assuming that absorption occurred only through the skin,

because as shown from Table 3, this assumption results in an estimated daily absorbed dose that is the highest for a given urinary excretion of triclopyr. This ensures that the worst case scenario is retained. Fig. 2 depicts the time-courses of the cumulative urinary excretion of triclopyr expressed as the fraction of daily absorbed dose (i.e.,  $F_{exc}(t)$ ) predicted for the eight workers with a backpack unit. The curves shown in Fig. 2 are obtained from sets of model parametric values which give the lowest and highest values of  $F_{exc}(22 \text{ hrs})$  and from the average parameter set. Fig. 2 exhibits the three estimated values for the fraction of the absorbed dose recovered in the 22-hr urinary samples: 0.259, 0.349 and 0.477. Similarly, simulating the work timetable of the two workers who pulverized Garlon 4<sup>®</sup> with the tractor-mounted boom spray, the estimated values of  $F_{exc}(22 \text{ hrs})$  are: 0.230, 0.314 and 0.433.

The absorbed dose for each worker was calculated starting from their urinary biomarker level presented in Table 2 and the above estimations of  $F_{exc}(22 \text{ hrs})$ . Table 4 gives the lower- and upper-bound estimates of the daily absorbed dose for each worker in addition to the value obtained from the average parameter set. For each worker, these three estimations of the daily absorbed dose were divided by their body weight, for comparison with the rat NOEL. Table 5 presents the results of this comparison. The upper-bound estimations of the workers daily absorbed doses were found to be 13.3% or less of the rat NOEL. On the other hand, only the worker number 4 absorbed a daily dose lower than the RfD, since there is a 100-fold safety factor included in this criteria.

## ***DISCUSSION***

A novel strategy was presented in this study for biomonitoring occupational exposure to triclopyr and for assessing the associated human health risks. While it is already well-known that the kinetics of a substance is necessary for reconstruction of the absorbed dose starting from excreted biomarkers (Carmichael, 1989; Lauwerys and Hoet, 2001), rare are the biomonitoring studies that consider the gradual exposure occurring in typical work shifts. When the work-schedule is known, the system of differential equations with the appropriate input function allows simulations of the time-course of the gradual absorption of the substance and the biomarker excretion rate corresponding to that specific exposure scenario. The health risk assessment can consequently be determined more accurately by taking full advantage of this mathematical tool. To wit, if, instead of employing the specific input function governed by the given timetable of exposure, the daily absorbed dose had been estimated from simulations of a bolus administration in the skin at the beginning of the work-day, the daily absorbed dose estimations presented in Table 4 would have been reduced by a factor of 1.3.

For the reconstruction of the daily absorbed dose, some assumptions were made to avoid underestimations. For one, only the dermal route was considered, even if, according to the study of Middendorf *et al.* (1994) on occupational exposure to triclopyr, the pulmonary route accounts on average for 13.8% of the daily absorbed dose and the dermal route for 86.2%. Model simulations with this combination show

that the estimates of the daily absorbed dose would be approximately 1.2 times lower than the estimates based on dermal absorption only. Given that in the study at hand it is impossible to know the relative contributions of the two entry routes, the safest dose estimates arise from the assumption that 100% of absorption is through the skin. Also, the estimates of daily absorbed dose carried out assume single day exposure. However, as a result of the slow urinary elimination arising from the low dermal absorption rate, an accumulation of triclopyr is expected to occur in the body of workers. This slow elimination was noticed by Carmichael *et al.* (1989) where the volunteers still excreted amounts of triclopyr three days after dermal administration of triclopyr. Therefore, the amounts recovered in the urinary samples collected the last day of a 5 day work-week stem not only from the amounts of triclopyr absorbed during that day, but also from the remains of amounts absorbed the previous days. Had the model simulations incorporated this bioaccumulation phenomena by simulating 5 days of exposure instead of single one, the estimates of the dose absorbed during the last day would have been about 2 times lower.

It is interesting to compare the level of triclopyr exposure measured in the current field study with other studies. In particular, the study of Middendorf *et al.* (1994) estimated the daily absorbed doses of 21 workers who applied a diluted form of Garlon 4<sup>®</sup> with a backpack unit. These workers collected all their urinary samples during 4 days following the onset of a work-day. Middendorf *et al.* (1994) calculated their daily absorbed doses by dividing the amounts of triclopyr measured in the urinary samples by a factor of 0.789. This value is equal to the mean fraction of the absorbed dose

found in urine ( $F_u$ ) after a long time as determined from the volunteers orally exposed to 0.5 mg/kg of triclopyr in Carmichael *et al.* (1989). According to these dose estimates, the workers in Middendorf *et al.* (1994) absorbed between 0.207 and 7.690 mg of triclopyr in the monitoring day, with a geometric mean value of 1.1 mg. The comparison between these daily absorbed doses and the ones presented in Table 4 reveals that the workers in the current study were much more exposed; this is so even from comparison using the lower-bound estimates of Table 4. This important difference is possibly due to the different procedures used to reconstruct the absorbed daily doses as well as from the different field conditions (e.g., mixing procedures, equipment maintenance, work practices)

One of the advantages of simulating the time-course of the biomarker excretion rate for a given exposure scenario is the opportunity to choose any convenient period of urinary collection. In practice, it is important to specify a period which suits the workers as well as the employers. Sensitivity tests carried out on the model parameters ( $k_{abs}$ ,  $k_{SB}$ ,  $k_{BS}$ ,  $k_e$ ,  $F_u$ ) show that the longer the urinary collection period is, the smaller is the impact of the human kinetics variability on the estimation of daily absorbed dose. Of course, for a collection period of 5 days or longer following the beginning of a single exposure day, only the total fraction of the absorbed dose eventually excreted in urine,  $F_u$ , affects the daily dose reconstruction. In addition to being very demanding for workers, this long period is unfortunately not suitable for employers because the workers would have to cease exposure to triclopyr during the four days of the collection period following their work day. Alternatively, a unique micturition at the

end of the work-shift, as ACGIH<sup>®</sup> proposed for almost BEI<sup>®</sup> (ACGIH, 2002), or a 12-hr cumulative urinary excretion following the onset of exposure are not suitable either because, in both instances, estimations of the daily absorbed dose are too dependent on the wide variability in dermal absorption rates. The latter are known to vary according to the anatomical region of the skin exposed, the skin condition and the environmental temperature and humidity (Bronaugh and Maibach, 1999). It is well to remember that urinary concentrations measured in a single micturition depend on the variable urinary flow and also, the amounts adjusted on creatinine depend on the creatinine excretion rates which are subject to inter-individual variations as well as to the intra- and inter-day variations (Boeniger *et al.*, 1993). Consequently, the estimates from a single urinary sample are less reliable. For the biomonitoring of triclopyr, urinary collections of 24-, 48- or 72-hr following the onset of the last day of a week of exposure appear to be the more appropriate periods.

For future field studies, biological reference values (BRV) should be established from the present results to prevent adverse health effects at an early stage in workers exposed to triclopyr. The BRV could take the form of amounts of triclopyr recovered in urinary samples over a given period that correspond to an absorbed dose that is considered safe. For the convenient collection periods proposed, 24-, 48- and 72-hr following the onset of a work-day of exposure, the BRV amounts in urine corresponding to a NOEL dose can be obtained by simulating a typical worker exposure scenario and using the set of model parametric values which results in the lowest cumulative urinary values. The typical exposure scenario retained is an 8-hr

work-shift, without break time, where the NOEL daily dose (5 mg/kg-bw) is assumed to be entirely absorbed through the skin (See Appendix for the input conditions). This dose would result in a cumulative urinary excretion of triclopyr equal to 1.45 mg/kg-bw for a 24-hr collection, 2.63 mg/kg-bw for a 48-hr collection and 2.83 mg/kg-bw for a 72-hr collection. However, since there is no observed effect in humans exposed to triclopyr, no one can prove that the NOEL established for rats corresponds to a safe dose for humans. Thus, the future biomonitoring studies can also be based on the above BRV divided by appropriate uncertainty factors.

Comparisons between the estimated daily doses absorbed by the workers of this study and the RfD show that there is a potential health risks for these workers under the current conditions. The RfD used here was proposed by U.S. EPA to prevent significant adverse health effects, assuming repeated daily exposure in the general population over a lifetime (U.S.EPA, 1998). The default uncertainty factors of 100-fold were used to established this RfD from the rat NOEL. However, according to WHO (1994), it is often suitable for an occupational exposure to use lower safety factors than the proposed default factors, since the occupational population does not include the more vulnerable persons (i.e., children, sick and elderly). In the current study, to bypass the interspecies uncertainty and the variability in the kinetics of triclopyr, the model simulations were designed to result in the highest estimate of the daily absorbed dose corresponding to a given cumulative amount in urine. Also, since the workers in this field study are exposed only three months per year, Renwick (1999) judged that it may be more appropriate to assess their health risks with a guidance value derived from

a NOEL established for sub-chronic exposure rather than a NOEL established for chronic exposure.

The results of this study were reported to the managers supervising these workers so that tighter security measures may be implemented during manipulations of the product in order to minimize worker contact with the product. Worker education and serious supervision were also recommended to insure that neoprene gloves and rubber boots or boot covers are worn at all times. The company ensures that these recommendations will be implemented.

***ACKNOWLEDGMENTS***

The authors thank the Institut de Recherche Robert-Sauvé en Santé et Sécurité du Travail (IRSST) and Hydro-Québec for providing financial support for this study.

## APPENDIX

### *Functional representation of the kinetics of triclopyr*

#### Differential equation system

*From Fig. 1, the following differential equations are obtained (see Table 1 for the description of each symbol):*

$$\frac{dD(t)}{dt} = g_{\text{skin}}(t) - k_{\text{abs}} \times D(t)$$

$$\frac{dB(t)}{dt} = g_{\text{lungs}}(t) + k_{\text{abs}} \times D(t) + k_{\text{SB}} \times S(t) - (k_e + k_{\text{BS}}) \times B(t)$$

$$\frac{dS(t)}{dt} = k_{\text{BS}} \times B(t) - k_{\text{SB}} \times S(t)$$

$$\frac{dU(t)}{dt} = F_u \times k_e \times B(t)$$

$$\frac{dN(t)}{dt} = (1 - F_u) \times k_e \times B(t)$$

#### Input conditions

The following equations describe the input conditions of the time tables simulated by the kinetic model (see the description of variables and parameters in Table 1):

Dose input rate for the exposure scenario of workers with backpack units (amount of the unit daily absorbed dose per hour):

$$g_{\text{skin}}(t) = \begin{cases} \frac{1 \times f_{\text{skin}}}{7 \times \text{hr}} & \text{for : } (0 < t < 2 \cdot \text{hr}), (2.25 \cdot \text{hr} < t < 4 \cdot \text{hr}), (4.5 \cdot \text{hr} < t < 6 \cdot \text{hr}), (6.25 \cdot \text{hr} < t < 8 \cdot \text{hr}) \\ 0 & \text{otherwise} \end{cases}$$

$$g_{\text{lungs}}(t) = \begin{cases} \frac{1 \times f_{\text{lungs}}}{7 \times \text{hr}} & \text{for : } (0 < t < 2 \cdot \text{hr}), (2.25 \cdot \text{hr} < t < 4 \cdot \text{hr}), (4.5 \cdot \text{hr} < t < 6 \cdot \text{hr}), (6.25 \cdot \text{hr} < t < 8 \cdot \text{hr}) \\ 0 & \text{otherwise} \end{cases}$$

with the initial conditions:  $D(0) = Q(0) = U(0) = N(0) = 0$ .

Dose input rate for the exposure scenario of workers with tractor-mounted boom spray  
(amount of the unit daily absorbed dose per hour):

$$g_{\text{skin}}(t) = \begin{cases} \frac{1 \times f_{\text{skin}}}{10.5 \times \text{hr}} & \text{for : } (0 < t < 2 \cdot \text{hr}), (2.25 \cdot \text{hr} < t < 4 \cdot \text{hr}), (4.25 \cdot \text{hr} < t < 8.75 \cdot \text{hr}), (9.25 \cdot \text{hr} < t < 11.5 \cdot \text{hr}) \\ 0 & \text{otherwise} \end{cases}$$

$$g_{\text{lungs}}(t) = \begin{cases} \frac{1 \times f_{\text{lungs}}}{10.5 \times \text{hr}} & \text{for : } (0 < t < 2 \cdot \text{hr}), (2.25 \cdot \text{hr} < t < 4 \cdot \text{hr}), (4.25 \cdot \text{hr} < t < 8.75 \cdot \text{hr}), (9.25 \cdot \text{hr} < t < 11.5 \cdot \text{hr}) \\ 0 & \text{otherwise} \end{cases}$$

with the initial conditions:  $D(0) = Q(0) = U(0) = N(0) = 0$ .

Dose input rate for the determination of the biological reference value (mg/kg-bw per  
hour):

$$g_{\text{skin}}(t) = \begin{cases} \frac{1 \times f_{\text{skin}}}{8 \times \text{hr}} & \text{for : } (0 < t < 8 \cdot \text{hr}), \\ 0 & \text{otherwise} \end{cases},$$

$$g_{\text{lungs}}(t) = \begin{cases} \frac{1 \times f_{\text{lungs}}}{8 \times \text{hr}} & \text{for : } (0 < t < 8 \cdot \text{hr}) \\ 0 & \text{otherwise} \end{cases}$$

with the initial conditions:  $D(0) = Q(0) = U(0) = N(0) = 0$ .

**REFERENCES**

ACGIH. (2002) Documentation of the Threshold Limit Values and Biological Exposure Indices, 7th Ed. Cincinnati, OH : American Conference of Governmental Industrial Hygienists.

Boeniger MF, Lowry LK, Rosenberg, J. (1993) Interpretation of urine results used to assess chemical exposure with emphasis on creatinine adjustments: a review. *Am Ind Hyg Assoc J*; 54: 615-627.

Bouchard M, Gosselin NH, Brunet RC, Samuel O, Dumoulin M-J, Carrier G. (2003). A Toxicokinetic model for malathion and its metabolites as a tool to assess human exposure and risk through measurements of urinary biomarkers. *Toxicol Sci*; 73: 182-194.

Bronaugh RL, Maibach HI. (1999) Percutaneous Absorption. *Drugs – Cosmetics – Mechanisms – Methodology*, 3rd ed.. New York: Marcel Dekker.

Carmichael, NG. (1989) Assessment of hazards to workers applying pesticides. *Food Addit Contam*; 6: S21-S27.

Carmichael NG, Nolan RJ, Perkins JM, Davies R, Warrington SJ. (1989) Oral and dermal pharmacokinetics of triclopyr in human volunteers. *Human Toxicol*; 8: 431-437.

Carrier G, Brunet RC. (1999) A toxicokinetic model to assess the risk of azinphosmethyl exposure in humans through measures of urinary elimination of alkylphosphates. *Toxicol Sci*; 47: 23-32.

Gosselin NH, Bouchard M, Brunet RC, Dumoulin M-J, Carrier G (2005). Toxicokinetic modeling of parathion and its metabolites in humans for the determination of biological reference values. *Toxicol. Mech. Methods*; 15:33-52.

Lauwerys R, Hoet P. (2001) *Industrial Chemical Exposure: Guidelines for Biological Monitoring*. Boca Raton, London: Lewis Publishers.

Middendorf P, Timchalk C, Kropscott B, Rick D. (1994) Forest worker exposure to Garlon™ 4 herbicide. *Appl Occup Environ Hyg*; 9: 589-594.

Renwick AG. (1999) Duration of intake above the ADI/TDI in relation to toxicodynamics and toxicokinetics. *Regul Toxicol Pharmacol*; 30: S69-S78.

U.S. EPA. (1998) Reregistration eligibility decision: Triclopyr. Washington, DC: Office of Prevention, Pesticides and Toxic Substances, Environmental Protection Agency.

WHO. (1994) Assessing Human Health Risks of Chemicals: Derivation of Guidance Values for Health-Based Exposure Limits, Environmental Health Criteria, Vol. 170. Geneva: World Health Organization.

**Table 1. Symbols used in the conceptual and functional representation of the modified kinetics model of triclopyr developed by Carmichael *et al.* (1989)**

Symbols	Description
<b>Variables</b>	
$g_{skin}(t)$	Dermal dose bioavailable per unit of time which can describe different time tables of exposure (mg/kg-bw/hr)
$g_{lungs}(t)$	Inhaled dose bioavailable per unit of time which can describe different time tables of exposure (mg/kg-bw/hr)
$D(t)$	Burden of triclopyr at the skin surface as a function of time (mg/kg)
$B(t)$	Burden of triclopyr in blood and tissues in dynamical equilibrium with blood as a function of time (mg/kg)
$S(t)$	Burden of triclopyr in storage tissues as a function of time (mg/kg)
$U(t)$	Cumulative excretion of triclopyr in urine as a function of time (mg/kg)
$N(t)$	Cumulative excretion of triclopyr not observed in urine as a function of time (mg/kg)
<b>Parameters</b>	
$k_{abs}$	Dermal absorption rate constant of triclopyr ( <i>i.e.</i> transfer rate from skin surface to blood) ( $hr^{-1}$ )
$k_{BS}$	Blood to storage tissues transfer coefficient of triclopyr ( $hr^{-1}$ )
$k_{SB}$	Storage tissues to blood transfer coefficient of triclopyr ( $hr^{-1}$ )
$k_e$	Elimination rate constant of triclopyr ( $hr^{-1}$ )
$F_u$	Total fraction of the absorbed dose of triclopyr eventually excreted in urine
$V_d$	Apparent volume of the blood compartment $B(t)$ (ml/kg)
$f_{skin}$	Fraction of the daily absorbed dose from the dermal route
$f_{lungs}$	Fraction of the daily absorbed dose from the pulmonary route

**Table 2. Amounts of triclopyr measured in the 22-hr cumulative urinary samples (mg) of the workers and their body weights (kg)**

Workers	Amount of triclopyr measured in the 22-hr cumulative urine sample (mg)	Body weight (kg)
1 <sup>a</sup>	2.71	77
2 <sup>a</sup>	2.40	77
3 <sup>a</sup>	4.23	68
4 <sup>a</sup>	1.04	81
5 <sup>a</sup>	12.98	75
6 <sup>a</sup>	1.36	73
7 <sup>a</sup>	3.04	75
8 <sup>a</sup>	5.54	91
9 <sup>b</sup>	3.61	73
10 <sup>b</sup>	5.27	66

<sup>a</sup> Workers applying Garlon 4<sup>®</sup> with the backpack unit.

<sup>b</sup> Workers pulverizing Garlon 4<sup>®</sup> with the tractor-mounted boom spray.

**Table 3. Effect of variations in the relative contributions of the dermal and pulmonary routes on model predictions of different exposure parameters following a 8-hr exposure to triclopyr resulting in a 22-hr cumulative urinary excretion of triclopyr equal to 56.4  $\mu\text{g}/\text{kg}$**

Exposure parameters	Fraction of the daily absorbed dose from the dermal route ( $f_{\text{skin}}$ ) and from the pulmonary route ( $f_{\text{lungs}}$ )				
	$f_{\text{skin}}=1$ $f_{\text{lungs}}=0$	$f_{\text{skin}}=0.75$ $f_{\text{lungs}}=0.25$	$f_{\text{skin}}=0.5$ $f_{\text{lungs}}=0.5$	$f_{\text{skin}}=0.25$ $f_{\text{lungs}}=0.75$	$f_{\text{skin}}=0$ $f_{\text{lungs}}=1$
Daily absorbed dose of triclopyr (mg/kg-bw) <sup>a</sup>	0.162	0.124	0.101	0.085	0.073
Peak of blood concentration of triclopyr (mg/L) <sup>b</sup>	0.077	0.088	0.106	0.118	0.127
Area under the blood concentration time-curve of	2.802	2.156	1.751	1.474	1.273

Note: The model simulations were carried out with the parametric set obtained from the average of each individual parametric set of Carmichael et al<sup>1</sup> (i.e.,  $k_{\text{abs}}=0.04 \text{ hr}^{-1}$ ;  $k_{\text{BS}}=0.14 \text{ hr}^{-1}$ ;  $k_{\text{SB}}=0.28 \text{ hr}^{-1}$ ;  $k_{\text{BU}}=0.30 \text{ hr}^{-1}$ ;  $F_{\text{u}}=0.81$ ,  $V_{\text{d}}=194.1 \text{ ml}/\text{kg}$ ).

<sup>a</sup>

$$\text{Daily absorbed dose} = \frac{0.56 \mu\text{g}/\text{kg} - \text{bw}}{\text{simulated fraction of the daily absorbed dose recovered in the 22 - hr urinary samples}}$$

<sup>b</sup> The blood concentration time-curve of triclopyr  $C_{\text{blood}}(t)$  is obtained by the following equation:

$$C_{\text{blood}}(t) = \frac{B(t)}{V_{\text{d}}}$$

° The area under the blood concentration time-curve of triclopyr AUC is obtained by the following equation:

$$\text{AUC} = \int_0^{\infty} C_{\text{blood}}(t) dt .$$

**Table 4. The lower-bound, the mean and the upper-bound estimates of daily absorbed dose (mg) for each worker assuming that the absorption occurs only via the skin**

Workers	Estimates of the daily absorbed dose (mg) <sup>a</sup>		
	Lower-bound	Mean	Upper-bound
1 <sup>b</sup>	5.69	7.77	10.46
2 <sup>b</sup>	5.03	6.87	9.24
3 <sup>b</sup>	8.88	12.13	16.32
4 <sup>b</sup>	2.19	2.99	4.02
5 <sup>b</sup>	27.23	37.18	50.04
6 <sup>b</sup>	2.85	3.89	5.24
7 <sup>b</sup>	6.37	8.70	11.71
8 <sup>b</sup>	11.63	15.87	21.36
9 <sup>c</sup>	8.33	11.49	15.69
10 <sup>c</sup>	12.16	16.78	22.91

<sup>a</sup> The estimations were calculated using the following equation:

$$\text{Daily absorbed dose} = \frac{\text{amounts of triclopyr measured in the 22 - hr urinary samples}}{\text{fraction of the daily absorbed dose recovered in the 22 - hr urinary samples}}$$

<sup>b</sup> The lower-bound, the mean and the upper-bound estimates of the absorbed dose were calculated with three values of the simulated fraction of the absorbed dose recovered in the 22-hr urinary samples: 0.477, 0.349 and 0.259.

<sup>c</sup> The lower-bound, the mean and the upper-bound estimates of the absorbed dose were calculated with three values of the simulated fraction of the absorbed dose recovered in the 22-hr urinary samples: 0.433, 0.314 and 0.230.

**Table 5. Comparison of the lower-bound, mean and upper-bound estimates of daily absorbed dose (mg/kg-bw) with the dose corresponding to the no-observed-effect level (NOEL) observed in rats: 5 mg/kg-bw**

Workers	Daily absorbed dose <sup>a</sup> / NOEL		
	Lower-bound	Mean	Upper-bound
1	0.015	0.020	0.027
2	0.013	0.018	0.024
3	0.026	0.036	0.048
4	0.005	0.007	0.010
5	0.073	0.099	0.133
6	0.008	0.011	0.014
7	0.017	0.023	0.031
8	0.026	0.035	0.047
9	0.023	0.032	0.043
10	0.037	0.051	0.070

<sup>a</sup> See Table 4 for the estimates of the daily absorbed dose of each worker.

## CAPTIONS TO FIGURES

**Figure 1 :** Modified model of the kinetics of triclopyr developed by Carmichael *et al.* (1989). Symbols are described in Table 1.

**Figure 2 :** Model simulations of the time-course of cumulative excretion of triclopyr in urine (expressed as a fraction of the daily absorbed dose) following the onset of an 8-hour day with two 15-minute breaks in the morning and in the after-noon and a 30 minutes break for lunch with absorption only through the skin: (—)  $k_{abs}=0.04 \text{ hr}^{-1}$ ,  $k_{BS}=0.13 \text{ hr}^{-1}$ ,  $k_{SB}=0.46 \text{ hr}^{-1}$ ,  $k_e=0.19 \text{ hr}^{-1}$ ,  $F_u=0.74$  ; (·-·-·-·-·)  $k_{abs}=0.06 \text{ hr}^{-1}$ ,  $k_{BS}=0.13 \text{ hr}^{-1}$ ,  $k_{SB}=0.23 \text{ hr}^{-1}$ ,  $k_e=0.35 \text{ hr}^{-1}$ ,  $F_u=0.90$  ; (-----)  $k_{abs}=0.04 \text{ hr}^{-1}$ ,  $k_{BS}=0.14 \text{ hr}^{-1}$ ,  $k_{SB}=0.28 \text{ hr}^{-1}$ ,  $k_e=0.30 \text{ hr}^{-1}$ ,  $F_u=0.81$ .

FIGURE 1.

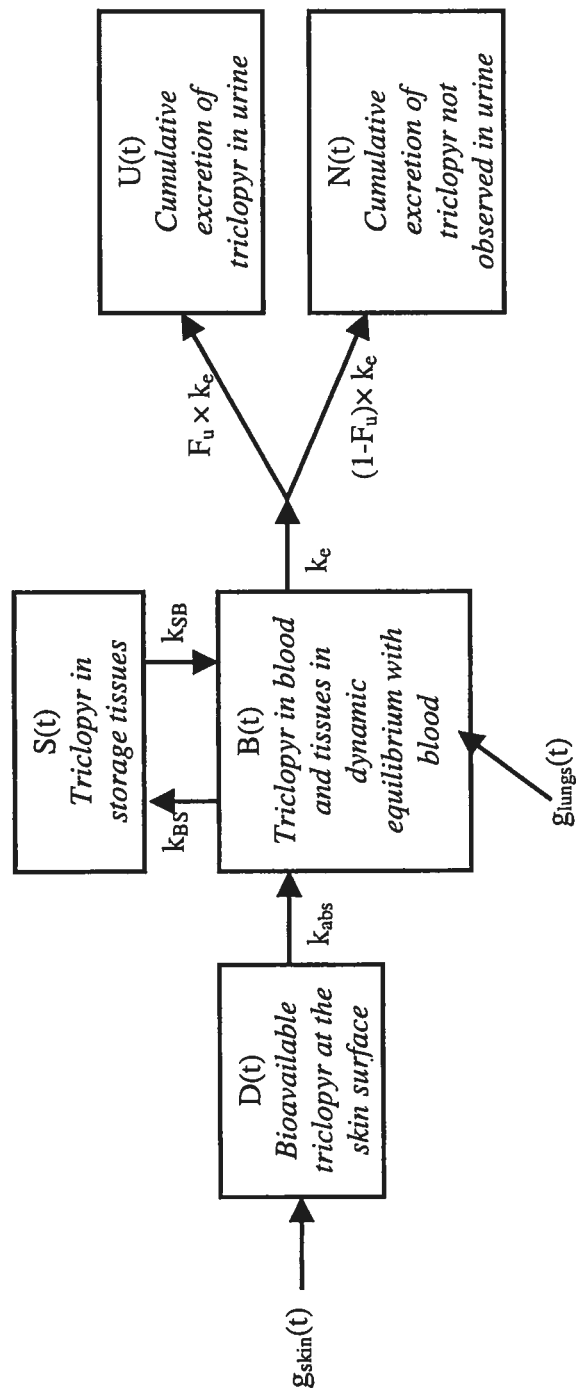
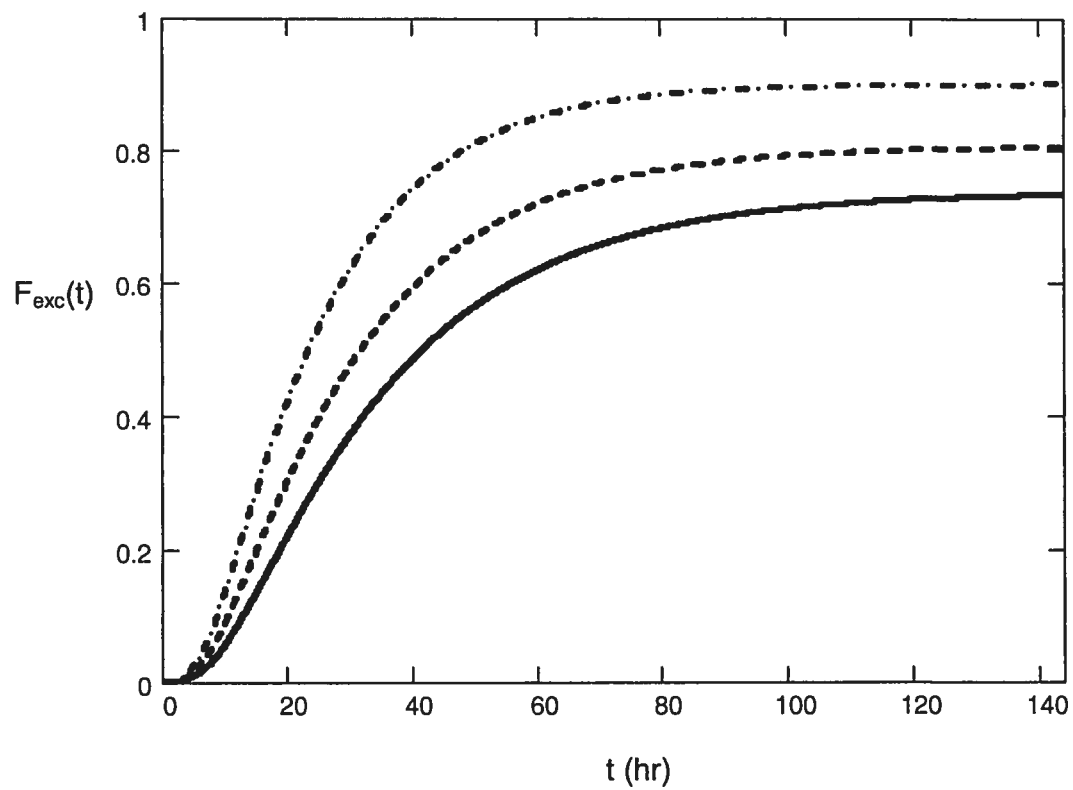


FIGURE 2.



**CHAPITRE 7 : ARTICLE 5, MÉTHYLMERCURE**

Cette version finale de l'article a été acceptée le 10 février 2005 pour publication dans *Journal of Exposure Analysis and Environmental Epidemiology*.

## RECONSTRUCTION OF METHYLMERCURY INTAKES IN INDIGENOUS POPULATIONS FROM BIOMARKER DATA

Nathalie H. Gosselin<sup>1</sup>, Robert C. Brunet<sup>2</sup>, Gaétan Carrier<sup>1</sup>, Michèle Bouchard<sup>1</sup>, Mark  
Feeley<sup>3</sup>

<sup>1</sup> Chaire en analyse des risques toxicologiques pour la santé humaine and Département de santé environnementale et santé au travail, Faculté de Médecine, Université de Montréal, P.O. Box 6128, Main Station, Montreal (Quebec), Canada, H3C 3J7

<sup>2</sup> Département de Mathématiques et de Statistique and Centre de Recherches Mathématiques, Faculté des arts et des sciences, Université de Montréal, P.O. Box 6128, Main Station, Montreal (Quebec), Canada, H3C 3J7

<sup>3</sup> Health Canada, Chemical Health Hazard Assessment Division, Bureau of Chemical Safety, Food Directorate, Sir F. Banting Bldg, Tunney's Pasture, Ottawa (Ontario), Canada, K1A 0L2

Reprint requests: Gaétan Carrier  
Département de Santé environnementale et santé au travail  
Université de Montréal  
P.O. Box 6128, Station centre-ville, Montreal (Quebec) H3C 3J7  
CANADA  
Telephone number: (514) 343-6111 ext 3108  
Fax number: (514) 343-2200  
E-mail: gaetan.carrier@umontreal.ca

Running title: Reconstruction of methylmercury intakes  
Key words: methylmercury, biomonitoring, toxicokinetics, biomarker

**ABSTRACT**

Significant amounts of methylmercury (MeHg) can bioaccumulate in fish and sea mammals. To monitor MeHg exposure in individuals, organic and inorganic mercury are often measured in blood samples or in hair strands, the latter being by far the best integrator of past exposure. With knowledge of the MeHg kinetics in humans, the levels of both biomarkers can be related to MeHg body burden and intakes. In the present study, we use the toxicokinetic model of Carrier et al. (2001), describing the distribution and excretion of MeHg in humans, to reconstruct the history of MeHg intakes of indigenous women of the Inuvik region in Canada starting from total mercury concentrations in hair segments. From these reconstructed MeHg intakes, the corresponding simulated mercury blood concentrations are found to be good predictors of the concentrations actually measured in blood samples. An important conclusion of this study is that, for almost all subjects, the reconstructed history of their MeHg intakes provides much lower intake values than intakes estimated from questionnaires on food consumption and estimated MeHg levels in these foods ; the mean value of the reconstructed MeHg intakes is  $0.03 \mu\text{g}/\text{kg}/\text{day}$  compared with the mean value of  $0.20 \mu\text{g}/\text{kg}/\text{day}$  obtained from questionnaires. The model was also used to back-calculate the MeHg intakes from concentrations in hair strands collected from aboriginals of the Amazon region in Brazil, a population significantly more exposed than the population of the Inuvik region.

## ***INTRODUCTION***

The 1956 industrial mercury spillage in the bay of Minamata in Japan has irrefutably demonstrated the harmful effects of acute methylmercury (MeHg) exposure on the human nervous system (Tsubaki and Irukayama, 1977). In 1971, another major incident of MeHg poisoning occurred in Iraq; the use of barley and wheat seed treated with mercury fungicides induced severe cases of poisoning following the consumption of bread made from the contaminated grains (Bakir et al., 1973). This incident confirmed the neurological effects of MeHg on the foetus of the exposed mothers (Marsh et al., 1980, 1981).

Nowadays, the major source of MeHg exposure is through the consumption of contaminated fish (World Health Organization (WHO), 1990). Populations that get a substantial amount of their food through subsistence fishing, such as Canadian aboriginals, have the potential to be highly exposed to MeHg. Many epidemiological surveys have been conducted to monitor the level of MeHg exposure in these populations with the aim of limiting the health hazards arising from their diet (Mc Keown-Eyssen and Ruedy, 1983 ; Wheatley and Paradis, 1996 ; Dewailly et al., 2001 ; Muckle et al., 2001). The MeHg exposure can be inferred from biomarker levels expressed as the concentration of total mercury (organic and inorganic form) in blood and/or in hair samples. The MeHg consumption can also be assessed by estimating the daily intake of MeHg by means of a questionnaire about the past ingestion of food potentially contaminated with MeHg or from an analysis of a duplicate diet during a

given period. In order to evaluate the associated health hazards of MeHg intake, these MeHg exposure markers are compared with reference values proposed by public health and environmental organizations (WHO, 1990 ; United States Environmental Protection Agency (USEPA), 1997 ; Health Canada, 1998 ; Food and Agriculture Organization of the United Nations (FAO), 2003). These values, which are based on scientific investigations of the plausible relations between the levels of MeHg biomarkers and the harmful effects on human health, are considered acceptable by those organizations.

To relate the levels of MeHg biomarkers to the corresponding daily intakes of MeHg, an empirical one-compartment kinetic model describing the fate of MeHg in the human body has so far been used (WHO, 1990 ; USEPA, 1997 ; FAO, 2003). More often than not, the steady-state conditions (i.e., the intake equals the excretion) are assumed in establishing the relationship, resulting in a constant ratio between the MeHg daily intake and the total mercury measured in the biological matrices. However, since the amounts of MeHg measured in fish fluctuate greatly (Morgan et al., 1997) and the consumption patterns of fish and sea mammals vary with seasons (Sherlock et al., 1982), the MeHg exposure generally varies too much throughout time to satisfy the conditions of steady-state. This exposure variation is identified by the variable total mercury levels measured in sequential segments of hair strands of individuals from fish eating populations (Phelps et al., 1980; Dolbec et al., 2001).

Recently, a biologically-based dynamical model was developed by Carrier et al. (2001) to predict in humans the distribution and elimination of MeHg and its inorganic metabolite for a variety of MeHg ingestion scenarios. This model can relate MeHg daily intakes to the total mercury levels measured in accessible biological matrices. The model follows the dynamics of intakes and elimination, without steady-state assumptions, for any dietary exposure scenario and any data collection time. The toxicokinetic model of Carrier et al. (2001) is based on a system of differential equations where each equation describes the evolution of the organic or inorganic mercury burden in a compartment. Each compartment stands for either a single organ or a group of organs or tissues. An input function incorporated in the differential equation of the gastrointestinal compartment allows simulations of any oral MeHg exposure scenario. This function represents the variable rate of MeHg daily intakes during a chosen period, a daily intake being the total of the amounts of food ingested multiplied by their respective MeHg concentrations. The values of the model parameters in Carrier et al. (2001) were determined using the available published data of the *in vivo* time-profiles of total mercury in blood and in hair of volunteers orally exposed to MeHg. These profiles were obtained from several experimental studies on healthy men and women (Aberg et al., 1969; Miettinen et al., 1971; Birke et al., 1972; Kershaw et al., 1980; Sherlock et al., 1984; Smith et al., 1994).

Before proceeding with the reconstruction of MeHg intakes in aboriginal populations, the present study seeks to understand the impact of the toxicokinetics of organic and inorganic mercury on the determination of amounts of MeHg ingested that can be

inferred from the concentrations of total mercury measured in biological matrices. For this purpose, the model of Carrier et al. (2001) was used to investigate the relationships between MeHg intake and biomarker levels for different exposure scenarios, particularly those where steady-state conditions are far from being attained. Also, the variability in MeHg biomarker levels stemming from the inter-individual variability of the MeHg blood elimination half-life and of the ratio between the total mercury concentration in hair and that in blood was assessed. Similarly, the effect of various collection times post exposure on MeHg biomarker levels were examined.

Using the model and the measured concentrations of total mercury in sequential centimeters of hair strands, reconstruction of the likely monthly MeHg intakes was carried out for indigenous populations of Canada and Brazil without the need for knowledge of their dietary habits.

## ***METHODS***

For the present study, the differential equation system of the toxicokinetic model of Carrier et al. (2001) was programmed in MathCad 2000 Professional (MathSoft Inc., Cambridge, MA). The mathematical resolution of the differential equation system, with the input function describing an ascribed ingestion sequence, was based on the numerical method of Runge-Kutta included in this software. All model simulations were carried out with the mean parametric values presented in Carrier et al. (2001), except when assessing the impact of the inter-individual variability of the elimination half-life of MeHg in blood and of the ratio between total mercury concentration in hair and that in blood. Since the model is based on the conservation of mass in the system at all times, it predicts initially the amounts of organic or inorganic mercury in each model compartment. To convert mercury blood amounts to concentrations, blood volume was taken to be 8.2% of the body weight (Brown et al., 1997). Also, to depict the time-profiles of total mercury levels in hair, it was assumed that hair grew at the rate of 1 centimeter (cm) per month (WHO, 1990).

### ***Main factors governing levels of methylmercury biomarkers***

**Methylmercury blood elimination half-life** : Carrier et al. (2001) determined averages for this parameter by fitting their kinetic model to time-profile data observed in controlled intake studies. Average MeHg blood elimination half-lives of 47.1, 50.2, 50.2, 51.7 and 54.8 days were respectively obtained from the data of Aberg et al. (1969), Miettinen et al. (1971), Smith et al. (1994), Sherlock et al. (1984) and Kershaw

et al. (1980). The underlying MeHg demethylation rate (Al-Shahristani and Shihab, 1974; Al-Shahristani et al., 1976) is subject to large variations among individuals and is plausibly the most determinant parameter for the elimination of MeHg from blood (WHO, 1990). To address this large variation, we allowed the MeHg blood elimination half-life to vary from 39 to 70 days, based on the extreme values measured in subjects under controlled and uncontrolled intake exposures (WHO, 1990). Its impact on the maximum total mercury concentration in blood and, in turn in hair, was examined for individuals ingesting MeHg under different exposure scenarios.

**Ingestion sequence :** Before attempting reconstruction of individual intake histories, it was deemed useful to assess the impact of the time sequence of ingestion on the time course of biomarkers. The kinetic profiles of total mercury concentrations in blood and in hair were simulated for different durations of MeHg ingestion and different ingestion rates. These template scenarios represent individuals consuming either a single meal contaminated with MeHg, or the same meal every day for one week, one month, 3 months and 21 months (only after this latter length of time is steady state practically attained). The progression of total mercury in biological matrices was also simulated for individuals ingesting one contaminated meal per week during 3 and 14 month periods. Every meal corresponded to an arbitrary dose of  $1 \mu\text{g}$  of MeHg/kg of body weight (BW) and the MeHg background before the onset of exposure was considered nil. Also, the ratios of total mercury concentration in the 1<sup>st</sup> cm of hair closest to the root to total mercury concentration in the corresponding blood sample were evaluated as function of collection times and exposure scenarios. The

concentration of total mercury in the 1<sup>st</sup> cm closest to the scalp was retained in the analysis of hair-to-blood ratio because it is available in almost all the exposed individuals, also this concentration reflects the integration of blood exposure during the month just prior to collection.

**Ratio between the total mercury concentration in hair and that in blood :** In

Carrier et al. (2001), the values of the transfer rates of organic and inorganic mercury from blood to hair were determined from the mean data set of Kershaw et al. (1980) on the time courses of total mercury in the hair and blood of exposed volunteers. Since these model parameters mainly govern the ratio between the total mercury concentration in hair and that in blood, sensitivity tests on these transfer rates were implemented to establish the impact of variability of the hair-to-blood ratio on the MeHg biomarker levels. Simulations of the exposure scenarios presented above were executed by varying by  $\pm 50\%$  the mean values presented in Carrier et al. (2001). This variation was chosen based the data set of Walker et al. (2002) described in the section below.

***Reconstruction of methylmercury intakes in indigenous populations***

Two databases of MeHg biomarkers were supplied to our research team. These databases originated from MeHg exposure studies on indigenous populations living in Canada and in Brazil.

**Indigenous population from Canada :** From June 1<sup>st</sup> 1998 to June 1<sup>st</sup> 1999, 104 pregnant Inuit women, between ages of 15 and 45 years, agreed to participate in a biomonitoring study on environmental contaminants (Walker et al., 2002). These women were from communities in the Inuvik region of the Northwest Territories, Canada. The day of delivery, samples of maternal blood and strands of hair were collected. Total mercury concentration was measured in blood samples and in each consecutive segment of 1 or 2 cm cut in the strand of hair. The limit of detection for the concentration of total mercury in blood was 0.2  $\mu\text{g/l}$ , for hair it was 0.4  $\mu\text{g/g}$ . In addition, Walker et al. (2002) distributed to these women a dietary questionnaire about their food consumption and estimated thereafter their average daily intake of MeHg from the amount of each food item multiplied by its known MeHg concentration. The available database provides the concentration in hair for 80 women, the concentration in blood for 94 women and the average daily intake as assessed from the questionnaire for 86 women.

Since the concentration of total mercury in each segment of hair represents an integration over time of the mercury transferred from blood to hair roots during the period corresponding to the segment growth, indirect information about past MeHg exposure is thus available for women who provided hair samples. Of course, the period for which the exposure history can be estimated was determined by the length of the collected hair strand. In the present work, the model of Carrier et al. (2001) was used to estimate the temporal profile of MeHg daily intakes starting from total mercury concentrations in hair strands. These back calculations were carried out by iterations,

varying the estimated MeHg intake rates until an optimal adjustment was achieved between model simulations and actual data on the total mercury concentration in each sequential segment of the hair strand. To fit the concentration of mercury in the segment at the tip of the hair strand (i.e., the segment corresponding to the most distant time for which past exposure to mercury can be estimated), the model simulations assumed that, before that month, the MeHg exposure occurred under steady-state conditions. Also, with the aim of not underestimating the MeHg intakes, the concentration in the segments of hair with no detectable mercury was set to the limit of detection. The MeHg daily intakes estimated through this back-calculation were later compared with the ones estimated from the food frequency questionnaire.

Using the model, the reconstructed temporal profile of MeHg consumption gave, for each woman providing a hair strand, an estimation of the total mercury concentration in blood on the day of childbirth. This simulated blood concentration was compared with the one measured in their blood sample. The comparison could meaningfully be done only for women whose mercury level in the 1<sup>st</sup> cm of hair cut closest to the root was above the limit of detection.

**Indigenous population from Brazil :** A study was undertaken in the Amazon in Brazil with the aim of verifying the relationship between the nervous system dysfunction and levels of MeHg exposure in a fish eating population (Lebel et al., 1996, 1998; Dolbec et al., 2001). The targeted populations were natives that lived in Amazonian villages situated on the edge of the river Tapajós in Brazil. The MeHg

exposure was evaluated by the total mercury concentration in collected hair strands. These strands were cut in segments of 1 cm and, the total mercury concentration was measured for every segment. The available database includes these concentrations for 108 aboriginals. For 45 of them, the hair was collected in 1995, for the other 63, in 2000.

In the current study, the temporal profiles of daily MeHg intakes of 20 natives men and women (pregnancy status not specified), were estimated by the same procedure as for the Inuvik women. The 20 individuals were chosen to afford representative levels of MeHg exposure in the cohort; to do so, two individuals were selected at random in every decile group. These deciles were ranked according to the average concentrations obtained upon pooling their hair segments.

## **RESULTS**

### ***Main factors governing levels of methylmercury biomarkers***

**Methylmercury blood elimination half-life** : Table 1 presents simulations of biomarker levels in exposed individuals with varying MeHg blood elimination rates. Increasing the residence time of total mercury in the body (longer MeHg blood elimination half-lives) results in an increase in maximum biomarker levels. For a chronic daily exposure, using a MeHg blood elimination half-life of 70 days, the maximums of the total mercury concentrations in hair and in blood are approximately 1.6 times higher than the ones obtained with a half-life of 39 days. This increase is however not noticeable for short exposure periods. In addition, the model simulations presented in Table 1 show that changing the MeHg blood elimination half-life has little impact on the hair-to-blood ratio.

**Ingestion sequence** : The simulations of the temporal profiles of the total mercury concentration in blood show that the contaminated meals consumed during the days, and even the months preceding a blood sampling, significantly influence the blood concentration. For example for an individual ingesting a daily meal equivalent to a dose of  $1 \mu\text{g MeHg/kg BW}$  during one week, the model estimates the maximum concentration of total mercury in blood immediately after ceasing ingestion at  $6.2 \mu\text{g/l}$ ; this is, respectively, 3.7 and 7.8 times less than the maximum concentration attained at the end of one month or 3 months with the same daily dose. The model also showed that to attain a steady-state blood concentration, the daily exposure needs to occur for 21 months, which would result in a blood concentration of  $68.3 \mu\text{g/l}$ .

According to the model simulations, the total mercury concentrations in the 1<sup>st</sup> cm of hair cut closest to the root increases following a kinetic pattern similar to the one in blood. However, there is a time-delay between the mercury level in blood and the concentration in the proximal cm hair segment as hair concentration stems from the average blood levels in contact with hair roots over one month. This time-delay effect diminishes only when the exposure conditions come close to steady-state conditions. The analysis of the time-profiles of total mercury concentration in hair simulated for a single MeHg intake and for daily MeHg intakes during a week or a month shows that the maximum concentrations in the proximal cm of hair are reached about one month following the end of MeHg exposure, whereas, for daily intakes over three months, the maximum concentration in hair is reached 10 days after the end of exposure. Also, the simulated time-profile of total mercury level in hair indicates that the steady-state is attained after 21 months of a constant daily intake. If the ingestion of contaminated foods stops when steady-state is reached, the maximum concentration in the proximal cm is obtained when the hair strand is collected on the termination day.

Figure 1 presents the time-profiles of total mercury concentration in blood and in hair following the onset of ingestion of one meal of 1  $\mu\text{g}$  of MeHg/kg BW per week for periods of 3 and 14 months. Between each ingested contaminated meal (seven days), approximately 7% of total mercury in blood was eliminated; this appears in Figure 1 as oscillations in the time-profiles of blood concentration. However, no oscillation in the hair concentration is observed given that the MeHg exposure remains the same month

after month and the amount in each one-cm of the hair strand stems from the integration of the total mercury levels in blood during the month corresponding to the one-cm growth. As a result of the integration of MeHg blood exposure, the total mercury concentration in hair is approximately the same as the concentration that would be obtained following the daily ingestion of a meal of  $0.14 \mu\text{g}$  of MeHg/kg BW instead of  $1 \mu\text{g}$  MeHg/kg per week (i.e.,  $1 \mu\text{g}$  of MeHg/kg of BW divided by 7).

Figure 1 illustrates a detectable time-delay between the maximum of the total mercury concentration in blood and the maximum in the proximal cm of hair for the weekly MeHg intakes throughout the three months intake, while no time-delay was detectable for the weekly exposures for 14 months. For both duration periods, after the first month without MeHg ingestion, the concentrations in hair and blood follow similar decay profiles, showing that after this initial time period, a dynamical equilibrium sets in between blood and hair concentrations. This feature is also observed for all the daily exposure scenarios after one month following the last ingestion.

**Ratio between the total mercury concentration in hair and that in blood :**

Simulated ratios between the total mercury concentration in the 1<sup>st</sup> cm of hair closest to the root and the concentration in blood are presented in Table 2 for different durations of MeHg daily intake and time of collection. It can be seen that hair-to-blood ratio depends on the duration of MeHg intakes; it increases when the duration of exposure increases. The ratio is close to a constant value when exposure gets nearer to steady-state conditions, since the time-delay observed between the blood and hair

concentrations then decreases. According to the model of Carrier et al. (2001) with the mean parametric values, this constant steady-state ratio is equal to 342. Table 2 shows that this value is only reached in the case of a chronic daily exposure. Even for a chronic ingestion of one MeHg contaminated meal per week (see Figure 1B), the hair-to-blood ratio is not constant. Since the blood levels decrease during the days following ingestion, this ratio depends on the day of blood collection, varying during the week between 331 and 354.

Also from Table 2, the hair-to-blood ratio is much lower if the collection is carried out on the termination day of MeHg exposure rather than if collection is done one month after. One month after intake cessation, the ratio is close to a constant value because the hair and blood concentrations are changing at a similar rate. In fact, the hair-to-blood ratio does not necessarily depend on the duration of MeHg intakes when the biological matrices are collected one month or more following the end of exposure, and this is true even for the once a week exposure scenario. That ratio ranges from 406 to 431 (see Table 2)

The total mercury concentrations in blood predicted by the model of Carrier et al. (2001) were not sensitive to the presumed variability of the transfer rates of organic and inorganic mercury from blood to hair because these transfer rates are relatively small compared to the other blood elimination rates. However, concentrations in hair were widely influenced by this variability; in fact, the total mercury levels in hair varied proportionally to the value of these blood-to-hair transfer rates. As can be

verified from the results presented in Table 2, this proportional response is true for any ingestion sequences and collection times. Also, this Table shows that the exposure and sampling scenarios are more important in determining the hair-to-blood ratio than the values of the transfer rates of organic and inorganic mercury from blood to hair.

### *Reconstruction of methylmercury intakes in indigenous populations*

**Indigenous population from Canada :** The construction of past daily MeHg intakes in the 80 Inuvik women who supplied hair strands was estimated by adjusting possible intake rates until an intake profile coupled with the model kinetics yielded a fit to the measured total mercury concentrations in every consecutive segment of hair. The estimations of intake rates from the data of four exposed women in the cohort are illustrated in Figure 2A; they show that there is a reasonable adjustment between the simulations of the model and the temporal profile of the mercury concentrations measured in the hair of these women. Good fits were also achieved from total mercury concentration measured in the hair of the other Inuvik women (results are not shown).

Comparison of the time-profiles of intakes versus that of hair concentrations presented in Figure 2A illustrates the delay between the MeHg daily intake rates and the total mercury concentrations in hair. For example, MeHg daily intake has to increase substantially before the appearance of a detectable increase in the hair segment. This time-delay between intake rates and hair concentrations stems from an important mechanism at work: rising intake results in rapid rise in blood concentration (days), but blood concentration needs to be high for a substantial amount of time (weeks) before

the monthly average of blood-hair root contact, represented in a cm of hair, can rise similarly. The dose rate reconstructions and the measurements of the total mercury concentration in the hair segments in Figure 2A show wide variations in the monthly levels of exposure; in none of the Inuvik women was steady-state ever attained.

For each of the 80 women who provided a hair sample, the reconstructed time-profile of MeHg daily intakes allows estimation of their average MeHg daily intake for each of the pregnancy trimesters. Descriptive statistics on these intakes are presented in Table 3. Only 60 women supplied hair strands long enough to estimate the past exposure to MeHg during the first trimester of pregnancy. There is, on average, little difference between MeHg ingested during the trimesters.

In Table 3, descriptive statistics are presented for the average MeHg daily intakes estimated from the dietary questionnaire of the 69 women who responded to the questionnaire among the 80 women providing hair strands. The estimates of the MeHg consumption based on the questionnaire were much higher than the ones based on the previously described reconstruction of intakes from the total mercury concentrations in consecutive segments of hair. In fact, the questionnaire gave higher intake estimations in 58 women of the group of 69. For example, the questionnaire estimated an average daily intake of 2.73  $\mu\text{g}$  of MeHg /kg BW for a given woman whereas the highest daily intake based on her reconstructed time-profile is 0.02  $\mu\text{g}$  of MeHg /kg BW. However, for the woman having the highest mercury levels in her hair, average daily intake estimated by the questionnaire is less than half of the intakes reconstructed with the

model. Also, the woman with the highest daily intake as estimated by the questionnaire presented no detectable mercury in her hair.

Figure 2B presents, for 4 women in the Inuvik cohort, the model simulations of the temporal profile of their total mercury concentration in blood as well as the concentration measured in the maternal blood sample collected after childbirth. These blood concentration simulations were determined using the model kinetics and the reconstructed time-profile of MeHg daily intakes based on the observed concentrations in the consecutive segments of hair strands, independent of the mercury levels in blood. Figure 2B shows that the simulated values for concentrations of mercury in blood at the moment of childbirth are close to the values measured in the collected blood. Figure 3 presents the relation between the simulated ( $x$ ) and measured ( $y$ ) total mercury concentrations in blood for the 16 Inuvik women having total mercury concentrations in the proximal cm of hair above the detection limit. The points are fairly close to the plotted line of a would be perfect simulation ( $y = x$ ). A regression for the linear function  $\log(y) = m \cdot \log(x)$  was carried out by the least-squares method on the logarithms of the measured and simulated blood concentrations. The logarithm was used to avoid distortion of fit from high values because the difference between the lower and higher concentrations (the measured as well as the simulated) is more than one order of magnitude. The slope estimator ( $m$ ) is 0.86 and the 95% confidence interval of this estimator is  $IC(95\%) = (0.69, 1.02)$ . The determination coefficient ( $r^2$ ) of this regression is 0.90.

**Indigenous population from Brazil :** The adjustments of the model simulations on the mercury concentrations measured in every segment of hair allowed reconstruction of the variations in daily MeHg intakes for the 20 selected Amazonian aboriginals. Figure 4 presents the results of only two simulations carried out: for the two participants among 20 providing hair strands long enough to back calculate the MeHg daily intakes for 16 months. This figure shows that a good fit can be obtained between the model simulations and the measured values; which was also the case for the other 18 aboriginals (results no shown).

A comparison between the temporal profile of the mercury concentrations in hair and that of daily MeHg intakes illustrates again the delay between the variations of these two quantities. Also, as for the Inuvik women, the monthly levels of MeHg exposure vary, so steady-state assumptions are also not in order here. The variations in MeHg levels for Amazon natives have been previously reported by Lebel et al. (1997) and by Dolbec et al. (2001). These authors conclude that the variations are mostly due to different MeHg content within the types of fish caught during the dry season and the ones consumed during the rainy season.

## ***DISCUSSION***

The toxicokinetic model of Carrier et al. (2001) was developed for the purpose of simulating the fate of organic and inorganic mercury in humans exposed to MeHg via the dietary route. It allows bilateral links between the MeHg daily intake and the mercury concentration in blood and hair samples collected at any given time following the onset of any MeHg ingestion period.

### ***Main factors governing methylmercury levels of biomarkers.***

Due to the relatively long elimination half-life of MeHg, the duration of exposure has an important influence on biomarker levels. The model simulations of total mercury concentrations in blood as well as in hair showed that the MeHg daily intake necessary to attain a specified maximum concentration has to be much higher for an exposure of short duration (days or weeks) than for a chronic or extended exposure of several months. For example, simulations show that, after ingesting each day for one week a MeHg contaminated meal, the MeHg blood level would be just 10% of the level reached at steady-state under identical daily intakes. Only after 21 months of constant identical daily intakes are the conditions for steady-state met; these conditions are rarely met in real life situations, hence there are dangers of severely biased estimations if steady-state is assumed. The impact of temporal exposure scenarios may help explain the large study-to-study difference between uncontrolled and controlled intake studies with regard to the ratio: “mercury blood concentration / MeHg daily intake” (Sherlock

and Quinn, 1988; WHO, 1990); these studies often surmise that the fish-eating populations are exposed to MeHg under steady-state conditions, which is not the case.

As already mentioned, inter-individual variability in the MeHg blood elimination half-life was observed in controlled intake studies (Miettinen et al., 1971; Kershaw et al., 1980; Sherlock et al., 1980; Smith et al., 1994). In the present study, the impact of this variation on the biomarker levels was investigated for different durations of MeHg daily intakes. Under chronic exposure, the simulated maximum total mercury concentrations in blood and in hair are about twice as high when the elimination half-life of MeHg in blood is put equal to 70 days in comparison to 39 days. However, the consequences of this variation are much less important if the daily exposure has only occurred for a short period (see Table 1).

In addition to the inter-individual variability observed in MeHg blood elimination half-lives and in mercury hair-to-blood ratio, there is study-to-study variations in the observed hair-to-blood ratio: the mean hair-to-blood ratio reported by the observational and controlling dosage studies vary between 140-370 (FAO, 2003). However, these ratios must be interpreted very cautiously; as presented in Table 2, this wide range may stem mainly from differences regarding the exposure scenarios and sampling procedures. The variability due to the sampling procedure was observed in the study of Kershaw et al. (1980) where volunteers had ingested a single MeHg contaminated meal. These authors measured the total mercury concentration in blood sample and in 0.5-cm proximal segment of hair for each 2 weeks following the ingestion; a 95%

confidence range of 224-476 for the ratio was calculated for a volunteer who provided six blood and six hair samples. Nevertheless, model simulations show that the variations produced by the exposure durations become negligible when the sampling procedure is done one month after exposure cessation (see Table 2). Therefore, to assess inter-individual variability in the hair-to-blood ratio, blood and hair samples should be collected one month after cessation of MeHg exposure and the concentration in hair should be based on the proximal segment of the hair strand.

#### ***Reconstruction of methylmercury intakes in indigenous populations***

Using the model of Carrier et al. (2001), it was possible to reconstruct the temporal profiles of MeHg daily intakes of pregnant women in the Inuvik region starting from the total mercury concentration in each segment of the hair strand. Consequently, the reconstruction does not require the knowledge of the amounts of contaminated food consumed and their respective MeHg concentrations. While there is variability in the parameters of the MeHg kinetics (Stern, 1997; Clewell et al., 1999), the set of the mean parametric values from Carrier et al. (2001) allows for good predictive values of intake estimates, using as indirect validation the comparison between the simulated and measured concentrations of total mercury in the blood samples of the 16 women at child birth (see Figure 3). Despite these encouraging results, there still exist uncertainties concerning the real time-profile of MeHg intakes because the intra- and inter-individual variability in the kinetics of MeHg, in the blood volume and in the hair growth rate were not accounted for in the modeling. There is also a possible imprecision in mercury measurements in hair.

When reconstructing the time-profiles of the MeHg intakes, the variability in the model parameter values can however be considered. In fact, a range of MeHg daily intakes could be obtained by adjusting the model simulations to the hair concentrations using different MeHg blood elimination rates and transfer rates of the organic and inorganic mercury from blood to hair. Time-profiles of the MeHg intakes of the 16 women with detectable mercury levels in the proximal cm of hair were estimated by the model simulations with parametric values for the blood elimination half-life of MeHg at the extremes of the likely range, either 39 or 70 days. With the slower elimination rate (70 days), the estimates of MeHg intakes were reduced by factors ranging between 1.1 and 1.5 compared to the 50 day half-life, whereas they were multiplied by factors between 1.1 to 1.3 with the faster elimination rate (39 days). To assess the impact of variability in the transfer rate of organic and inorganic mercury from blood to hair, a range of MeHg daily intakes was back-calculated for each of these 16 women, using the mean transfer rate values  $\pm 50\%$ . This range of estimated intakes for a given women was then applied to predict an interval for her total mercury concentration in blood at delivery. It was found that the measured values of these blood concentrations were all within the simulated intervals.

Even with the above mentioned uncertainties, the MeHg intakes estimated by adjusting the model to the measured total mercury levels in the hair strands collected from the Inuvik women seem more accurate than the estimates based on their answers to the dietary questionnaire. In fact, the method proposed provides coherence between the

reconstructed MeHg intakes and the measured biomarker levels, whereas there are important inconsistencies between the questionnaire estimations and the amounts of total mercury measured in biological matrices. These inconsistencies, as reported in the Results section, lead one to doubt any inferences based on questionnaires. These dietary estimations are probably biased by inaccurate recollection of the frequency of fish and sea mammal consumption and from variations in the MeHg amounts in traditional/country foods collected in different areas. These biases can have significant impact when assessing health risks related to MeHg ingestion. For instance, the average daily MeHg intakes reconstructed by the model are much lower than  $0.2 \mu\text{g}/\text{kg}$  BW, the value recommended by Health Canada (Health Canada, 1998), whereas the ones estimated by the dietary questionnaire are close to this recommended value (see Table 3). Even when the extreme variability of both the MeHg blood elimination half-life and the hair-to-blood ratio are taken in, the estimated MeHg daily intakes reconstructed using the model by fitting on hair strand data was lower than the one estimated through the questionnaires for almost all women.

The back-calculations of the MeHg daily intakes based on the total mercury concentration in hair strands are applicable to a large range of MeHg exposures. Applied to data collected from the populations of the Amazon, the back calculations show that the most exposed aboriginal in that cohort presented a mercury concentration in the hair about 7 times higher than the most exposed woman in the Inuvik cohort.

## *CONCLUSION*

The results reported in this study may be useful in the design of further biomonitoring studies. Most important, the probable time duration of MeHg exposure should be carefully established when back-calculating with a model the MeHg intakes through the total mercury measured in the biological matrices. It was shown in the present study that mercury concentrations in every one-cm segment of hair are best to provide indications of the historical exposure to MeHg; hence, biomonitoring studies should give priority to hair sampling. The fit between the time-profiles of MeHg hair concentrations simulated by the toxicokinetic model of Carrier et al. (2001) and the observed hair concentrations allows good estimates of the daily intakes during the exposure period to the extent of the length of the hair strand. However, if the collected hair strand is not long enough, a dietary questionnaire about eating habits could be distributed to the exposed individuals just to decide whether the intake was constant, intermittent or acute. This questionnaire does not need to quantify the daily MeHg intake; it is only important to know the period during which the individual might have consumed contaminated food.

An important advantage of collecting hair strands to monitor the MeHg exposure is that the total mercury concentration in a one-cm segment is not substantially influenced by the most recent contaminated meal, contrary to the concentration in blood samples. According to the temporal profiles of the total mercury concentration in blood of volunteers in the study of Kershaw et al. (1980), the mercury level in blood is in

equilibrium with the one in tissues after 30 to 40 hours following the ingestion of a fish meal contaminated with MeHg. This implies that the mercury distribution from the blood to tissues is complete after this period without MeHg exposure. Thus, field workers collecting blood samples should ask the exposed individuals beforehand not to consume foods which might have been contaminated with MeHg for at least two days prior to the blood test.

***ACKNOWLEDGMENT***

The authors wish to thank the Northern Contaminants Program of Indian and Northern Affairs Canada and the Institut de Recherche Robert-Sauvé en Santé et Sécurité du Travail (IRSST) for providing financial support.

**REFERENCES**

Aberg B, Ekman L, Falk R., Greitz U, Persson G, Snihs JO. Metabolism of methyl mercury ( $^{203}\text{Hg}$ ) compounds in man. Excretion and distribution. *Arch. Environ. Health.* 1969; 19: 478-484.

Al-Shahristani H, Shihab KM, Al-Haddad IK. Mercury in hair as an indicator of total body burden. *Bull. World Health Organ.* 1976; 53: 105-112.

Al-Shahristani H, Shihab KM. Variation of biological half-life of methylmercury in man. *Arch. Environ. Health.* 1974; 28: 342-344.

Bakir F, Damluji SF, Murtadha M, Khalidi A, et al. Methylmercury poisoning in Iraq. *Science* 1973; 181: 230-241.

Birke G, Johnels AG, Plantin LO, Sjöstrand B, Skerfving S, Westermark T. Studies on humans exposed to methyl mercury through fish consumption. *Arch. Environ. Health* 1972; 25: 77-91.

Brown RP, Delp MD, Lindstedt SL, Rhomberg LR, Beliles RP. Physiological parameters values for physiologically based pharmacokinetics model. *Toxicol. Ind. Health.* 1997; 13: 407-484.

Carrier G, Bouchard M, Brunet RC, Caza, M. A toxicokinetic model for predicting the tissue distribution and elimination of organic and inorganic mercury following exposure to methyl mercury in animals and humans. II. Application and validation of the model in humans. *Toxicol. and Appl. Pharmacol.* 2001; 171: 50-60.

Clewell HJ, Gearhart JM, Gentry PR, et al. Evaluation of the uncertainty in an oral reference dose for Methylmercury due to interindividual variability in pharmacokinetics. *Risk Anal.* 1999; 19: 547-558.

Dewailly É, Ayotte P, Bruneau S, Lebel G, Levallois P, Weber JP. Exposure of the Inuit Population of Nunavik (Arctic Québec) to lead and mercury. *Arch. Environ. Health.* 2001; 56: 350-357.

Dolbec J, Mergler D, Larribe F, Roulet M, Lebel J, Lucotte M. Sequential analysis of hair mercury levels in relation to fish diet of an Amazonian population, Brazil. *Sci. Total Environ.* 2001; 271: 87-97.

Food and Agriculture Organization of the United Nations -FAO, World Health Organization -WHO. Summary and conclusions of the sixty-first meeting of the Joint FAO/WHO Expert committee on Food Additives (JECFA). JECFA/61/SC, Rome, 2003.

Health Canada. *Review of the tolerable daily intake for methylmercury : Rationale for proposed interim revision of the TDI*. Food Directorate, Health protection branch, Ottawa 1998.

Kershaw TG, Dhahir PH, Clarkson TW. The relationship between blood levels and dose of methylmercury in man. *Arch. Environ. Health*. 1980; 35: 28-36.

Lebel J, Mergler D, Lucotte M et al. Evidence of early nervous system dysfunction in Amazonian populations exposed to low-levels of methylmercury. *Neurotoxicology*. 1996; 17: 157-168.

Lebel J, Roulet M, Mergler D, Lucotte M, Larribe F. Fish diet and mercury exposure in a riparian Amazonian population. *Water, Air and Soil Pollut*. 1997; 97: 31-44.

Lebel J, Mergler D, Branches F et al. Neurotoxic effects of low-level methylmercury contamination in the Amazonian Basin. *Environ. Res. section A*. 1998; 79: 20-32.

Marsh DO, Myers GJ, Clarkson TW, Amin-Zaki L, Tikriti S, Majeed MA. Fetal methylmercury poisoning: clinical and toxicological data on 29 cases. *Ann. Neurol*. 1980; 7: 348-355.

Marsh, DO, Myers GJ, Clarkson TW et al. Dose-response relationship for human fetal exposure to methylmercury. *Clin. Toxicol*. 1981; 18: 1311-1318.

Mc Keown-Eyssen GE, Ruedy J. Methyl mercury exposure in Northern Quebec I. Neurologic findings in adults. *Am. J. Epidemiol.* 1983; 118: 461-469.

Miettinen JK, Rahola T, Hattula T, Rissanen K, Tillander M. Elimination of  $^{203}\text{Hg}$ -methylmercury in man. *Ann. Clin. Res.* 1971; 3: 116-122.

Morgan, JN, Berry MR, Graves RL. Effects of commonly used cooking practices on total mercury concentration in fish and their impact on exposure assessments. *J. Expo. Anal. Environ. Epidemiol.* 1997; 7: 119-133.

Muckle G, Ayotte P, Dewailly É, Jacobson SW, Jacobson JL. Prenatal exposure of the Northern Québec Inuit infants to environmental contaminants. *Environ. Health Perspect.* 2001; 109: 1291-1299.

Phelps RW, Clarkson TW, Kershaw TG, Wheatley B. Interrelationships of blood and hair mercury concentrations in a North American population exposed to methylmercury. *Arch. Environ. Health.* 1980; 35: 161-168.

Sherlock, JC, Lindsay DG, Hislop JE, Evans WH, Collier TR. Duplication diet study on mercury intake by fish consumption in the United Kingdom. *Arch. Environ. Health.* 1982; 37: 271-278.

Sherlock JC, Hislop J, Newton D, Topping G, Whittle K. Elevation of mercury in human blood from controlled chronic ingestion of methylmercury in fish. *Hum. Toxicol.* 1984; 3: 117-131.

Sherlock JC, Quinn M. Underestimation of dose-response relationship with particular reference to the relationship between the dietary intake of mercury and its concentration in blood. *Hum. Toxicol.* 1988; 7: 129-132.

Smith JC, Allen PV, Turner MD, Most B, Fisher HL, Hall LL. The kinetics of intravenously administered methyl mercury in man. *Toxicol. Appl. Pharmacol.* 1994; 128: 251-256.

Stern AH. Estimation of interindividual variability in the one-compartment pharmacokinetic model for methylmercury: implications for the derivation of the reference dose. *Regul. Toxicol. Pharmacol.* 1997; 25: 277-288.

Tsubaki T, Irukayama K. *Minamata Disease: Methylmercury Poisoning in Minamata and Nigata, Japan.* Elsevier Scientific: New York, NY 1977.

United States Environmental Protection Agency –USEPA. Mercury study report to Congress. Vol. V: Health effects of mercury and mercury compounds. US EPA - 452/R-97-007. Office of Air Quality Planning and Standards and Office of Research and Development, US EPA, 1997.

Walker V, Tofflemire K, Wrathall B, et al. Inuvik Regional Human Contaminants Monitoring Program. In: Sarah Kalthok, ed. *Synopsis of Research Conducted under the 1999-2000 Northern Contaminants Program*, Ottawa: Minister of Indian Affairs and Northern Development, 2002; pp.80-84.

World Health Organization -WHO. Methylmercury. Vol. 101. World Health Organization, International Programme on Chemical Safety, Geneva, Switzerland, 1990.

Wheatley B, Paradis S. Balancing human exposure, risk and reality: questions raised by the Canadian Aboriginal Methylmercury Program. *Neurotoxicology*. 1996; 17: 241-250.

**Table 1: Effect on the maximum concentration of total mercury in blood ( $\mu\text{g/l}$ ) and in hair ( $\mu\text{g/g}$ ) of variations in the value of the assumed metabolic rate of transformation of organic mercury into inorganic mercury.**

Maximum total mercury concentration in blood and hair				
Duration of methylmercury daily intake <sup>1</sup>	Biological matrix	Elimination half-lives of methylmercury from blood		
		39 days	50 days	70 days
Unique dose	Blood	0.92 $\mu\text{g/l}$	0.92 $\mu\text{g/l}$	0.93 $\mu\text{g/l}$
	Hair	0.25 $\mu\text{g/g}$	0.26 $\mu\text{g/g}$	0.27 $\mu\text{g/g}$
1 month	Blood	21.82 $\mu\text{g/l}$	23.01 $\mu\text{g/l}$	24.30 $\mu\text{g/l}$
	Hair	6.53 $\mu\text{g/g}$	6.81 $\mu\text{g/g}$	7.15 $\mu\text{g/g}$
3 months	Blood	42.30 $\mu\text{g/l}$	48.39 $\mu\text{g/l}$	55.99 $\mu\text{g/l}$
	Hair	13.99 $\mu\text{g/g}$	15.41 $\mu\text{g/g}$	17.22 $\mu\text{g/g}$
21 months	Blood	53.08 $\mu\text{g/l}$	67.98 $\mu\text{g/l}$	95.09 $\mu\text{g/l}$
	Hair	18.85 $\mu\text{g/g}$	23.28 $\mu\text{g/g}$	31.34 $\mu\text{g/g}$

Note: The concentrations are estimated from the model Carrier et al. (2001) using the parametric values presented by these authors, except for the values of the elimination half-life of MeHg from blood.

<sup>1</sup> Each ingested dose is equivalent to 1  $\mu\text{g}$  of methylmercury/kg body weight.

**Table 2 : Simulated ratio of total mercury concentration in the 1<sup>st</sup> centimeter of hair closest to the root ( $\mu\text{g/g}$ ) and in blood ( $\mu\text{g/ml}$ ) as function of collection times and different durations of methylmercury daily intakes.**

Ratio of hair-to-blood concentrations <sup>1</sup>					
Duration of methylmercury daily intake	Collection times (time elapsed since the cessation of exposure)				
	Day of cessation	One week	One month	Two months	Three months
Unique dose	4.5 (2.2- 6.7)	86 (43- 129)	407 (209- 629)	420 (210- 633)	423 (211- 635)
One week	39 (19- 58)	124 (62- 186)	419 (209- 630)	421 (210- 633)	423 (211- 635)
1 month	179 (90- 269)	267 (134- 401)	420 (210- 631)	422 (211- 634)	424 (212- 636)
3 months	306 (153- 459)	348 (174- 522)	421 (210- 633)	423 (211- 636)	425 (212- 639)
21 months	342 <sup>2</sup> (171- 513)	372 (186- 558)	425 (212- 639)	428 (214- 643)	431 (215- 648)

<sup>1</sup> The ratios were estimated from the Carrier et al. (2001) model using the parametric values presented by these authors (top). A variation of  $\pm 50\%$  on the transfer rate of organic and inorganic from blood to hair yields a range of hair-to-blood ratios (in parentheses).

<sup>2</sup> At the end of this exposure, the steady-state conditions are reached, but these conditions are lost at times after exposure ceases.

**Table 3 : Descriptive statistics on average daily intakes of methylmercury ( $\mu\text{g}/\text{kg}$  body weight) for the women from the Inuvik cohort (Walker et al., 2002): *i*) estimated from the model simulations based on the total mercury concentrations measured in the consecutive segments of hair; *ii*) average daily intakes as estimated by the questionnaire.**

Average daily intake of methylmercury ( $\mu\text{g}/\text{kg}$ body weight)				
	Estimated by the model from hair concentrations			Estimated by the questionnaire
	1 <sup>st</sup> trimester of pregnancy <sup>1</sup>	2 <sup>nd</sup> trimester of pregnancy <sup>1</sup>	3 <sup>rd</sup> trimester of pregnancy <sup>1</sup>	
Arithmetic mean	0.04	0.03	0.03	0.20
Standard deviation	0.07	0.07	0.05	0.35
Minimum	0	0	0.015	0
Maximum	0.49	0.56	0.34	2.73
Number of individuals	60	72	80	69

<sup>1</sup> Estimated by optimal adjustment of the simulations based on the Carrier et al. (2001) model to fit the data on the mercury concentration in each consecutive cm of the hair strand.

## CAPTIONS TO FIGURES

**Figure 1.** Model simulations of the time-profiles of total mercury concentration in blood (—) and in the 1<sup>st</sup> centimeter of hair closest to the root (----) following ingestion of a once a week intake of 1  $\mu\text{g}$  of methylmercury/kg of body weight: 3-months exposure (A) and 14-months exposure (B).

**Figure 2.** (i) Historical reconstruction of daily intakes of methylmercury ( $\mu\text{g}/\text{kg}$  of body weight) prior to the hair collection at time 0 (—) from model simulation (----) of the measured data ( $\square$ ) on mercury concentration in successive centimeters of hair ( $\mu\text{g}/\text{g}$ ) in 4 women from the Inuvik cohort (Walker et al., 2002). (ii) Simulated time-profile (-·-·-) of total mercury concentration in blood ( $\mu\text{g}/\text{l}$ ) from the reconstructed intake compared to measured data ( $\times$ ).

**Figure 3.** Comparison between measured and simulated total mercury concentration in blood ( $\mu\text{g}/\text{l}$ ) for the 16 women from the Inuvik cohort with mercury levels in the proximal cm of hair above the detection limit (Walker et al., 2002). The simulated value for each woman was obtained using the model of Carrier et al. (2001) in combination with their measured time-profile of total mercury concentration in hair. The line (—) represents the linear equation  $y=x$ .

**Figure 4.** (i) Historical reconstruction of daily intake of methylmercury ( $\mu\text{g}/\text{kg}$  of body weight) prior to the hair collection at time 0 (—) from model simulation (----) of the measured data ( $\square$ ) on mercury concentration in successive centimeters of hair ( $\mu\text{g}/\text{g}$ ) in 2 natives from the Amazon cohort (Lebel et al., 1998; Dolbec et al., 2001).

FIGURE 1

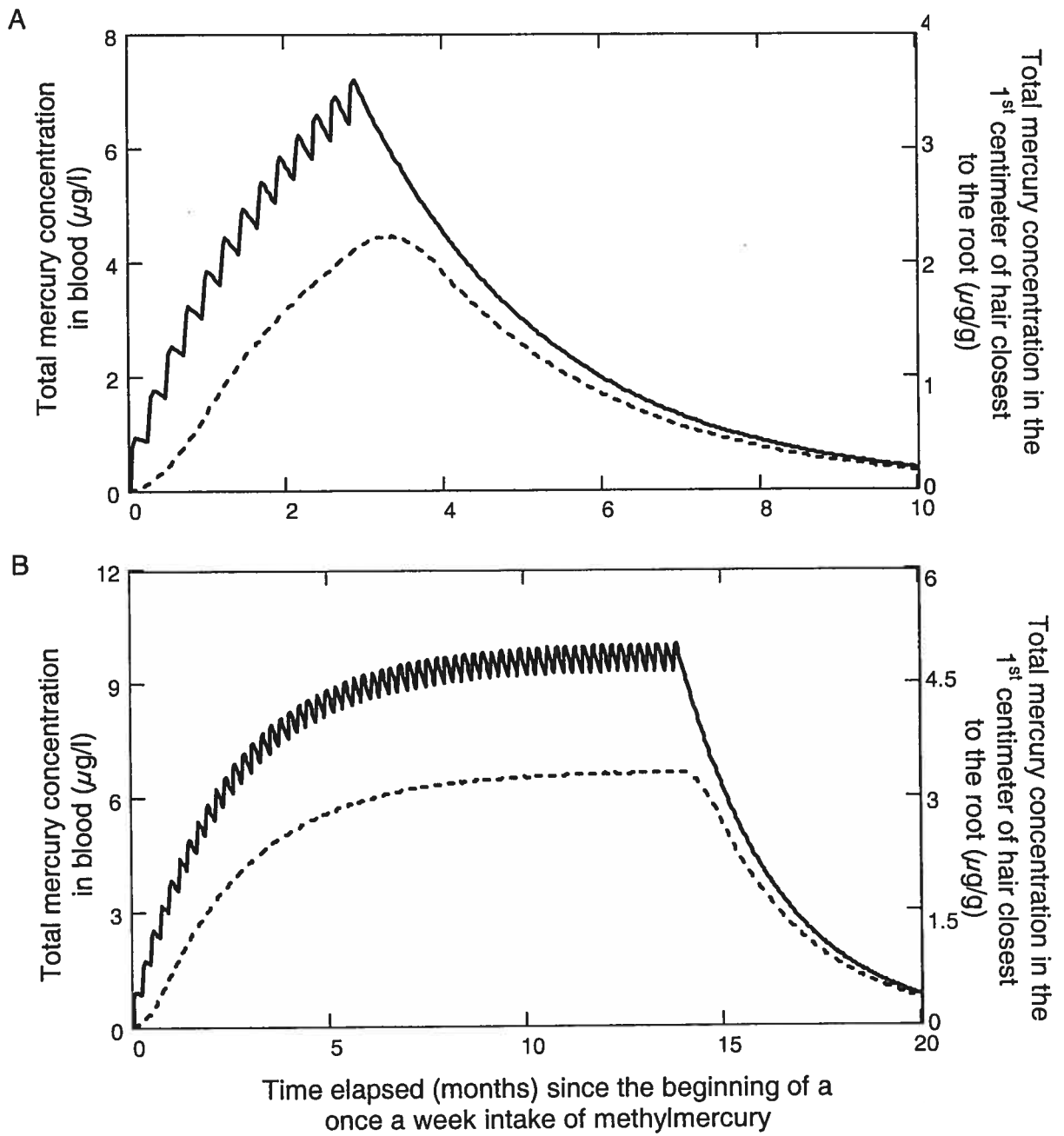
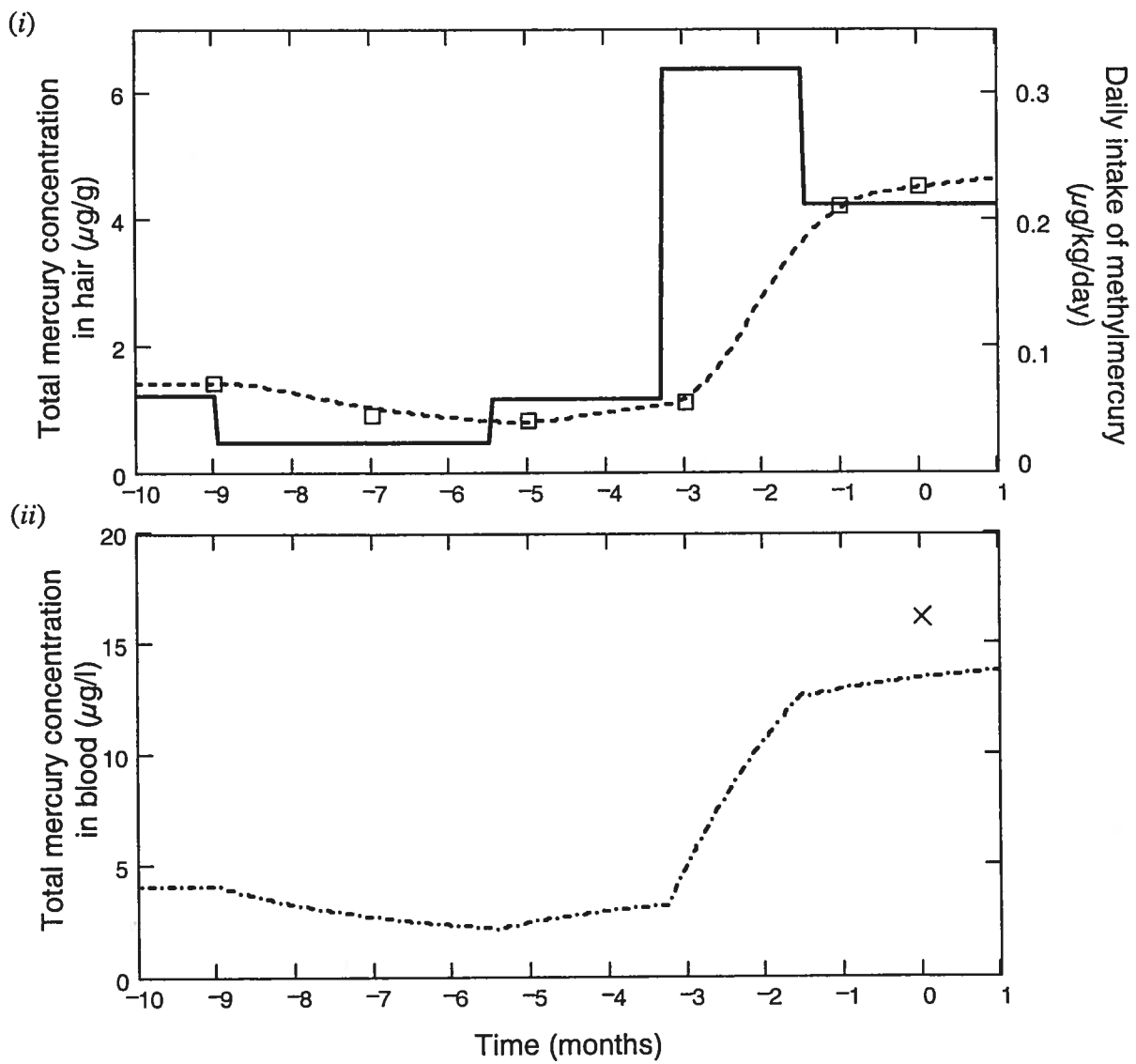
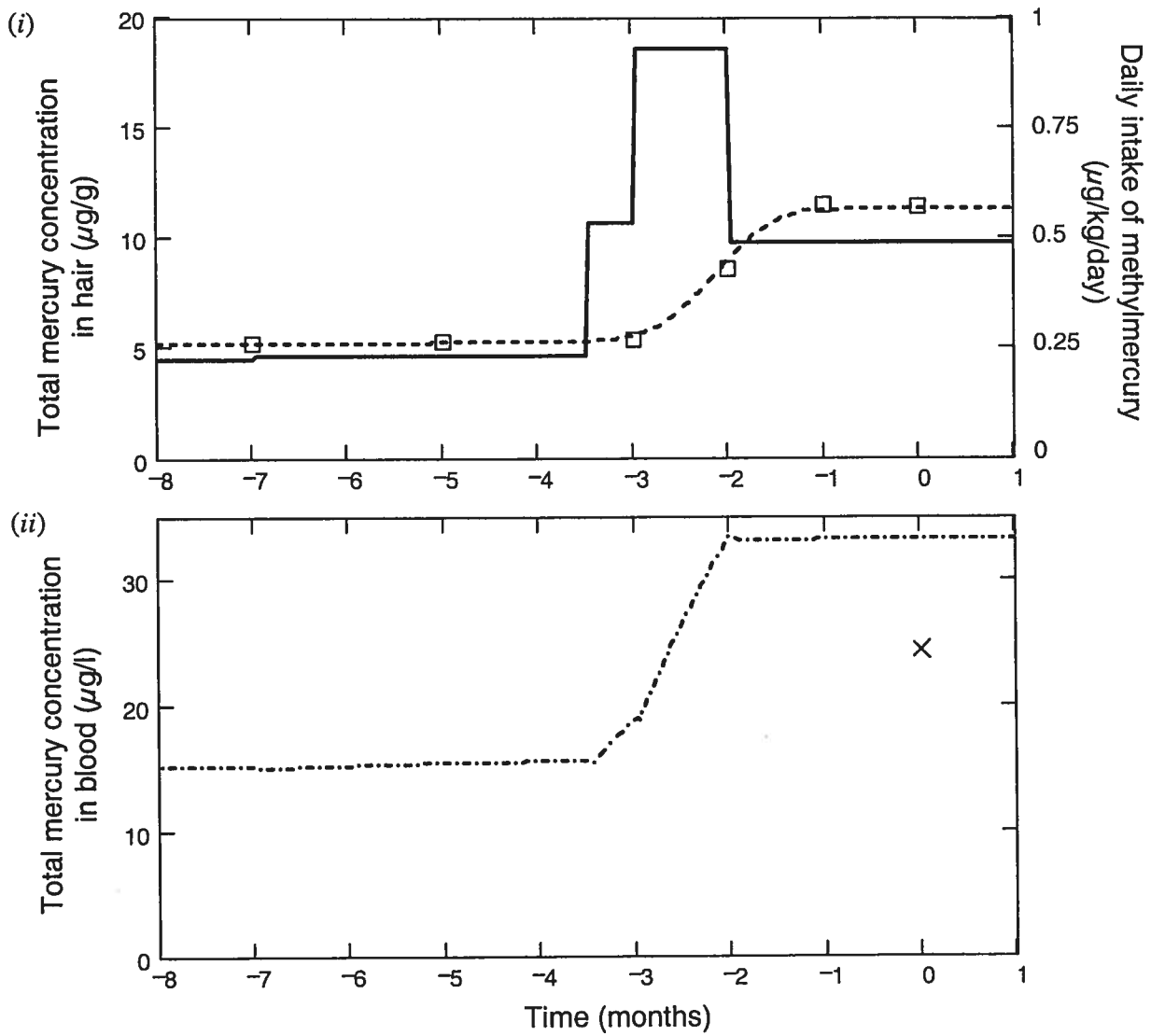


FIGURE 2

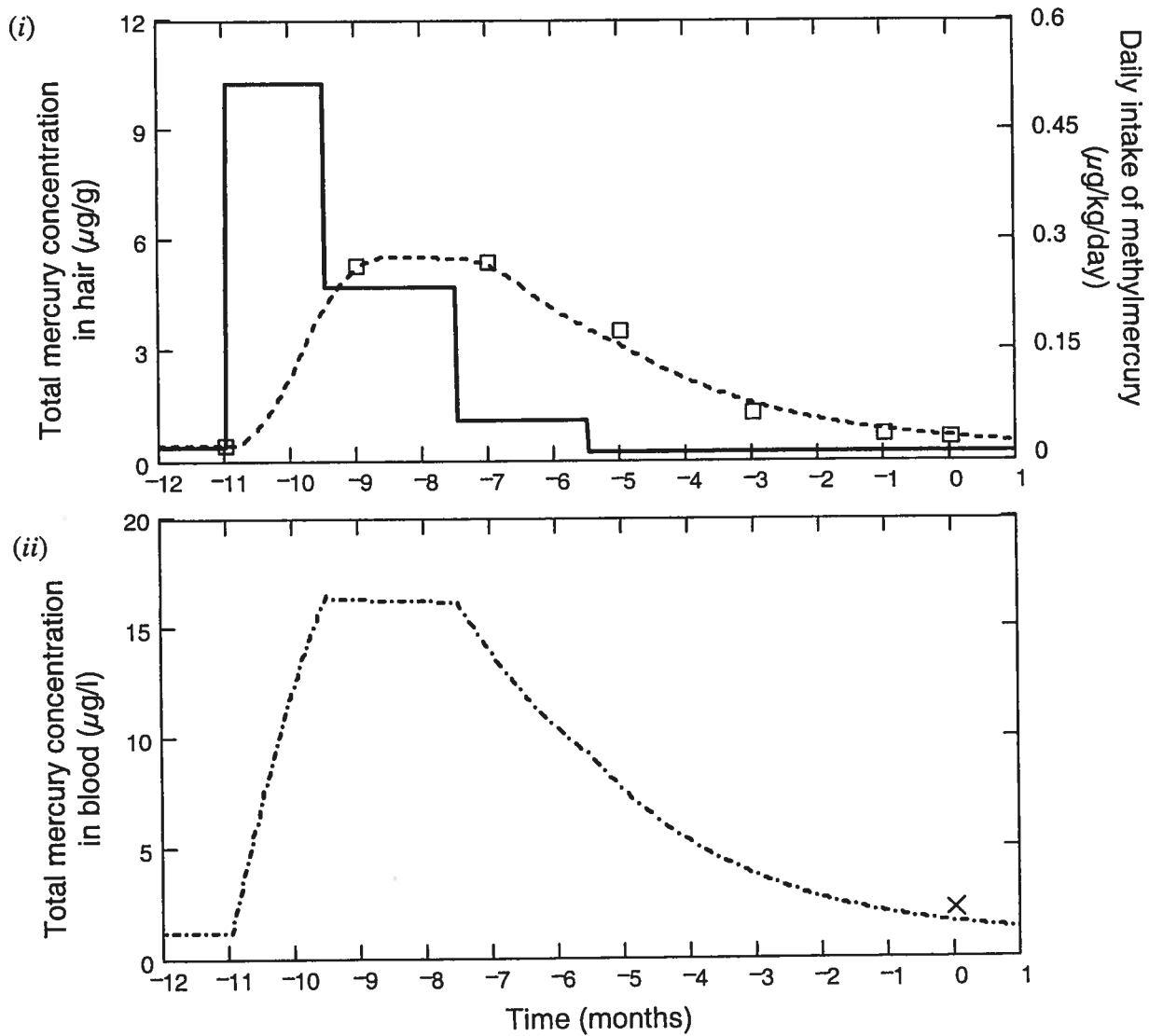
Woman A



Woman B



## Woman C



## Woman D

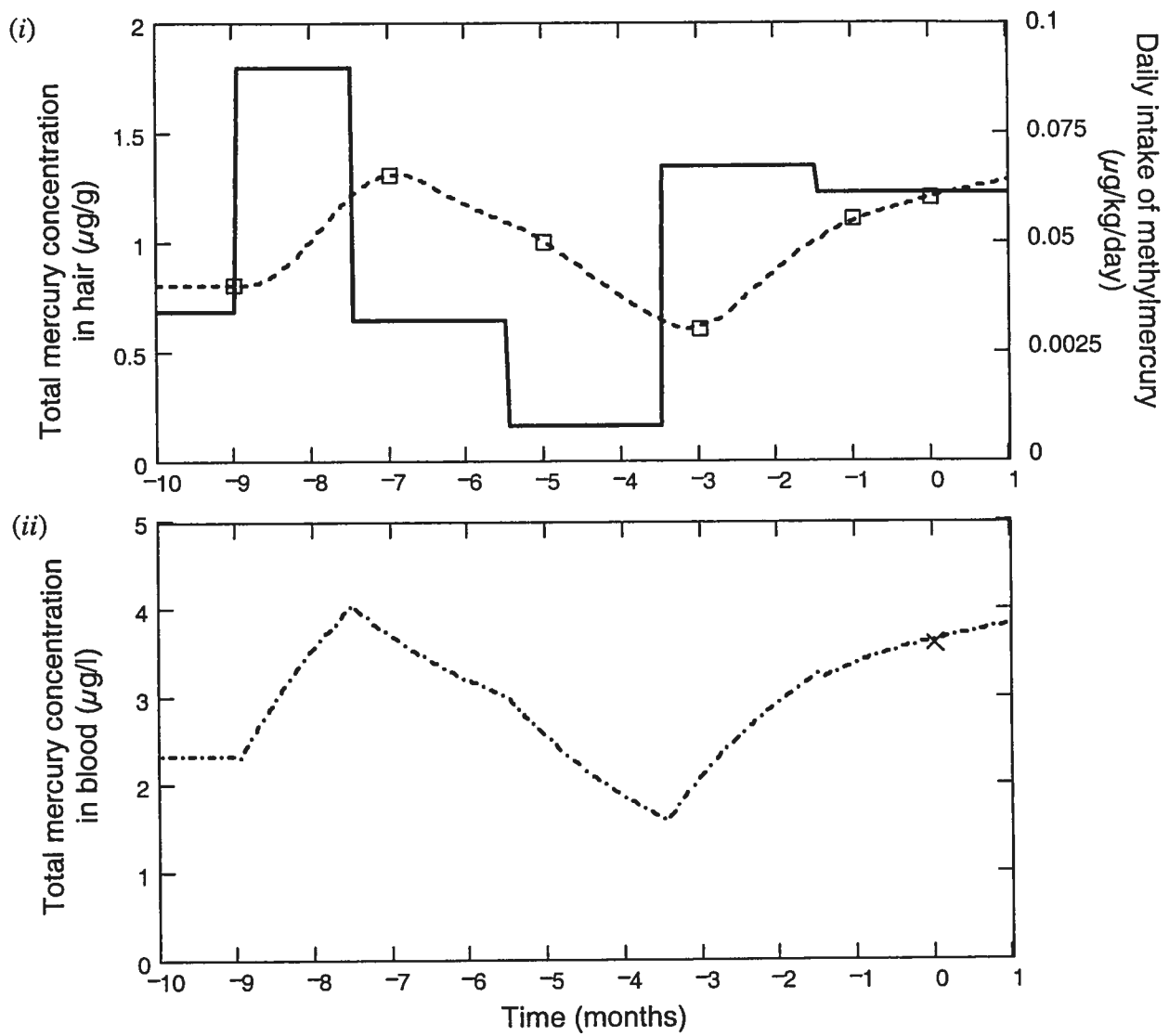


FIGURE 3

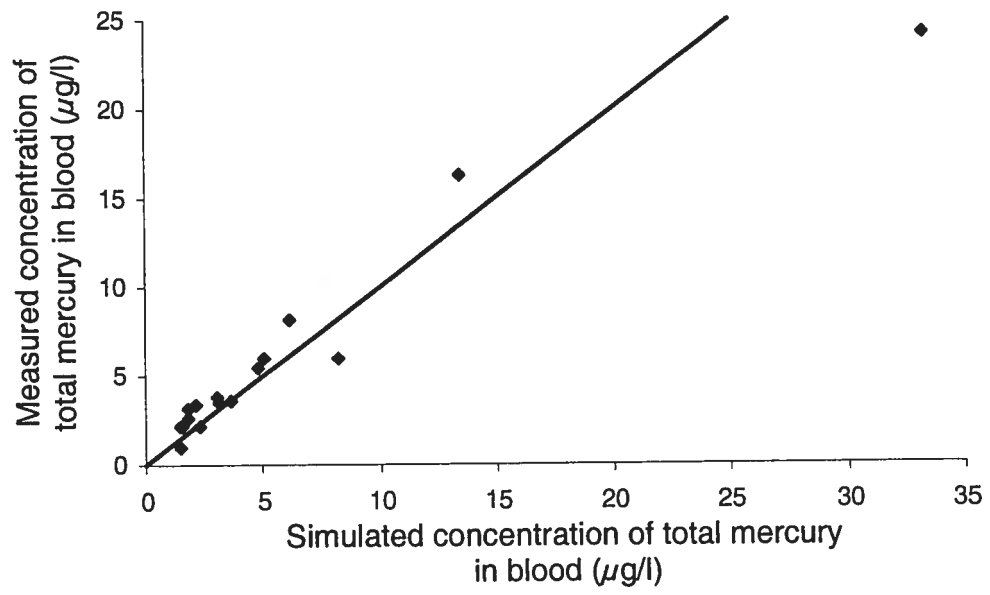
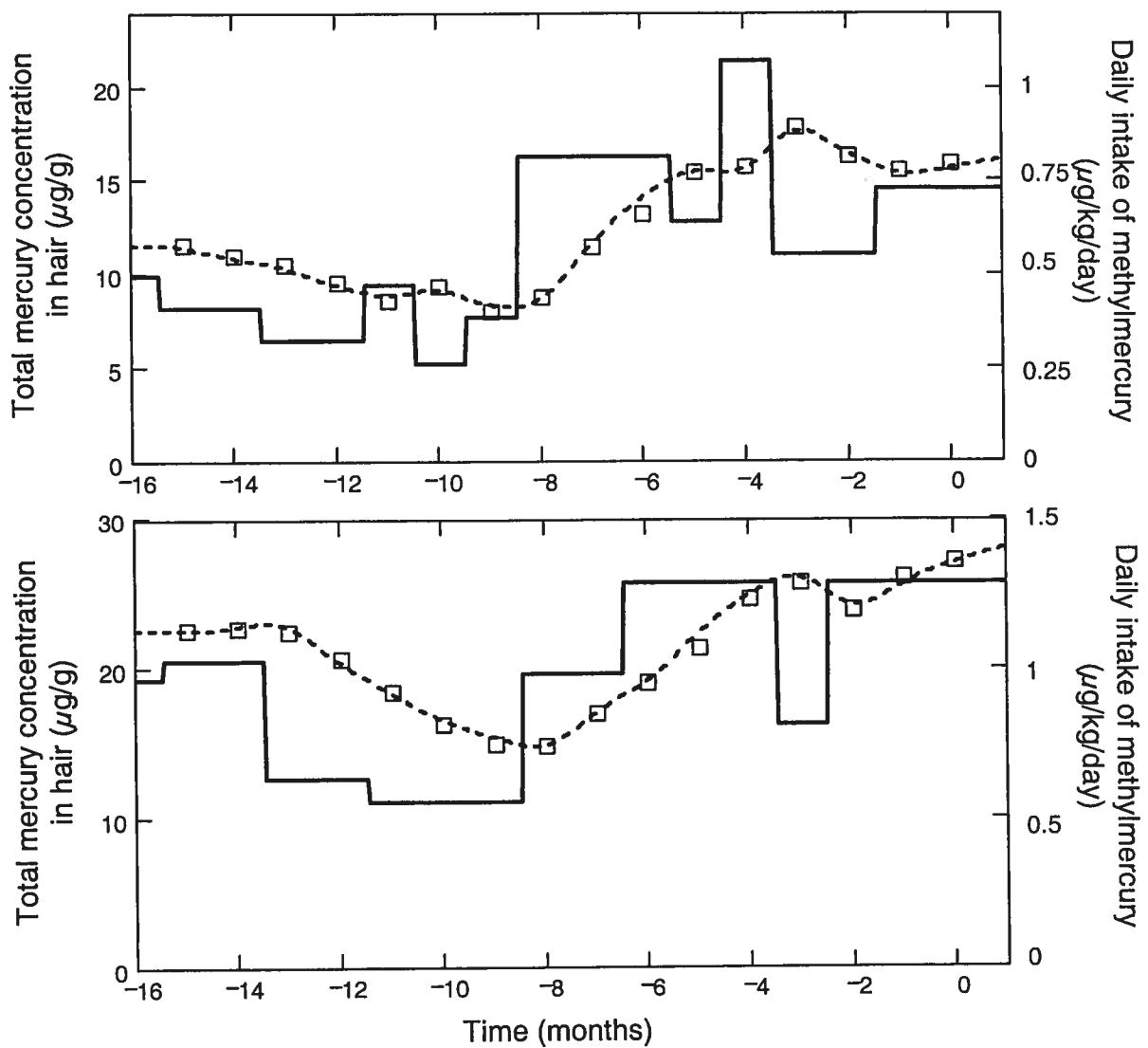


FIGURE 4



## **CHAPITRE 8 : CONCLUSION GÉNÉRALE**

Les travaux de cette thèse proposent aux intervenants de la santé des outils pour les aider à évaluer l'exposition et prévenir les risques encourus par les personnes exposées à cinq substances toxiques : trois insecticides de la famille des organophosphorés (parathion, malathion et chlorpyrifos), un phytocide largement utilisé comme herbicide (triclopyr), et finalement le méthylmercure. L'approche consiste à mesurer les niveaux de biomarqueurs de ces substances dans des matrices biologiques accessibles et à les comparer à des valeurs repères pour estimer l'exposition individuelle et le risque pour la santé associé à cette exposition. Les outils proposés possèdent toutes les qualités recherchées dans un test de dépistage : ils sont facilement applicables, ont un haut degré de spécificité et de sensibilité et permettent la détection de l'exposition bien avant l'apparition d'effets toxiques. En particulier, les mesures des métabolites des organophosphorés permettent de déceler le niveau d'exposition bien avant qu'il y ait inhibition détectable des cholinestérases. Le non-dépassement des valeurs repères, présentées sous forme de valeurs de référence biologiques, devrait permettre de prévenir les effets toxiques chez les individus les plus sensibles de la population ciblée. Des stratégies d'échantillonnage adaptées aux diverses substances étudiées et aux scénarios d'exposition les plus souvent rencontrés dans la réalité sont également proposées pour permettre l'évaluation précise de l'exposition interne de chaque sujet.

L'utilisation des niveaux de biomarqueurs comme mesures de l'exposition et indicateurs d'effets physiologiques de ces substances a été rendu possible grâce à une approche qui consiste, dans un premier temps, à développer ou à adapter des modèles

mathématiques de la cinétique de ces substances et de leurs métabolites à partir de leurs profils temporels dans des matrices biologiques collectées chez l'humain et, dans un deuxième temps, à établir les relations de type « dose absorbée–réponse toxique » à partir d'une revue de la littérature. La conjugaison de ces deux démarches a permis de déterminer des niveaux de biomarqueurs en deçà desquels aucun effet ne devrait être observé chez l'humain.

Cette approche permet d'utiliser des mesures de biomarqueurs en situations réelles pour estimer une dose absorbée dans le passé ou le devenir d'une dose sans avoir recours à des mesures de concentrations dans le milieu d'exposition et sans connaître la fraction d'absorption des diverses voies d'entrée dans l'organisme. De plus, pour la plupart des substances étudiées, les biomarqueurs sont sensibles et spécifiques, augmentant ainsi la validité et la pertinence de la mesure de l'exposition. Le présent travail fournit donc des outils très utiles à la réalisation d'études épidémiologiques qui viseraient à évaluer l'impact d'une exposition à une ou l'autre des substances étudiées.

Pour les quatre pesticides, des simulations avec les modèles cinétiques ont permis d'évaluer l'effet de divers scénarios temporels d'exposition, de diverses voies d'entrée et divers taux d'absorption sur l'estimation de la dose absorbée qui est reconstruite à partir des niveaux de biomarqueurs accumulés dans l'urine. Des tests de sensibilité ont démontré que le paramètre cinétique qui a le plus d'influence sur l'estimation de la dose absorbée est le taux d'absorption par voie cutanée, taux beaucoup plus faible et plus variable que les taux des voies orale et pulmonaire. Ces tests ont montré que les

résultats sont peu sensibles au taux de biotransformation et de distribution de la molécule-mère, puisqu'ils sont environ 15 fois plus élevés que les taux d'absorption cutanée et d'excrétion des métabolites qui s'avèrent déterminants pour la cinétique observée. Considérant ce résultat, les valeurs de référence biologiques, jugées sécuritaires pour une exposition professionnelle, ont été établies avec le scénario d'exposition qui est le plus conservateur : une exposition constante durant une période de huit heures consécutives, uniquement par la peau et où la charge corporelle du pesticide ou de ses métabolites au début de cette période est nulle. La marge de sécurité induite par ce scénario est expliquée en détails dans les articles portant sur les pesticides.

Une analyse a également été réalisée pour évaluer l'impact de différents scénarios d'exposition sur les niveaux de biomarqueur du MeHg. En effet, pour cette substance, le taux d'absorption n'a aucune influence sur les concentrations sanguines ni sur celles dans les cheveux et ce, quel que soit le scénario d'exposition. Ceci s'explique par la grande différence des échelles de temps gouvernant l'absorption et l'élimination ; la demi-vie d'élimination du MeHg est d'environ 50 jours alors que celle de l'absorption est tout au plus de 3 heures pour une absorption orale. Des variations dans le taux d'absorption ont alors peu de répercussions à moyen terme sur les niveaux de mercure dans le sang et les cheveux. Par ailleurs, la fréquence de consommation de produits contaminés au MeHg et la durée de l'exposition sont régies par des échelles de temps mesurées en semaines, tout comme la demi-vie d'élimination; les scénarios temporels de consommation ont donc un impact important sur les niveaux de biomarqueurs.

Toutefois, les variations mensuelles dans la consommation ont plus d'influence sur les niveaux biologiques que les variations de la demi-vie d'élimination du MeHg.

Une retombée importante de cette recherche touche les stratégies de collecte des échantillons biologiques pour les diverses substances étudiées. Par exemple, pour les pesticides étudiés, il ressort qu'une urine cumulative de 24 heures ou plus depuis le début d'une période d'exposition est souhaitable pour reconstruire avec un bon degré de précision la dose cumulative absorbée par les individus. Pour le MeHg, suite à de courtes périodes d'exposition (i.e., ingestion journalière durant un mois ou moins), il est suggéré d'effectuer la collecte de cheveux un mois après la fin de l'exposition afin de s'assurer que les cheveux aient eu le temps d'intégrer par leurs racines la présence du mercure dans le sang durant une période assez longtemps pour que cela apparaisse dans le centimètre proximal retenu pour le test.

L'utilisation du modèle cinétique du MeHg a permis une bonne adéquation entre les niveaux de biomarqueurs mesurés chez un individu et les quantités de MeHg ingérées. En effet, contrairement aux apports en MeHg estimés à partir d'un questionnaire alimentaire et de la contamination mesurée dans la nourriture, les apports reconstruits à partir du modèle de Carrier et coll. (2001) assurent une cohérence entre les apports estimés de MeHg et les quantités de mercure total mesurées dans les matrices biologiques.

L'application de l'approche proposée dans cette thèse à des données provenant de travailleurs exposés au malathion et au triclopyr et à celles provenant de populations autochtones exposées au MeHg montre bien l'utilité de ces outils dans un programme de prévention. Leur principale qualité comme signal de risque est de détecter l'exposition à des niveaux bien inférieurs à ceux induisant des effets toxiques et par le fait même à un stage beaucoup plus précoce que celui obtenu en utilisant des biomarqueurs d'effets.

## **BIBLIOGRAPHIE**

ACGIH. American Conference of Governmental Industrial Hygienists. 2003. Documentation of the Threshold Limit Values and Biological Exposure Indices, 8th Ed. Cincinnati, OH : American Conference of Governmental Industrial Hygienists.

Alessio, L., Berlin, A., Dell'Orto, A., Toffoletto, F., and Ghezzi, I. 1985. Reliability of urinary creatinine as a parameter used to adjust values of urinary biological indicators. *Int. Arch. Occup. Environ. Health* 55:99-106.

Boeniger, M.F., Lowry, L.K., and Rosenberg, J. 1993. Interpretation of urine results used to assess chemical exposure with emphasis on creatinine adjustments: a review. *Am. Ind. Hyg. Assoc. J.* 54:615-627.

Bouchard M., Brunet R.C., Droz P.O. and Carrier, C. 2001. A biologically based dynamic model for predicting the disposition of methanol and its metabolites in animals and humans. *Toxicol. Sci.* 64:169-184.

Carmichael, N.G., Nolan, R.J., Perkins, J.M., Davies, R., and Warrington S.J. 1989. Oral and dermal pharmacokinetics of triclopyr in human volunteers. *Human Toxicol.* 8: 431-437.

Carrier, G., Bouchard, M., Brunet, R.C., and Caza, M. 2001. A toxicokinetic model for predicting the tissue distribution and elimination of organic and inorganic mercury

following exposure to methyl mercury in animals and humans. II. Application and validation of the model in humans. *Toxicol. and Appl. Pharmacol.* 171: 50-60.

Carrier, G. and Brunet, R.C. 1999. A toxicokinetic model to assess the risk of azinphosmethyl exposure in humans through measures of urinary elimination of alkylphosphates. *Toxicol Sci.* 47: 23-32.

Carrier, C., Brunet, R.C. and Brodeur, J. 1995. Modeling of the toxicokinetics of polychlorinated dibenzo-p-dioxins and dibenzofurans in mammals, including humans, 1) nonlinear distribution of PCDD/PCDF body burden between liver and adipose tissues. *Toxicol. and Appl. Pharmacol.* 131: 253-266.

Curtis, G., and Fogel, M. 1970. Creatinine excretion : diurnal variation and variability of whole and part-day measures. *Psychosom. Med.* 32:337-350.

Dolbec, J., Mergler, D., Larribe, F., Roulet, M, Lebel, J, Lucotte M. 2001. Sequential analysis of hair mercury levels in relation to fish diet of an Amazonian population, Brazil. *Sci. Total Environ.* 271: 87-97.

Gosselin, N. 2001. Étude comparative de divers modèles toxicocinétiques. Mémoire de maîtrise, Département de mathématiques et statistique, Université de Montréal.

Greenblatt, D.J., Ransil, B.J., Harmatz, J.S., Smith, T.W., Duhme, D.W., and Koch-Weser, J. 1976. Variability of 24-hour urinary creatinine excretion by normal subjects. *J. Clin. Pharmacol.* 16:321-328.

L.R.Q, c, P-29 Loi sur les produits agricoles, les produits marins et les aliments, Éditeur officiel du Québec.

L.R.Q., c. Q-2, Loi sur la qualité de l'environnement, Éditeur officiel du Québec.

Lebel J., Mergler D., Branches, F., Lucotte, M., Marucia, A., Larribe, F. and Dolbec, J. 1998. Neurotoxic effects of low-level methylmercury contamination in the Amazonian Basin. *Environ. Res. section A.* 79: 20-32.

Lebel J., Mergler D., Lucotte M., Marucia, A., Dolbec, J., Miranda, D., Arantès, G., Rheault, I. and Pichet, P. 1996. Evidence of early nervous system dysfunction in Amazonian populations exposed to low-levels of methylmercury. *Neurotoxicology.* 1996; 17: 157-168.

Leung, HW. 1991. Development and utilization of physiologically based pharmacokinetic models for toxicological applications. *J. Toxicol. Environ. Health,* 32:247-267.

RQMT, 2001. Règlement sur qualité du milieu de travail, S-2.1, R-15, Éditeur officiel du Québec.

Segel, L.A. 1988. On the validity of the steady state approximation of enzyme kinetics. *Bull. Math. Biol.* 50:579-593.

Segel, L.A., and Slemrod, M. 1989. The quasi-steady state approximation: A case study in perturbation. *Society for Industrial and Applied Mathematics Review* 31:446-476.

Temple W., and Smith N.A. 1996. Insecticides. In: Human Toxicology, Chapter 20 (J. Descotes Ed.), Elsevier, New-York, pp 541-50.

Walker V., Tofflemire K., Wrathall, B., et al. Inuvik Regional Human Contaminants Monitoring Program. In: Sarah Kalhok, ed. *Synopsis of Research Conducted under the 1999-2000 Northern Contaminants Program*, Ottawa: Minister of Indian Affairs and Northern Development, 2002; pp.80-84.

**APPENDICE : CONTRIBUTION**

**CONTRIBUTION SPÉCIFIQUE DE LA CANDIDATE À CHACUN DES ARTICLES DE CETTE THÈSE**

**Malathion (Article 1) et Parathion (Article 2)**

- Contribution significative au développement du modèle cinétique :
  - Mise au point du système d'équations différentielles
  - Détermination et validation des valeurs paramétriques
- Contribution significative à l'application du modèle cinétique :
  - Réalisation des tests de sensibilité
  - Détermination d'un scénario d'exposition pour déterminer les valeurs de référence biologiques
- Contribution à l'analyse de la littérature pour déterminer la DSEO
- Contribution significative à la rédaction des articles :
  - Écrire l'article du parathion
  - Correction de l'article du malathion écrit par Michèle Bouchard

**Chlorpyrifos (Article 3)**

- Contribution au développement du modèle cinétique :
  - Détermination et validation des valeurs paramétriques
- Contribution significative à l'application du modèle cinétique :
  - Réalisation des tests de sensibilité
  - Détermination du scénario d'exposition pour déterminer les doses de référence biologique
- Contribution à la rédaction de l'article :
  - Correction de l'article écrit par Michèle Bouchard

**Triclopyr (Article 4)**

- Contribution significative au développement de l'analyse des risques toxicologiques chez les travailleurs de l'étude:
  - Adaptation du modèle de Carmicheal et coll. (1989)
  - Réalisation des simulations du modèle :
    - Reconstruction de leur dose absorbée à partir des urines cumulatives collectées par Amssetou Dosso
    - Tests de sensibilité
    - Établir les valeurs de référence biologiques
  - Recherche de la dose sans effet nocif observé
- Écrire l'article

**Méthylmercure (Article 5)**

- Contribution significative à l'application du modèle de Carrier et coll. (2001) :
  - Reconstruction de l'historique des apports quotidiens en méthylmercure chez les autochtones ciblés
  - Réalisation de simulations portant sur différents scénarios d'exposition afin d'effectuer une analyse de sensibilité des paramètres et variables impliqués
- Écrire l'article



Faint, illegible text at the bottom right corner of the page.